Sterile activation of invariant Natural Killer T cells by ER-stressed antigen presenting cells

Melissa Deborah Bedard

Radcliffe Department of Medicine
St. Edmund Hall
University of Oxford

This thesis is submitted for the degree of Doctor of Philosophy in Medical Sciences
43,813 words

Trinity Term 2019

Abstract

Invariant NKT (iNKT) cells are a subset of innate-like lymphocytes that recognize lipid antigen presented on monomorphic CD1d molecules. These cells have the unique ability to shape immunity during anti-tumour immune responses and other forms of sterile and non-sterile inflammation. Recent studies have highlighted a variety of classes of endogenous and pathogen-derived lipid antigens that can trigger iNKT cell activation under sterile and non-sterile conditions. However, the context and mechanisms that drive the presentation of self-lipid antigens in sterile inflammation remain unclear. Given that ER-stress is prevalent during tumourigenesis coupled with the intersection between the ER-stress pathways and lipid metabolism, we hypothesized that ER-stressed $CD1d^{+}$ cells might present immunogenic self-lipid(s) on CD1d molecules to activate iNKT cells in sterile conditions. We demonstrate that ER-stressed dendritic cells activated iNKT cells in a CD1d-dependent manner, which in turn promotes dendritic cell maturation. We illustrate that PERK signalling increases CD1d-mediated presentation of immunogenic endogenous lipid species. We demonstrate that the immunogenic self-lipid(s) are likely ceramide-based and loaded onto CD1d in the endosomal/lysosomal compartments. We also investigate the relevance of this mechanism in a human tumour setting by analysing iNKT cell responses to multiple myeloma cell lines and identifying ER-stressed myeloid cells in the tumour microenvironment. In conclusion, this work defines a previously unidentified mechanism that controls iNKT cell activation during sterile inflammation, with a potential role in human health and disease.

Acknowledgements

Firstly, I would like to thank my supervisors, Vincenzo Cerundolo, Mariolina Salio, and Christian Eggeling. I have truly realized how much I've learned from you all over the past three years, from writing to technical skills, and from experimental design to formal presentations, while writing this thesis. For this, I will always be grateful. I'd also like to thank my thesis committee, Drs. Adrian Harris and John Christianson, for the stimulating conversations and helpful feedback during my DPhil.

Secondly, I would like to thank the members of the Cerundolo lab, for the many professional and light-hearted conversations, technical support, and funny, memorable moments. My time in this lab has had an immense impact on my personal and professional development.

Thirdly, I would like to thank to my college friends, who I can rely on for emotional support, sound advice, boundless laughter, wild formal dinners and horror movie nights. You have made my time in Oxford an unforgettable experience.

Finally, I would like to thank the largely non-scientific support team that has had my back throughout my time in Oxford. To my family, especially my parents, whose wisdom, past and present, has ultimately guided me through this experience - without your love and support I could not have embarked on this journey. To Allison, whose description of the challenges and satisfaction of

completing the PhD has no doubt inspired my decision to take one on myself – I am grateful and proud to join you in the family PhD/DPhil club!

To my fiancé, Harry, who has been on this journey with me every step of the way since we met at the Jericho Tavern in our first year at Oxford – there was nothing I looked forward to more after a long day in lab than being with you. You took me to places I never thought I would see, prepared amazing food for me every night, and became a wonderful gym partner and dog spotter. You have and will always inspire me to be my best.

I love you all so much. I cannot dedicate this thesis to one of you in particular, so it is dedicated to you all.

Table of Contents

List of Figures and Tables

Commonly Used Abbreviations

αGC	α-galactosylceramide
ACER1	Alkaline ceramidase 1
APC	Antigen presenting cell
APC	Allophycocyanin
ALT	Alanine aminotransferase
ATF4	Activating transcription factor 4
ATF6	Activating transcription factor 6
ATG7	Autophagy Related 7
βGluCer	β-glucosylceramide
BiP	Binding immunoglobulin protein
BMDC	Bone marrow-derived dendritic cell
CD	Cluster of differentiation
CDR	Complementarity-determining regions
CHOP	C/EBP homologous protein
CV	Control vector
DC	Dendritic cell
DMSO	Dimethyl sulfoxide
DP	Double positive
eIF	Eukaryotic initiation factor
ER	Endoplasmic reticulum
FACS	Fluorescence activated cell sorting
FITC	Fluorescein
FCS	Fetal calf serum
GCN2	General control nonderepressable 2
GGC	α-galactose-(1,2)galactosylceramide
GMCSF	Granulocyte-macrophage colony stimulating factor
GPI	Glycosylphosphatidylinositol
GSL	Glycosphingolipid
HLA	Human leukocyte antigen

IFN	Interferon
iGB3	Isoglobohexosylceramide
IL	Interleukin
iNKT	Invariant natural killer T (cell)
IRE1	Inositol-requiring enzyme 1
ISRE	Integrated stress response
ISRIB	Integrated stress response inhibitor
KD	Knock down
LPS	Lipopolysaccharide
MAIT	Mucosal-associated invariant T (cell)
MHC	Major histocompatibility complex
MoDC	Monocyte-derived dendritic cell
MR1	Major histocompatibility complex, class 1 related
MS	Mass spectrometry
MTTP	Microsomal Triglyceride Transfer Protein
MyD88	Myeloid differentiation primary response 88
NAFLD	Non-alcoholic fatty liver disease
NASH	Non-alcoholic steatohepatitis
NK	Natural killer
pAPC	Profession antigen presenting cell
PBS	Phosphate buffered saline
PE	Phycoerythrin
PDI	Protein disulfide isomerase
PERK	PKR-like endoplasmic reticulum kinase
PLZF	Promyelocytic leukemia zinc finger
ROS	Reactive oxygen species
SERCA	Sarcoendoplasmic reticulum Ca^{2+} ATPase (pump)
TCR	T cell receptor
Th	T-helper
TLR	Toll-like receptor
TRAJ	T cell receptor alpha joining region

ULBP	UL16 binding protein
uORF	Upstream open reading frame
UPR	Unfolded protein response
WT	Wild type
XBP1	X-box binding protein 1

Chapter 1: Introduction and Project Aims

1.1 Overview of the immune system

[Section 1.1 is based on *Janeway's Immunobiology*, 9th Edition.]

The human immune system is comprised of two main branches: innate and adaptive. Together, the branches work to discriminate between 'self' and 'non-self', and through this distinction mount an appropriate immune response to maintain homeostasis and health.

The distinct roles of and essential cooperation between the innate and adaptive branches are highlighted in the immune response to a foreign infection. The first lines of defence against microbes are the barrier sites, such as skin, mucous membranes, gut epithelium etc. If such barriers are compromised, the pathogen can enter blood and body tissues. In this case, cells of the innate immune system, either circulating or tissue resident, sense the presence of non-self entities and initiate a rapid response in the early stages of infection. Upon uptake or phagocytosis by innate immune cells, pathogens are detected through recognition of pathogen-specific molecules, called pathogen-associated molecular patterns (PAMPs), by surface or intracellular pattern recognition receptors (PRRs). This mode of recognition is typical of macrophages, neutrophils, and dendritic cells (DCs). Another innate cell subset, natural killer cells, can sense viral infection by detecting the downregulation of MHC class I and upregulation of ligands for activating receptors on infected cells.

In response to this detection, innate immune cells secrete chemokines to recruit other immune cells to the site of infection, and cytokines to help polarize the

ensuing immune response towards a pathogen-clearing phenotype. Professional antigen presenting cells (DCs, macrophages, and mature B cells) might also process and present pathogen-derived antigens on antigen presenting molecules, including MHC class I, MHC class II (mainly expressed on professional antigen presenting cells, or pAPCs), CD1, or MR1. These antigens can be recognized by lymphocytes of the adaptive branch in the draining lymph node. This step that bridges innate and adaptive immunity is key to developing pathogen-specific long-term immunity.

While cells in the innate immune system exhibit a limited diversity in sensing mechanisms, mounting comparable responses to an array of pathogens, adaptive immunity confers a degree of specificity in its responses. The adaptive branch primarily consists of lymphocytes, including T and B cells. While their progenitors arise in the bone marrow, T cell precursors migrate to the thymus, whereas B cells complete maturation in the bone marrow. T cells bear a T cell receptor (TCR), which theoretically recognizes a unique epitope presented on antigen presenting molecules. TCR or BCR ‘combinatorial diversity’ stems from seemingly infinite genetic rearrangements in the gene segments, coding for the aptly named variable regions of the polypeptide chains. Another layer of diversification stems from the addition or subtraction of nucleotides at the junctions of the gene segments to create so-called ‘junctional diversity’. Together, these mechanisms give rise to numerous T cell clones that, by each recognizing a specific epitope, increase the breadth of antigens recognized by lymphocytes on MHC class I and II molecules. Positive selection, which selects for T cell clones

that are restricted to self-MHC molecules, and negative selection, which eliminates T cell clones that react too strongly to self-antigens, occur in the thymus. Similar processes lead to the diversification and selection B cell clones.

After selection, immature T and B cells migrate into the lymphatics and circulate around the body. During infection, pAPCs migrate to the lymph nodes where they present antigens to lymphocytes. In order to achieve activation, lymphocytes integrate multiple signals from the pAPC. These are 'signal 1' in the form of TCR/BCR-peptide:MHC recognition (or CD1:lipid antigen recognition), 'signal 2' in terms of signalling of costimulatory molecules, and 'signal 3' in terms of cytokine stimulation.

Activation of T and B cell clones initiates their proliferation and endows them with effector functions for targeted pathogen clearance and long-term immunity mediated by immunological memory. Activation of T cells gives rise to cellular immunity, whereas activation of B cells gives rise to humoral immunity, characterized by antibody secretion. T cell responses can be classified in part by the co-receptors that they bear; either CD8, which is usually a hallmark of cytotoxic abilities, or CD4, which usually correlates with a 'helper' phenotype. The profile of cytokines they release upon activation also classifies T cell responses. Th1 responses are typified by tumour necrosis factor α (TNFα) and interferon-γ (IFN-γ) release and cytotoxicity of tumour or virally-infected cells stemming from recognition of antigen on MHC class I by T cells expressing the transcription factor Tbet; Th2 responses are typified IL-3, IL-4 and IL-15 release from GATA3-expressing $CD4^+$ T cell recognition of antigen on MHC class II; Th17 responses,

associated with mucosal immune responses are typified by RORγT-expressing T cells that secrete IL-17 and IL-22 release; Th9 responses, which are similar to Th2 responses, are typified by high IL-9 secretion and immunity against tumours and extracellular pathogens; Tfh responses, restricted to T cells residing in follicles of the spleen of lymph nodes, provides B cell 'help' to mature them into effective antibody-secreting plasma cells; and Treg cells, which are $CD4^+$ cells typified by expression of the Foxp3 transcription factor and promotion of peripheral tolerance, and anti-inflammatory and immunoregulatory responses through secretion of anti-inflammatory cytokines such as IL-10. T cells can be polarized towards these responses by external factors such as a cytokines and the metabolic environment, and also exhibit a degree of plasticity, allowing them to shift between, for example, Th1 and Th2 phenotypes. B cells can similarly be polarized towards different Th profiles.

While the innate immune response is generated over the course of hours to days, the adaptive immune response is generated over a longer period of days to weeks, giving rise to effector lymphocytes. Many of these effector cells undergo apoptosis after the initial insult in cleared, but memory lymphocytes, a subset of reactive cells, are maintained after resolution of the initial infection. Upon secondary exposure to their cognate antigen, these central and effector memory lymphocytes (that reside in the lymph nodes and tissue respectively), mount a rapid and robust response to clear the pathogen. This immunological memory is a distinct feature of the adaptive branch.

An understanding of the nature of immune responses is at the core of understanding many diseases and therapies important to human health. The term ‘non-self’ originally referred to foreign pathogens, but can now be extended to tumours through recognition of danger associated molecular patterns (DAMPs) and neoantigens generated in neoplasmic cells. Failure to discriminate between ‘self’ and ‘non-self’ can give rise to harmful autoimmune responses. The concept of immunizations, arguably one of the most life-saving interventions developed by man, harnesses the power of the adaptive immune response and immunological memory to create long-term immune responses against certain pathogens that, in the case of smallpox, has eliminated a devastating disease world-wide. The inclusion of adjuvants, substances that enhance the immune response to an antigen with which it is mixed, has further improved the efficacy of immunizations. A similar immunization strategy, using tumour-specific neoantigens, is one of several types of immunotherapy that are revolutionizing cancer treatments (Schumacher and Schreiber, 2015). Current controversial but cutting edge immunology research on so-called ‘splice-itopes’ continues to push the boundaries of ‘self’ versus ‘non-self’ discrimination (Liepe et al., 2016). The boundaries between innate and adaptive cells have also been blurred with the discovery of innate-like lymphocytes that exhibit characteristics of both cell types. Since they sit at the interface between the two branches, it is becoming clear that their immunomodulatory effects can influence a wide range of immune cells. Amongst these unconventional innate-like lymphocytes are T cells that recognize lipid antigen in the context of CD1 molecules (Murphy and Weaver, 2016).

1.2 CD1 group molecules

CD1 molecules are functionally monomorphic antigen presenting molecules that present lipid antigens (Brigl and Brenner, 2004). Their corresponding genes are located on chromosome 1 in humans. All CD1 molecules consist of a transmembrane heavy chain with α1, α2, and α3 domains that folds and assembles with β2 microglobulin in the ER, in complex with lipid antigen, to form functional CD1 molecules, similar to MHC class I molecules. The folding requires calnexin and calreticulin, but is independent of TAP (Brigl and Brenner, 2004). Upon folding, CD1 molecules traffic through the Golgi, where they undergo glycosylation, and traffic to the cell surface. CD1 molecules consist of five isoforms, classified into two groups, group 1 and group 2 CD1 molecules, based primarily on sequence homology and expression patterns (Brigl and Brenner, 2004). CD1 genes can be traced back to birds and reptiles, although they are expressed differentially in certain mammals; rodents do not express group 1 CD1 molecules, whereas bovine species do not express group 2 CD1 molecules (Rogers and Kaufman, 2016).

1.2.1 Group 1 CD1 molecules

Group 1 CD1 molecules consist of CD1a, CD1b, CD1c, and CD1e. They are all expressed on mature and immature DCs and thymocytes (Brigl and Brenner, 2004). CD1a is highly expressed on skin-resident Langerhans cells (Kim et al., 2016), CD1b is expressed on macrophages (Kasinrerk et al., 1993, Porcelli, 1995) and CD1c is expressed on B cells (Delia et al., 1988). All three molecules

can be intracellularly recycled to exchange lipid antigens and return to the cell surface, albeit through slightly different routes. CD1a undergoes ‘cortical’ recycling in the early endosome (Barral et al., 2008a), whereas CD1b requires trafficking deeper into the late endosome and lysosome to undergo lipid exchange (Jackman et al., 1998). CD1c can recycle into both compartments to facilitate lipid exchange (Sugita et al., 2000). This recycling is mediated by adaptor protein interactions with a tyrosine sorting motif on the cytoplasmic tail of the CD1 molecules, which targets the molecules to the different intracellular compartments (Sugita et al., 2004). CD1e represents a minor class of CD1 molecules, as it does not directly present lipid antigens at the cell surface but rather acts as chaperone to aid lipid loading on the other CD1 molecules in the Golgi, endosomes and lysosomes (de la Salle et al., 2005, Facciotti et al., 2011). It is sometimes classified separately as a group 3 CD1 molecule (Angenieux et al., 2000).

CD1a, CD1b, and CD1c all exhibit characteristic deep, hydrophobic clefts for lipid binding, with charged residues surrounding the top of the molecule where the TCR docks and recognizes the antigen (Rossjohn et al., 2015). However, specific structures of these molecules vary, reflecting the types of lipid antigens each molecule can bind and present. In analysing the crystal structure of CD1a bound to sulfatide, the heavy chain forms two hydrophobic pockets termed the A’ and F’ pockets (Zajonc et al., 2003). The A’ pocket forms a semi-circular channel in the molecule, while the F’ pocket bind lipids in a straighter orientation. The head group protrudes from the centre of the binding groove to interact with a cognate TCR. Typical CD1a-binding lipids include sphingomyelin, certain phospholipids,

fatty acids, urushiol and cholesterol derivatives, such as squalene (Le Nours et al., 2018). The observation that headless and relatively small autoreactive lipids can activate CD1a-restrictied T cells has given rise to the 'absence of interference' model, whereby CD1a adopts a conformation that is recognized by the TCR even in the absence of a polar moiety on the lipid antigen (Van Rhijn et al., 2015, de Jong et al., 2014). The crystal structure of CD1b bound to phosphatidylinositol or ganglioside GM2, reveals a distinct network of four hydrophobic tunnels deep in the molecule: the A', C', and F' tunnels, which are interconnected by the T' tunnel (Gadola et al., 2002). Together, these pockets can accommodate lipid tails of over 70 carbons. The A' and C' tunnels allow for antigen recognition by the TCR. Typical classes of CD1b binding lipids include an array of phospholipids, gangliosides, and mycolic fatty acids derived from *Mycobacteria* (Le Nours et al., 2018). However, some of these classical CD1b lipid antigens fit in the A' and C' pockets, but do not fully occupy the other two binding pockets of molecule, therefore jeopardizing the folding and stability of the CD1b molecule. This issue is remedied by an ancillary F' tunnel opening to allow for the binding of an additional foreign or self-lipids, termed scaffold or spacer lipids, in the F' and T' tunnel (Huang et al., 2011). This feature expands the number and type of lipid antigens capable of binding CD1b. Based on the crystal structure of CD1c bound with mannosyl-β1-phosphomycoketide, CD1c consists of an A' and F' pocket, similar to CD1a (Scharf et al., 2010). However, it exhibits unique features: the existence of the D' and E' portal, located underneath the α1 domain, which allows for the overhang of long-chained lipids; and the open conformation of the F' pocket, which

is accessible to solvent. While certain fatty acids, phosphatidic acids, and phosphomycoketides are typical CD1c-binding lipids (Le Nours et al., 2018), the open nature of the F' pocket draws speculation the glycopeptides might bind CD1c (Adams, 2013).

Lipid antigens that bind group 1 CD1 molecules are typically derived from endogenous and bacterial lipids, predominantly from *Mycobacteria* such as *M. tuberculosis*. The noteworthy absence of group 1 CD1 in mice, but presence in animals such as humans and cows, which are naturally susceptible to *Mycobacteria*, might highlight their importance in defence against *Mycobacterial* infection (Van Rhijn et al., 2006). Furthermore, perhaps in part due to their ability to present numerous self-lipid antigens, group 1 CD1 molecules have been shown to contribute to autoimmune and allergic inflammation. For example, CD1a has been implicated in skin inflammatory conditions (de Jong et al., 2014, Kim et al., 2016), including, psoriasis, contact dermatitis, and allergic reactions to bee venom (Hardman et al., 2017, Cheung et al., 2016, Jarrett et al., 2016, Subramaniam et al., 2016). Humanized mouse models illustrate that autoreactive CD1b-restricted T cells contribute to hyperlipidemia-induced skin inflammation (Bagchi et al., 2017). Allergen-driven upregulation and lipid presentation by CD1c on respiratory tract resident DCs has been implicated in atopic asthma (McCarthy et al., 2007). CD1-restricted T cell responses can take on different Th phenotypes, but the extent to which they can mount regulatory responses and their degree of plasticity is an area of continuing research.

1.2.2 Group 2 CD1 molecules

Group 2 CD1 molecules include the best-characterized CD1 member, CD1d. Like the other CD1 family members, CD1d is functionally monomorphic, (limited polymorphism are detectable but not in the antigen binding groove), a striking feature that contributed to its discovery (Han et al., 1999). CD1d is widely expressed on murine and human cells of hematopoietic origin, particularly on antigen presenting cells such as DCs, thymocytes, and splenic B cells (Koch et al., 2005). It can also be expressed on hepatocytes and intestinal and lung epithelial cells (Crosby and Kronenberg, 2018). Like group 1 CD1s, CD1d is expressed in birds and reptiles, and is highly evolutionarily conserved in most mammals, including rodents and humans (Rogers and Kaufman, 2016). Nascent CD1d is folded in the ER as previously described, where lipid-loading machinery enables folding of CD1d with a self-lipid antigen. It is glycosylated and translocates through the Golgi to the cell surface for antigen presentation to invariant natural killer T (iNKT) cells (Freigang et al., 2010, van den Elzen et al., 2005). CD1d continuously presents endogenous lipids on the cell surface, either through *de novo* synthesis in the ER or through turnover of recycling CD1d (Jayawardena-Wolf et al., 2001). It undergoes a pattern of recycling through the endosome and lysosome, similar to that of CD1c, to facilitate lipid exchange through the activity of saposins, particularly saposin B (Salio et al., 2013, Yuan et al., 2007).

The lipid-binding structure of human CD1d was determined from its crystal structure in the presence and absence of the classical iNKT cell agonist, α-galactosylceramide (αGC) (Koch et al., 2005). Similar to the other CD1 molecules,

it consists of deep channels of hydrophobic residues that bind lipid tails of glycolipids allowing the polar head group to emerge at top of the molecule for TCR recognition. In human CD1d, the channels are termed A' and C' channel, and A' and F' in the mouse. The difference in nomenclature between species stems from the F' channel in human CD1d more closely resembling the C' channel in CD1b than the F' channel in murine CD1d. The A' and C' pockets of human CD1d can bind glycolipids with shorter lipid tails (max 26 and 18 carbons, respectively) than most other CD1 molecules (Koch et al., 2005). The length and chemical composition of the lipid tails can have important consequences on iNKT cell activation, as discussed later.

A combination of high performance liquid chromatography and mass spectrometry techniques has been used to annotate the range of natural lipids that bind human CD1d molecules (Cox et al., 2009). A large number of lipid classes were identified as binding ligands for CD1d. They fell primarily into two groups: (1) glycerophospholipids, including species of lysophospholipids, diacylglycerol, phosphatidic acid (PA), phosphatidylglycerol (PG), phosphatidylserine (PS), phosphatidylinositol (PI), phosphatidylcholine (PC) and phosphatidylethanoline (PE) and (2) sphingolipids, including species sphingomyelin and neutral or acidic glycosphingolipids (GSLs). A commonality between all these CD1d-binding lipids is the presence of two lipid tails to bind in the A' and C' channels and a polar moiety that mediates TCR recognition. Our well-defined understanding of CD1d-binding lipids, and the characteristics of the lipids that impart immunogenicity when

recognized by iNKT cells, has allowed for engineering of synthetic analogues used to modulate iNKT cell activation, which will be discussed later.

In mice, there exists two isoforms of CD1d, CD1d1 and CD1d2 (Bradbury et al., 1988). The CD1d1 isoform dominates CD1d expression in most cells of hematopoietic lineage with the exception of thymocytes, where expression of the two isoforms is almost equal. Analysis of the crystal structure of these two isoforms reveals that CD1d2 slightly deviates from CD1d1 in that the A' channel in CD1d2 cannot accommodate as many carbon units the A' channel in CD1d1 (Sundararaj et al., 2018). The authors postulate that this difference might give preference to the presentation certain self-lipids in the thymus involved in thymic iNKT cell selection. However, CD1d2 alone is not sufficient for positive selection of iNKT cells in the thymus (Chen et al., 1999).

1.3 Lipid antigen-restricted T cells

So-called 'conventional' T cells refer to a pool of T cells expressing diverse, polyclonal αβ TCRs that recognize peptide antigen presented in the context of MHC class I or class II molecules (with exception of HLA-E restricted T cells, which recognize peptide antigen but express semi-invariant TCRs) (Godfrey et al., 2015). However, there exist so-called 'unconventional' αβ T cells, which include iNKT cells and MAIT cells. They are innate-like lymphocytes as they exhibit characteristics of both innate and adaptive immune cells (Godfrey et al., 2015). Their activation is driven by antigen recognition, a characteristic of conventional adaptive immune cells. However, unlike conventional T cells, iNKT and MAIT cells

bear a semi-invariant TCR that recognizes antigens presented on monomorphic CD1d and MR1 molecules, respectively (Godfrey et al., 2015). This recognition manner has been likened to a pattern recognition mode (Jones et al., 2007). They further deviate from conventional T cells by their ability to rapidly secrete copious amounts of cytokines shortly upon activation – a characteristic reminiscent of innate immune responses, and which is imparted at the epigenetic level by their unique developmental program (Beyaz et al., 2017, Coquet et al., 2008, Stetson et al., 2003, Wesley et al., 2008).

CD1a, CD1b and CD1c-restricted T cells are less well characterized than MAIT or iNKT cells, owing in part to the absence of mouse models and difficulties in identifying putative TCR clones that recognize particular lipid ligands. However, the establishment of CD1a, CD1b, and CD1c tetramers has aided this area of research, allowing for a broader sampling of reactive TCRs. This was particularly important in classifying populations of CD1b-restricted T cells reactive against *Mycobacterial* lipids: (1) the GEM T cells, reactive against mycolic acids, with a conserved TRAV1-2 and TRAJ9 TCR (Van Rhijn et al., 2013, Chancellor et al., 2017) and (2) the LDN-5 like T cells with TRBV4-1 usage (Moody et al., 1997).

Apart from αβ T cells, certain γδ T cell subsets can recognize lipids presented on CD1 molecules. γδ T cells that recognize CD1c are reported (Adams, 2013); Vδ1 γδ T cells are known to recognize CD1d presenting αGC and sulfatide (Bai et al., 2012, Uldrich et al., 2013). The γδ TCR recognizes lipid antigens presented on CD1d in a manner distinct from iNKT cells, namely it terms

of docking contact by the CDR3 loop (Uldrich et al., 2013). The functionally consequences of γδ TCR:CD1d interactions are not entirely clear.

The coming chapters will focus on type I NKT cells, or iNKT cells.

1.4 Characterization of iNKT cells

1.4.1 iNKT cell development

iNKT cells follow a similar pattern of thymic development as conventional αβ T cells to the point of becoming $CD4^+CD8^+$ or double positive (DP) thymocytes in the thymic cortex (Gapin, 2008, Bendelac, 1995). While conventional T cells undergo thymic education through TCR interactions with MHC class I and II molecules expressed on cortical thymic epithelial cells, recognition of CD1d molecules on DP thymocytes, with costimulation provided by SLAM receptor signalling, directs other DP thymocytes towards iNKT cell differentiation (Griewank et al., 2007). The pool of selected DP thymocytes features an invariable TCR α-chain. At this point iNKT cell differentiation diverges from that of conventional T cells, as the iNKT-destined DP thymocytes (Stage 0 iNKT cells) express higher levels of the Egr2 transcription factor than required for conventional T cell differentiation (Seiler et al., 2012). Egr2 drives the transcription of *Zbtb16*, the gene encoding the transcription factor PLZF (Dutta et al., 2013). This transcription factor, long considered a hallmark of iNKT cells, instils iNKT cells with the memory-like phenotype they acquired early during ontogeny (Kovalovsky et al., 2008, Savage et al., 2008). Another level of regulation in iNKT cell development stems from epigenetic regulation within DP thymocytes to permit PLZF expression

(Dobenecker et al., 2015). With this transition, the DN or $CD4^{+}PLZF^{hi}$ cells continue to diverge into functional subsets as dictated by the expression of Tbet (iNKT1), Gata3 (iNKT2), and RORγT (iNKT17). These cells eventually exit into the periphery (Gapin, 2016).

There are several unanswered questions relating to thymic iNKT cell development. One surrounds the identity of the self-lipid antigen(s) mediating positive selection. It is thought that the strength of signalling between TCR on DP thymocytes and the lipid in complex with CD1d might in part dictate the functional phenotype of the developing iNKT cell, suggesting that there might be more than one selecting lipid ligands (Gapin, 2016). Isoglobohexosylceramide (iGB3) is a self-lipid antigen that can activate both mouse and human iNKT cells and was a putative selecting lipid during positive selection. However, given the normal development of iNKT cells in mice lacking Gb3-synthase (Porubsky et al., 2012) and the notion that the Gb3 synthase (iGb3S) gene in the human genome appears to be a pseudogene (Taylor et al., 2003) the physiological relevance of iGB3 as the self-lipid antigen involved in thymic selection of iNKT cells or in peripheral activation of iNKT cells remains controversial (Porubsky et al., 2007, Speak et al., 2007). The reported existence of α-linked GSLs in mammals lends itself to the possibility that they might serve of the selecting ligand in iNKT cell development, partially illustrated by the staining of the thymus with antibodies that specifically recognize αGC:CD1d complexes (Kain et al., 2014). However, the existence of α-linked GSLs in mammals is controversial (Lairson et al., 2008).

Another question in iNKT cell development surrounds the factors that drive iNKT cell differentiation into particular functional subsets, beyond TCR signalling. NOTCH signalling (Oh et al., 2015), miRNAs (Fedeli et al., 2009), components of autophagy (Salio et al., 2014, Pei et al., 2015) and chromatin rearrangements are amongst some of the cell intrinsic events that contribute to iNKT cell development and lineage commitment (Gapin, 2016). Surface expression of Slamf8 receptor seems important in balancing the development of iNKT cell subsets, as mice deficient in Slamf8 exhibit a higher proportion of iNKT2 cells (De Calisto et al., 2014). CCR7 expression permits precursor iNKT cells to migrate to the thymic medulla where they fully differentiation into iNKT1s in the presence of IL-15 (Pobezinsky et al., 2015). iNKT17 cell subset maintenance is restricted by the transcription factor Bcl11b (Uddin et al., 2016) and the transcription factor TH-POK, whose expression is epigenetically regulated by miR-133 (Di Pietro et al., 2016, Tsagaratou et al., 2017). These findings illustrate that a variety of cell intrinsic and extrinsic factors, beyond TCR signalling are coordinated for proper iNKT development and functional differentiation.

Under steady-state conditions, circulating human iNKT cells are typically $CD161^{+}CD27^{+}CD28^{+}CD45RO^{high}CD62L^{low}$ (Montoya et al., 2007). There is limited evidence indicating peripheral iNKT cell functional plasticity. Signals from specific tissue niches are likely important to maintain certain subsets of iNKT cells.

1.4.2 Tissue distribution of iNKT cells

Although some iNKT cells are retained in the thymus, most migrate into the periphery, where populations are established in the blood and at a variety of tissue sites. The frequency of human iNKT cells ranges from 0.01 - 0.1% in peripheral blood (far lower than in mice), but this frequency is still orders of magnitude higher than that of naïve peptide-specific T cells (Jenkins et al., 2009). Apart from lymphatic tissues, iNKT cells populate the lungs, intestine, adipose tissue, and most notably, the liver, where in humans iNKT cells constitute about 1% of total lymphocytes (Berzins et al., 2011). Homing to these tissues is likely reflects their expression of CXCR6 (Liew et al., 2017). The proportion of functionally distinct subsets varies at different tissue sites. For example, iNKT1 cells predominate over other subsets in the liver, whereas iNKT2 populations are enriched in the lung, and iNKT2 and 17 can be found in the skin and lymph nodes (Crosby and Kronenberg, 2018). The maintenance of these populations is not predominantly dependent on continued CD1d-TCR signalling, similar to memory T cells. However, cytokines are required for peripheral iNKT cell homeostasis, such as IL-15 for iNKT1 cells (Ranson et al., 2003) and IL-7 for iNKT17 cells (Webster et al., 2014). The role of iNKT cells in maintaining homeostasis or driving pathology varies across tissues, a point which will be discussed later.

There are two iNKT cell subsets that develop in the periphery upon antigenic stimulation: iNKTfh and iNKT10 cells. iNKTfh are found in the germinal centres of the spleen, where they provide B cell ‘help’ in boosting affinity maturation and promote antibody secretion (King et al., 2011, Chang et al., 2011,

Barral et al., 2010). iNKT10 cells, enriched in adipose tissue, are noted for secretion of IL-10, driving their immunoregulatory function (Lynch et al., 2015). Notably this subset does not express PLZF but rather the E4B4 transcription factor, which likely imparts their immunoregulatory activities (Motomura et al., 2011).

1.4.3 The iNKT TCR

Perhaps one of the most striking features of iNKT cells is their semi-invariant TCR, which recognizes a range of lipid agonists presented by CD1d. In the mid-1980s, Taniguchi and colleagues recognized the existence of a T cell population stemming from a murine T cell hybridoma with a predominant TCR α-chain arrangement Vα14Jα18 (Sumida et al., 1984, Imai et al., 1986). This finding was followed by a report of a DN T cell population with preferential TCR β-chain usages in mice (Fowlkes et al., 1987); similar findings were reported later in humans (Porcelli et al., 1993, Dellabona et al., 1994). These observations laid the foundation for the identification of a lymphocyte population expressing natural killer cell markers and a semi-invariant TCR. Later work demonstrated that this TCR recognized antigen presented on CD1d (Bendelac et al., 1995, Exley et al., 1997). Today, the iNKT cell TCR is hallmarked by the expression of an invariant α-chain, either Vα14Jα18 in mice or Vα24Jα18 in humans, paired with a restricted number of β-chains, namely Vβ2, 7, and 8 in mice and Vβ11 in humans. β-chain pairings with the invariant α-chain can bias recognition of different types of lipids presented on CD1d molecules; for example, in mice, iNKT cells bearing a Vβ7 chain make

up the majority of iNKT cells responsive to high affinity GSL presentation, whereas iNKT cells reactive to GSLs with shorter lipid tails, such a OCH, expressed Vβ8 (Cameron et al., 2015). Furthermore, in this study, subtle changes in reactivity were detected across iNKT cells with diversity in the Jβ region, particularly in human iNKT cells.

1.4.4 Type II NKT cells

In addition to type I NKT or iNKT cells, there exist type II NKT cells that similarly recognize lipid antigen in the context of CD1d molecules. Unlike their type I counterparts, type II NKT cell TCRs are not semi-invariant and use a wide repertoire of α and β chains. Type II NKT do not recognize αGC, but other lipids, amongst them sulfatide, a type of sulfated glycolipid, and β-mannosylceramide (Terabe and Berzofsky, 2018). As such, CD1d-sulfatide tetramers are used to better study this cell type. Type II NKT cells are as typified by their immunoregulatory and anti-inflammatory properties upon activation, namely through IL-13 secretion and promoting myeloid-derived TGF-β secretion (Terabe et al., 2000, Terabe et al., 2003). Their activation in a tumour setting promotes pro-tumourigenic responses, particularly with respect to metastases in the lung and liver, where these type II NKT cells are enriched (Terabe and Berzofsky, 2018). Another mechanism by which these cells inhibit anti-tumour immunity is through cross-talk with type I iNKT cells, as illustrated in CT26 lung metastases models where mice co-treated with αGC and sulfatide demonstrated an increase tumour burden compared to αGC-injected mice (Ambrosino et al., 2007). In the liver,

Kumar et al. demonstrated that injection of sulfatide and activation of type II NKT cells reduced conacanavalin A (ConA) hepatic injury mediated by type I iNKT cells (Halder et al., 2007). Knowledge of type II NKT cells, and their role in modulating iNKT cell responses, has implications when using TRAJ18$^{-/-}$ mice, deficient in type I iNKT cells, or CD1d$^{-/-}$ mice, deficient in both types I and II iNKT cells, in *in vivo* studies.

1.5 Activation of iNKT cells

1.5.1 Lipid antigens that activate iNKT cells

iNKT cell responses to CD1d have been best described in the context of foreign infection. In some cases these investigations by have led to the identification of new classes of lipid antigen. Work by Kronenberg and colleagues identified diacylglycerol-based glycolipids from various bacteria, including species of *Sphingomonas*, *Streptococcus*, and *Borrelia burgdorferi,* triggers a protective Th1 and Th17 response (Tupin et al., 2007). APCs exposed to toll-like receptor (TLR) agonists are altered to present more immunogenic self-lipid antigens, in conjunction with IL-12 and IL-18 to augment iNKT cell activation (Montoya et al., 2006, Paget et al., 2007, Salio et al., 2007, Mattner et al., 2005). A subset of lysophospholipids is presented on intestinal epithelial cells upon Hepatitis B virus (HBV) infection activates iNKT cells (Zeissig et al., 2012). CD1d-dependent Th1 and Th2 responses from iNKT cells are reported in other viral infections, such as respiratory syncytial virus and encephalomyocarditis virus (Johnson et al., 2002, Exley et al., 2001). It is unclear in many cases of viral infection whether

immunogenic self-lipids are presented during viral infection, as described by Zeissig et al., or whether activation is mainly driven by cytokines. Like MHC class I, downregulation of CD1d is common in a range of viral infections (Miura et al., 2010), perhaps underscoring the importance of CD1d-dependent iNKT cell activation in anti-viral immune responses.

While the repertoire of activating self-lipid CD1d-restricted antigens presented during sterile inflammation is less well understood, previous studies have broadened our knowledge of the subject. Lysophosphatidylcholine (LPC) has been identified as an activating self-lipid antigen, inducing enhanced GMCSF and IL-13 secretion from iNKT cells, when presented on CD1d molecules (Fox et al., 2009). However, lack of IFN-γ secretion upon recognition of CD1d-LPC complexes perhaps can be accounted for by its low affinity to CD1d (~2μM) (Lopez-Sagaseta et al., 2012). iGB3, as previously discussed, is a murine self-lipid antigen. However, these studies fall short of describing a sterile, physiological context in which these self-lipid antigens would be presented to iNKT cells.

1.5.2 Mechanism of CD1d-dependent iNKT cell activation

The first crystal structure of the iNKT-TCR interacting with αGC:CD1d shed light on the structural mechanics mediated CD1d-dependent activation (Borg et al., 2007, Gadola et al., 2006). Unlike conventional αβ TCR recognition of peptide antigens in MHC class I, where both the TCR α- and β-chains contact the peptide in the groove, the invariant α-chain of the iNKT-TCR makes contact with the sugar moiety that protrudes out of the CD1d cleft, and the β-chain docks at the edge of

the CD1d molecule; this unusual footprint makes sense given wide variety of lipids with a polar head group that drives iNKT cell activation. The CDR3α and CDR2β loops are perhaps most important CD1d-dependent iNKT cell activation, as they make the main contact with the polar head group and the surface α-helices of CD1d, respectively. The CDR3α loop, whose residues correspond with the Jα18 region of the TCR, is responsible for conserved CD1d-lipid recognition (Borg et al., 2007, Li et al., 2010).

The nature of the glycosidic linkage between the fatty acid tails and the sugar moiety in GSLs likely also confers the degree of immunogenicity of lipid antigens. α-linked sugars tend to adopt an ideal conformation for interaction with CDR3α loop, where β-linked sugars are oriented at a sub-optimal angle for this interaction (Sidobre et al., 2004, Wun et al., 2011). Furthermore, the CDR1α and CDR3α loops contact the 2', 3' and 4' hydroxyl group on the carbon ring of the sugar moiety, which explains why galactose rings are typically more stimulatory than their mannose or glucose counterparts (Sidobre et al., 2004, Wun et al., 2011).

While αGC stimulation of iNKT cells is robust, it comes with a drawback. CD1d-mediated iNKT cell activation, particularly with a strong lipid agonist, can readily induce iNKT cell anergy (Silk et al., 2008). In the context of conventional T cells, anergy refers to stimulation of T cells with 'signal 2' and 'signal 3' in the absence of 'signal 1' aka TCR interaction (Sullivan and Kronenberg, 2005). The lack of sufficient signalling imprints impaired T cell function in the form of hypo-responsiveness, termed anergy. Anergic phenotypes are comparable in iNKT

cells, but the mechanism underpinning iNKT cell anergy is distinct – it is a consequence of strong TCR signalling, and can be induced by restimulation with αGC. This deviation from conventional T cells might reflect that iNKT cells express a more limited number of costimulatory receptors (amongst the most dominant is CD40L, which can mediate iNKT-DC crosstalk) (Sullivan and Kronenberg, 2005, Matsuda et al., 2003, Fujii et al., 2004). TCR signalling is necessary and, for some strong ligands, sufficient to induce an initial iNKT cell response – the caveat is that repeated stimulation will induce iNKT anergy (Parekh et al., 2005). Blockade of PD1 reduces anergy of glycolipid-activated iNKT cells in a tumour setting (Parekh et al., 2009).

1.5.3 CD1d-independent modes of activation

iNKT cells can mount responses in a CD1d-independent manner. iNKT cells constitutively express cytokine receptors that correlates with chromatin modifications at the corresponding cytokine loci (Stetson et al., 2003). IL-12 and IL-18 are the best-characterized iNKT cell activating cytokines. In cases where CD1d-TCR engagement is dispensable for driving iNKT cell activation, for example during murine cytomegalovirus infection, DC-derived IL-12 propagates IFN-γ secretion by iNKT cells (Tyznik et al., 2008). In contrast, TLR7 and 9-stimulated Kuppfer cells drive liver-resident iNKT cell activation primarily through secretion of type I interferons, not IL-12 (Paget et al., 2007), suggesting that iNKT cell tissue residency influences cytokine-mediated signalling and activation. iNKT cell activation during *Salmonella typhrimurium* infection, a bacterium which does

not appear to harbour CD1d-bound lipid antigens, drives iNKT cell activation through TLR signalling as well as IL-12 signalling (Brigl et al., 2011).

These cytokines can also boost iNKT cell activation to weak or self-lipid agonists. IL-12 promotes iNKT cell activation to self-lipid antigens on TLR-exposed APCs during microbial infection (Brigl et al., 2011), and IL-18 boosts CD1d-dependent iNKT-cell mediated inflammation during atopic eczema (Lind et al., 2009).

Another CD1d-independent mode of activation stems from the expression of NK receptors on iNKT cells, namely NKG2D. The expression of this receptor is restricted to $CD4^-$ iNKT cells. Like NK cells, engagement of NKG2D on $CD4^-$ iNKT cells with its cognate ligands, including MICA/B, ULBPs etc. triggers perforin and granzyme B release, driving iNKT-cell mediated cytotoxicity (Kuylenstierna et al., 2011). This mechanism contributes to iNKT-cell mediated cytolysis in certain haematological cancers (Wang et al., 2008).

1.5.4 Influence of activated iNKT cells on other immune cells

Endowed with the ability to modulate multiple immune cell subsets, iNKT cells can be critical in shaping immune responses. Activated iNKT cells not only secrete of a variety of cytokines, but also enhance CD40L-dependent maturation of DCs and activation of B cells (Kawakami et al., 2003, Nieuwenhuis et al., 2002, Park et al., 2003, De Santo et al., 2008, Galli et al., 2003, Silk et al., 2004, Hermans et al., 2003). iNKT cell-dependent DC maturation results in increased antigen-specific enhanced $CD4^+$ and $CD8^+$ T cell priming (Hermans et al., 2003,

Fujii et al., 2007), while B cell activation results in enhanced secretion of antibodies and isotype switching (Barral et al., 2008b, King et al., 2011). Activated iNKT cells provide for cognate and non-cognate help to B cells. Cognate help is provided when iNKTfh cells recognize lipid antigen on CD1d molecules of B cells (Lang et al., 2006) whereas non-cognate help stems from the release of cytokines including IL-2, BAFF, and APRIL from iNKTfh cells to promote antibody secretion and plasma cell maintenance (Shah et al., 2013).

Neutrophils can activate iNKT cells and influence their function, for example, by licensing iNKT cells to regulate B cell responses (Hagglof et al., 2016). In turn, activated iNKT cells influence neutrophil recruitment. This has been illustrated in the setting of cystic fibrosis, where iNKT cells with a Th17 profile attract neutrophils and macrophages to the lung (Siegmann et al., 2014), and in murine models of αGC-induced hepatic injury, where IL-4 secretion from activated liver-resident iNKT cells promotes accumulation of neutrophils (Wang et al., 2013). Additionally, IFN-γ secretion from iNKT cells drives transactivation of NK cells (Smyth et al., 2002, Carnaud et al., 1999), which has been implicated in murine tumour clearance (Smyth et al., 2001).

1.6 iNKT cells and the microbiota

The importance of iNKT cells in combatting infection is emphasized by reports of disease progression in patients deficient in iNKT cells. These patients were particularly susceptible to viral infections, including Epstein-Barr and the varicella virus (Levy et al., 2003). iNKT cell numbers are modulated in a variety of

bacterial infections, including *M. tuberculosis* (Kee et al., 2012). While iNKT cells are generally protective against microbial pathogens, as previously described, it begs the question whether similar mechanisms are involved in interactions with microbiota.

iNKT cell interactions with microbiota are primarily studied in the intestine. Microbiota can regulate the nature and quality of iNKT cell responses in the gut (Zeissig and Blumberg, 2013). While conventional αβ T cell numbers are typically reduced in specific pathogen free (SPF) or germ free mice, iNKT cell numbers expand with a lack of commensal bacteria (Wingender et al., 2012). Diversity in the iNKT-TCR usage differed in SPF mice, as reflected in the decreased proportion of $V\beta7^+$ iNKT cells, and iNKT cells were hyporesponsive, particularly with respect to TNFα secretion (Wingender et al., 2012). Microbiota are theorized to shape iNKT cell populations and responses by acting as a source of glycolipid antigens (Iyer et al., 2018) and modulating myeloid cell maturation (Olszak et al., 2014). In turn, IFN-γ secreted from activated iNKT cells acts on Paneth cells in the intestine, altering the secretion of antimicrobial peptides that regulate microbiota composition (Nieuwenhuis et al., 2009, Farin et al., 2014). Furthermore, CD1d presentation on intestinal epithelial cells can polarize iNKT cells to secrete IL-13, which can disrupt barrier integrity (Olszak et al., 2014). On the other hand, retrograde CD1d-signalling in intestinal epithelial cells (Olszak et al., 2014) and lipid presentation by $CD11c^+$ DCs (Saez de Guinoa et al., 2018) maintain intestinal homeostasis. This bidirectional crosstalk between the microbiota and iNKT cells can regulate gut homeostasis.

1.7 iNKT cells in sterile inflammation

1.7.1 Hepatic disease

Under steady-state conditions, hepatic iNKT cells contribute to liver tissue repair through secretion of IL-4 from M2 macrophages and hepatocyte proliferation (Liew et al., 2017). However, there is evidence supporting iNKT cell involvement in sterile hepatic pathologies, including non-alcoholic fatty liver diseases (NAFLD) ranging from mild hepatic steatosis to non-alcoholic steatohepatitis (NASH). Liver pathologies are hallmarked by lipid dysfunction, particularly with respect to triglycerides, which can be induced by high fat or choline-deficient diets in mice (Wu et al., 2012). Increased expression of hepatic CD1d and accumulation of iNKT cells in the liver was also observed during disease progression. This observation was complimented by alanine aminotransferase (ALT) detection in the serum (as a measure of liver injury), increased fibrosis, and progression towards NASH. To bolster these findings, NAFLD pathology was markedly reduced in TRAJ18$^{-/-}$ and CD1d$^{-/-}$ mice (Wu et al., 2012). Furthermore, secretion of IL-13, which contributes to fibrogenesis, was partially derived from iNKT cells (Fichtner-Feigl et al., 2006). ConA murine models of acute hepatitis, where this lectin directly activates iNKT cells to drive immune-mediated liver damage, show a similar pathology to NAFLD (Zeissig et al., 2017). In humans, increased liver iNKT cell numbers are correlated with increased cirrhosis and liver damage (Syn et al., 2010).

1.7.2 Obesity and metabolic disorders

iNKT cells associated with adipose tissue are largely of a Th2 and regulatory phenotype. Studies on the role of adipose-resident iNKT cells revealed that they help maintain adipose tissue homeostasis and confer resistance against metabolic dysregulation and inflammation induced by high fat, high sugar diets (Lynch et al., 2015, Schipper et al., 2012). This finding complimented the observation that iNKT cell numbers, both circulating and in adipose tissues, were decreased in obese individuals and leptin-deficient mice, a phenotype that could be reversed upon weight loss (Lynch et al., 2012). Furthermore, absence of iNKT cells in mouse models resulted in the accumulation of pro-inflammatory or M1 macrophages that contribute to metabolic syndrome, whereas adoptive transfer of iNKT cells in these mice restored homeostasis, which could be further improved upon αGC-mediated activation (Lynch et al., 2012). Along these lines, glucagon-like peptide 1, a gut hormone that regulates glycaemia and satiety and promotes weight loss, can activate iNKT cells to protect against pathogenic inflammation and consequent metabolic dysfunction (Lynch et al., 2016). In contrast to these findings, activated iNKT cells in murine models of obesity are reported to take on a pro-inflammatory phenotype, promoting hepatic disease and insulin resistance (Wu et al., 2012).

1.7.3 Allergies and autoimmune diseases

The role of iNKT cells in allergies and asthma remains somewhat controversial. Intranasal αGC administration induces acute lung inflammation,

which when coupled with intranasal administration of ovalbumin, boosted an asthma-like Th2 response and increased eosinophilia, an effect that was reversed in CD1d$^{-/-}$ mice (Nie et al., 2015). iNKT cell activation can exacerbate inflammation to other environmental antigens, such as house dust mite extract (Wingender et al., 2011). However, other studies point to the irrelevance of iNKT cells in allergic asthmatic responses in both mouse models (McKnight et al., 2017) and human disease (Vijayanand et al., 2007).

Numerous studies have provided insights into the involvement of iNKT cells in rheumatic disease, namely arthritis. However, the nature of iNKT cell activation and disease context dictates whether iNKT-cell induced inflammation is protective or harmful (Coppieters et al., 2007). Research into the biology and mechanisms of iNKT cells in arthritis mirrors the complexity of the situation. Mutations in the crucial TCR signalling transducer, Zap70, influence thymic development of iNKT cells, likely by modulating TCR signalling strength during selection, resulting in an altered proportion of iNKT cell functional subsets (Zhao et al., 2018). The results of this study suggested that iNKT1 cells are expanded in mice bearing hypoactive Zap70, and that expanded iNKT1 cells in the synovial fluid are protective against arthritis as opposed to the iNKT17 subset (Zhao et al., 2018). The biases in iNKT-TCR repertoire in rheumatoid arthritis influence Th polarizations during disease progression, as proliferative capacity of high-affinity TCR clones was reduced in early disease compared to controls and the functionality of the clones was shifted towards a Th2 profile (Mansour et al., 2015). More work is required to clarify the role of iNKT cells in rheumatoid arthritis.

In models of multiple sclerosis (MS), namely experimental autoimmune encephalomyelitis (EAE) mouse models, the repeated subcutaneous or intraperitoneal injection of αGC with the MS-related autoantigen myelin oligodendrocyte glycoprotein (MOG) induced protective immune responses, where iNKT cell acts as cellular adjuvants and secrete IL-4 (Singh et al., 2001). Building on this result, co-injection of MOG with OCH further improved protection against EAE, suggesting that biasing the iNKT cell response towards Th2 phenotype shifts Th1 autoimmune responses driving MS pathologies towards a Th2 profile, thus ameliorating the disease (Miyamoto et al., 2001).

iNKT cells activated by αGC are effective at ameliorating other autoimmune pathologies, including Type 1 diabetes. Analysis of NOD CD1d$^{-/-}$ mice illustrated that IL-4 secretion from activated iNKT cells was protective in Type 1 diabetes development (Hong et al., 2001, Sharif et al., 2001).

1.7.4 Cancer

The ability of iNKT cells to orchestrate immune responses against cancer is perhaps the most striking example of their role in disease. Work from the lab led by Dale Godfrey highlighted the essential role for iNKT cells in tumour immunity by demonstrating that mice lacking iNKT cells were more susceptible to methylcolanthrene-induced sarcomas, consistent with the role of iNKT cells in immunosurveillance (Crowe et al., 2002). This effect was reversed upon iNKT cell reconstitution, an observation that further supports their role in tumour clearance. Although the anti-tumour effector activity of iNKT cells upon αGC injection was

recently confirmed using newly generated Jα18 deficient mice ($TRAJ18^{-/-}$), which bear an otherwise normal T cell repertoire (Dashtsoodol et al., 2016), the role of iNKT cells in immunosurveillance of methylcholanthrene-induced sarcomas was called into question in a separate study (Kammertoens et al., 2012).

iNKT cells' ability to modulate various immune subsets is key to their role in anti-tumour immune responses. iNKT cells can mature DCs, activate $CD4^+$ T cells, $CD8^+$ T cells and B cells, and transactivate NK cells (Hermans et al., 2003, Fujii et al., 2003). In murine models of lung and liver cancers, the anti-tumour effect of αGC administration was attributed to IFN-γ secretion from iNKT cells and transactivated NK cells, which culminated in NK perforin-mediated cytolysis of tumour cells (Fujii et al., 2003). iNKT cell-derived IFN-γ is also responsible for enhanced activation of tumour antigen-specific $CD8^+$ T cells (Moreno et al., 2008, Hermans et al., 2003, Silk et al., 2004). Additionally IL-12 derived from iNKT cell-matured DCs helps priming of tumour antigen-specific T cells (Hermans et al., 2003, Fujii et al., 2007).

iNKT cells can also augment an anti-tumour response by diminishing the immunosuppressive activities of immune subsets that promote tumourigenesis. It has been shown that iNKT cells can have a profound effect on the number and function of pro-tumourigenic myeloid populations (De Santo et al., 2010, Song et al., 2009, De Santo et al., 2008). Tumour associated macrophages (TAMs), which secrete immunosuppressive molecules such as IL-6 and TGF-β that dampen T-cell responses to MHC-presented tumour antigen, are found in the tumour microenvironment of a variety of cancers, including renal cell carcinomas and

neuroblastoma (Song et al., 2009). In primary human neuroblastoma samples, iNKT cells specifically killed the tumour-antigen-loaded TAMs rather than neuroblastoma cells, in part relieving the immunosuppressive tumour microenvironment and limiting metastases (Song et al., 2009). iNKT cells are also capable of reducing myeloid-derived suppresser cell (MDSC) numbers and immunosuppressive activity (De Santo et al., 2010, De Santo et al., 2008). These findings beg the question of how iNKT cells remain unaffected by the immunosuppressive microenvironment. It is reported that in patients with head and neck cancer, iNKT cells, unlike conventional T cells, are resistant to hydrogen peroxide produced by $CD15^+$ MDSCs (Liu et al., 2012). This observation potentially explains their persistent activation and cytotoxic activity within an immunosuppressive tumour microenvironment.

While iNKT cells are best known to potentiate their anti-tumour effect through enhancing the immunogenic activities of a variety of immune cell subsets, they are capable themselves of recognizing and killing $CD1d^+$ tumour cells. Such is true for the EL4 T-cell lymphoma model, where both *in vitro* and *in vivo* iNKT cells directly executed perforin-mediated cytolysis of lymphoma cells in a CD1d-dependent manner (Gorini et al., 2017, Bassiri et al., 2014). Furthermore, in a TRAMP murine model of $CD1d^+$ prostate cancer iNKT cells directly and predominantly reduce tumourigenesis, to a greater extent than cytotoxic T lymphocytes (Bellone et al., 2010). In addition, in naturally expressing $CD1d^+$ human osteosarcoma cell lines, iNKT cells selectively killed the tumour cells through Fas-FasL interaction, while leaving co-cultured $CD1d^-$ osteoclasts and

$CD1d^+$ mesenchymal stem cells unaffected (Fallarini et al., 2012). Glioma and breast cancer cell lines transduced with CD1d enabled iNKT cells to lyse the tumour cells (Dhodapkar et al., 2004, Hix et al., 2011). These results collectively indicate that iNKT cells are capable of directly killing $CD1d^+$ tumours. In cases where tumours are $CD1d^-$, tumour-infiltrating $CD1d^+$ myeloid populations might activate iNKT cells either within the tumour or in distal lymphoid tissues enriched in iNKT cells.

1.8 iNKT cells as a therapeutic target

iNKT cells have been implicated in a variety of pathologies, but their manipulation has proven particularly useful in sterile pathologies. Most studies have mainly focused on the adjuvant behaviour of iNKT cells and efficient methods of αGC delivery, often in combination with tumour antigens, to trigger an all-encompassing immune response against the cancer. On the other hand, lipid antigen can be manipulated to drive iNKT cell responses that resolve certain damaging autoimmunity. More recent studies have focused on incorporating iNKT cells in new, promising cancer immunotherapies.

While αGC is a naturally occurring iNKT cell agonist, to enhance the adjuvant effect of iNKT cells in cancer, there is a focus on identifying stronger iNKT cell agonists, either by modifying αGC or identifying novel molecules based on medicinal chemistry programs. Such efforts are supported by the structural knowledge of CD1d bound to αGC and of the iNKT-TCR either in isolation or during cognate interaction with CD1d-lipid complexes (Koch et al., 2005, Gadola et

al., 2006). In screening a panel of αGC analogues for enhanced iNKT cell activation, glycolipids that produce a strong Th1 response from iNKT cells tend to feature an aromatic ring (or, more specifically, a phenyl ring) within their acyl tails; their consequent iNKT-cell activation can be stronger than with αGC *in vitro* (Hung et al., 2017, Chang et al., 2007, Aspeslagh et al., 2011, Huang et al., 2014). Several of these analogues are able to induce a stronger and prolonged anti-tumour immune response in *in vivo* models of lung and breast cancer (Chang et al., 2007). Importantly, these phenyl-analogues, unlike αGC, do not induce either iNKT cell anergy or MDSC recruitment, thought to be due to alarmin release from iNKT-targeted cells (Huang et al., 2014). The synthetic glycolipid ABX196, based upon the structure of αGC, is currently entering clinical trials as a vaccine adjuvant (Tefit et al., 2014).

Another factor to consider in investigating new or modified stimulatory glycolipids is the stability of the CD1d-lipid complex for prolonged signalling. αGC analogues that feature the aromatic ring as discussed above trigger a more stable induced fit within the CD1d cleft due to anchoring of the aromatic ring in addition to conventional anchoring of the hydrophobic tails (Wu et al., 2011, Aspeslagh et al., 2011). The affinity and avidity of the CD1d-phenyl analogue complexes might also be factor in their enhanced Th1 polarizing effect, as suggested by their lower Kd values (Wu et al., 2011, Aspeslagh et al., 2011).

Avidity might play a more important role in iNKT cell activation than previously considered, especially iNKT cell activation by self-lipid antigen repertoire. Alterations in the actin cytoskeleton are evidenced to create CD1d

nanoclusters of higher avidity, increasing basal iNKT autoreactivity (Torreno-Pina et al., 2016).

Since the polar head group of CD1d-bound lipids is key for recognition by the iNKT-TCR, cellular enzymes that might either catabolize some iNKT-cell agonists or redirect them away from lipid-antigen presentation pathways might in part drive sub-optimal iNKT cell responses. This observation coupled with a deficiency of iNKT cell agonists has fuelled work that led to the identification of a novel class of iNKT cell agonists, based on modifications of αGC, that possess non-carbohydrate structures as the hydrophilic head of the ceramide residue (Tashiro et al., 2010). One of these compounds, threitolceramide (ThrCer), is very efficient in augmenting antigen-specific T cell responses and minimizing iNKT cell over-stimulation and iNKT cell-dependent DC lysis, is capable of rectifying the deficiencies of αGC (Silk et al., 2008). This second generation of iNKT cell agonists provides a series of compounds amenable to medicinal chemistry optimization, including the recently characterized compound IMM60, which today is on the of the strongest iNKT cell agonists (Jukes et al., 2016). Given that the coupling of iNKT cell agonists with PLGA-nanoparticles enhances their immune adjuvant potential by orders of magnitude (Dolen et al., 2016), a phase I clinical trial in ovarian cancer and prostate cancer patients will be carried out with IMM60 conjugated to PLGA-nanoparticles with NY-ESO-1 full length protein.

Efficient delivery of potent lipid iNKT cell agonists is essential in manipulating the adjuvant effects of iNKT cells. Optimizing delivery methods and combining the stimulatory lipid with tumour-specific antigens are critical to

ensuring that the adjuvanted immune response is targeted predominantly towards the tumour. In that vein, the use of exosomes as a means of co-delivering αGC and ovalbumin has proved highly successful in reducing the tumour burden and increasing survival in mice inoculated with OVA-expressing melanoma compared with injection of soluble αGC and OVA together (Gehrmann et al., 2013). Since exosomes naturally bear surface markers to direct them to a particular destination, - and for this reason are utilized by breast cancer cells themselves to create a 'metastatic niche' at a location of future metastasis (Hoshino et al., 2015) - they make excellent conduits for delivery of this potential 'cancer vaccine' directly to the tumour site, whilst perhaps protecting the contents from degradation during delivery. Synthetic nanoparticle delivery systems also hold great promise. Similar to exosomes, delivery of αGC or TLR 3 and 7/8 agonists polyI:C and R848, and OVA in biodegradable poly (lactic-co-glycolic acid) nanoparticles proved efficient in stimulating $CD8^+$ antigen-specific T cell responses against OVA-B16 independent of $CD4^+$ T cell help (Dolen et al., 2016). Encapsulation of the contents was essential, as injection of a mixture of αGC, TLR ligands, and OVA did not induce a comparable anti-tumour T cell response (Dolen et al., 2016).

The recent emergence of monoclonal antibody therapies to checkpoint regulators has revolutionized the field of cancer immunotherapy, particularly antibodies targeting the PD1-PD1L axis and CTLA4. While these therapies are studied predominantly in the context of $CD8^+$ cytotoxic T cells, iNKT cells are not exempt from their influence. Much like conventional T cells, iNKT cells upregulate PD1 on their cell surface upon activation as means of eventually resolving the

immune response (Durgan et al., 2011). Blockade of PD1 using anti-PD1 antibodies injected simultaneously with αGC results in iNKT cell activation but prevents iNKT cell anergy, a common occurrence after potent αGC stimulation (Durgan et al., 2011). In fact, blockade of PD1 during αGC -mediated iNKT cell activation in a B16 melanoma mouse model lead to a persistent anti-metastatic immune response (Durgan et al., 2011).

Another emerging T cell-based cancer immunotherapy centres on the chimeric antigen receptor (CAR) T cell therapy. CAR T cell therapy works on the principle that genetically engineered $CD8^+$ T cells expressing TCRs specific for a tumour antigen fused to their native CD3 domain or modified with the endodomain of a co-stimulatory molecule can become activated and expand into a population of tumour specific $CD8^+$ cytotoxic T cells (Fesnak et al., 2016). This approach has recently been applied to iNKT cells (Heczey et al., 2014). A CAR specific for GD2 ganglioside, an abundant neuroblastoma antigen, was expressed in primary human iNKT cells (Heczey et al., 2014). CAR.GD2 iNKT cells took on a Th1 profile and localized directly in the tumour site when transplanted in NSG. CAR.GD2 iNKT cells were highly cytotoxic against neuroblastoma cells, and when fused with CD28 and 41BB endodomains, increased long-term survival in a murine model of the disease (Heczey et al., 2014). With conventional T cells, a frequent adverse effect of CAR therapy in NSG mice is that adoptive transfer of the engineered T cells can induce graft-versus-host disease (GVHD) (Heczey et al., 2014). However, there is no evidence of GVHD in *in vivo* models utilizing CAR.GD2 iNKT cells (Heczey et al., 2014). For this reason, CAR iNKT cells might become an

alternative to conventional T cells as vectors for CAR therapy. So far, however, CAR iNKT cell therapy has not been translated into clinical trials due to a poor understanding of the mechanisms underlying their *in vivo* proliferation and persistence (Tian et al., 2016). There have been no clear markers to differentiate effector and memory iNKT cells. Recently, a subset of iNKT cells that express the adhesion marker CD62L (also found in naïve and central memory T cells) has been identified (Tian et al., 2016). As expected, this population rapidly expands and can persist upon stimulation. In iNKT cells transduced to express a CD19.CAR, it was the $CD62L^+$ population that achieved persistent activation and proliferation *in vivo*, and was responsible for lymphoma and neuroblastoma regression (Tian et al., 2016).

Clinical trials utilizing iNKT cell-based therapy have underscored their role and therapeutic promise as an immunotherapeutic target in cancer. Clinical trials in which MoDCs pulsed with αGC were injected into patients show improved clinical responses, with limited adverse effects, compared to those receiving injection with αGC alone. Phase I clinical trials involving patients with lung cancer demonstrated that injection αGC-pulsed DCs results in an increase in IFN-γ producing cells and prolonged patient survival (Takami, 2018). In a similar trial involving patients with head and neck squamous cell carcinoma, the accumulation of iNKT cells around the tumour correlated with objective clinical responses (Takami, 2018). Furthermore, multiple myeloma patients receiving three cycles αGC-pulsed DCs in combination with lenalidomide exhibited a degree of tumour regression that correlated with increased endogenous iNKT cells activation

(Richter, 2013). Future clinical work building on these studies extends to injection of modified αGC-based agonists such as IMM60 (results unpublished) as well as adoptive iNKT cell therapy in melanoma patients (Exley, 2017).

1.9 iNKT cells versus MAIT cells

Mucosal-associated invariant T cells, or MAIT cells, are a population of innate-like lymphocyte that closely resembles iNKT cells. Both recognize non-peptide antigens (MAIT cell recognize riboflavin metabolites) in the context of monomorphic MHC class I-like molecules (MR1 for MAIT cells) using a limited diversity of semi-invariant TCRs (Kurioka et al., 2016). Recognition of riboflavin-derived antigens or cytokine-mediated stimulation induces an innate-like response similar to that of iNKT cells (van Wilgenburg et al., 2016), hallmarked by rapidly acquired effector functions and cytokine secretion (Kurioka et al., 2016) . Furthermore, like iNKT cells, activated MAIT cells can enhance maturation of APCs through CD40:CD40L interactions (Salio et al., 2017). Given their similarities, it is tempting to speculate that iNKT and MAIT cells play redundant roles. However, distinct characteristics of each cell type support the notion that they have overlapping but individual roles in immunity.

MAIT cell frequency in mice and humans differ from that of iNKT cells. In humans, MAIT cells are far more abundant that iNKT cells in the blood (up to 10% versus 0.1% of circulating lymphocytes), whereas iNKT cells are far more abundant in mice (Kurioka et al., 2016). Thymic development (Koay et al., 2016) and human tissue distribution (Salou et al., 2019) of both cell types is comparable,

particularly with respect to enrichment in the liver. MAIT cells express the transcription factor PLZF, but due to their dichotomous expression of Tbet or RORγt, they only differentiate into Th1 or TH17 phenotypes (Rahimpour et al., 2015, Salou et al., 2019). They bear semi-invariant TCRs that, like iNKT cells, stem from a relatively constant α-chain usage (TRAV1-2/TRAJ33/12/20) (Reantragoon et al., 2013) with a limited repertoire of β-chains (Lepore et al., 2014). MAIT cells require similar stimulatory signals to iNKT cells for activation, with the exception of IL-18 as the predominant stimulatory cytokine in MAIT cell activation (IL-12 is predominant in iNKT cell activation) (Brigl et al., 2011). It follows that MAIT cells similarly express the surface markers CD161 and CD44 (to reflect their effector memory phenotype) and CXCR6 (to reflect their homing to the liver) but differ from iNKT cells in their constitutive expression of IL-18R (Kurioka et al., 2016). In contrast to iNKT cells, the majority of MAIT cells are $CD8^+$ with a portion being double negative, and a small percentage being $CD4^+$ (Gherardin et al., 2018).

Peripheral MAIT cell activation and expansion appears to be driven by the presentation of riboflavin metabolites from the vitamin B2 synthetic pathway (Kjer-Nielsen et al., 2012). Many of the enzymes involved in the generation of these MAIT cell agonists exist in a variety of bacteria and yeast species, including *S. typhimurium*, *E. coli*, *P. aeruginosa*, *K. pneumoniae*, *M. tuberculosis*, *C. albicans*, and *S. cerevisiae* (Corbett et al., 2014). Interestingly, bacteria that lack the enzymes required for synthesis of the riboflavin-derived agonists, including species of *Streptococcus* and *Listeria*, fail to activate MAIT cells (Corbett et al.,

2014). This observation is consistent with notion that MAIT cells primarily exert anti-microbial immune responses against pathogens while maintaining homeostasis with the microbiota (Dias et al., 2017).

The development of MR1-tetramers now opens the field of MAIT research to address some unanswered questions surrounding their thymic positive selection and their interactions with the microbiota, to name a few. In seeking answers to these questions, we will understand more about MAIT cell biology and how this population converges or diverges phenotypically from iNKT cells.

1.10 Overview of ER-stress and the Unfolded Protein Response

The endoplasmic reticulum (ER) is a large, dynamic organelle consisting of a network of undulating membranes. The ER can be described as ‘smooth’ or ‘rough’ depending on the presences of ribosomes on its cytoplasmic surface. As the ribosome translates mRNA into peptides, the nascent peptides are translocated in the ER lumen where the ER exerts its primary function – to properly fold nascent proteins into functional protein that eventually either translocate into the appropriate intracellular compartment or are secreted into the extracellular space (Bettigole and Glimcher, 2015). The process of protein folding is aided by chaperones, which recognize and bind strings of hydrophobic residues (Koldewey et al., 2016). Chaperones can be classified as foldases, holdases, and disaggregases, with the former and latter types requiring ATP hydrolysis to function (Mattoo and Goloubinoff, 2014). Additionally, the ER functions to maintain intracellular homeostasis by regulating both ion flux into the cytosol and lipid

metabolism (Bettigole and Glimcher, 2015). In order to carry out its activities, the ER must maintain a specific set of subcellular conditions. Therefore perturbations to the ER homeostasis can induce ER-stress. The main consequences of ER-stress is the inability to (1) maintain an adequate rate of folding of nascent unfolded proteins and (2) target misfolded proteins, primarily through ubiquination, for proteasomal degradation (Bettigole and Glimcher, 2015). The accumulation of unfolded or misfolded proteins in the lumen induces the unfolded protein response (UPR).

The UPR consists of three individual yet intersecting pathways aimed at relieving the protein burden and restoring ER homeostasis. They are inositol requiring enzyme 1 (IRE1), PKR-like endoplasmic reticulum kinase (PERK), and activating transcription pathway 6 (ATF6), each named for the three initiating sensors in ER lumen. In steady state conditions, the chaperone binding immunoglobulin protein (BiP) binds to the luminal domains of these three sensors, rendering them inactive in a monomer configuration (Amin-Wetzel et al., 2017). However, when there is an increased protein burden in the ER, BiP, which is a chaperone, has a higher affinity for unfolded polypeptides and preferentially binds them, thereby unleashing the three pathways of the UPR (Amin-Wetzel et al., 2017).

1.11 Sources of ER-stress that trigger the UPR

1.11.1 ER-stress and UPR inducing reagents

While there are multiple reagents used to induce ER-stress through different mechanisms of action, two of the best-studied reagents are (1) thapsigargin, a plant-based sesquiterpene lactone, and (2) tunicamycin, a fungus-derived antibiotic (**Figure 1.1**). Thapsigargin induces ER-stress by blocking the activity of the sarcoendoplasmic reticulum Ca^{2+} ATPase (SERCA) pump. SERCA pumps calcium ions (Ca^{2+}) from the cytosol into the ER, where they serve as important cofactors for functional chaperones. When SERCA pumps are non-competitively inhibited by thapsigargin, the low concentration of calcium ions in the ER prevents chaperone from functioning properly, leading to an accumulation of misfolded proteins. Tunicamycin induces ER-stress by a different mechanism – it inhibits UDP-HexNAc: polyprenol-P HexNAc-1-P family of enzymes, including GlcNAc phosphotransferase, which catalyses the transfer of N-acetylglucosamine-1-phosphate from UDP-N-acetylglucosamine to dolichol phosphate in the first step of glycoprotein synthesis (Reiling et al., 2011). This blockade of N-linked glycosylation prevents correct folding and secretion of proteins from the ER, inducing the UPR. Though dosing, length of treatment, and the cell type affect the ER-stress response upon exposure to these drugs, the response is general rapid and sustained given that both reagents are irreversible. Another common ER-stress-inducing reagent is 2-deoxy-D-glucose, which inhibits glycolysis, in turn driving oxidative stress and depleting certain sugar molecules available for protein glycosylation (Yu and Kim, 2010). Certain chemotherapeutic agents, particularly

platinum-based ones such as cisplatin, operate through induction of immunogenic cell death (ICD) induced overwhelming ER-stress in target cells (Mandic et al., 2003).

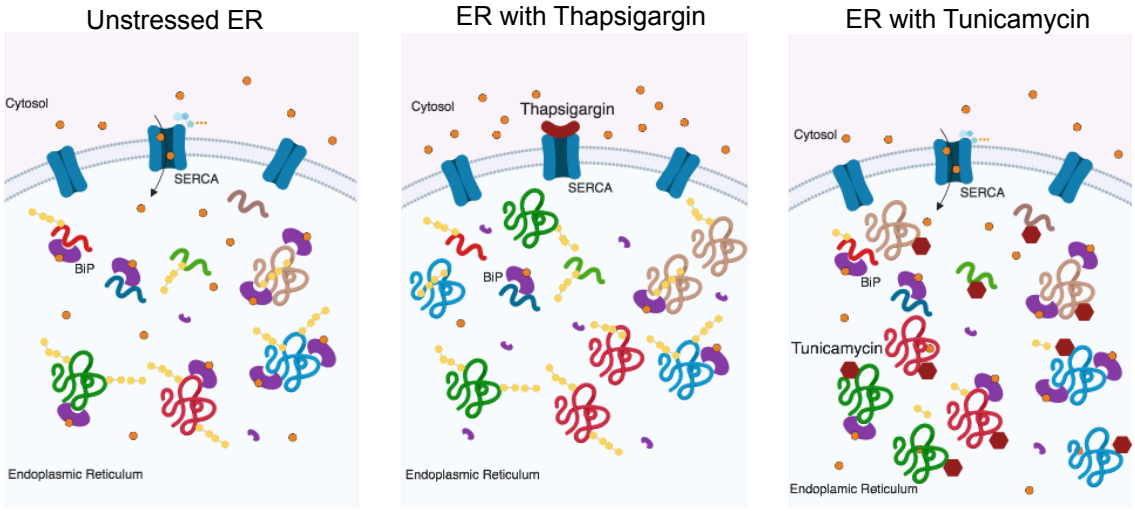

Figure 1.1 The mechanisms of action of thapsigargin and tunicamycin. In the ER of an unstressed cell (left), functional chaperones (large, purple) bind Ca^{2+} ions (orange) as cofactors and attempt to fold polypeptides, some of which are glycosylated (yellow). Thapsigargin blocks the SERCA pump, depleting ER Ca^{2+} stores to block chaperone activity leading to an accumulation of misfolded proteins (centre). Tunicamycin blocks N-linked glycosylation, preventing proper folding and egress from the ER (right).

One of the main issues surrounding the use the ER-stress inducing agents is their off-target effects which might give rise to a phenotype unrelated to the UPR. As such, the recent discovery of the SubAB5 toxin, resolves this issue, as it specifically induces the UPR in the absence of off-target effects. This toxin, isolated from a strain of Shiga-toxigenic *E. coli* specifically cleaves the ER chaperone and master regulator of the UPR, BiP, near the C-terminal domain of the protein (Paton et al., 2006), as shown in **Figure 1.2**. An inactive version of the toxin, which differs from the wild type toxin only in a single amino acid in the catalytic cleft to prevent BiP cleavage (Paton et al., 2006). These sorts of reagents are invaluable, as they uncouple real UPR responses and off-target effects.

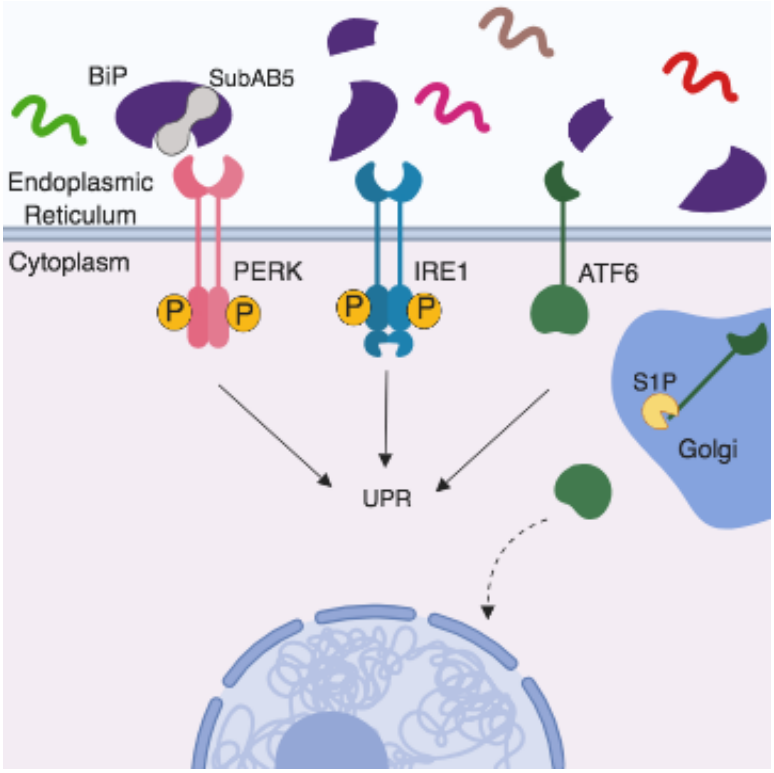

Figure 1.2 The mechanism of action of the SubAB5 toxin. The SubAB5 toxin (grey) cleaves BiP, creating two distinct fragments and preventing binding to the sensors of UPR, unleashing the three pathways.

1.11.2 Physiological Drivers of ER-stress and the UPR

1.11.2.1 Cell intrinsic

Reactive Oxygen Species (ROS)

ROS are formed as by-products of cellular oxygen metabolism and/or produced by NADPH oxidase and have pleotropic effects on cellular homeostasis (Nguyen et al., 2017). They are positively utilized in phagocytes, including macrophages and neutrophils, for 'oxidative bursts' to kill phagocytized or intracellular pathogens (Nguyen et al., 2017). However, inappropriate ROS production or failed sequestration can result in oxidative damage and stress. The 'redoxisome', consisting of membrane contacts between the mitochondria, peroxisomes, and ER, is recently reported to sense cellular ROS levels and is the site of redox

regulation between the organelles (Yoboue et al., 2018). The ER is particularly sensitive to this stress, as particular redox conditions are required for proper BiP and protein disulfide isomerases (PDI) function. BiP and PDI are redox-sensitive chaperones that must maintain a specific redox state to carry out their folding activity (Xu et al., 2016a, Wang and Sevier, 2016, Kranz et al., 2017). Furthermore, the redox status of thiol groups in cysteine residues acts as a barometer for sufficient protein folding (Ellgaard et al., 2018). While the subcellular environment in ER tends to be more oxidizing than that of the cytosol, the ability to discriminate highly oxidized, unfolded proteins versus more reduced, properly folded ones for export is crucial for ER-homeostasis (Ellgaard et al., 2018). Aberrant ROS production and subcellular compartmentalization is implicated in a number of pathologies related to ischemia and mitochondrial dysfunctions (Holmstrom and Finkel, 2014), and ROS accumulation has been associated with aging (Reichmann et al., 2018).

Lipid disequilibrium

The relationship between ER-stress and lipid metabolism is bidirectional. While ER-stress can modulate lipid biosynthesis in a protective manner, modified lipids and dysregulated lipid metabolism can trigger the UPR (Bettigole and Glimcher, 2015). Aberrant lipid composition, often stemming from increased saturated lipids of the ER membrane, gives rise to lipid bilayer stress, which activates the UPR (Volmer et al., 2013). Attenuation of phosphatidylcholine synthesis in *C. elegans* drives IRE1 activation resulting in lipid droplet accumulation and initiation of autophagy (Koh et al., 2018, Hou et al., 2014).

Accumulation of peroxidized lipids jeopardizes membrane integrity, which can trigger lipid bilayer stress (Catala, 2014).

Genetic predisposition

ER-stress can stem from a variety of pathologies, but **Table 1.3** specifies several human diseases in which the pathology is conferred, at least in part, by mutations that specific affect the UPR.

Disease	*Gene*	*Mutation*	*Affected tissue*	*Effect on UPR*	*Pathology*
Inflammatory Bowel Disease (Grootjans et al., 2016)	*XBP1* *ATG16L1* *ORMDL3*	SNP-hypomorphic variant	Intestine	Loss of UPR transcription factor Impaired autophagy in response to PERK Altered ER Ca^{2+}	Spontaneous enteritis, increased susceptibility to colitis
Cystic fibrosis (Ntimbane et al., 2009)	*CFTR*	Frameshift, ΔF508	Lung	Protein misfold and ER-retention	Mucus buildup, lung inflammation, pancreatitis
Wolcott-Rallison Syndrome (Julier and Nicolino, 2010)	*EIF2AK3* (PERK)	Various, loss of function	Pancreas, bone, liver	Loss of UPR pathway	Early-onset diabetes, skeletal dysplasia, liver failure
α1 anti-trypsin syndrome (Greene and McElvaney, 2010)	*SerpinA1*	SNP - Glu342Lys	Liver and lung	Misfolding and aggregation of protein	Hepatitis and cirrhosis, COPD

Table 1.3 Diseases with a genetic predisposition to ER-stress. Human diseases where mutations that alter UPR signalling are directly implicated in pathology.

1.11.2.2 Cell extrinsic

At steady-state most cells in the body are equipped to function within a certain range of external stress that triggers the UPR. However, malignant cells

often bear mutations that allow them to survive with a high ER-stress burden that would otherwise trigger apoptosis (Cubillos-Ruiz et al., 2017). This trait combined with their high proliferative potential drives abnormal consumption of glucose, oxygen, and nutrients from the extracellular milieu (Cubillos-Ruiz et al., 2017). Although they are typically less sensitive to ER-stress in this suboptimal environment, other untransformed cells in the tumour microenvironment are more susceptible to strong ER-stress responses in this environment (Cubillos-Ruiz et al., 2017). These microenvironmental sources of ER-stress are not restricted to cancer settings, but are best characterized in this context.

Hypoxia and glucose deprivation

Hypoxic cells switch from oxidative phosphorylation to glycolysis to generate ATP, at the expense of large amounts of glucose. A deficiency in glucose interferes with N-linked glycosylation of nascent proteins, as it disrupts equilibrium in the conversion of glucose into UDP-GlcNAc (Wang et al., 2014). One of the proteins implicated in this pathway, GFAT1, is upregulated by sXBP1-mediated transcription due glycolytic stress (Denzel et al., 2014, Wang et al., 2014). The metabolic shift to glycolysis can also alter ROS and redox conditions in the cell, inducing oxidative stress and UPR activation (Yu et al., 2017). The interplay between hypoxic and glycolytic responses and the UPR synergizes transcription of VEGFα through cooperation between HIF1-α and ATF4 transcription factors (Pereira et al., 2014). In tumours, the PERK signalling confers an advantage in hypoxic stress (Pereira et al., 2014). Indeed eIF2α phosphorylation under hypoxic

conditions is PERK-dependent. However, the exact mechanisms underpinning hypoxia-induced UPR remain unclear.

Amino acid deprivation

Amino acids can be classified as essential, conditionally essential, and non-essential. Non-essential amino acids can be readily synthesize by cells, whereas maintenance of sufficient cellular levels of essential and conditionally essential amino acid relies on amino acid transport across cellular membranes (Timosenko et al., 2017, Timosenko et al., 2016). A deficiency in amino acids results in a failure to incorporate specific amino acids during translation of nascent peptides (Mazor et al., 2018). In turn, the altered pattern of hydrophilic and hydrophobic residues crucial for chaperone recognition might jeopardize protein folding in the ER (Koldewey et al., 2016).

The General Control Non-derepressible 2 (GCN2) is the primary cellular sensor for a deficiency in intracellular amino acids. When tRNAs are covalently linked to their specific amino acid, they are aminoacylated or ‘charged’. GCN2 is a kinase that can be activated through a conformational change when binding ‘uncharged’ tRNAs, or tRNAs lacking an amino acid load. Activation of GCN2 results in the phosphorylation of eIF2α and triggering of the ISRE. Consequently, protein translation is suppressed and in parallel ATF4 induction can enhance the expression of amino acid transporters (Timosenko et al., 2016) to replenish cellular stores.

1.12 The three branches of the UPR

1.12.1 IRE1

The IRE1 pathway is the most evolutionarily conserved pathway of the UPR, existing in both higher and lower eukaryotes, including unicellular organisms such as yeast (Mori, 2009). The sensor is a transmembrane protein consisting of two important cytosolic domains: and serine/threonine kinase and an endoribonuclease (Bettigole and Glimcher, 2015). Upon BiP unbinding from the ER lumen, the IRE1 monomers dimerize, activating the kinase domains. Autophosphorylation of the serine/threonine kinases on the dimer activates the C-terminal endoribonuclease domain, which splices specific substrates, in particular the mRNA XBP1. Full length, unspliced XBP1 mRNA is transcribed by the ATF6 transcription factor (Yoshida et al., 2001). The endoribonuclease splices and excises a 26 base pair intron. This activity results in a frame shift in the coding sequence that leads to the translation of the sXBP1 isoform of the protein (**Figure 1.4**).

sXBP1 recognizes and binds cAMP-responsive elements (CRE) upstream the promoter of target genes, which contained the conserved core sequence ACGT (Acosta-Alvear et al., 2007). Target genes are typically involved in chaperone folding and ER-Golgi machinery that are actively transcribed under low-stress conditions (Acosta-Alvear et al., 2007). Other distinct binding motifs have been identified which are preferentially utilized under more stressful conditions. These include genes containing CAACG boxes and UPR elements upstream of the promoters (Acosta-Alvear et al., 2007). These target genes are distinct from those featuring the ACGT sequence core, and are largely involved in lipid

biosynthesis, DNA replication, ion channels and transporters, cell survival and apoptosis, and cell differentiation, amongst others (Acosta-Alvear et al., 2007).

While XBP1 is its best-described substrate, the IRE1 endoribonuclease targets other mRNAs in a highly conserved process termed regulated IRE1-dependent decay (RIDD), in which mRNAs are degraded by the IRE1 endoribonuclease through splicing at consensus sites similar to XBP1 splicing sites (5'CUGCAG'3), followed by digestion of free 5' and 3' ends by ribonucleases. When RIDD was first described in *Drosophila*, targeted mRNAs seem to code exclusively for ER-resident proteins (Moore and Hollien, 2015). However, it has become clear that this is not a strict requirement for substrates, and it remains unclear whether targeting is a somewhat stochastic activity or if there are other subtle levels of regulation in mRNA targeting (Maurel et al., 2014) beyond the presence of CUGCAG sites.

In part due to its conservation in yeast, IRE1 remains a well-studied component the UPR. Consequently, researchers are regularly identifying new layers of IRE1 regulation. The degree to which IRE1 is phosphorylated can greatly influence its function; too little and the endoribonuclease does not function, too much and the protein becomes unstable (Korennykh et al., 2011, Rubio et al., 2011). The role of BiP in activating IRE1 dimerization has been called into question. An alternative model indicates the IRE1 binds directly to unfolded proteins, which triggers IRE1 activation, while BiP binding to IRE1 instead promotes IRE1 stability to ensure a consistent, adequate level of IRE1 monomers in the ER-membrane (Credle et al., 2005, Gardner and Walter, 2011). There is

evidence that lipid disequilibrium in the ER, even in the absence of an unfolded protein burden, is sufficient to trigger IRE1 signalling (Volmer et al., 2013). Given that the evolutionary conservation of IRE1 underscores its central role in maintaining ER homeostasis, insights into IRE1 biology could greatly benefit our understanding of ER-stress response as whole.

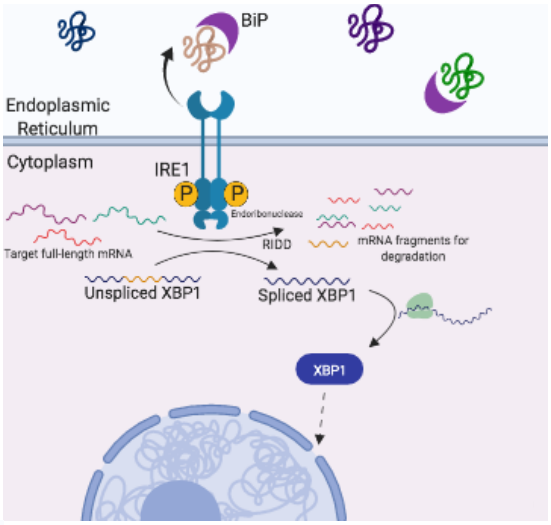

Figure 1.4 Schematic of the IRE1 pathway

1.12.2 ATF6

ATF6 was first identified in 1998 by the Mori lab and is a branch of the UPR that emerged relatively recently in evolution, as it is only found in mammalian cells (Yoshida et al., 1998). ATF6 is sequestered at the ER-membrane through the binding of BiP to its luminal domain (Bettigole and Glimcher, 2015). However, if BiP unbinds in response to an accumulation of misfolded proteins, ATF6 translocated to the Golgi for regulated intramembrane proteolysis, where it is cleaved by site 1 and 2 and proteases (S1P and S2P). This cleavage event releases the C-terminal as a 50kDa transcription factor (**Figure 1.5**).

The ATF6 protein exists in two isoforms: ATF6α, which is transiently expressed and serves as a strong transcription factor, and ATF6β, which exhibits a longer half-life but is a weaker transcription factor (Thuerauf et al., 2007). They can form both homodimers and heterodimers at ER-stress response elements (ERSE) upstream of the promoter of target genes, adding a layer of transcriptional regulation. Consensus ERSE sequences contain the motif CCAAT-N(9)-CCACG (Yoshida et al., 2000) or ATTGG-N-CCACG (Kokame et al., 2001). They are distinct from UPRE sequences implicated in XBP1-driven transcription, but are often found on the same target genes. This redundancy is an example of intersections between the branches of the UPR, and is ascribed as an additional regulatory mechanism.

ATF6-targeted genes are involved in a more narrow functional scope – namely proteostasis (Okada et al., 2002). These targets include chaperones and components of ER-associated degradation (ERAD) to reduce the protein burden. As previously mentioned, ATF6-mediated transcription generates unspliced XBP1, and important precursor for XBP1-driven transcription. Given its relatively late emergence in evolution, this target might seem somewhat surprising given the yeast express an ortholog of XBP1, *Hac1*, in the absence of ATF6 (Lee et al., 2002). However, given the increased complexity of mammalian cells versus yeast, it is not surprising that mammals have gained versatility by evolving additional cis-acting transcriptional elements and addition branches of the UPR to regulate key transcriptional responses (Okada et al., 2002).

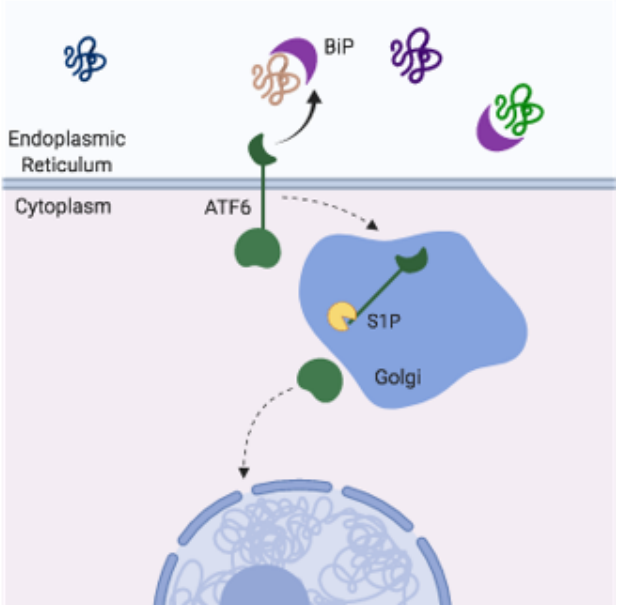

Figure 1.5 Schematic of the ATF6 pathway

1.12.3 PERK

Unlike the previous two pathways, whose responses are primarily aimed a driving the transcription of genes directly involved in coping with an enhanced protein burden, PERK pathway is more suited to deal with intense UPR signalling and is largely responsible for fate decisions in the event of overwhelming ER-stress (Bettigole and Glimcher, 2015). The Brostrom group in 1993 demonstrated that treatment with thapsigargin, which induces ER-stress, is associated with polysome disassembly and correlated with phosphorylation of serine 51 of the translation initiation factor eIF2α, thereby blocking general translation (Wong et al., 1993). The lab of David Ron first discovered this ER-membrane kinase, deemed PERK, in 1999, in attempt to build on this previous observation (Harding et al., 1999). This kinase was named for interferon-inducible RNA-dependent protein kinase (PKR) with which it shares a high degree of amino acid homology in its C-

terminal region. On the other hand, the N terminal region of PERK exhibits a greater degree of homology with IRE1. Similar to IRE1, PERK monomers are bound by BiP, and disassociation of BiP leads to PERK-dimerization and autophosphorylation at serine 731 near the C terminus. This autophosphorylation event activates an additional PKR-like C-terminal kinase that is responsible for phosphorylating eIF2α (Harding et al., 1999).

PERK is not the sole kinase responsible for the phosphorylation of eIF2α. Prior to its discovery, PKR and the heme-regulated eIF2α kinase (HRI) phosphorylated eIF2α in response to pathogens and cytokines or heme levels, heat-shock, and oxidative stress, respectively (Bettigole and Glimcher, 2015). The general control nonderepressable 2 (GCN2) pathway also phosphorylates eIF2α.

The transcriptional and translation response that arises from the phosphorylation of eIF2α is termed that Integrated Stress Response (ISRE), referring the multiple different inputs that can signal through the four kinases and converge on a common factor, eIF2α. The consequent response is manifested in two ways: a block in protein translation and initiation of a specific transcriptional programme. This phosphorylation event inhibits the eIF2b-dependent exchange of GDP to GTP, thereby interfering with the reformation of the active 43S pre-initiation complex and subsequent ribosome complex during protein translation (Young and Wek, 2016). The protein translation block effects a wide range of proteins, but in order to be targeted for translation inhibition, mRNA must contain a certain sequence and distribution of upstream open reading frames (uORFs) where translation machinery docks on mRNAs prior to the coding sequence

(Young and Wek, 2016, Vattem and Wek, 2004). In an unstressed cell, GTP is abundant for rapid disassembly and reassembly of the 43S pre-initiation complex to scan multiple subsequent uORFs, including patterns of activating and inhibitory uORFs (Young and Wek, 2016). When cells become stressed and eIF2α is phosphorylated, the decreasing levels of GTP results in 'delayed re-initiation' (Young and Wek, 2016). For most mRNAs, the failure to re-initiate at the downstream activating uORFs prevents protein translation (Young and Wek, 2016). On the other hand, for mRNAs with a specific pattern of activating and inhibitory uORFs, the 43S pre-initiation complex fails to reassemble to scan the inhibitory uORFs, resulting in the translation of the protein (Young and Wek, 2016). This selectively drives preferential translation of mRNAs coding for proteins involved in restoring ER-homeostasis, while suppressing the translation of protein not immediately relevant to coping with the ER-stress (Vattem and Wek, 2004). The best-characterized mRNAs preferentially translated during the ISRE code for ATF4 and CHOP (**Figure 1.6**). ATF4 mediates a variety of stress response proteins involved in amino acid transport and protection by oxidative stress, amongst other processes (Vattem and Wek, 2004). CHOP is typically upregulated upon long-term ER-stress, and is largely responsible to activating pro-apoptotic signalling pathways (Fusakio et al., 2016).

Since PERK signalling primarily governs cell survival in the face of ER-stress, it is not surprising that PERK activation also promotes autophagy (Song et al., 2018b). Components of the PERK pathway feed into the autophagic process during prolonged stress responses; selective translation by p-eIF2α favours

production of ATG12, a key factor in LC3-I to LC3-II conversion, and ATF4 drives transcription of numerous autophagy-related genes including ATG3, ATG16, and p62 (Liu et al., 2015). PERK can also phosphorylate AMP kinase, which in turn inhibits mTOR, a kinase that regulates cellular metabolism and blocks autophagy (Liu et al., 2015). PERK signalling is also implicated in mitochondrial health and mitophagy, likely due to the preferential transcription of ATF5, which drives the mitoUPR upon oxidative stress (Shpilka and Haynes, 2018).

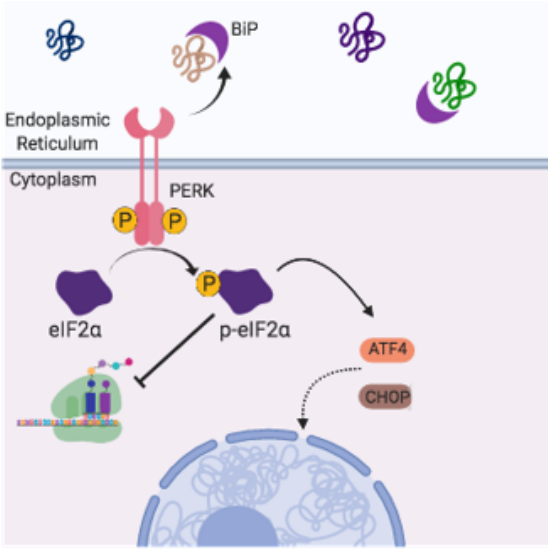

Figure 1.6 Schematic of the PERK pathway

1.13 ER-stress in steady-state immunity

Signalling through the three branches of the UPR is critical in development and function of multiple immune cell subsets. While there is constitutive low level UPR signalling at steady-state conditions to maintain ER homeostasis, many cells require a rapid turnover of proteins during differentiation to take on a new phenotype and carry out newly acquired functions (Sugiura et al., 2009, Lu et al., 2013). Certain immune cells, particularly those with a high secretory capacity, require stronger constitutive UPR signalling to properly function.

Plasma cells constitute a terminally differentiated form of B cell endowed with the ability to secrete large amount of immunoglobulin. Consequently, the demands on protein folding in the ER are relatively high (Bettigole and Glimcher, 2015). The UPR, more specifically XBP1, is indispensible in plasma cell survival and function. This link was first observed when Blimp-deficient mice failed to upregulate XBP1 expression in B cells upon plasma cell differentiation compared to wild type (WT) mice (Shaffer et al., 2004). Interestingly, immature and mature B cells do not exhibit the same dependency on UPR signalling for differentiation and function. This finding was further confirmed when *in vitro* plasma cell differentiation by LPS and IL-4 induced activation of IRE1 as well as ATF6 (but not PERK) (Ma et al., 2010). However, with respect to robust antibody production, only IRE1 signalling is necessary (Aragon et al., 2012).

DCs are an example of a non-secretory immune cell that requires UPR at steady state (Iwakoshi et al., 2007). Differentiation of particular DC subsets relies on signalling through specific branches of the UPR. For example, PERK signalling is higher on $CD11b^{+}$ monocyte derived DCs (MoDCs) than other subsets, XBP1 splicing is higher on plasmacytoid DCs (pDCs) than other subsets (their numbers decreased by about 25% in $XBP1^{-/-}$ mice) (Iwakoshi et al., 2007), and PERK and IRE1 signalling occurs constitutively on $CD8\alpha^{+}$ DCs in mice. The requirement for high resting XBP1 activity in pDCs might be reflect that pDCs are typically primed for rapid IFN-α synthesis in the ER (Worah et al., 2016). cDC1s, typified by surface expression of XCR1, DNGR1, and CD103, are particularly efficient in priming $CD8^{+}$ T cells, a process which are involved cross-presentation (Medel et

al., 2018). In mice, the use of CD11c-Cre XBP1$^{-/-}$ mice illustrated that the IRE1-XBP1 signalling pathway was crucial in cDC1 cells' ability to cross-present dead cell antigens to CD8^{+} T cells on MHC class I. The underlying mechanism driving this defect was the over-activation of RIDD in the absence of XBP1, which degraded mRNAs that code for key components of the cross-presentation pathway (Osorio et al., 2014).

While its direct role in T cell development is not clear, differential UPR signalling plays a role in sculpting T cell functional responses. For CD4^{+} T cells, the IRE1-XBP1 axis is implicated in Th2 differentiation of human and murine T cells and innate lymphoid cell 2s (Henriksson et al., 2019); deletion of XBP1 or blocking the IRE1 endoribonuclease with small molecule inhibitors reduced secretion of IL-4, IL-5, and IL-13 (Kemp and Poe, 2019). Induction of ER-stress by physiological stresses, such as hypoxia and glucose deprivation, seems to promote Th17 differentiation, as measured by IL-17 secretion (Dang et al., 2011). These effects are mitigated by IRE1 and PERK inhibition. Granzyme B production in cytotoxic CD8^{+} T cell responses is positively correlated with levels of the chaperone BiP, as illustrated by comparing CD8^{+} T cells from wild type and BiP$^{+/-}$ mice (Chang et al., 2012). Induced regulatory T cells (iTregs) exhibit a narrow range of plasticity between a regulatory phenotype, hallmarked by high expression of Foxp3 and IL-10 secretion, and a slight Th1 phenotype, hallmarked by low expression of Foxp3 and IFN-γ secretion (Zhang et al., 2015). This functional plasticity is reportedly related to ATF4 levels, with increased expression of ATF4 in iTregs promotes a shift towards a Th1 phenotype (Yang et al., 2018). Finally,

secretion of Th1 and Th17 cytokines from TCR-activated iNKT cells requires IRE1 signalling, which serves to stabilize the cytokine mRNAs (Govindarajan et al., 2018).

1.14 ER-stress in infection

The interactions between pathogens and the ER-stress response are bidirectional in nature; host immune responses intersect with the UPR, and certain microbes co-opt the UPR during pathogenesis. Innate immune cells can sense intracellular and extracellular pathogens, including a broad array of viruses and bacteria, through TLRs. TLR2 and 4 signalling specifically drives XBP1-mediated transcription through IRE1 activation, which results in the sustained production of pro-inflammatory cytokines in macrophages, including IL-6, TNFα, and IFN-β, required for intracellular bacterial clearance, while suppressing ATF4-CHOP signalling to promote macrophage survival during infection (Martinon et al., 2010). Integration of TLR4 and 8 and PERK signalling synergizes IL-23 production, a process that requires CHOP (Goodall et al., 2010). ER-stress also activates the NLRP3 inflammasome, which promotes caspase dependent cleavage and generation of IL-1β (Shenderov et al., 2014). In a *Brucella* infection model, this link is made through IRE1 sensing of mitochondrial dysfunction and consequent IRE1 and PERK signalling to modulate NFκB and MAP kinase signalling, which contributes to the production of pro-inflammatory cytokines (Bronner et al., 2015). Virulence factors from *P. aeruginosa* triggers the IRE1-XBP1 axis, which in turn protects against infection-induced cytotoxcity of airway epithelial cells (van 't Wout

et al., 2015). Infection of hepatocytes with HBV induced the XBP1-dependent upregulation of lipid antigen on CD1d to activate iNKT cells (Zeissig et al., 2012).

Numerous reports confirm the involvement of ER-stress pathways in the production of type 1 interferons, namely IFN-β through XBP1-mediated transcription, which are important in viral immune defences (Smith et al., 2008). Furthermore, the PKR kinase can trigger the ISRE through detection of dsRNA as part of the interferon antiviral response (Lemaire et al., 2008). Given this link between ER-stress and antiviral responses, it is unsurprising that viruses have developed a number of ways to co-opt the UPR. Briefly, viruses manipulate different components of the UPR promote replication and infection, stemming from activation of RIDD to degrade mRNAs coding for host defence proteins, or blocking PERK signalling to permit translation of viral proteins and prevent cell apoptosis to allow for viral replication (Bhattacharyya, 2014).

1.15 ER-stress in sterile inflammation

ER-stress responses in autoimmune disease and sterile immune pathologies, particularly hepatic disease and cancer, are well documented. Whether they play protective or pathological roles in sterile immune responses is highly varied and likely context dependent. There are multiple sterile pathologies where non-immune cells exhibit ER-stress, but the remaining part of this section will focus specifically on the influence of ER-stressed immune cells in sterile tumourigenesis.

Work from the Glimcher and Cubillos-Ruiz labs has provided key insights into the involvement of ER-stress in anti-tumour immune responses. Splicing of XBP1, a downstream transcription factor in the IRE1 branch of the UPR, in tumour-associated DCs alters lipid metabolism and protein-antigen presentation, leading to inhibited anti-tumour T cell responses in ovarian cancer (Cubillos-Ruiz et al., 2015). Consistent with this finding, loss of XBP1 signalling in ovarian tumour-infiltrating T cells improved anti-tumour immune responses by promoting influx of glutamine that is necessary to maintain mitochondrial respiration and metabolic fitness in these T cells (Song et al., 2018a). PERK signalling and consequent translation suppression reduces Tbet levels within $CD8^+$ effectors TILs in mice bearing lung and ovarian tumours, thereby blunting anti-tumour immune responses at those sites (Cao et al., 2019). IRE1-XBP1 axis is also important in proliferation of NK cells through support of mitochondrial activities including oxidative phosphorylation, which supported NK-mediated anti-tumour responses against B16 melanoma lung metastases (Dong et al., 2019).

1.16 ER-stress as a therapeutic target

Given its prevalence in a variety of diseases, the UPR pathways are attractive targets for therapy. Perhaps the most promising setting for UPR-based therapy is in treating neurodegenerative diseases. A common feature of prion-based, Alzheimer's, Parkinson's, and Huntington's diseases is protein misfolding (Scheper and Hoozemans, 2015). Markers of the UPR, particularly the PERK pathway, are used in immunohistochemistry to help identify region of tauopathy or synucleinopathy in human brain tissue sections (Stutzbach et al., 2013). A

genome wide association (GWAS) study identified single nucleotide polymorphisms (SNPs) *EIF2AK3*, the gene corresponding to PERK, associated with increased risk of tauopathies (Hoglinger et al., 2011). Administration of small molecule inhibitors that target the central node of the ISRE, eIF2α, has dramatic effects on neurodegenerative disease progression in mice. In murine experiments, the PERK inhibitor GSK2606414 reduces clinical symptoms of prion disease (Moreno et al., 2013). Furthermore, it exerted neuroprotection and improved memory responses in fronto-temporal dementia and Alzheimer's disease models (Radford et al., 2015). Another drug that targets the ISRE is salubrinal, which blocks the phosphatases responsible for eIF2α dephosphorylation (Boyce et al., 2005). Its role in helping or hindering neuroprotection in neurodegenerative disease remains controversial (Moreno et al., 2012, Colla et al., 2012), but bolsters evidence that the PERK pathway and the ISRE holds promise in this setting. While the mechanism by which PERK signalling contributes to neurodegenerative pathology, particular Alzheimer's, is likely related to UPR responses, there is evidence of second mechanism whereby PERK activates Glycogen Synthase Kinase 3β (GSK3β), which phosphorylates Tau and drives pathogenic aggregations (Nijholt et al., 2013, van der Harg et al., 2014).

The monogenic disease cystic fibrosis stems from a mutation in the gene coding for CFTR, and transmembrane chloride ion channel highly expressed in lung epithelial cells, as well as epithelium of the pancreas, intestine and exocrine glands. When functioning properly CFTR pumps chloride ions out the cells, which maintains correct osmotic pressure and water balance between the cell and

extracellular milieu (Cutting, 2015). However, the homozygous mutations associated with cystic fibrosis, namely the ΔF508 mutation responsible for nearly two-thirds of cases in Caucasian populations, prevents the CFTR protein from folding properly, thus it is retained in the ER and eventually degraded (Cutting, 2015). The failure of CFTR to translocate and function properly in the cell membrane results disrupts the ion gradient between the cell and extracellular space, drawing excess water into the cell. This aberrant effect that contributes to the rigid, stagnant mucus typical of the cystic fibrosis pathology (Cutting, 2015).

Though the driver of the disease is not immune related, inflammation at later stages can exacerbate the pathology, particularly as impaired clearance of mucous renders patients susceptible to lung infections (Ratner and Mueller, 2012). Patients are also more prone to autoimmune responses, included allergic and asthmatic responses (Cutting, 2015). Neutrophils, monocytes/macrophages, and numerous granulocytes reportedly mount dysfunctional immune responses in cystic fibrosis, leading to abnormal T helper and B cell responses (Ratner and Mueller, 2012).

Overcoming the improper folding of CFTR is the goal of frontline therapy. One such drug is Orkambi®, consists of two components: lumacaftor, which helps fold the mutated CFTR protein to escape the ER and traffic to the cell surface, and ivacaftor, which improves its chloride transport ability. By the non-specific mechanism of action, lumacaftor likely ameliorates the UPR in cells with a misfolded protein burden (Deeks, 2016).

Since coping with ER-stress is essential to their survival and can contribute to chemotherapeutic resistance, the UPR is an attractive target in certain tumour settings. ER-stress in cancer is a double-edge sword – heightened ER-stress responses might hinder tumour progression, while in other instances it promotes tumourigenesis (Urra et al., 2016). In the case of multiple myeloma, proteasome inhibitors such as bortezomib (and new versions carfilzomib and ixazomib) are frontline treatments. Plasma cells develop from B cells, and are distinctive in their ability to produce and secrete antibodies (Cooke et al., 2016). Antibodies are composed of two identical heavy chains of one of 5 subtypes: α (IgA) γ (IgG) ε (IgE) δ (IgD) and μ (IgM) They also contain two identical light chains of one of two subtypes: κ or λ. Chromosomal breakages and rearrangements of the long arm (q arm) of chromosome 22 induce genetic changes that give rise to various specificities and affinities of the BCR. These processes, which occur at different stages of B cell maturation, include VDJ recombination, somatic hypermutation, and, later, affinity maturation. While these are natural process in B cell biology, this genomic instability can promote oncogenic mutations, for example, if an antibody promoter is rearranged upstream of an oncogene. In multiple myeloma, these aberrant rearrangements can result in the copious production of immunoglobulins. The burden of folding these nascent immunoglobulin peptides drives the UPR in these malignant cells. Multiple myelomas have adapted mechanisms, particularly with downstream components of the UPR, to cope with a level of overwhelming ER-stress that would otherwise trigger cell death in nonmalignant plasma cells; they often lie on the brink of survival. While UPR activation is a hallmark of the

disease, it is also exploited for therapeutic intervention. Drugs such as bortezomib and its analogues serve to inhibitor the proteasome, which prevents malignant cells from degrading apoptotic proteins, pushing the myeloma cells to proteotoxicity and apoptosis (Lee et al., 2003). Naturally, this mechanism of action augments UPR signalling, particularly through the PERK pathway (Obeng et al., 2006). Other UPR-targeting drugs, including those targeting BiP, are currently in clinical trials to treat melanoma (Bu and Diehl, 2016).

1.17 Project Aims

1.17.1 Question

While several mechanisms modulating iNKT cell activation in non-sterile conditions have been identified, it remains unclear what mechanisms drive iNKT cell activation during sterile inflammation, including in cancer.

1.17.2 Rationale

Pathways, including the UPR, involved in modulating lipid biosynthesis leading to an altered repertoire of immunogenic lipid species are reported to drive iNKT cell activation in non-sterile conditions (Zeissig et al., 2012). Cells undergoing the UPR exhibit marked increased in genes involved in lipid metabolism, including *PPARγ*, *SREB1/2*, and *VLDLR* (Oyadomari et al., 2008, Bobrovnikova-Marjon et al., 2008, Jo et al., 2013). In hepatic diseases, such as non-alcoholic fatty liver disease (NAFLD), non-alcoholic steatohepatitis, and hepatic steatosis, ER-stress

contributes greatly to dysregulated lipid metabolism (Oyadomari et al., 2008, Jo et al., 2013). Notably, iNKT cells contribute to the sterile inflammatory component of these pathologies (Adler et al., 2011, Tajiri et al., 2009). ER-stress also is a hallmark in a variety of cancers, a sterile pathology where iNKT cells are known to play a central role in immunosurveillance. Cubillos-Ruiz et al. illustrated that splicing of XBP1, a downstream transcription factor in the IRE1 branch of the UPR, in tumour-associated DCs altered lipid metabolism and protein-antigen presentation, leading to inhibited anti-tumour T cell responses (Cubillos-Ruiz et al., 2015).

1.17.3 Hypothesis

We hypothesize that ER-stress, triggering the UPR, in $CD1d^+$ myeloid cells drives CD1d-dependent activation of iNKT cell during sterile inflammation.

To address our hypothesis, we set out the following aims for the project:

1) To determine whether treatment of APCs with inducers of the UPR, in the absence of any foreign or synthetic agonist, can trigger iNKT cell activation;
2) To characterize the nature and quality of the iNKT cell response to ER-stressed APCs;
3) To determine the molecular mechanism driving ER-stressed APC-mediated iNKT cell responses;

4) To understand the biological relevance of the mechanism in human health and disease.

Chapter 2: Materials and Methods

2.1 Human cell culture

2.1.1 Immortalized cell lines

The following cell lines were used as APCs for human *in vitro* assays: THP1 – a human monomyelocytic cell line, U266 – a lymphoblastic myeloma cell line, JIM3 – a myeloma cell line, and JJN3, a plasma cell leukaemia cell line. These cell lines were passaged between 10-20 times before being discarded and fresh aliquots thawed for future experiments. All these cell lines are non-adherent, and were split every two to three days depending on confluency. Cells were screened for *Mycoplasma* contamination two to three times per year.

2.1.2 Media

Primary immune cells and all human cell lines were cultured in Roswell Park Memorial Institute (RPMI-1640) media (Sigma) supplemented with the following: 10% heat inactivated fetal calf serum (Gibco), 2mM L-glutamine (Sigma), penicillin-streptomycin 100X (Sigma), 1mM sodium pyruvate (Gibco), MEM non-essential amino acids 100X (Gibco), 10mM HEPES buffer solution (Gibco), 50μM β-mercaptoethanol (Gibco). This complete medium (R-10) was refrigerated for up to one month, at which point unused medium was discarded. R-10 supplemented with 1000U/mL IL-2 (from supernatants from J588L cell line) was used for human iNKT cell expansion. Sorted human iNKT cells were maintained in Iscove's Modified Dulbecco's Medium (Sigma) supplemented with 5% human serum (NHS Blood and Transfer Unit) and 1000U/mL IL-2 (hereafter referred to as

T cell medium). This T cell media was refrigerated for up to two months, at which point unused medium was discarded. Freezing medium containing heat inactivated fetal calf serum (Gibco) with 20% DMSO (Sigma) was sterile filtered each time before use. Cells, at counts ranging from 10,000 to 3 million, were resuspended in freezing medium to make 1mL aliquots in cryovials. All supplements were passed through a 0.2μm filter when added to base medium in an effort to keep the medium sterile.

2.1.3 Generation of monocyte-derived DCs (MoDCs)

Blood from leukocyte cones (purchased from the NHS Blood and Transport unit) was diluted in RPMI-1640 with 10mM HEPES at a 1:12 dilution. The mixture was overlaid on 15mL of LymphoPrep (STEMCELL Technologies) and centrifuged for 30min at 2000rpm with no acceleration or brake. The peripheral blood mononuclear cell (PBMC) layer was collected and washed twice with RPMI + 10mM HEPES, first at 1500rpm for 15 minutes with brake, and then 1000rpm for 10 minutes with brake. The PBMCs were incubated with $CD14^+$ beads (Miltenyi) for 15 minutes in MACS buffer (PBS+10%FCS+2mM EDTA), washed, passed through a Celltrics 30μm single cell filter (Sysmex) to remove clumps and then purified using positive selection magnetic LS MACS columns (Miltenyi). Purified $CD14^+$ monocytes were washed in R-10 and cultured at 900,000 cells/well in 6-well plates. Monocytes were differentiated into DCs with the addition of 50ng/mL granulocyte macrophage- colony stimulating factor (GMCSF) (Peprotech) and 100ng/mL IL-4 (from supernatants). After 5 days, the MoDCs were used in

experiments. During initial experiments, the MoDCs were tested for markers of successful differentiation, including downregulation of CD14. MoDCs differentiated from previously frozen $CD14^+$ cells were often used at Day 4. $CD14^-$ cells, containing the T cells, were frozen down during MoDC differentiation.

2.1.4 Generation of human primary iNKT cells

Upon MoDC differentiation, the $CD14^-$ cells were thawed and rested at 37°C in R-10 for 2-3 hours. Simultaneously, a fraction of the autologous MoDCs were pulsed with 1µg/mL αGC in 1mL R-10 at 37°C for 2-3 hours. The pulsed MoDCs and $CD14^-$ cells were counted and co-cultured together in R-10+IL-2 at the following proportion: $6X10^5$ αGC-pulsed MoDCs and $6X10^6$ autologous $CD14^-$ cells (a ratio of 1:10 MoDCs:$CD14^-$ cells, the raw numbers varied slightly) in 24-well plates. This co-culture was expanded over the course of 2-3 weeks. At this point, the co-culture was harvested and iNKT cells were sorted to purity (~70-95%) into T cell medium on the FACS ARIA with a 30mm nozzle. The iNKT cells were plated in two-wells of a 48-well plate and re-stimulated using a mixture of irradiated (30min at 3000rads) allogeneic PBMCs in R-10 at final concentration of $5X10^6$cells/mL and 1µg/mL phytohaemagluttin. A well containing the restimulation mixture was cultured in parallel to ensure that the feeders did not proliferate. iNKT cells were expanded in T cell medium over the next 10 days before being checked for purity and used in functional assays (delay due to downregulation of the iNKT-TCR by restimulation).

2.1.5 Generation of human primary MAIT cells and γδ T cells

PBMCs were isolated as previously described. These cells were then incubated with CD2 beads (Miltenyi) for 15 minutes, washed, and passed through a Celltrics filter to remove clumps and the purified using positive selection magnetic LS MACS columns (Miltenyi). MAIT cells and γδ T cells were sorted to purity from this population and cultured in separate 48-well plates.

2.2 Murine cell culture

2.2.1 Immortalized cell lines

Lewis lung carcinoma (3LL) cell line was used as a model murine tumour cell line. Cells were trypsinized every 2-3 days or when they reached 70% confluency. DN32 cells were cultured in R-10. Frozen aliquots were provided by senior lab members, and were tested for mycoplasma before use. These non-adherent cells split every 2-3 days.

2.2.2 Media

3LL cells were maintained in high glucose Dulbecco's Modified Essential Medium (Sigma) and supplemented with the following: 10% heat inactivated fetal calf serum (Gibco), 2mM L-glutamine (Sigma), penicillin-streptomycin 100X (Sigma), 1mM sodium pyruvate (Gibco), MEM non-essential amino acids 100X (Gibco), 10mM HEPES buffer solution (Gibco), 50μM β-mercaptoethanol (Gibco). This complete medium (D-10) refrigerated for up to two months, at which point unused medium was discarded. DN32 cells were maintained in R-10.

2.2.3 Generation of bone marrow-derived DCs (BMDCs)

Mice were culled following the guidelines of a Schedule 1 procedure. The long bones (tibias and femurs) were removed, cleaned, and sterilized in 70% isopropanol/methanol solution. The ends of the bones were cut and the marrow was flushed out using a 0.5 inch, 26-gauge needle filled with RPMI-1640 into a single cell strainer over a 50mL Falcon tube to create a single cell suspension. The marrow was mashed using a 5mL syringe plunger, washed with RPMI-1640 or PBS for 5 min at 1500rpm and treated with 5mL of red blood cell lysis buffer (Qiagen) for 10 minutes at room temperature. The marrow cells were spun at 1500rpm for 5min, resuspended in R-10 and plated in 6-well plates, 5mL per well, at a density of $4X10^5$cells/mL. The R-10 was supplemented with 50ng/mL murine GMCSF (Peprotech). This supplemented medium was replenished every 2 days, for a total of 6-8 days. Around this time, the cells were tested by flow cytometry for the percentage $CD11c^+CD11b^+$ cells. If cells were less than 85% double positive, the BMDCs were incubated with $CD11c^+$ beads and then purified using positive selection magnetic LS MACS columns (Miltenyi) as previously described, as tested in **Figure 2.1**.

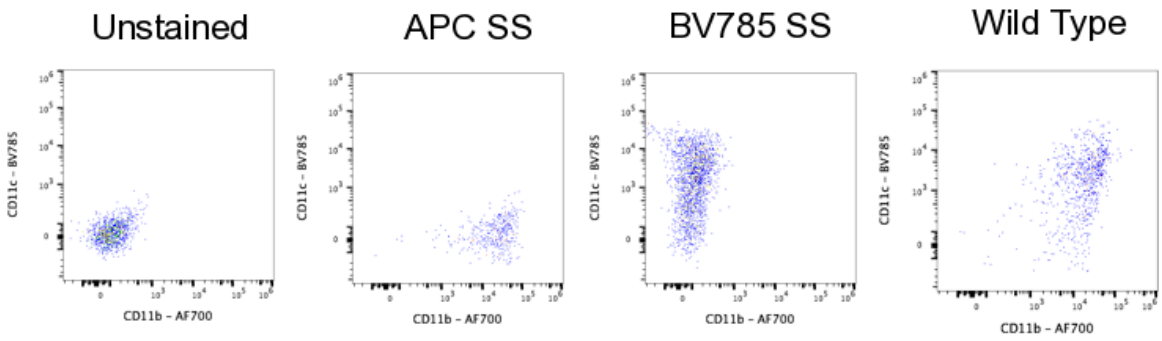

Figure 2.1 Confirmation of CD11c$^+$ BMDCs. Flow cytometry confirms that CD11c$^+$ DCs have differentiated to high purity from bone marrow precursors. Dot plots are representative of N=3

2.3 iNKT cell agonists

2.3.1 Inducers of ER-stress

Thapsigargin (Sigma) was resuspended in DMSO (Sigma) and aliquoted in 1μM stocks. Tunicamycin (Sigma) was resuspended in DMSO (Sigma) and aliquoted in 1μg/mL stocks. SubAB5 toxin was discovered by Dr. James Paton and provided Dr. John Christianson through his material transfer agreement with Dr. James Paton. Also provided was the mutant SubAB5 toxin, which has a single amino acid mutation ($S_{272}A$) that abolishes its enzymatic activity, and serves a negative control. Both toxins were resuspended in 50% glycerol in sterile H_20 (v/v) at 1mg/mL or 1.5mg/mL.

2.3.2 iNKT lipid agonists

α-galactosylceramide (αGC)

αGC used in the experiments was either: (1) synthesized as a powder by Gurdyal Besra and Natacha Veerapen, University of Birmingham or (2) purchased commercially in film form as KRN7000 (Enzo Life Sciences). αGC from both

sources was resuspended first in 100μL 2:1 chloroform:methanol in glass vials. PBS-Tween was immediately added to make a stock concentration of 100-200μg/mL. The solution was subject to roughly 5 repeated cycles of 5 minutes water-bath sonication, 5 minutes in a 55°C water bath until the solution was clear and the αGC had fully dissolved. New stocks were tested functionally in a titration curve against old batches pulsed on THP1-CD1d cells to measure iNKT cell activation.

C20:2 and α-galactose-(1,2)galactosylceramide (GGC)

C20:2 was synthesized by Natacha Veerapan and Gurdyal Besra and resuspended as previously described at a stock concentration of 100μg/mL. Likewise, GGC was synthesized by Natacha Veerapan and Gurdyal Besra, and resuspended as previously described at a stock concentration of 100μg/mL.

2.4 Small-molecule inhibitors

2.4.1 PERK inhibitors

The PERK kinase inhibitor GSK2606414 (Sigma) was resuspended in DMSO to a final concentration of 500μM, aliquoted and stored at -20°C. The p-eIF2α inhibitor Integrated Stress Response Inhibitor (ISRIB) (Sigma) was resuspended in DMSO to a stock concentration of 5mM, aliquoted and stored at -20°C.

2.4.2 IRE1 inhibitors

Dr. John Christianson provided the IRE1 inhibitor 4μ8C, which inhibits the IRE1 endoribonuclease responsible for splicing XBP1. It was resuspended in DMSO at a stock concentration of 50μM, aliquoted, and stored at -20°C. The IRE1 endoribonuclease inhibitor MCK-3964 (Calbiochem) was resuspended in DMSO at a stock concentration of 1mM. The IRE1 endoribonuclease inhibitor STF-083010 (Sigma) was resuspended in DMSO at a stock concentration of 1mM. These inhibitors were aliquoted and stored at -80°C. The products were protected from light as per manufacturer instructions.

2.4.3 ATF6α inhibitor

Ceapin-A7 was provided by Dr. John Christianson and purchased via Sigma-Aldrich. It was resuspended in DMSO at a stock concentration of 2mg/mL, aliquoted and stored at -20°C.

2.5 Flow cytometry antibody/staining panels

2.5.1 Human iNKT cell activation panel

Live/Dead staining was performed in PBS, followed by antibody staining in PBS+10% FCS for 20 – 30 minutes.

Target	*Conjugated fluorophore*	*Dilution*	*Clone*	*Supplier*	*Catalogue Number*
CD3	APC	1:10	HIT3α	BD Pharmingen	555342
CD4	APC	1:10	RPA-T4	BD Pharmingen	555349
CD4	FITC	1:10	RPA-T4	BD Pharmingen	5097644

CD4	PE	1:20	RPA-T4	BD Pharmingen	555347
CD69	FITC	1:10	FN50	BD Pharmingen	555530
CD25	PE	1:20	M-A251	BD Pharmingen	555432
CD25	APC	1:10	M-A251	BD Pharmingen	555434
CD25	PerCP-Cy5.5	1:10	BC96	Biolegend	302625
Fixable Aqua (Live/Dead stain)	BV510	1:100	Dye	invitrogen	L34957

2.5.2 Human DC panel

Fixable Aqua Live/Dead staining was performed in PBS, followed by antibody and in some cases propidium iodide staining in PBS+10% FCS.

Target	*Conjugated fluorophore*	*Dilution*	*Clone*	*Supplier*	*Catalogue Number*
CD14	APC	1:10	M5E2	BD Pharmingen	555399
CD80	PE	1:20	L307.4	BD Pharmingen	557227
CD83	FITC	1:10			5051731
CD86	APC	1:10	2331 (FUN-1)	BD Pharmingen	555660
HLA-ABC	FITC	1:10	G46-2.6	BD Pharmingen	555552
Propidium iodide (Live/Dead stain)	PE-Cy7	1:100 (10ug/mL)	Dye	Thermo Fisher	P3566
Fixable Aqua	BV510	1:100	Dye	invitrogen	L34957

2.5.3 Other human antibodies

Target	*Conjugated fluorophore*	*Dilution*	*Clone*	*Supplier*	*Catalogue Number*
iNKT-TCR tetramer	PECF-594	1:100	N/A	N/A	N/A
TCR Vδ2	PE	1:50	123R3	Miltenyi	130-095-796

CD1d	PE	1:20	42.1	BD Pharmingen	550255
Vα7.2	PE	1:33	3C10	Biolegend	333108
CD161	APC	1:12	HP-3G10	Biolegend	339911
γδ	BV421	1:12	B1	Biolegend	331217

2.5.4 Murine splenic iNKT cell activation panel

Fc block, Live/Dead staining, and CD1d-αGC tetramer staining was performed in PBS at room temperature for 10 minutes, all other antibody staining was performed after on ice at a 1:1 ration of PBS+10%FCS and Brilliant Stain Buffer (BD Horizon). The gating strategy is illustrated in **Figure 2.2**.

Target	*Conjugated fluorophore*	*Dilution*	*Clone*	*Supplier*	*Catalogue Number*
Fc block (CD16/32)	N/A	1:100	93	eBioscience	14-0161-85
Fixable Aqua (Live/Dead)	BV510	1:100	N/A	invitrogen	L34957
CD1d-αGC tetramer	PE	1:20	N/A	N/A	N/A
NK1.1	AF-488	1:15	PK136	BioLegend	108717
PD1	APC	1:20	J443	eBioscience	17-9985-82
CD69	PE-Cy7	1:75	H1.2F3	eBioscience	25-0691-82
CD44	Alexa-700	1:75	IM7	eBioscience	56-0441-82
TCR-β	ef780	1:75	H57-597	eBioscience	47-5961-82
CD62L	BV605	1:20	MEL-14	BioLegend	104437
CD25	BV650	1:15	PC61	BioLegend	102038
B220	BV510	1:20	RA3-6B2	BioLegend	103248
CD4	PECF-594	1:500	RM4-5	BD Biosciences	562314
CD8	BV711	1:75	53-6.7	BioLegend	100747

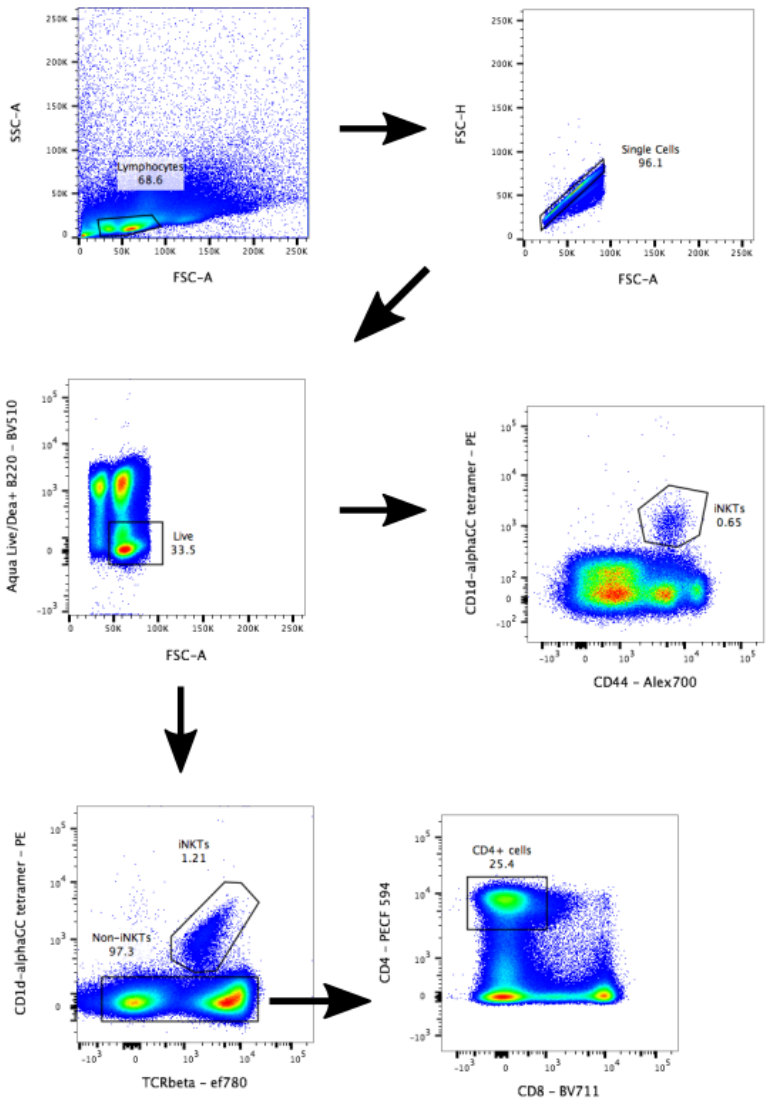

Figure 2.2 Gating strategy for analysing iNKT cells *in vivo*. Flow chart of the gating strategy used to analyse the iNKT cells in mice for based on an uninjected control mouse. Briefly, lymphocytes were gated based on forward and side scatter, then single cells on forward scatter area versus height, dead cells and B cells were excluded, and finally iNKT cells using the CD1d-αGC tetramer, from which expression levels of the activation markers CD25 and PD1 were determined. From the CD1d-αGC tetramer negative population, $CD4^+$ cells were analysed for expression levels of the activation markers PD1 and CD25.

2.5.5 Murine DC panel

Fc block and Live/Dead staining were performed in PBS at room temperature for 10 minutes, all other antibody staining was performed on ice in a 1:1 ration of PBS+10%FCS and Brilliant Stain Buffer (BD Horizon).

Target	*Conjugated fluorophore*	*Dilution*	*Clone*	*Supplier*	*Catalogue Number*
Fc block (CD16/32)	N/A	1:100	93	eBioscience	14-0161-85
Fixable Aqua (Live/Dead)	BV510	1:100	N/A	Invitrogen	L34957
CD11b	Alexa700	1:75	M1/70	eBioscience	56-0112-82
CD11c	BV785	1:20	N418	BioLegend	117335
MHC II	ef780	1:500	M5/114.15.2	eBioscience	47-5321-80

2.5.6 Human iNKT sorting panel

CD1d-αGC tetramer staining was performed in PBS at room temperature for 10 minutes, all other antibody staining was performed on ice in a 1:1 ration of PBS+10%FCS.

Target	*Conjugated fluorophore*	*Dilution*	*Clone*	*Supplier*	*Catalogue Number*
CD1d-αGC tetramer	PE	1:500	N/A	N/A	N/A
CD3	APC	1:10	HIT3α	BD Pharmingen	555342
CD4	FITC	1:10	RPA-T4	BD Pharmingen	5097644

2.5.7 Making the CD1d-αGC tetramer

CD1d-αGC biotinylated monomer was tetramerized used Steptavidin (SAV)-PE (eBioscience, 12-4317-87) following guidelines from NIH tetramer website. Briefly, based on the molecular weight of CD1d (59kDa) and SAV-PE, 12.5μL of the monomer (stock concentration 0.5mg/mL) was tetramerized by adding 16.25μL (2.6μL/μg monomer) in 10 steps (1.6μL every 15min) on ice in the dark.

2.5.8 Making the iNKT-TCR tetramer

Soluble iNKT-TCR biotinylated monomer was tetramerized used Streptavidin (SAV)-PECF594 (Biolegend, 405207) following guidelines from NIH tetramer website. Briefly, based on the molecular weight of the TCR (38kDa) and SAV-PECF594, 12.5µL of the monomer (stock concentration 0.5mg/mL) was tetramerized by adding 6.25µL (1µL/µg monomer) in 10 steps (0.625µL every 15min) on ice in the dark.

2.6 Flow cytometry protocol

2.6.1 Staining protocol

Cells were stained in a 96-well round bottom plate (Costar). If cells had been previously cultured in a 96-well flat well plate (such as DCs), they were washed and incubated at 37°C for 10minutes in PBS+EDTA, loosened gently by pipetting, and transferred to 96-well round bottom plate. Cells were washed with PBS, spun to pellet at 1500rpm for 2-5 minutes, and stained at room temperature with Fixable Aqua (including Fc block in certain cases) diluted in PBS for 10 minutes in the dark. Next, cells were washed, pelleted and stained with tetramers or the antibody mix in PBS+10%FCS (+Brilliant Violet Staining Buffer in some cases) on ice in the dark for 20-30min. Subsequently, cells were washed and pelleted to remove unbound antibody and resuspended for acquisition.

2.6.2 Flow cytometry and FACS acquisition protocol

Flow cytometry data was collected on the Cyan (Beckman-Coulter), BD FACS Canto, Fortessa X50, or NxT Attune (life technologies). Cell sorting was performed on the BD FACS Aria under the direction of Craig Waugh (**Figure 2.6**). Voltages were set using unstained cells (matching the cell type that would be primarily analysed, to account for autofluorescence), and single colour controls consisted either of (1) single-stained cells or (2) compensation beads (BD^{TM} CompBeads, Cat#552845). Briefly, cells were gated based on forward and side scatter, then gated on singlets, and then dead cell were excluded. All data was analysed after acquisition in FlowJo, where the acquisition-based compensation matrix was adjusted as necessary.

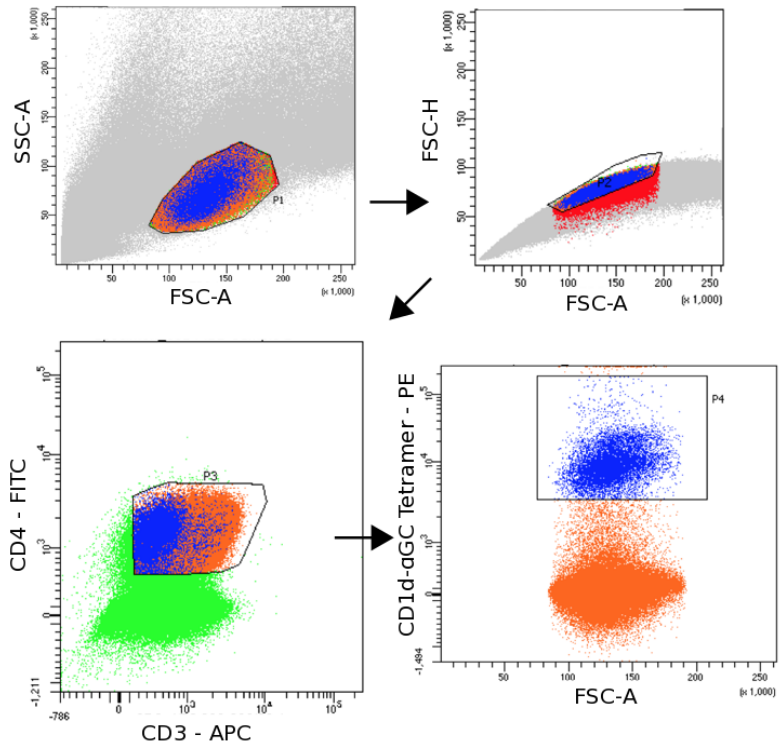

Figure 2.3 Gating strategy to sort primary human iNKT cells. Flow chart of the basic gating strategy used to sort the iNKT cells expanded from PBMCs from healthy donors. Briefly, lymphocytes were gated based on forward and side scatter, then singlets on forward scatter area

versus height, then T cells based on CD4/CD3 staining (which is often lower after CD1d-αGC tetramer staining), and then sorting on CD1d-αGC tetramer positive cells. In this example, only $CD4^+$ iNKT cells were sorted, but in most cases both $CD4^+$ and $CD4^-$ iNKT cells were sorted together.

2.7 Enzyme-linked Immunosorbent Assay (ELISA)

2.7.1 Antibodies and reagents

Human

Reagent	*Stock Concentration*	*Dilution/Starting concentration*	*Supplier*	*Catalogue Number*
IFN-γ Coating Antibody	1.0mg/mL	1:250	BD Pharmingen	551221
Recombinant IFN-γ standard	200µg/mL	10-20µg/mL	Peprotech	300-02-20
Biotin-Conjugated IFN-γ Detection Antibody	0.5mg/mL	1:500	BD Pharmingen	554550
IL12p40 Coating Antibody	1.0mg/mL	1:250	BD Pharmingen	511227
Recombinant IL12p40 standard	200µg/mL	20-40µg/mL	Peprotech	200-12p40-10
Biotin-Conjugated IL12 Detection Antibody	0.5mg/mL	1:500	BD Pharmingen	554660
IL-4 Coating Antibody	0.5mg/mL	1:250	BD Pharmingen	554515
Recombinant IL-4 standard	200µg/mL	10-20µg/mL	Peprotech	200-4-20
Biotin-Conjugated IL-4 Detection Antibody	0.5mg/mL	1:500	BD Pharmingen	554483
GMCSF Coating Antibody	1.0mg/mL	1:250	eBioscience	88-6339-CP
Recombinant GMCSF standard	200µg/mL	10-20µg/mL	Peprotech	300-03-20
Biotin-Conjugated GMCSF Detection Antibody	1.0mg/mL	1:500	eBioscience	88-6339-DT

IL-13 Coating Antibody	0.5mg/mL	1:250	eBioscience	14-7139-81
Recombinant IL-13 standard	200µg/mL	10-20µg/mL	Peprotech	200-13-20
Biotin-Conjugated IL-13 Detection Antibody	1.0mg/mL	1:500	eBioscience	13-7138-81

Murine

Reagent	*Stock Concentration*	*Dilution/Starting concentration*	*Supplier*	*Catalogue Number*
IL-2 Coating antibody	0.5mg/mL	1:500	eBioscience	14-0722-85
Recombinant IL-2 Standard	200µg/mL	2µg/mL	Peprotech	212-12-20
Biotin-Conjugated IL-2 Detection Antibody	0.5mg/mL	1:250	eBioscience	13-7021-85

2.7.2 Protocol

Costa half area, high binding polystyrene 96-well plate (Corning) was coated with 2µg/mL purified coating antibody diluted in coating buffer (0.1M $NaHCO_3$ pH 9) and incubated at 4°C overnight. The plate was then washed with washing buffer (PBS with 0.1% Tween-20) and blocked for 1 hour at room temperature with blocking buffer (PBS with 10% FCS). The titrated cytokine standard and the samples were added to the plate and incubated overnight at 4°C. The plate was washed and biotin anti-human detection antibody was added at 1µg/mL for 1 hour at room temperature. The plate was washed again and 250µg/mL avidin-peroxidase (Sigma), diluted in blocking buffer, was added for 45 minutes at room temperature. The plate was washed again and substrate added to develop the ELISA. The reaction was quenched with 2N H_2SO_4. The OD490 was

measure on a plate reader and the sample concentrations were calculated from the OD measurement of the standard curve.

2.8 Western blotting

2.8.1 Primary Antibodies

Target (Clone)	*Species*	*Clonality*	*Clone*	*Supplier*	*Catalogue Number*
ATF4	Rabbit	Monoclonal	D4B8	Cell Signalling Technology	11815S
BiP	Rabbit	Monoclonal	C50B12	Cell Signalling Technology	3177S
CHOP	Mouse	Monoclonal	L63F7	Cell Signalling Technology	2895S
eIF2α	Rabbit	Polyclonal	D7D3	Cell Signalling Technology	9722S
p-eIF2α	Rabbit	Polyclonal	D9G8	Cell Signalling Technology	9721S
GAPDH	Mouse	Monoclonal	6C5	Santa Cruz	Sc-32233
GAPDH XP(R)	Rabbit	Monoclonal	D16H11	Cell Signalling Technology	5174S
HERPUD1	Rabbit	Polyclonal	Q15011	abcam	ab155778
IRE1	Rabbit	Monoclonal	14C10	Cell Signalling Technology	3294S
PERK	Rabbit	Monoclonal	D11A8	Cell Signalling Technology	5683S
PDI	Rabbit	Monoclonal	C81H6	Cell Signalling Technology	3501S

2.8.2 Protocol

Cytosolic protein was extracted from cell lysates prepared by resuspending about 1 million cells in cold Co-IP buffer (20mM Tris-HCl [pH 7.5], 150mM NaCl, 1mM ethylenediaminetetraacetic acid (EDTA), 1% Triton X-100, 1mM EGTA, 2.5mM sodium-pyrophosphate decahydrate, 1mM β-glycerophosphate) with protease inhibitors (Roche). Protein in the lysates was quantified using a BCA assay with a BSA standard (Thermo Scientific). A constant amount of protein (~20µg) was loaded into pre-cast gels (4-12 or 10% polyacrylimide) and run at 120V until bands of the ladder (Precision Plus Dual Standard, New England Biolabs) were well separated. Protein was transferred onto a PVDF membrane and blocked for 1 hour with 5% BSA in PBS+0.1% Tween-20. The blots were washed in PBS+0.5% Tween before the secondary antibodies, IRDye800CW goat anti-rabbit (Licor, 1mg/mL) and IRDye680RD goat anti-mouse (Licor 1mg/mL), were added at 10,000X dilution for 45 minutes. The blots were washed and dried and visualized using Licor Odyssey scanner and imaging software.

2.9 RNA and PCR analysis

2.9.1 RNA extraction

Cell pellets were washed in PBS and underwent a freeze-thaw cycle before being resuspended in 350µL Buffer RLT (Qiagen). RNA was subsequently extracted using the RNeasy Kit (Qiagen) following the manufacturer's instructions. The concentration of extracted RNA was measured using NanoDrop ONE^{c} (Thermo Scientific).

2.9.2 Reverse transcription

500ng of RNA in 10µL nuclease free water was added to the reverse transcription mastermix prepared from the High-Capacity RT-PCR kit with RNase inhibitors (Applied Biosystems) following the manufacturer's instructions. Briefly, the mastermix was prepared as follows:

Component	*Volume per reaction (total volume 10uL)*
10X RT Buffer	2µL
10X Random Primers	2µL
RNase inhibitors	1µL
Multiscribe Reverse transcriptase	1µL
dNTPs	0.8µL
Nuclease free water	3.2µL

'No Reverse transcriptase' and 'No RNA' controls were included. The reverse transcription reaction was carried out on the ProFlex PCR System (Applied Biosystems by Life Technology) using the following program:

Step	*Temperature (°C)*	*Duration (min)*
1	25	10
2	37	120
3	85	5
4	4	∞

2.9.3 XBP1 PCR

Human XBP1 mRNA was amplified from the 20ng cDNA by PCR using the OneTaq 2X Master Mix with Standard Buffer (New England Biolabs) following the manufacturer's instructions. The forward primer was: 5'-TTACGGGAGAAAACTCACGGC-3'. The reverse primer was: 5'-GGGTCCAACTTGTCCAGAATGC-3'. These primers were based on previously published designs from the Walter lab (Hollien et al., 2009). The PCR reaction was

carried out on the ProFlex PCR System (Applied Biosystems by Life Technology) using the following program:

Step	*Temperature (°C)*	*Duration (seconds)*	
1	74	0.5	
2	74	20	30X
3	59	21	
4	68	40	
5	68	300	
6	4	∞	

The PCR product was mixed with GelPilot® loading buffer (Qiagen) and was run with a ladder on a 2.25% agarose gel at 100V and visualized using SYBR Safe (invitrogen).

2.10 Lentiviral transduction of cell lines

2.10.1 THP1 cells overexpressing modified CD1d

THP1 cells overexpressing wild type and tail$^{-/-}$ CD1d were described previously (Salio et al., 2013). THP1 cells overexpressing GPI-linked CD1d were made by transducing cells with a CD1d lentiviral vector containing the GPI sequence used in the construct as previously described (Wild et al., 1999).

2.10.2 CD1d overexpression in multiple myeloma lines

Transfection to generate lentivirus

HEK293T cells were cultured in T-75 flasks in 12mL high glucose D-10 to reached 80-90% confluency for the day of transfection. The DNA mix for transfection was prepared in a separate microtube by adding the following: 1.5µg of the gag-pol expressor, 1.5µg of VSV-G expressor, and 2.3µg of either the untagged CD1d plasmid or a GFP plasmid. Water was added to a total volume of

50μL. Meanwhile 27μL of XTreme-gene (Roche) was added to 200μL of OptiMEM medium (Gibco), mixed by flicking, and DNA was added to form liposomes containing the DNA plasmids. The lipocomplexes were added to the medium in the flask and incubated for 72 hours. At 72 hours, the cells were visualized under a fluorescent microscope to estimate the efficiency of the transfection.

Transduction of cells

Supernatant from the transfected H293T cells was spun at 1500rpm for 15minutes. The top 10mL of the total 12mL was carefully transferred to a separate Falcon tube without the disturbing the pellet, and spun again for 15minutes at 1500rpm, and separate from any precipitating cells. 100,000 cells of U266, JIM3, JJN3 human myeloma cell lines were seeded in 100μL of R-10 in separate 48 well plates. 100μL of the transfection supernatants was added to each of the seeded cell line wells. 24 hours later, the wells were topped up with 1mL of R-10. The cells were expanded, diluting the virus over a week before being sorted based on CD1d surface expression.

2.10.3 PERK, IRE1, ATF6α KD in THP1 cells

Mission® lentiviral particles containing shRNAs targeting PERK, IRE1, and ATF6α, as well a pKLO.1 control (containing an shRNA targeting a bacterial sequence) were purchased from Sigma. Four different shRNAs were selected based on the following criteria: (1) targeting in different regions in the gene of interest and (2) previous validation by the company. THP1 WT cells were infected in a volume of 100μL R-10 with 50,000 viral particles (MOI 2.5). The infected cells

were topped up the following day with 1mL of R-10 and split via a 2X dilutions. At day 3, 3µg/mL puromycin dihydrochloride (Life Technologies) was added to select for the transduced cells, and the cells were maintained thereafter in R-10+1µg/mL puromycin.

2.11 Lipid functional assays

2.11.1 Lipid extraction and fractionation

Equal numbers of WT or PERK KD THP1 cells (~25 million cells) were cultured overnight with or without thapsigargin 0.03µM in T-75 flasks, at a cell concentration comparable to the 96-well plate assays. After treatment, the cells were spun at 1500rpm for 5min. Medium was removed from the pellet, which was then snap frozen in dry ice. The cells were lysed through additional freeze-thaw cycles, and were taken up in 2:1 chloroform:methanol to extract and dissolved the cellular lipids. The resulting lipid mixture was loaded onto SPE amino-propyl columns for fractionation as previously described (Alvarez and Touchstone, 1992). Briefly, fractions were obtained using the following elution solvents, with wash steps in between:

Fraction	*Elution solvent*	*Lipids eluted*
Pre-loading	Aqueous	Upper phase Gangliosides
Lower phase/washing fraction	Chloroform	Unbound material
Fraction I	Diethyl-ether	Cholesterol, Triglyceride, Diglyceride
Fraction II	$CHCl_3$/MeOH 23:1	Ceramides and Monoglycerides
Fraction III	Di-isopropyl-ether/acetic acid 98:4	Free Fatty Acids and OH Fatty Acids
Fraction IV	Acetone/MeOH 9:1:2	Neutral

		glycosphingolipids and Sphingoid Bases
Fraction V	$CHCl_3$/MeOH 2:1	Neutral Phospholipids, PC, PE, sphingomyelin

The amount of lipid (by volume) loaded on the separation column was normalized to total protein in each sample, so as to better compare fractions across samples. The fractions were then dried down under nitrogen gas and resuspended in DMSO for functional assays.

2.11.2 Lipid digestion

Each lipid fraction was resuspended in 2:1 chloroform:methanol and split into the separate tubes for each digestion. The fractions were dried down under nitrogen gas. The dried lipids were resuspended with 10µL of each enzyme in the commercial buffer, vortexed, and incubated at 37°C overnight. The next day, 50µL of 2:1 chloroform:methanol was added to the enzyme-lipid mix and centrifuged at 2500rpm for one minute. This centrifugation formed an aqueous layer on top containing enzyme and an organic phase containing lipids in the 2:1 chloroform:methanol bottom layer. Using gel-loading tips, the bottom layer was carefully pipetted into smaller tubes. The digested lipid C/M solution was dried down as previously described.

2.11.3 CD1d plate bound assay

Streptavidin-coated 96-well flat-bottom plates (Thermo Fisher Scientific, Cat. 15124) were coated with 10µg/mL of biotin-conjugated CD1d monomers (produced in house) in 50µL/well PBS overnight. The following day, the plate was washed twice with PBS and the lipid fractions were added, in duplicate, in 50µL 50mM citrate-phosphate buffer pH5-6. Citrate phosphate buffer was prepared by

mixing 17.9mL of 0.1M citric acid solution (19.21g of citrate to 1L water) and 32.1mL 0.2M dibasic sodium phosphate solution (53.65 g of Na_2HPO_4• $7H_2O$ or 71.7 g of Na_2HPO_4•$12H_2O$ in 1 L). The plate was incubated overnight at 37°C. The following day the plate was washed three times and iNKT cells were added at a concentration of 20,000 cells/well in 200µL/well of R-10. IL12p70 (Peprotech, Cat. 200-12-H-2) was added to the culture at a concentration of 0.05ng/mL for costimulation. The plate was incubated overnight at 37°C and activation was assessed the following day.

2.12 Mass spectrometry and lipidomics

2.12.1 Chemicals and lipid standards for mass spectrometry analysis

Common chemicals and solvents were LC-MS grade from Sigma–Aldrich Chemie (Munich, Germany) and methanol (LiChrosolv grade) from Merck (Darmstadt, Germany). Synthetic lipid standards were purchased from Avanti Polar Lipids, Inc. (Alabaster, AL, USA). Stocks of internal standards were stored in sealed glass ampules at −20 °C. Internal standard mix was prepared in methyl-*tert*-butyl ether (MTBE)/methanol (MeOH) (5:1.5; v/v) containing 1299.73 pmol of cholesterol ester (CE)-D7 16:0; 2133.62 pmol of Chol-D7; 1457.65 pmol of TG-D5 50:0; 145.35 pmol of DG-D5 34:0; 1100.88 pmol of phosphatidylcholine (PC) 25:0; 692.61 pmol of phosphatidylethanolamine (PE) 25:0; 383.62 pmol of phosphatidylinositol (PI) 25:0; 334.07 pmol of phosphatidylserine (PS) 25:0; 77.06 pmol of phosphatidic acid (PA) 25:0; 163.21 pmol of LPC 13:0; 106.33 pmol of lyso-phosphatidylethanolamine (LPE) 13:0; 140.63 pmol of lyso-

phosphatidylinositol (LPI) 13:0; 113.51 pmol lyso-phosphatidic acid (LPA) 13:0, 272.42 pmol of Cer 30:1:2; 554.90 pmol of SM 30:1:2 and 135.88 pmol of galactosylceramide (GalCer) 30:1:2 and stored at −20 °C until the analysis. Whole lipid extracts were also included as a control to ensure that lipids from the fractions reflected the cellular lipid content, and not extracellular contamination introduced during the sample processing.

2.12.2 Lipid quantification by shotgun mass spectrometry

700µl of a mixture of internal standards in MTE/MeOH (5:1.5; v/v) were added to the dried lipid fractions. Mass spectrometric analyses were performed as previously described (Schuhmann et al., 2012). Lipid extracts were vacuum dried and re-suspended in ethanol/chloroform 5:1 (v/v) containing 0.1% triethylamine for analysing PS to avoid overlapping with formate adducts of odd-chain PCs or in isopropanol/methanol/chloroform 4:2:1 (v/v/v) containing 7.5 mM ammonium formate for other lipids. Mass spectrometric analysis was performed on a Q Exactive instrument (Thermo Fisher Scientific, Bremen, Germany) equipped with a robotic nanoflow ion source TriVersa NanoMate (Advion BioSciences, Ithaca NY, USA) using nanoelectrospray chips with the diameter of spraying nozzles of 4.1 µm. The ion source was controlled by the Chipsoft 8.3.1 software (Advion BioSciences). Ionization voltage was +0.96 kV in positive and −0.96 kV in negative mode; backpressure was 1.25 psi in both modes by polarity switching. The temperature of the ion transfer capillary was 200 °C; S-lens RF level was 50%. Targeted-selected ion monitoring (t-SIM) spectra were acquired within the range of

m/z 300–1000 in positive mode and in negative mode respectively, at a mass resolution of $R_{m/z200} = 140000$ and with automated gain control of 5×10^4. Free Chol was quantified by parallel reaction monitoring Fourier transform (FT) MS/MS in positive mode. For FT MS/MS, the number of micro scans was set to 1, isolation window to 0.8 Da, normalized collision energy to 12.5%, AGC to 5×10^4. Spectra was filtered based on repetition rate as previously described (Schuhmann et al., 2017) and stitched together by a lab-developed script. Lipids were identified by LipidXplorer software (Herzog et al., 2011). Molecular Fragmentation Query Language (MFQL) queries were compiled for PC, PC O-, LPC, LPC O-, PE, PE O-, LPE, PI, LPI, PG, PS, PA, LPA, Cer, SM, hexosylceramide (hexCer), Chol, CE, TG, and DG lipid classes. Lipids were identified based on accurately determined intact lipid masses (mass accuracy better than 5 ppm) and quantified by comparing the isotopically corrected abundances of their molecular ions with the abundances of internal standards of the same lipid class. Only lipids whose monoisotopic peaks were detected with a signal-to-noise ratio above the value of 5 were quantified. Lipid amount was either normalized to corresponding protein amount to total lipids in each fraction and represented as percentage of total.

2.13 VITAL Assay

The VITAL was performed as previously described (Hermans et al., 2004). Briefly, $3X10^6$ target cells were either (1) left unpulsed, (2) pulsed for three hours with 100ng/mL αGC in 1mL of R-10, or (3) pre-treated with thapsigargin 0.03μM for six hours and washed the previous day. Half of the cells for each treatment

were washed in PBS and the other half washed with R-10. The cells washed in PBS were labelled with 333nM CFSE (Life Technologies) at room temperature for 8 minutes, and then washed twice in R-10 to quench the reaction. The cells washed in R-10 were labelled with 10μM CMTMR (Life Technologies) in R-10 for 15 minutes at 37°C, and then washed and incubated in fresh R-10 for another 15 minutes at 37°C, and washed twice more. 6000 targets cells of each CFSE and CMTMR populations were added to one well of a 96-well plate. iNKT cells were added at the different ratios described, and the co-culture was incubated for about 4 hours with THP1 WT cells and overnight for the myeloma lines.

2.14 *In vivo* murine experiments

Animal studies were performed with appropriate UK Home Office Project and Personal licenses, with ethical approval from the University of Oxford. C57BL/6 WT and CD1d$^{-/-}$ (C57BL/6-*Cd1d1*$^{tm1.2Aben}$/J, JAX stock # 017294) were cared for at the Biomedical Service Unit (John Radcliffe Hospital, Oxford, UK). Intravenous tail-vein injections were performed using 500,000 *ex vivo* differentiated bone marrow-derived DCs suspended in 100μL PBS. Recipient mice were culled 24 hours later. Spleens were harvested, processed into a single cell suspension, and treated with red blood cell lysis buffer before being stained for flow cytometry analysis. A total of 129 mice were culled for this project.

2.15 Immunohistochemistry

2.15.1 Antibodies

Marker	*Dilution*	*Species*	*Clone*	*Supplier*	*Catalogue Number*
BiP	1:400	Rabbit	C50B12	Cell Signalling Technology	3177S
CD11c	1:20,000	Rabbit	EP1347Y	abcam	ab52632

2.15.2 Protocol

The Oxford Centre for Histopathology Research (OCHRe) provided human tumour sections under the project code 16/A194 and 19/A075. Slides of paraffin-embedded tissue sections where immersed in Histoclear II (national diagnostics) for 5 minutes each to remove the paraffin. The tissue sections were rehydrated through washes in 100%-95%-70% ethanol, for 3 minutes each before being washed in distilled water for 5min. Heat-induced antigen retrieval was performed by submerging the slides in Dako Antigen Retrieval Buffer and steaming them in a microwave for 20 minutes. The slides were cooled to ~30°C and washed in TBS-T. Treating the tissue sections with Dako Peroxidase Block for 15min at room temperature quenched endogenous peroxidase activity. The slides were washed 3 times with TBS-T. The slides were blocked in Daku protein-free blocking solution for 15 minutes at room temperature. The blocking solution was drained before adding 150µL of primary antibody diluted in Dako Antibody Diluent to the slides for 1 hour at room temperature. After washing 3 times with TBS-T, the secondary antibody (Envision anti-rabbit/mouse, HRP conjugated) was added for 30 minutes at room temperature. The slides were washed 3-5 times before adding the DAB

chromogen substrate (1 drop DAB enhancer in 1mL of DAB substrate, Dako) for ~3 minutes followed by rinsing the slides with distilled water. To counterstain the sections, Meyer's Haematoxylin was added for 3 minutes, washed off with distilled water (until the water runs clear), and then treated with ammoniated water (1-2 drops of ammonium hydroxide solution into 50mL of distilled water~1% solution). Slides were washed in water and left to dry completely at room temperature overnight. The following day, slides were covered slipped using Limonene (abcam) and left to dry overnight. Images were acquired using the Olympus BX60 with Infinity3S Lumenera® software.

2.16 Statistical Analysis

Statistical analysis was performed where biological replicates N were equal to or greater than three. Cytokine secretion was assumed to follow a Gaussian distribution and analysis was performed. Normality tests were performed when necessary. Points represent the mean of technical duplicates for each biological experiment, and the error bars represent standard error around the mean. Statistical analysis was performed in Graphpad Prism Version 5.0a.

Chapter 3: ER-stressed CD1d$^+$ cells activate iNKT cells in a CD1d-dependent manner

The mechanisms underlying iNKT cell activation against foreign pathogens, including bacteria and viruses, have been extensively studied *in vitro* and *in vivo*. iNKT cells can also modulate immune responses in sterile pathologies, but the mechanism(s) driving their activation in these situations has not been fully elucidated. We demonstrate that ER-stressed CD1d$^+$ cells activate iNKT cells *in vitro* and *in vivo* via signalling through CD1d-presentation with IL-12 stimulation.

3.1 The iNKT cell response to DCs treated with classical inducers of ER-stress: Thapsigargin and Tunicamycin

To determine if ER-stress in CD1d$^+$ APCs can activate iNKT cells, we pre-treated monocyte-derived DCs (MoDCs) from healthy donors with a dose-curve of thapsigargin and tunicamycin, washed the cells, and co-cultured them overnight with allogeneic polyclonal human iNKT cells expanded from healthy donors. As a control we assessed the viability of the monocultured, pre-treated MoDCs, as strong and/or persistent signalling through the UPR can trigger cell death. As shown in **Figure 3.1.1**, we observed that with decreasing concentrations of the two reagents there was an increase in MoDC viability, approaching the same viability as the DMSO solvent control. Neither drug induced a detectable amount of IL-

12p40 secretion from the monocultured, pre-treated MoDCs (**Figure 3.1.1A**).

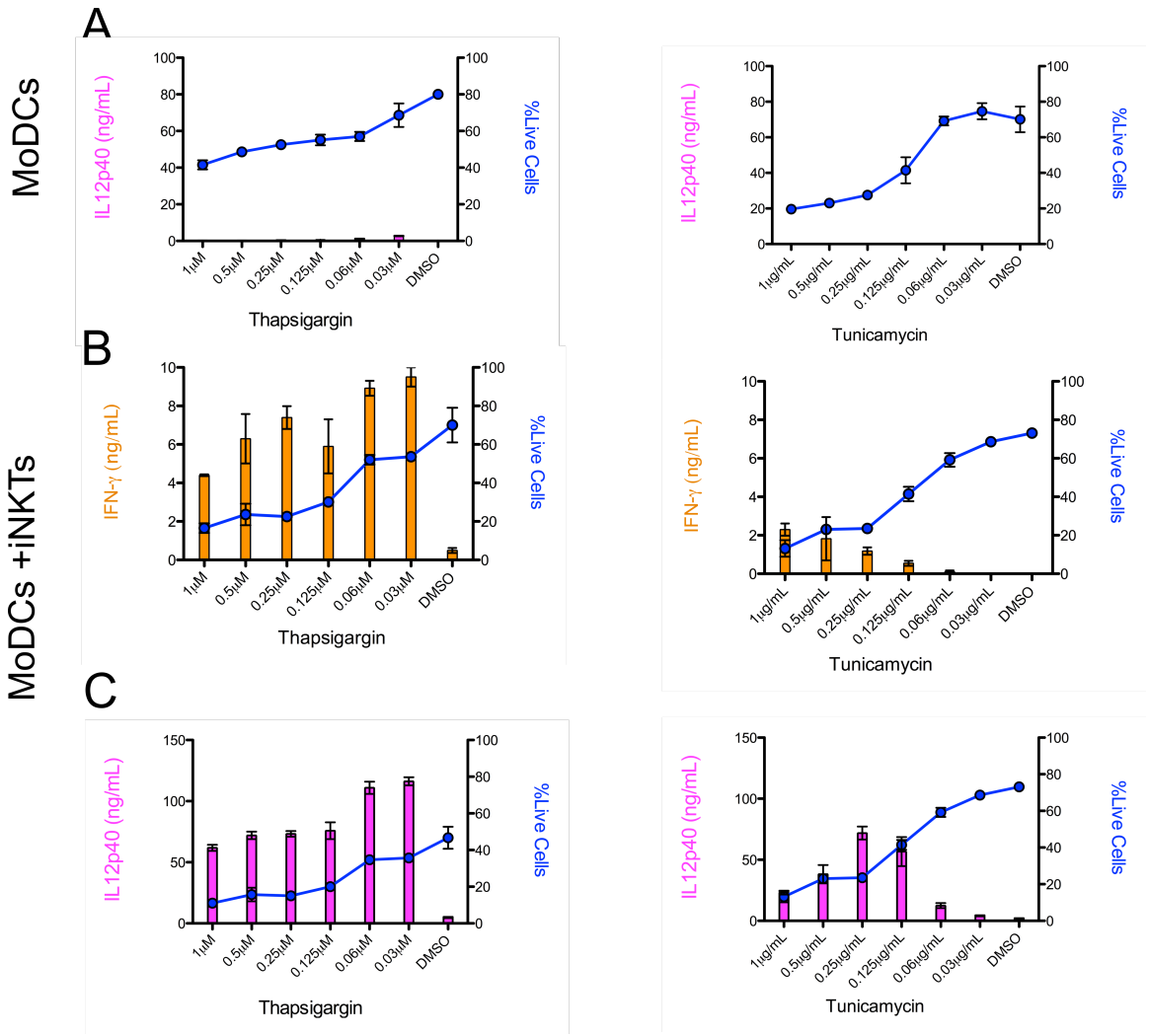

Figure 3.1.1 The dose-dependent effects of thapsigargin and tunicamycin on MoDC survival, IL-12p40 secretion, and IFN-γ secretion from co-cultured human iNKT cells. (A) IL-12p40 secretion (pink) and cell death (blue) was measured in MoDCs pre-treated with decreasing doses of thapsigargin (left) and tunicamycin (right). **(B)** MoDCs pre-treated with decreasing doses of thapsigargin (left) and tunicamycin (right) were co-cultured with iNKT cells overnight. Cell death of MoDCs in the co-culture (blue) and activation of iNKT cells was measured by IFN-γ secretion (orange) **(C)** MoDCs pre-treated with decreasing doses of thapsigargin (left) and tunicamycin (right) were co-cultured with iNKT cells overnight. Cell death of MoDCs in the co-culture (blue) and maturation of MoDCs by iNKT cells was measured by IL-12p40 secretion (pink). Cytokine secretion and cell death measurements represent the average of N=2 biological replicates, each performed in technical duplicate.

However, upon co-culture with iNKT cells, thapsigargin-treated MoDCs induced IFN-γ secretion, which increased with decreasing concentrations of thapsigargin

(**Figure 3.1.1B**). The increased MoDC viability with decreasing thapsigargin concentrations might explain this inverse correlation. Tunicamycin did not induce appreciable IFN-γ secretion and followed a direct correlation with drug concentration. Similarly, IL-12p40 secretion from pre-treated MoDCs increased upon co-culture with iNKT cells, but particularly upon pre-treatment with thapsigargin (**Figure 3.1.1C**). In this case, the activated iNKT cells likely fed back on the MoDCs to enhance MoDC maturation. Activated iNKT cells killed the thapsigargin pre-treated MoDCs in co-culture.

We wanted to ensure that the concentrations of thapsigargin used in the functional assays did induce the UPR. To this end, we prepared protein lysates from THP1 WT cells treated with different concentrations of thapsigargin from the dose curve and the highest concentration of tunicamycin. We observed upregulation of chaperones like BiP and PDI, which are largely regulated by the ATF6 and IRE1 pathway respectively, as well as ATF4 and CHOP, transcription factors downstream the PERK pathway in the treated cells (**Figure 3.1.2A**). Furthermore, *XBP1* splicing by PCR analysis was evident in thapsigargin-treated cells compared to the controls (**Figure 3.1.2B**).

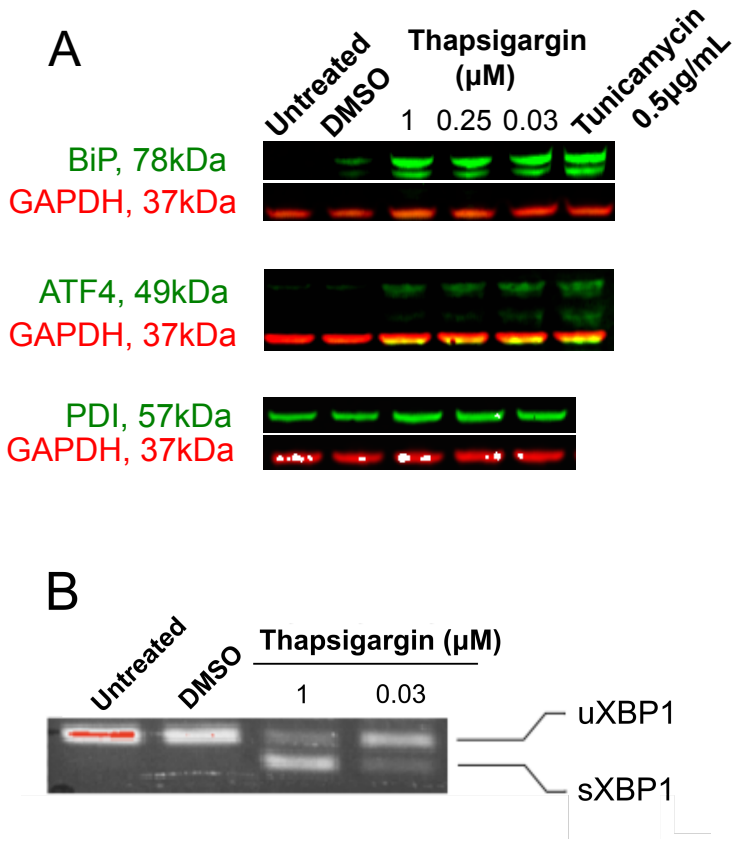

Figure 3.1.2 Thapsigargin and tunicamycin trigger the unfolded protein response in treated THP1 cells. (A) Western blot validation of ER stress and UPR in THP1 cells treated with the indicated concentrations of thapsigargin and tunicamycin. Green bands represent protein expression of BiP (left) PDI (centre) and CHOP (right); red bands represent loading controls (GAPDH). **(B)** mRNA splicing of the transcription factor XBP1 upon thapsigargin treatment of THP1 cells, indicating increased ER-stress and UPR activation. Experiments are representative of N=3 biological replicates.

Given that both thapsigargin and tunicamycin induced the UPR, yet only thapsigargin pre-treated MoDCs activated iNKT cells, we wondered whether the their specific mechanisms of action could account for these different effects. iNKT cells can be activated through cognate interactions between their semi-invariant TCR and lipid-loaded CD1d on the surface of APCs. CD1d molecules, like other antigen presentation molecules destined for the cell surface, are glycosylated at multiple sites in the ER to allow for egress through the Golgi network to the plasma membrane (Bagriacik et al., 1996, Sriram et al., 2008). However, since

tunicamycin blocks N-linked glycosylation on proteins in the ER, we hypothesized that CD1d might not reach the cell surface in tunicamycin pre-treated MoDCs, therefore failing to activate iNKT cells even while undergoing the UPR. To address this possibility, we tested whether THP1-CD1d overexpressing cells (THP1-CD1d) cells pre-treated with thapsigargin or tunicamycin showed different CD1d surface expression compared to the solvent control (DMSO). As an additional control, we investigated the effect of these pre-treatments on MHC class I expression. While thapsigargin pre-treated THP1-CD1d cells expressed CD1d and MHC class I levels comparable to the DMSO control, tunicamycin pre-treated THP1-CD1d cells expressed lower CD1d and MHC class I levels (**Figure 3.1.3**), suggesting that the lack of activation of iNKT cells in tunicamycin-treated MoDCs might be due to the reduced surface levels of CD1d.

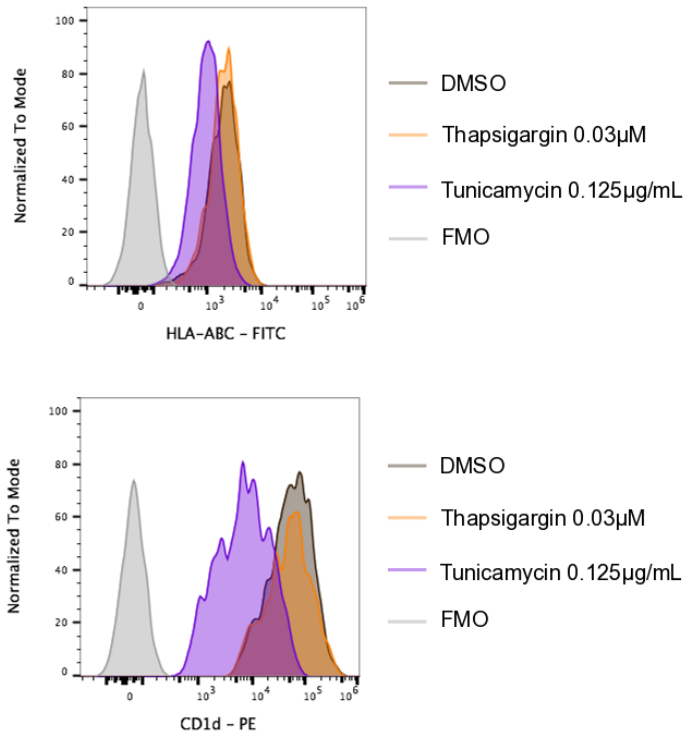

Figure 3.1.3 Tunicamycin treatment results in the downregulated surface expression of MHC class I and CD1d. THP1-CD1d overexpressing cells pre-treated with thapsigargin 0.03μM, tunicamycin 1.25μg/mL, or solvent control DMSO, were stained and analysed by flow cytometry for **(A)** MHC class I (HLA-ABC) surface expression and **(B)** CD1d expression. The histograms represent an N=2 biological replicates, each performed in technical duplicates.

While our primary cytokine readout for iNKT cell activation was IFN-γ, we assessed the secretion of alternate cytokines. These included the cytokines IL-4, IL-13, and GMCSF, the latter of which enhances myeloid cell maturation. Secretion of all three of these cytokines from iNKT cells was augmented upon co-culture with thapsigargin pre-treated MoDCs (**Figure 3.1.4**). As we were primarily interested in whether ER-stressed APCs can elicit a Th1 response in iNKT cells, future experiments focused on IFN-γ secretion.

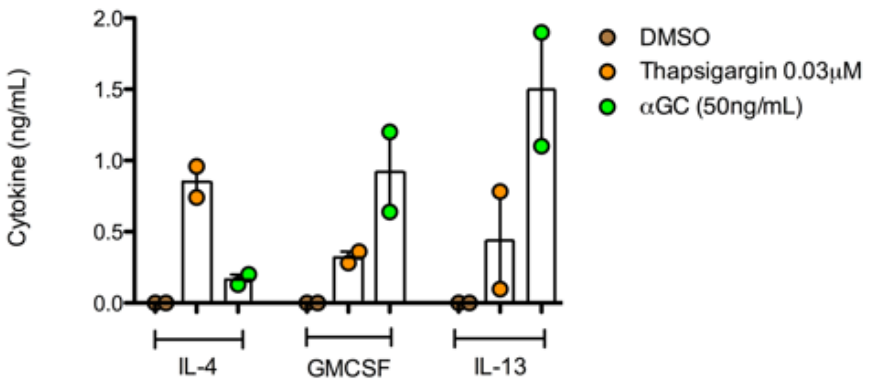

Figure 3.1.4 Thapsigargin pre-treated MoDCs induce secretion of multiple cytokines from human iNKT cells. IL-4, GMCSF, and IL-13 secretion in co-cultures of iNKT with untreated, thapsigargin-treated, or αGC-pulsed MoDCs. Average of N=2 biological replicates, each performed in technical duplicates.

We wondered how iNKT cell activation by thapsigargin pre-treated MoDCs compared to that of other classical iNKT cell agonists. To this end, we compared thapsigargin pre-treated MoDCs to those pulsed with the CD1d-binding antigenic lipid αGC and to MoDCs pre-treated with LPS, a bacterial endotoxin and TLR4

agonist that promotes CD1d-presentation of immunogenic self-lipids (Salio et al., 2007) (**Figure 3.1.5**). Readouts for activation included (**A**) IFN-γ secretion from activated iNKT cells, (**B**) upregulated surface expression of the IL-2 receptor CD25 on iNKT cells (**C**) augmented IL-12p40 secretion from the MoDCs, which undergo enhanced maturation in response to activated iNKT cells, and (**D**) upregulated surface expression of the co-receptors CD83 and CD86 on the MoDCs upon enhanced maturation. αGC, a strong exogenous lipid antigen, represents the near maximal degree of iNKT cell activation through primarily cognate CD1d:TCR interaction. Direct thapsigargin treatment of iNKT cells failed to activate them, supporting the notion that any residual thapsigargin in the co-culture was not directly activating the iNKT cells through calcium flux/signalling. Thapsigargin pre-treated MoDCs activated iNKT cells to a degree similar to LPS, which activates iNKT cells through a combination of weak CD1d:TCR interaction and cytokine signalling events.

The similarity in thapsigargin and LPS pre-treated MoDC-mediated iNKT cell activation begged the question of whether the commercially acquired thapsigargin is contaminated with endotoxin or is signalling through an alternative common pathway in the APC to activate the iNKT cells. To test this, we pre-treated BMDCs cultured from wild type or MyD88$^{-/-}$ mice with thapsigargin and a panel of TLR ligands, and measured IL-12p40 secretion from the BMDCs with and without iNKT cells. As expected, IL-12p40 secretion induced by TLR agonists was reduced in MyD88$^{-/-}$ BMDCs compared to the WT ones (**Figure 3.1.6**). The response to thapsigargin did not appear to change dramatically between pre-

treated WT and MyD88$^{-/-}$ BMDCs compared the DMSO controls, but when comparing to the untreated condition, there was a decrease in IL-12p40 secretion within MyD88$^{-/-}$ BMDCs compared to WT upon iNKT cell co-culture. The different interpretation, depending on which control one compares, makes it difficult to draw a solid conclusion from this experiment.

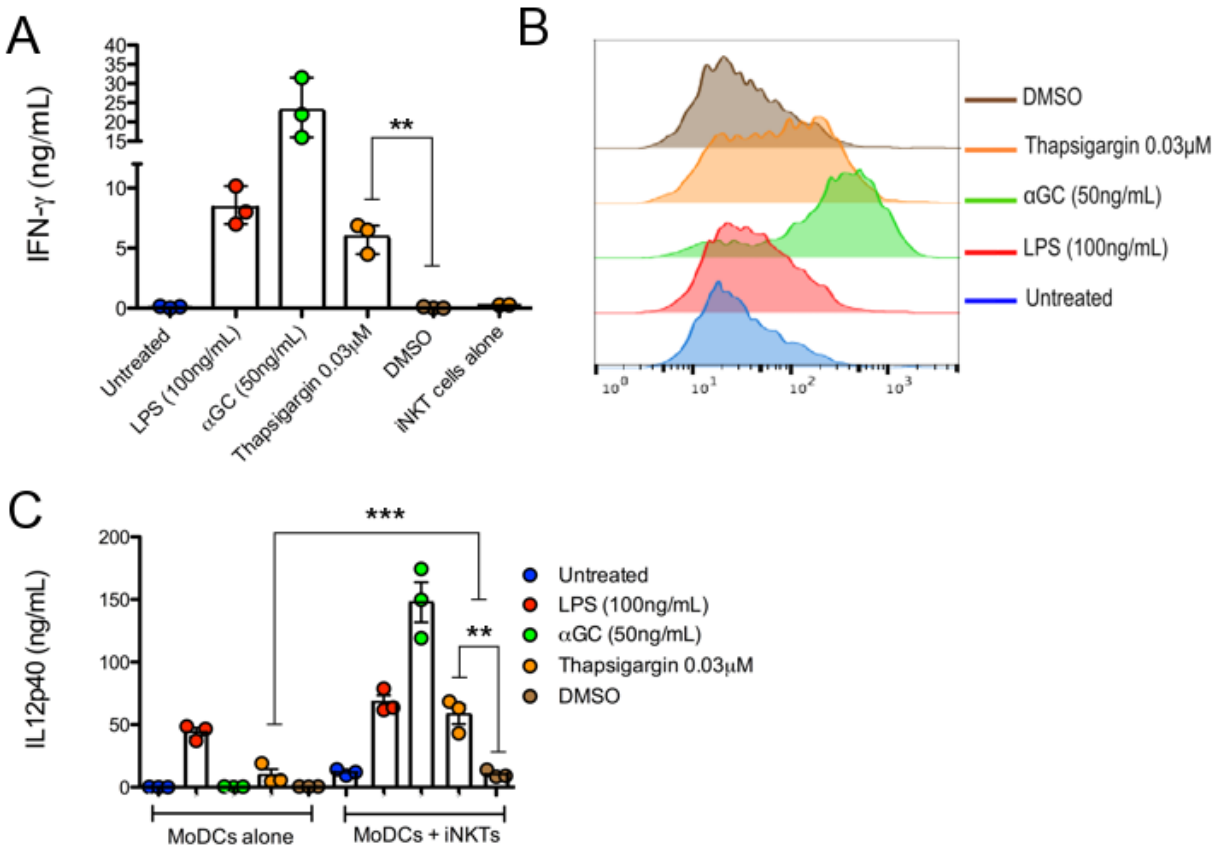

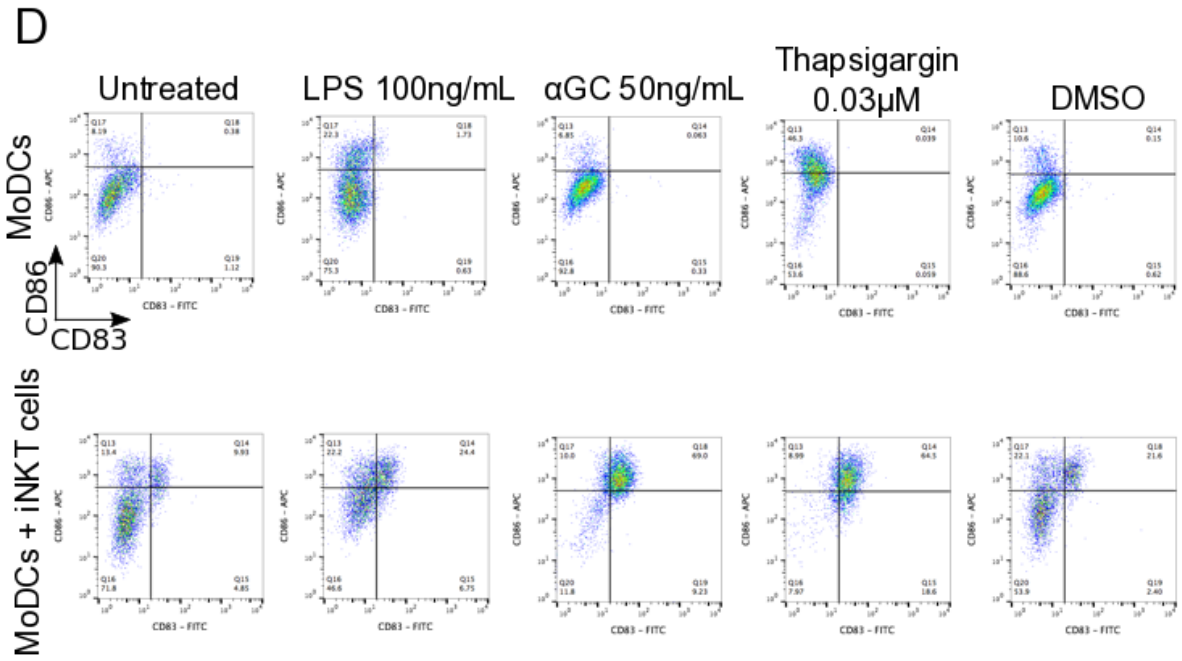

Figure 3.1.5 Thapsigargin pre-treated MoDCs induce iNKT cell activation that enhances MoDC maturation. Human monocyte-derived DCs (MoDCs) treated as indicated were co-cultured with human iNKT cells. iNKT cell activation was measured by secretion of IFN-γ from iNKT cells **(A)** and by increased surface expression of CD25 on iNKT cells **(B)**. ** represents $p<0.005$ by an unpaired, two-tailed t test. IFN-γ secretion is the average of N=3 biological replicates, and the CD25 histograms are representative of N=3 biological replicates, each performed in technical duplicates. MoDCs treated as indicated were either left untreated (MoDCs alone) or co-cultured with human iNKT cells. MoDCs maturation is measured by **(C)** IL-12p40 secretion in the supernatants or **(D)** surface expression of CD83 and CD86 on MoDCs. ** and *** represents $p<0.005$ and $p<0.001$, respectively, by a one-way ANOVA with a Bonferroni post-test. The histograms or representative of and IL-12p40 secretion is the average of N=3 biological replicates, each performed in technical duplicates.

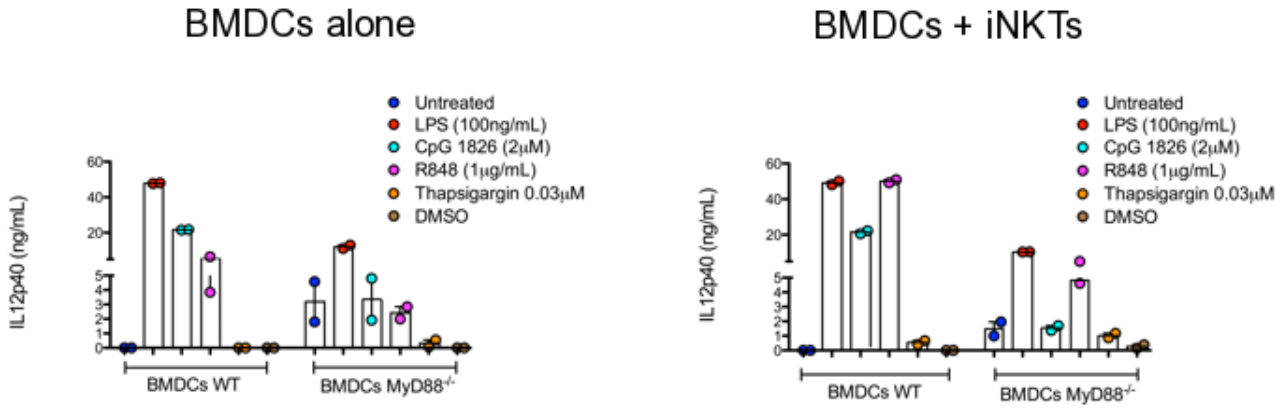

Figure 3.1.6 iNKT cell activation by thapsigargin pre-treated BMDCs might require MyD88-mediated signalling events. BMDCs from wild type or MyD88$^{-/-}$ mice were pre-treated as indicates and either cultured alone (left) or with human iNKT cells (right). Maturation of BMDCs was measure of IL-12p40 secretion in the supernatants. IL-12p40 secretion is the average of N=2 biological replicates, each performed in technical duplicates.

3.2 How ER-stressed APCs alter 'unconventional' T cell activation: MAIT, γδ, iNKT cells with ER-stressed MoDCs

Since tunicamycin both fails to activate iNKT cells and reduces surface expression of CD1d on APCs, we suspected that ER-stressed APC-mediated iNKT cell activation was, at least in part, CD1d-dependent. However, given the result in **Figure 3.1.6**, we realized that additional signalling events might affect APC maturation and potentially influence different T cell populations. To address these questions, we tested if ER-stressed APC-mediated activation was restricted to iNKT cells or could apply to other unconventional T cells, including human MAIT cells and γδ T cells, the latter of which expresses a distinct γδ (as opposed to αβ) TCR capable of recognizing a variety of antigens through unconventional means of presentation (Melandri et al., 2018). Both types of T cells, in addition to iNKT cells, were co-cultured with thapsigargin pre-treated MoDCs as previously described. While the positive controls for each cell type illustrated that they could

secrete IFN-γ (**Figure 3.2A**) and upregulate CD25 (**Figure3.2B**) upon activation, thapsigargin pre-treated MoDCs only activated iNKT cells. This finding suggested that ER-stressed APC-mediated activation modulated CD1d:TCR interaction, as opposed to TCR interactions with other antigen presenting molecules. Furthermore, this result indicated that soluble mediators that influence iNKT and MAIT cell activation, like IL-12 and IL-18, or signalling through innate pathways in the APCs, like the MyD88 pathway that would likely effect activation of broad subsets of T cells (Brutkiewicz, 2016), are likely not primarily responsible for ER-stressed APC-mediated activation.

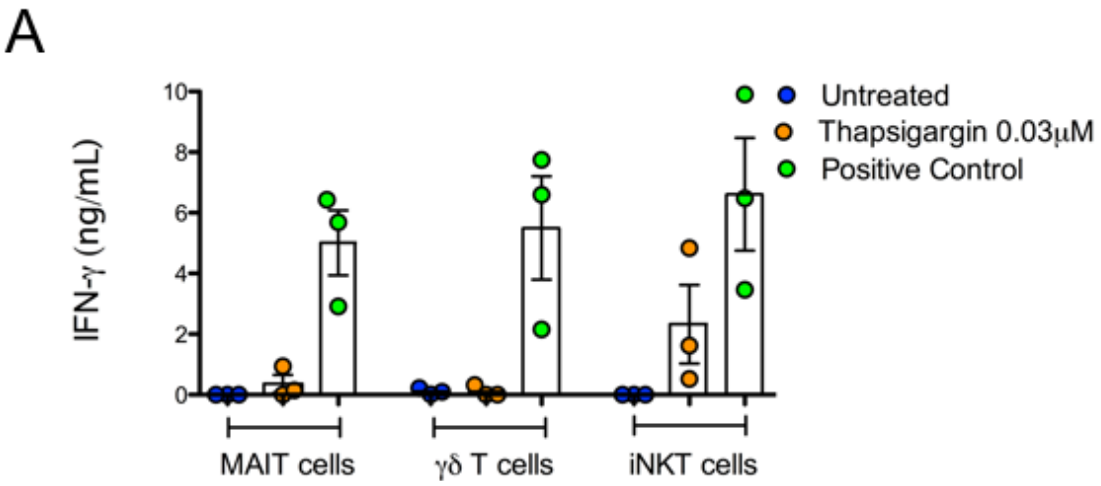

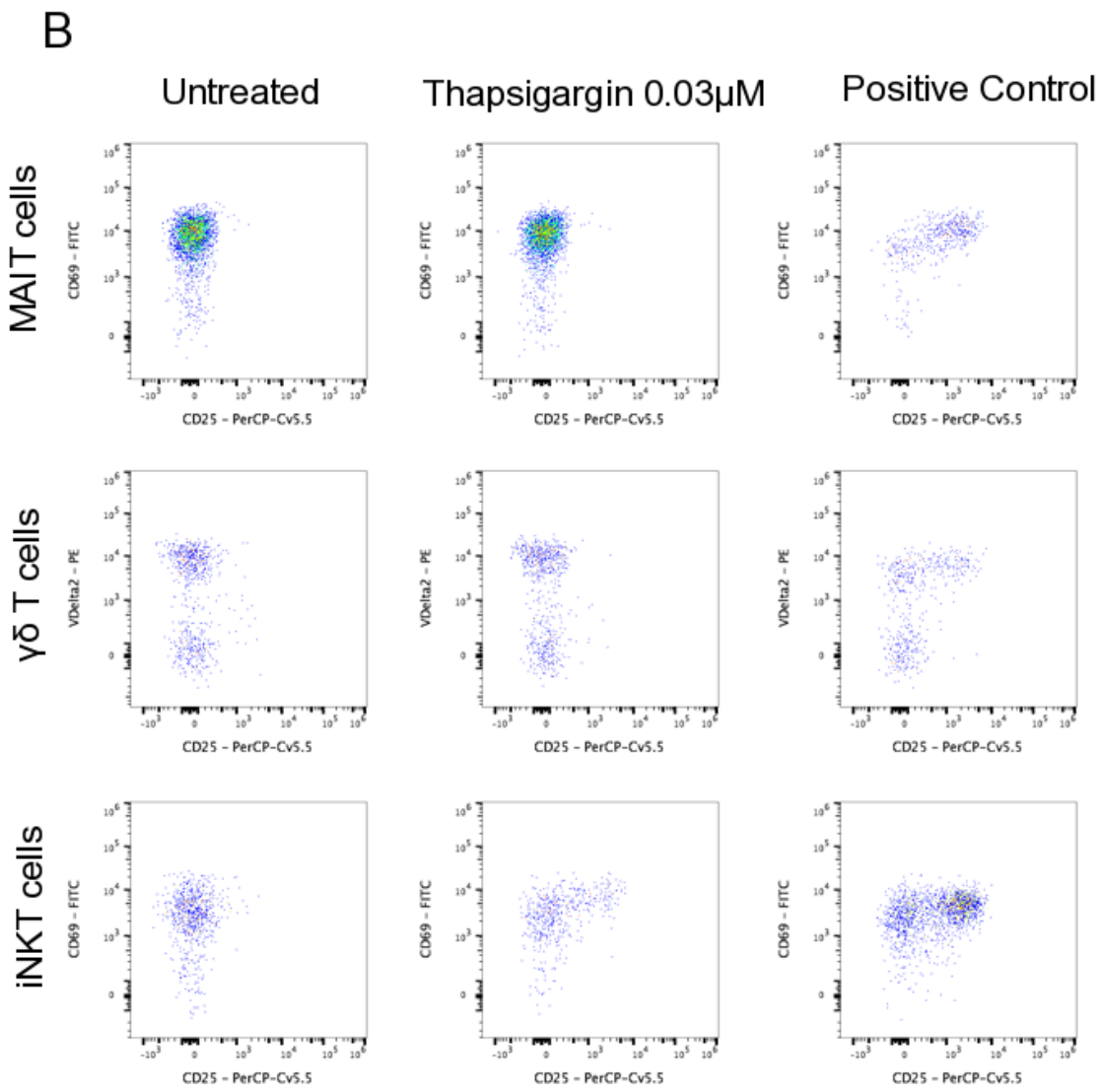

Figure 3.2 Thapsigargin pre-treated MoDCs do not induce activation of human MAIT and γδ T cells. MoDCs were either left untreated, treated with thapsigargin, αGC (50ng/mL), 5ARU (1μg/mL) + Methyl Glyoxal (50μM), or HMBPP (1μM) as positive controls and co-cultured with either iNKT, MAIT or γδ T cells. Activation was measured by (**A**) IFN-γ in the supernatants and by increased (**B**) CD25 expression on the T cells. The dot plots are representative of and IFN-γ secretion is the average of N=3 biological replicates, each performed in technical duplicates.

3.3 Sterile activation of iNKT cells requires cognate interaction with CD1d

Following from section 3.2, we sought to determine whether CD1d:TCR interactions and signalling drive ER-stressed APC-mediated iNKT cell activation. To address this question, we pre-treated BMDCs from WT or CD1d$^{-/-}$ mice as listed in **Figure 3.3.1**, and co-cultured the BMDCs with human iNKT cells. αGC

was presented efficiently by WT BMDCs and activated iNKT cells, inducing IFN-γ secretion (**Figure 3.3.1A**) and CD25 upregulation (**Figure 3.3.1B**), which was abrogated with the $CD1d^{-/-}$ BMDCs. In contrast, WT and $CD1d^{-/-}$ BMDCs pre-treated with LPS, which can activate iNKT cells through a combination of CD1d-dependent self-lipid presentation and CD1d-independent cytokine secretion, activated iNKT cells (albeit the activation is partially reduced with the $CD1d^{-/-}$ BMDCs as expected). Thapsigargin pre-treated WT BMDCs activated iNKT cells, whereas their $CD1d^{-/-}$ counterparts failed to do so. This finding suggested that thapsigargin-mediated iNKT activation is predominantly CD1d-dependent. Furthermore, there was a dose-dependent decrease in CD25 expression on the iNKT cells when varying the E:T ratio with WT BMDCs. However, there was no activation of iNKT cells with any proportion of $CD1d^{-/-}$ BMDCs (**Figure 3.3.1C**). A dose dependency in iNKT cell activation was also observed when comparing thapsigargin pre-treated THP1-CD1d cells versus THP1 WT cells (**Figure 3.3.1D**). To compliment this result, we tested whether ER-stressed APC-mediated iNKT cell activation could be reduced with the addition of a CD1d blocking antibody (**Figure 3.3.1D**). Addition of the CD1d blocking antibody, with both THP1 WT and CD1d cells, reduced iNKT cell activation, compared to isotype controls. CD1d-blockade reduced only partially iNKT cell activation in response to LPS and αGC.

Since blocking antibodies can have adverse effects by retroactively signalling through their target, we were aware that the reduced iNKT cell activation upon the addition of the blocking antibody might be due to killing of the THP1 cells, particularly with the THP1-CD1d cells. When assessing unpulsed and αGC-pulsed

THP1-CD1d cell viability upon addition of the antibodies, there was an increase in cell death with the blocking antibody compared to the isotype control, particularly when CD1d was bound to αGC (**Figure 3.3.1E**). This adverse effect might be a confounding factor in this experiment.

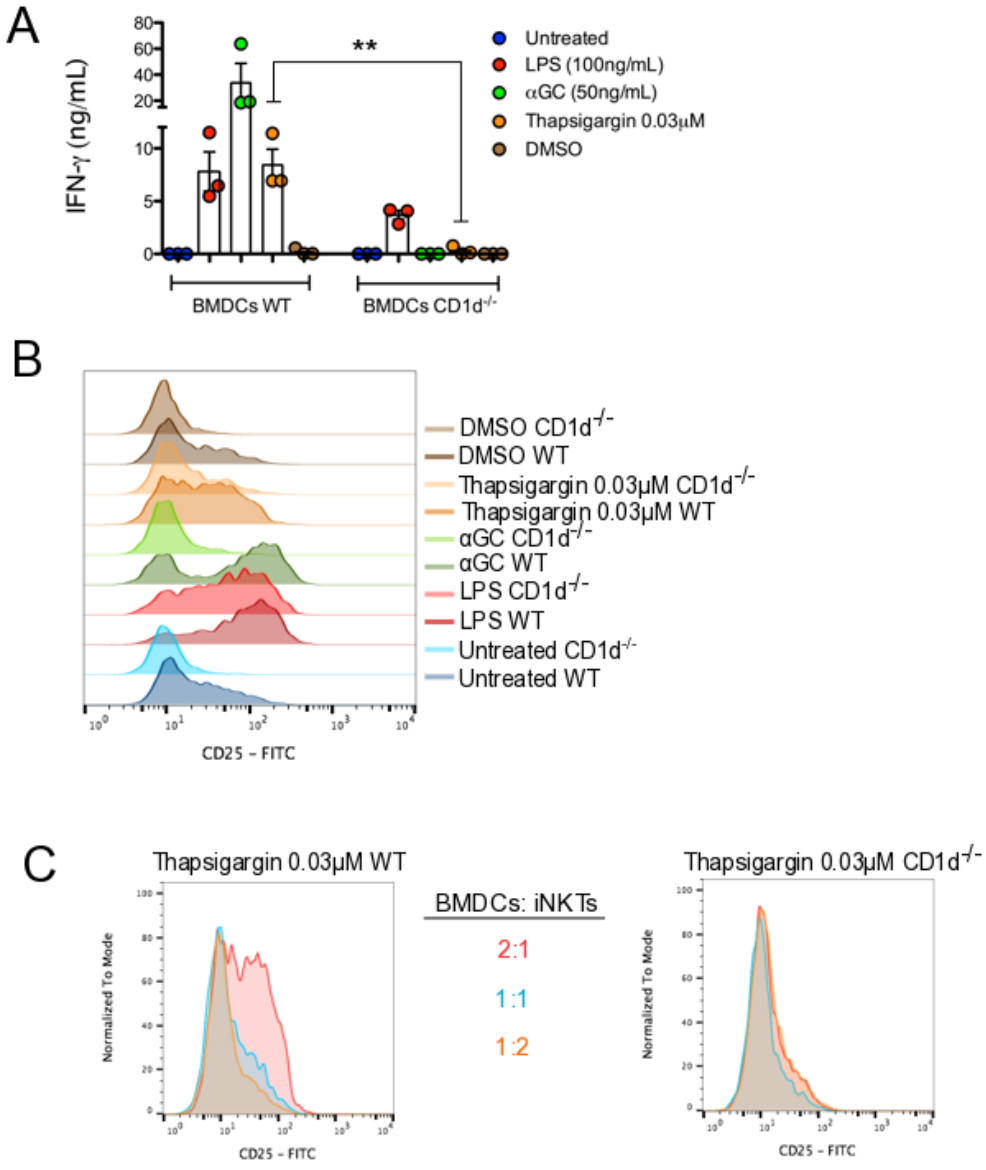

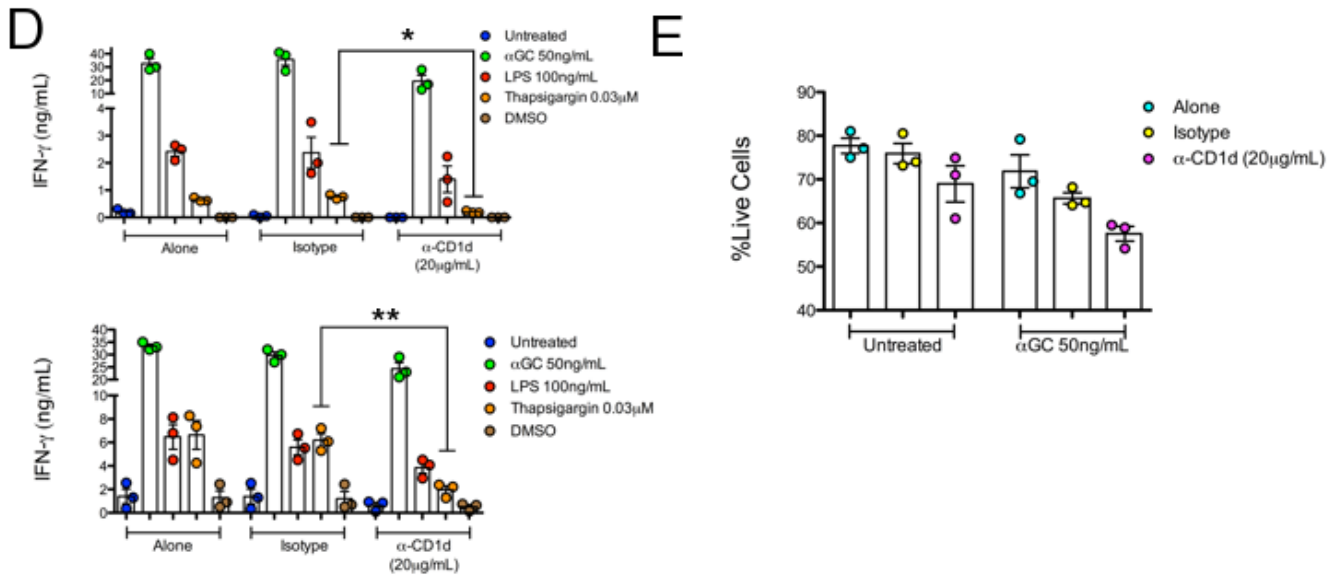

Figure 3.3 Thapsigargin pre-treated APCs activate iNKT cells in a CD1d-dependent manner. Bone marrow derived DCs (BMDCs) from wild type and CD1d$^{-/-}$ mice were co-cultured with human iNKT cells. iNKT cell activation was measured by **(A)** IFN-γ secretion and **(B)** CD25 upregulation. ** represents p<0.005 by an unpaired, two-tailed t test. IFN-γ secretion is the average of N=3 biological replicates, and the CD25 histograms are representative of N=3 biological replicates, each performed in technical duplicates. **(C)** Human iNKT cells were co-cultured with a decreasing proportion of thapsigargin-treated wild type or CD1d$^{-/-}$ BMDCs (BMDCs:iNKTs) and iNKT cell activation was assessed by CD25 upregulation. These histograms are representative of N=3 biological replicates, each performed in technical duplicates**. (D)** THP1 cells treated as indicated then co-cultured with human iNKT cells in the presence of CD1d blocking antibody (20μg/mL) or the appropriate isotype control. ** represents p<0.005 by an unpaired, two-tailed t test. IFN-γ secretion is the average of N=3 biological replicates, each performed in technical duplicates. **(E)** Cell death is measured for THP1 cells treated as indicated in the presence of CD1d blocking antibody (20μg/mL) or the appropriate isotype control. These results are representative of an N=3, performed in technical duplicates.

3.4 IL-12 boosts ER-stressed APC-mediated iNKT cell activation

A number of sufficient 'signals' from APCs are collectively required to generate a T cell response. 'Signal 1' generally refers to the recognition of antigen on antigen-presenting molecules, like CD1d, by the cognate TCR. 'Signal 2' refers to signalling through the binding of costimulatory receptors to their ligands, for example CD28 on T cells binding CD80/CD86 on APCs. 'Signal 3' refers to cytokine stimulation to boost the other signals to achieve T cell activation. Certain

exogenous, foreign antigens, like αGC, exhibit high TCR affinity, such that signal 1 is sufficient to reach the minimum signalling threshold required for T cell activation. However, weaker antigens, like self-lipids, require an additional boost beyond signal 1 to achieve iNKT cell activation. For iNKT cells, where certain costimulatory molecules i.e. signal 2, are ubiquitously expressed (van den Heuvel et al., 2011), the boost comes from signal 3. Therefore, we wondered if cytokines or other soluble factors provide a 'signal 3' in this mode of iNKT cell activation.

To broadly address this issue, supernatants from thapsigargin pre-treated wild type and CD1d$^{-/-}$ BMDCs were added to human iNKT cells overnight, and then assessed for CD25 upregulation. While supernatants from LPS pre-treated BMDCs, both WT and CD1d$^{-/-}$, activated iNKT cells through soluble factors, supernatants from thapsigargin pre-treated BMDCs failed to do so (**A**). However, some cytokines exhibit limited cross-reactivity between mouse and human cells. To this end, we tested whether adding an IL-12 blocking antibody would reduce iNKT cell activation to thapsigargin pre-treated human MoDCs. We observed that the IL-12 blocking antibody did partially reduce IFN-γ secretion from iNKT cells (**Figure 3.4B**), suggesting that IL-12 might provide a signal 3 to boost activation to self-lipid antigens presented on CD1d.

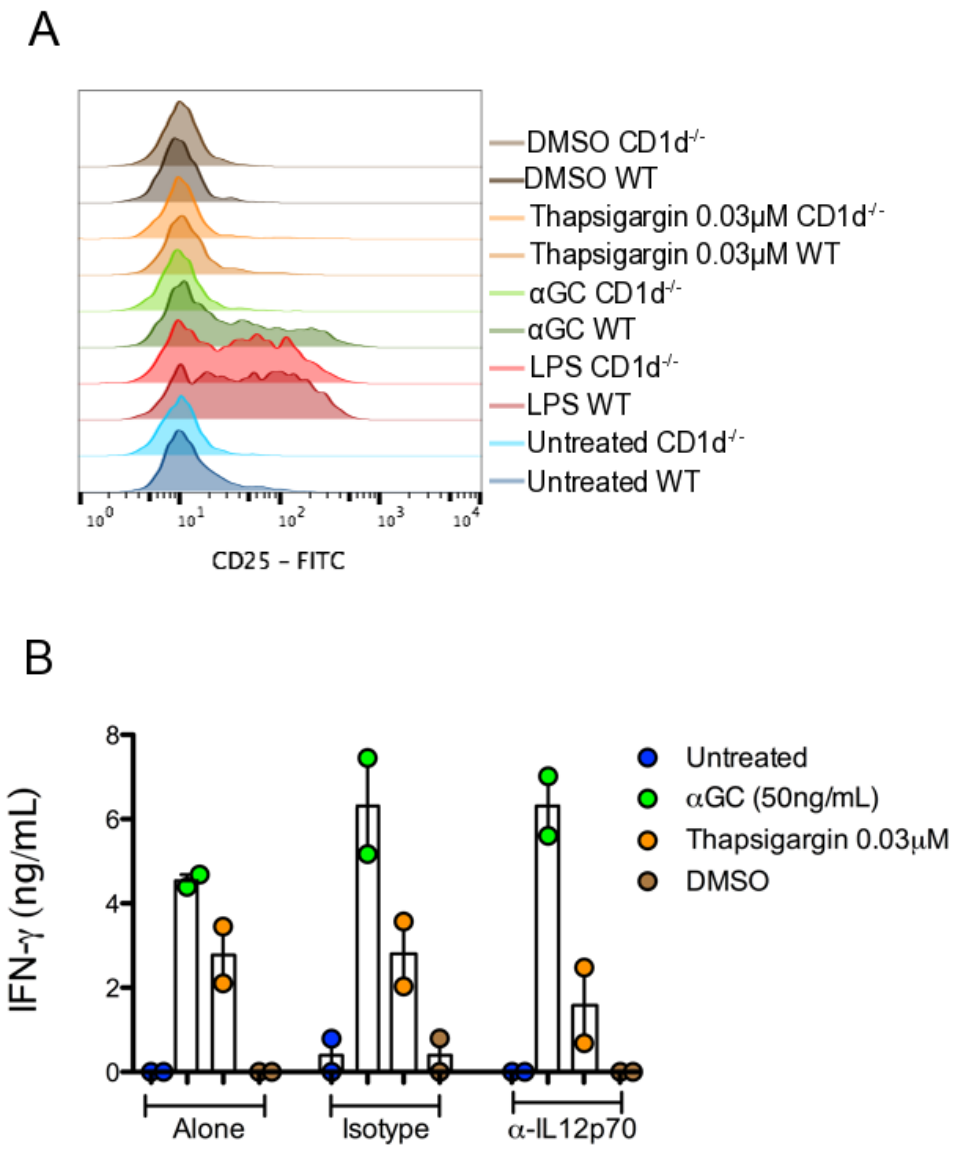

Figure 3.4 Thapsigargin pre-treated APCs secrete IL-12 to enhance CD1d-dependent iNKT cell activation. (A) Human iNKT cells were cultured overnight in supernatants from BMDCs pre-treated as indicated. Activation was measured by increased CD25 surface expression on the iNKT cells. The histogram is representative of an N=3. **(B)** MoDCs treated as indicated were co-cultured with human iNKT cells in the presence of IL-12p70 blocking antibody (20μg/mL) or the appropriate isotype control. IFN-γ secretion is the average of N=2 biological replicates, each performed in technical duplicate.

3.5 A role for NKG2D/NKG2DL interactions in ER-stressed APC-mediated iNKT cell activation

Cellular stress, including ER-stress, has been linked to the upregulation of NKG2D ligands, which are structurally similar to MHC class I molecules (Raulet, 2003). The murine NKG2D ligand MULT1 was upregulated on ER-stressed intestinal epithelial cells and implicated in activating innate lymphoid cells (ILCs) (Hosomi et al., 2017). This finding lead us to wonder if the human ortholog, UBLP, is contributing to ER-stressed APC-mediated activation of iNKT cells. First we investigated whether the human iNKT cells we expanded express the NKG2D. Since human iNKT cells are either $CD4^+$ or DN, we investigated whether NKG2D was differentially expressed in these two sub-populations. As a positive control for NKG2D expression, we stained human γδ cells (Das et al., 2001, Nedellec et al., 2010). DN iNKT cells expressed higher levels of NKG2D compared to $CD4^+$ iNKT cells (**Figure 3.5A**), in agreement with previous reports (Kuylenstierna et al., 2011). Therefore we hypothesized that at least a fraction of the iNKT cells used in our co-culture experiment might be activated through NKG2D:NKG2DL signalling (that might also account for the bimodal CD25 expression). Secondly, we wanted to determine which, if any, of the several isoforms of the ULBP ligand were expressed on THP1 WT cells, and whether they were upregulated upon thapsigargin treatment. While all the ULBP isoforms are expressed on THP1 WT cells, three isoforms (that cannot be distinguished by FACS analysis), ULBP 2/5/6 were particularly upregulated upon thapsigargin treatment (**Figure 3.5B**).

Therefore, NKG2D:ULBP interactions might contribute to ER-stressed APC-mediated iNKT cell activation.

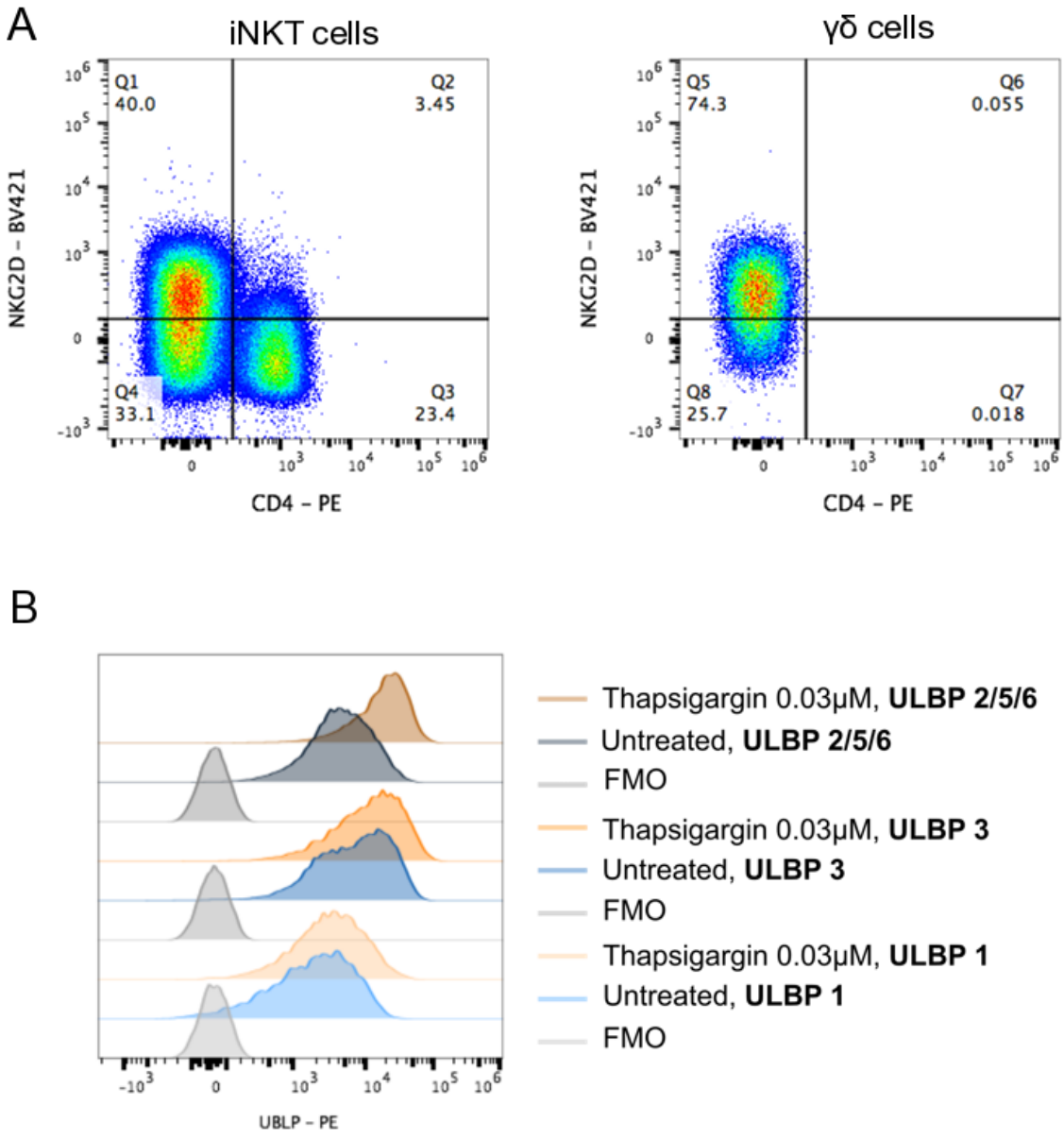

Figure 3.5 NKG2D is expressed on DN iNKT cells and ULBPs are expressed on thapsigargin-treated THP1 cells. (A) NKG2D surface expression on human $CD4^+$ and DN ($CD4^-$) iNKT cells, with γδ T cells as a positive control. **(B)** ULBP surface expression on untreated or thapsigargin-treated THP1 cells. Representative of N=2, each performed in technical duplicates.

3.6 ER-stressed CD11c^{+} DCs activate iNKT cells *in vivo* in a CD1d-dependent manner

Since most of our investigation used *in vitro* assays, we wondered whether ER-stressed APCs could activate iNKT cells *in vivo* via CD1d presentation. We pre-treated CD11c^{+} BMDCs from WT and CD1d$^{-/-}$ mice with thapsigargin 0.03μM**.** After washing and resting overnight, these BMDCs were injected intravenously into wild type recipient mice, which were sacrificed 24 hours later and the spleens were harvested. We then analysed the splenic iNKT cells for signs of activation by FACS, using the gating strategy previously described. Activation was measure by a decrease in CD1d-αGC tetramer positivity, which corresponds with the early activation event of downregulating the TCR (**Figure 3.6A and E**), upregulation of CD25 (**Figure 3.6B and F**), upregulation of the co-inhibitory receptor PD1 (**Figure 3.6C and F**), and downregulation of NK1.1, a C-type lectin expressed on iNKT cells, NK cell and some other CD3^{+} subset (**Figure 3.6D and G**). In mice that received ER-stressed WT BMDCs, iNKT cells showed signs of activation compared to those from untreated WT BMDC recipient mice. However, in mice receiving ER-stressed CD1d$^{-/-}$ BMDCs, iNKT cells were not activated compared to those from untreated CD1d$^{-/-}$ BMDC recipient mice. Unlike splenic iNKT cells, the activation state of other generic CD4^{+} T cells in spleen was not affected by the injection of BMDCs after 24 hours (**Figure 3.6H**). Together these results indicate that the *in vitro* results generated thus far can be recapitulated in an *in vivo* setting, where murine iNKT cells in the spleen were activated by thapsigargin pre-treated BMDCs in a CD1d-dependent manner.

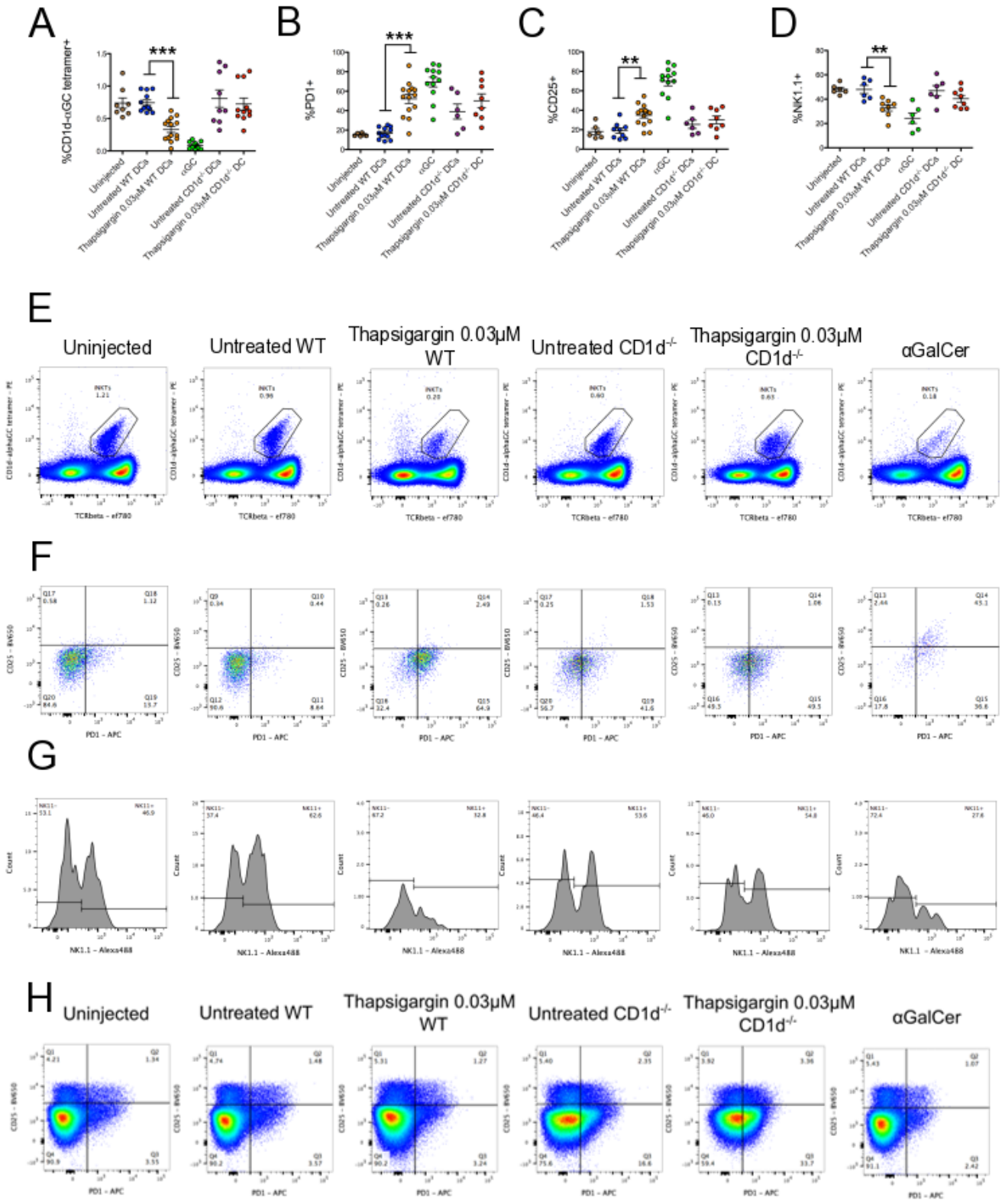

Figure 3.6 Thapsigargin pre-treated murine DCs activate iNKT cells *in vivo*. Murine iNKT cell frequency **(A)** and phenotype **(B, C, D)** in spleens isolated from C57BL/6 mice, 24 hours after injection of untreated or thapsigargin-treated WT or $CD1d^{-/-}$ $CD11c^{+}$ BMDCs. Representative dot

plots from one of the three experiments are shown below. ** and *** represents $p<0.005$ and $p<0.001$, respectively, by an unpaired, two-tailed t test. Each dot represents a recipient mouse; animals collated from three independent experiments. Dots plots indicating decreased frequency of **(E)** CD1d-αGC tetramer, **(F)** PD1 and CD25 expression, and **(G)** NK1.1 expression on splenic iNKT cells. **(H)** PD1 and CD25 expression on non-iNKT $CD4^+$ T cells in recipient mice. These are representative FACS plots of mice from one of three experiments described.

3.7 Discussion

The results of this chapter indicate that pre-treatment of APCs with thapsigargin, which triggers the UPR, induces iNKT cell activation in a CD1d-dependent manner. This mode of CD1d-dependent iNKT cell activation, initially described via *in vitro* experiments with MoDCs, BMDCs, and THP1 cells, was replicated in an *in vivo* setting.

One of the first surprising pieces of data we encountered was the difference in iNKT cell activation by thapsigargin and tunicamycin pre-treated MoDCs. Given that both agents induced the UPR, we wondered if the difference in activation was due to their differing mechanisms. Thapsigargin, by restricting calcium flux between the cytosol and the ER, had the potential to affect multiple signalling pathways within treated cells. Intracellular calcium ions can act as secondary messengers in various signalling transduction pathways (Clapham, 2007), particularly from G-coupled protein receptors involved in cell motility (Rac and Rho), as well growth and differentiation processes. Often in such pathways, calcium ions allosterically modulated a variety of proteins and enzymes, including ion channels, enzymes like isocitrate dehydrogenase in the Krebs cycle, and, perhaps best characterized, calmodulin, which is activated upon calcium binding and modulates a variety of downstream kinases and phosphatases. In DCs, cytosolic calcium can trigger the phospholipase C pathway, which induces DC

maturation. Furthermore, calcium signalling is necessary to form the immunological synapse between the APC and T cells, and LAT/ZAP70 interactions immediately downstream TCR engagement triggers phospholipase C signalling as an early activation step in T cells (Kumari et al., 2014). Given the wide-ranging effects of altered intracellular calcium distribution in modulating APC maturation and T cell activation, we initially wondered if the increase in intracellular calcium rather than the UPR drove the observed activation with thapsigargin and not tunicamycin.

Although thapsigargin pre-treated APCs were washed at least three times before being co-cultured with iNKT cells, we were initially concerned that the residual thapsigargin in the co-culture would stimulate the iNKT cells directly. Not only was calcium signalling in thapsigargin-treated iNKT cells a concern, but UPR signalling specifically through the IRE1 pathway is reported to drive altered cytokines secretion from iNKT cells (Govindarajan et al., 2018). Thapsigargin-treated MoDCs alone expressed higher surface levels of the co-stimulatory markers, CD83 and CD86, suggesting that thapsigargin induces their maturation, therefore contributing to the iNKT cell activation. We also observed increased IL-12 secretion compared to untreated or DMSO-treated cells, consistent with enhanced DC maturation. This finding is contradictory to a previous report that thapsigargin-treated MoDCs do not secrete IL-12p40 in the absence of a TLR agonist (Goodall et al., 2010). This contradiction alerted us of possible endotoxin contamination, an issue that we attempted to address using the MyD88$^{-/-}$ BMDCs.

One way to help confirm whether the iNKT cell activation to thapsigargin pre-treated iNKT cells is driven by altered calcium flux in the APCs was to repeat the protocol with a compound that alters calcium distribution within the cell. Ionophores are typically divalent cation carriers that ferry ions across membranes independent of specific transporters. A23187 binds a variety of ions including Ca^{2+}, Mg^{2+} and Mn^{2+} (Babcock et al., 1976), whereas ionomycin is a potent and selective Ca^{2+} ionophore, traditionally used with PMA to induce T cell activation and cytokine secretion in an APC-independent manner. Whereas thapsigargin blocks the SERCA pump, preventing the Ca^{2+} re-entry into the ER after store depletion (results in a higher cytosolic Ca^{2+} concentration), ionomycin mimics this distribution by carrying extracellular and intracellularly-stored Ca^{2+} across membranes, in a transporter-independent manner, into the cytosol (Morgan and Jacob, 1994). We performed initial experiments with MoDCs pre-treatead with the ionophore A23187 at concentrations comparable to the thapsigargin concentration and found there was abundant iNKT cell activation, beyond that of αGC, but this was accompanied with massive MoDC cell death. In hindsight, given that A23187 targets a variety of divalent cations, the use of a calcium-specific ionophore would have been better suited. A collaborator included ionomycin in his studies, and found that neither ionomycin pre-treated BMDCs nor directly-treated iNKT cells triggered to iNKT cell activation.

Rather than focusing on the thapsigargin-mediated iNKT activation as an off-target effect of the drug, we focused on whether tunicamycin was negatively effecting iNKT cell activation. N-linked glycosylation is an important checkpoint in

protein folding quality control. In this case, attachment of dolichol lipid to the nitrogen atom in asparagine in the ER is the first steps for building glycan chains and, as the protein traffics through the Golgi network, more complex oligosaccharides are added. Glycosylation stabilizes the newly folded protein and is required for many proteins to traffic to the cell surface and/or be secreted (Reiling et al., 2011). This holds true for CD1d, specifically CD1d1, which bears 5 exposed asparagine residues that are predicted glycosylation sites (Sriram et al., 2008). In this report, site-specific mutagenesis that converted the asparagine residues to glutamine resulted in disrupted glycosylation at certain sites, impaired CD1d surface expression and functionality, and ablation of all the glycosylation sites prevented CD1d surface expression and abolished iNKT cell activation to αGC. The reduced CD1d surface expression in APCs treated with tunicamycin is consistent with the fact that impaired N-linked glycosylation might limit functional CD1d surface expression and iNKT cell activation to endogenous lipids. This effect could be confirmed by pulsing tunicamycin-treated APCs with αGC and measuring iNKT cell activation.

Soluble factors such as cytokines would likely require glycosylation in order to be secreted from cells. IL-12 and GMCSF are just two inflammatory cytokines for which glycosylation is essential for their functional secretion (Carra et al., 2000). The IL-12p35 and IL-12p40 subunits responded slightly differently to the inhibition of N-linked glycosylation. The p35 protein is heavily glycosylated during biosynthesis, whereas the p40 subunit is not as dramatically modified by glycosylation although the secretion of p40 homodimers was not detected in

tunicamycin treated monocytes (Carra et al., 2000). This illustrates the potential for tunicamycin to prevent iNKT cell activation, beyond reduced CD1d surface expression, by limiting co-stimulatory cytokine secretion or a 'signal 3' to boost iNKT cell activation.

We found that upon co-culture with human iNKT cells, MAIT cells, or γδ T cells, thapsigargin pre-treated MoDCs only appreciably activated iNKT cells. This result is key for our understanding of ER-stress-mediated activation. Since it is restricted to CD1d-reactive iNKT cells, it supports the hypothesis that this mode of activation requires CD1d. Cytokine-mediated T cell activation via IL-12, -15 and -18 is not likely primarily responsible for the activation, as MAIT cells are responsive to such cytokines, primarily IL-18, and would also likely be activated. Similarly, if activation by NKG2D:NKG2DL engagement contributed greatly to the ER-stress activation phenotype, we would expect that γδ T cells, which constitutively express NKG2D, would exhibit higher levels of activation. Furthermore, when analysing conventional $CD4^+$ T cells in the spleens of mice injected with thapsigargin pre-treated BMDCs, but there were no clear differences in their activation. Previous work described that intratumoural ER-stressed $CD11c^+$ DCs impaired anti-tumour responses from $CD4^+$ and $CD8^+$ TILs (Cubillos-Ruiz et al., 2015). However, this study looked specifically TILs and not T cells in the lymphatic tissue, where the immune cells exist a different microenvironment. Furthermore, the analysis did not account for the proportion of Tregs amongst the TIL population and other factors that might confound the results.

When considering factors other than CD1d expression that might influence ER-stressed APC-mediated iNKT cell activation, we cannot ignore the potential role of the inflammasome. Despite a report that NLRP3 inflammasome activation is UPR-independent (Menu et al., 2012), several reports have linked ER-stress and signalling through the UPR sensor IRE1 and PERK to assembly of the inflammasome and caspase-dependent production of IL-1β and IL-18 (Shenderov et al., 2014, Kim et al., 2014). Although, as previously discussed, our findings suggest that CD1d is the primary driver of ER-stress mediated iNKT cell activation, reactivity to self-antigens as 'signal 1' typically requires a boost from cytokines. It is not known whether IL-1β can drive activation of iNKT cells.

Since there exists a wide range of soluble factors that are reported to modulate iNKT cell activation, such as exosomes (Deng et al., 2013) or alarmins like IL-33 (Bourgeois et al., 2009), etc. we took an unbiased approach to determine whether supernatants containing soluble factors secreted from thapsigargin-treated BMDCs could activate human iNKT cells in the absence of direct interaction with the APC. However, since cytokine stimulation is typically not as conserved as CD1d:iNKT-TCR interaction across species, the interpretation of this experiment might be incorrect due to potentially limited murine-human cytokine cross-reactivity. The iNKT cell activation from supernatants from LPS-treated BMDCs might contain certain cross-reactive cytokines, but we cannot rule out the possibility that residual LPS, DAMPs or necrotic cell debris, or exosomes, which are know to be released by DCs, might also be influencing iNKT cell activation. Given that IL-18 secretion would influence MAIT cells as well and iNKT

cell activation, we demonstrated that IL-12 augments CD1d-dependent ER-stress mediated iNKT cell activation in a wholly human system. An important positive control missing from that experiment is an LPS condition, which can boost iNKT cell activation in a partially IL-12-dependent manner.

In this work, the primary readouts for iNKT cell activation are CD25 surface expression and IFN-γ secretion. However, other markers of iNKT cell activation, measurable by flow cytometry, include PD1, ICOS, KLGR1 (van den Heuvel et al., 2011). While we investigated IL-4, GMCSF, and IL-13 secretion from iNKT cells co-cultured with ER-stressed APCs, we could have assess secretion of cytokines from different Th profiles, including TNFα, IL-17, and IL-10, perhaps using a multiplexed ELISA approach. There might also be an element of tissue-specificity in polarizing the iNKT cell response to ER-stressed APCs, for example in the spleen versus the liver.

The use of tissue from $CD1d^{-/-}$ mice confirmed that thapsigargin mediated iNKT cell activation was CD1d-restricted, both *in vitro* and in an *in vivo* model. Recent studies illustrate that CD1d2 can present endogenous lipid antigen with shorter hydrophobic tails and with less efficiency than CD1d1 (Sundararaj et al., 2018). The mice used our study are $CD1d1^{-/-}$ mice that have the CD1d2 gene intact. The markedly reduced activation using BMDCs from these mice compared to the wild type suggests that CD1d1 is primarily responsible for ER-stress mediated iNKT cell activation, but we cannot rule out the possible minor contribution of presentation by CD1d2, particularly in the thymus.

In order to perform our *in vivo* experiments, bone marrow precursors were differentiated into $CD11c^+$ DCs using GMCSF. However, murine DCs can be differentiated into distinct subsets through different cell culture conditions (Durai and Murphy, 2016). For example, differentiation with Flt3 ligand can promote a population of $CD8\alpha^+$ $DEC205^+$ cross-presenting subset, which upon ER-stress might differentially activate iNKT cells. Another subset, $CD103^+$ DCs, are also capable of cross-presentation and are typically enriched at barrier and mucosal sites such as the gut (del Rio et al., 2010). Injection of ER-stressed $CD103^+$ DCs, and monitoring activation of iNKT cells in the liver might reveal differential activation through this mechanism by different DC subsets at different tissue sites.

As we optimized these *in vivo* experiments we realized that the time of injection after stressing the cells was crucial in generating a splenic iNKT cell response. In initial experiments, we injected the DCs immediately after thapsigargin pre-treatment, but found little to no difference in splenic iNKT cell activation in the recipient mice compared to those injected with untreated control. We realized that the kinetics of the self-lipid generation and CD1d loading are unknown, but likely takes longer than the pre-treatment time of six hours. From *in vitro* experiments, the activating CD1d-lipid complexes likely appear on the cell surface sometime during the overnight co-culture with iNKT cells, which in turn are activated by the morning. We therefore modified the protocol to allow the thapsigargin-treated DCs to rest overnight, during which the CD1d-lipid complexes are expressed at the cell surface, and inject them into recipient mice the following morning. This change in timing results in a robust activation phenotype in iNKT

cells in the thapsigargin pre-treated WT DC-recipient mice compare to the controls.

In initial experiments, we also injected mice with αGC-pulsed WT and $CD1d^{-/-}$ DCs, but found that the αGC-pulsed $CD1d^{-/-}$ DC-recipient mice still had activated splenic iNKT cells. We attributed this either to residual αGC in the injection mix despite washes, or cell death of the DCs, releasing αGC in the mouse to be pick up and loaded by endogenous APCs. We opted to instead inject soluble αGC into the mice, rather than loading the DCs. While not necessarily the best comparison with the other experimental groups that received cell-based injections, it did serve as a good positive control to determine maximal iNKT cell activation.

Having established this *ex vivo/in vivo* model, we will continue to analyse the downstream consequences of thapsigargin-mediated iNKT cell activation. One of the most striking properties of activated iNKT cells is their ability to transactivate NK cells, which are highly cytotoxic against virally-infected and tumour cells. This phenomenon is particularly evident in a murine model of B16 lung metastases. Intravenously injected B16 tumour cells migrate to the lung, where they form dark metastases that can be easily quantified (Fujii et al., 2002). Injection of αGC activates iNKT cells that in turn transactivates NK cells, which kill the lung metastases in B16 challenged mice via IFN-γ (Fujii et al., 2002). It would be interesting to see if iNKT cells activated by injected ER-stressed DCs would be able to transactivate NK cells and reduce the B16 lung metastases burden in challenged mice.

Another downstream effect exerted by activated iNKT cells is enhanced priming of DCs to present peptide antigen to conventional $CD4^+$ and $CD8^+$ T cells. This could be tested in our model by injecting SIINFEKL into mice that have either received unstressed or stressed DCs, and measuring the percentage of SIINKFEKL tetramer positive $CD8^+$ T cells, as they would be activated and proliferate more readily with enhanced priming from iNKT cell help. We would also co-inject OVA-specific $CD8^+$ T cells, pre-labelled with CFSE, and measure their proliferation.

A more subtle concern that could apply to many avenues of biomedical research is whether overexpression of proteins can itself modulate ER-stress responses. Protein overexpression, due to lentiviral or retroviral transduction, has been used in mechanistic experiments and as a form of therapy for specific diseases, such as cystic fibrosis, is an area of intensive research (van Haasteren et al., 2018). In this project, we overexpressed CD1d in THP1 cells. It is possible that overexpression of proteins can itself modulate ER-stress responses. In our case overexpression of CD1d results in at least a log-fold increase in surface detection. There is a possibility that the enhanced iNKT cell activation to CD1d-overexpressing cells, while predominantly due to increase CD1d expression, might also be a synergistic effect of protein overexpression and thapsigargin inducing ER-stress. Comparing the UPR in THP1 WT versus THP1-CD1d might shed light on this possibility. Co-overexpression a chaperone molecule, such as BiP might be a possible method to circumvent this issue, as increasing the production of BiP

and other chaperones increases the capacity of protein folding in the ER, leading to reduced UPR signalling (Gu et al., 2010).

Chapter 4: UPR signalling through the PERK pathway drives ER-stressed APC-mediated iNKT cell activation

ER-stress is the main trigger of the unfolded protein response (UPR), which refers collectively to three individual yet intersecting pathways aimed at restoring ER homeostasis. Given that pre-treatment of APCs with the ER-stress inducing agent thapsigargin led to CD1d-dependent activation of iNKT cells, we investigated whether the UPR, and which branches in particular, contributes to this the phenotype.

4.1 Pre-treatment of THP1 cells with the SubAB5 toxin leads to CD1d-dependent activation of iNKT cells

We have primarily used thapsigargin to induce ER-stress in our experimental design. By blocking the SERCA pumps of the ER, ER calcium stores are depleted and the Ca^{2+} concentration rises in the cytosol, which could influence multiple unrelated pathways. Ca^{2+} are involved in a number of steps in the phospholipase C (PLC) signalling pathway, including when it is released by activated IP3 receptor channels, or by binding and activating protein kinase C (Hokin, 1966, Michell et al., 1977, Streb et al., 1983). This has potentially confounding implications in our model, as the PLC pathway can induce DC maturation (Bagley et al., 2004). We were therefore wary that the effect of

thapsigargin treatment on APC-mediated activation of iNKT cells might not be specific to the ER-stress response, but driven by enhanced dendritic cell maturation via signalling by re-distributed subcellular Ca^{2+}.

To address this concern, we decided to test a relatively new reagent – the SubAB5 toxin, which cleaves BiP to induce the UPR. We harvested protein from THP1 WT cells treated with the WT SubAB5 toxin at different time points to determine via western blot an optimal time point where BiP is cleaved. The SubAB5 toxin cleaved the BiP protein at the reported residue, to generate the expected 28kDa cleavage fragment upon treatment (Paton et al., 2006) (**Figure 4.1.1A**). Furthermore, the treatment induced substantial upregulation of the total BiP signal (full length and cleavage product combined), due to UPR activation by the toxin. The negative controls, including the 50% glycerol solvent control lysate and the lysate from cells treated with the inactive mutant toxin, neither induced BiP cleavage nor upregulation. Thapsigargin, which induces the UPR by a separate mechanism, upregulated BiP protein levels, but did not cleave BiP to produce the 28kDa fragment.

We assessed XBP1 splicing to confirm UPR induction by the SubAB5 toxin. Here we demonstrated that the solvent controls and inactive mutant toxin failed to induce XBP1 splicing, whereas thapsigargin, at both high and low doses, induced XBP1 splicing in THP1 WT cells. Similarly the WT SubAB5 toxin induced XBP1 splicing in a time-dependent manner (**Figure 4.1.1B**).

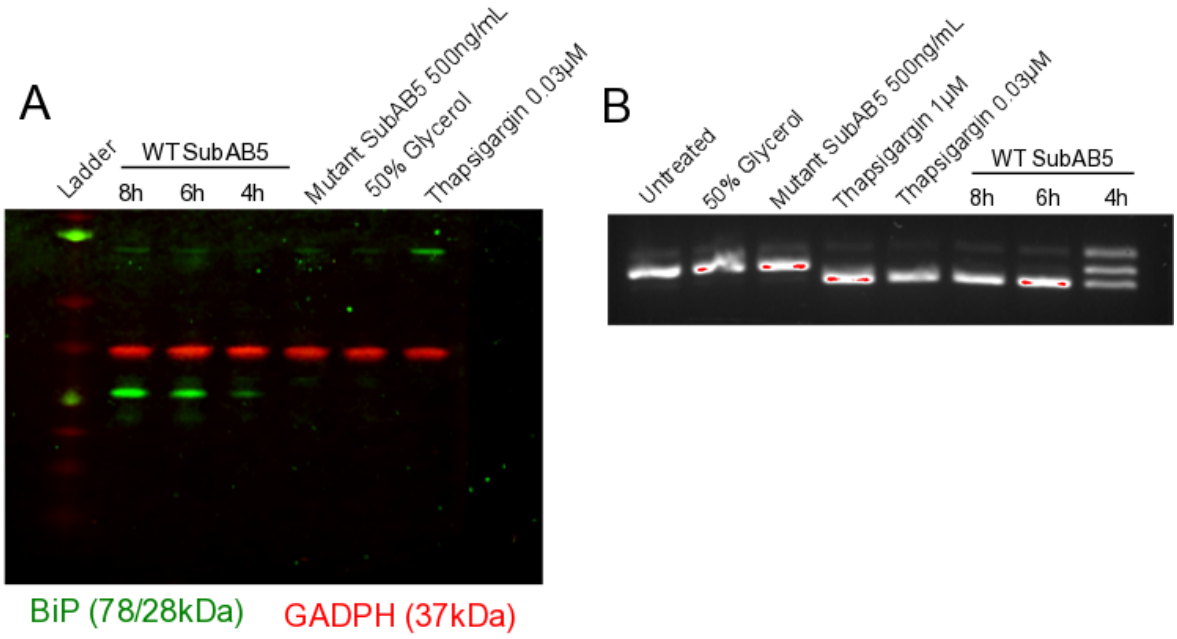

Figure 4.1.1 The SubAB5 toxin induces the UPR. (A) Activity of the SubAB5 toxin in THP1 cells at the 500μg/mL for different timepoints is demonstrated by cleavage of the full-length BiP protein, and detection of the BiP cleavage product, by western blot. The inactive mutant SubAB5 toxin was used as a negative control. **(B)** XBP1 splicing induced by the SubAB5 toxin, where thapsigargin acts as the positive control and the inactive mutant SubAB5 toxin as the main negative control.

To determine whether treated cells could induce CD1d-dependent activation of iNKT cells, we co-cultured WT SubAB5-treated cells with human iNKT cells, and measured any consequent activation by IFN-γ secretion. We also compared the viability of THP1 WT cells treated with the toxin, to see if APC cell death might be affecting iNKT cell activation. We found that cell death increased in a time-dependent manner and that toxin pre-treatment induced iNKT cell activation at an optimal time point of 6 hours (**Figure 4.1.2A**). We also found that this iNKT cell activation could be abrogated with a CD1d-blocking antibody (**Figure 4.1.2B**), suggesting that the activation achieved with thapsigargin, which is also CD1d-dependent, is in part UPR driven, rather than solely an off-target effect. Furthermore, pre-treatment with the inactive mutant toxin, which does not induce the UPR, failed to induce iNKT cell activation.

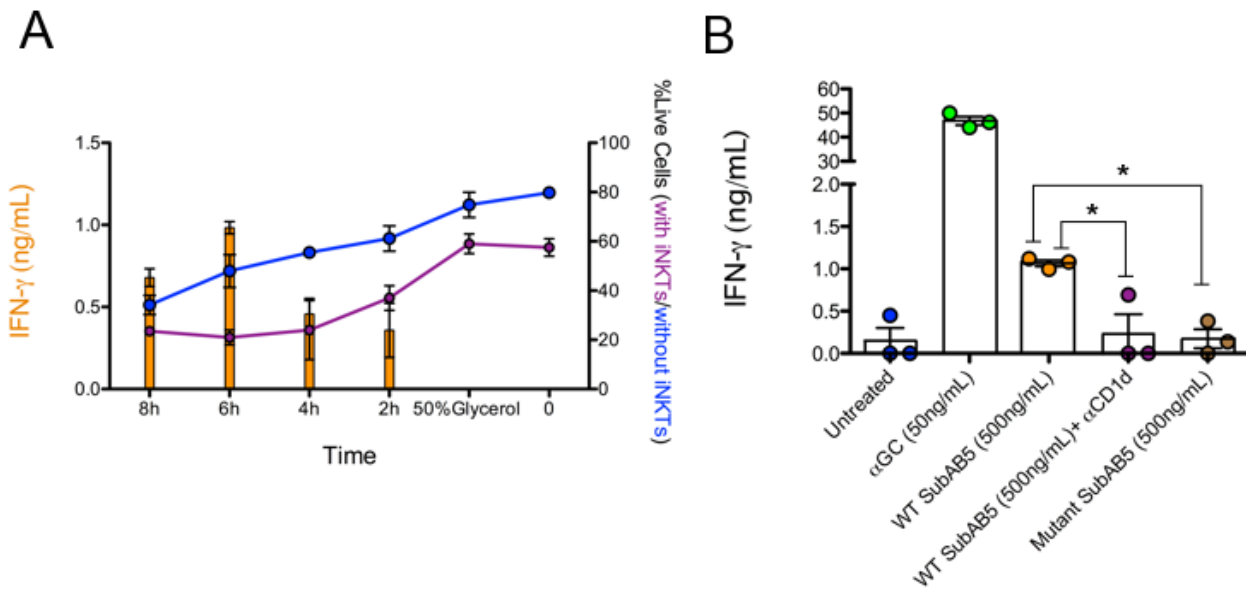

Figure 4.1.2 ER-stressed APC-mediated iNKT cell activation is UPR-dependent. (A) Cell death of MoDCs treated with the SubAB5 toxin over a time course was measured, either alone (blue) or when co-cultured with human iNKT cells (purple). Activation of iNKT cells co-cultured with SubAB5-pre-treated THP1 WT cells was measure by IFN-γ secretion (bottom, orange). Cell death and IFN-γ secretion is the average of N=2 biological replicates, each performed in technical duplicates. **(B)** Activation of human iNKT cells co-cultured with SubAB5-pre-treated THP1 WT cells in the presence or absence of CD1d blocking antibody (20μg/mL) was measured by IFN-γ secretion (right). The inactive mutant SubAB5 toxin was used as a negative control (right). * represents $p<0.01$ by an unpaired, two-tailed t test. IFN-γ secretion is the average of N=3 biological replicates, each performed in technical duplicates.

4.2 Knockdown of the three sensors of the UPR reveals a role for PERK pathway signalling in ER-stressed APC-mediated iNKT cell activation

After confirming involvement of the UPR in ER-stressed APC-mediated iNKT cell activation, we turned our focus onto determining which branch(es) of the UPR might contribute to this phenotype. To this end, we decided to knock down the three sensors of the UPR in THP1 WT cells: IRE1, PERK, and ATF6α. To carry out the knock down, we ordered lentiviral particles containing an shRNA targeted towards each of the sensors. For each sensor, we used multiple different shRNAs to increase the chance of generating knock down (KD) cells. shRNAs

were selected to target a variety of regions and specific locations within the gene of interest (determined using SerialCloner and SnapGene online software), in case targeting of certain regions produced a more efficient KD, detailed in **Table 4.2.1**.

Target	*shRNA#*	*Sequence*	*Region*	*TRC*
IRE1	6	CCGGGGAATCCTCTACATGGGTAAACTCGAG TTTACCCATGTAGAGGATTCCTTTTTG	CDS	**TRCN0000356311**
	9	CCGGAGAGGAGGGAATCGTACATTTCTCGAG AAATGTACGATTCCCTCCTCTTTTTTG	3'UTR	**TRCN0000235529**
PERK	6	CCGGGTTGTGCTAGCAACCCTAATACTCGAG TATTAGGGTTGCTAGCACAACTTTTTTG	3'UTR	**TRCN0000197197**
	9	CCGGATCATAGCAACAACGTTTATTCTCGAG AATAAACGTTGTTGCTATGATTTTTTG	CDS	**TRCN0000262377**
	13	CCGGCACTTTGAACTTCGGTATATTCTCGAG AATATACCGAAGTTCAAAGTGTTTTTG	CDS	**TRCN0000262381**
	14	CCGGGGAACGACCTGAAGCTATAAACTCGAG TTTATAGCTTCAGGTCGTTCCTTTTTG	CDS	**TRCN0000262380**
ATF6α	1	CCGGCCCAGAAGTTATCAAGACTTTCTCGAG AAAGTCTTGATAACTTCTGGGTTTTT	CDS	**TRCN0000017853**
	4	CCGGGCAGCAACCAATTATCAGTTTCTCGAG AAACTGATAATTGGTTGCTGCTTTTT	CDS	**TRCN0000017855**
	7	CCGGGATGCAAGAGAACAATGTTTCCTCGAG GAAACATTGTTCTCTTGCATCTTTTTTG	3'UTR	**TRCN0000415981**
	16	CCGGCAGAGAACCAGAGGCTTAAAGCTCGAG CTTTAAGCCTCTGGTTCTCTGTTTTTTG	CDS	**TRCN0000422247**

Table 4.2.1 shRNA sequences delivered in lentiviral particles to knock down the three sensors of the UPR. shRNA sequences were selected from the list provided Sigma Mission® based on previous validation and target location within the gene sequence. The sense shRNA sequence is highlighted red, the loop sequence in blue, and the anti-sense sequence in green, followed by the polyT tail to signal transcription termination. 2 of the 4 purchased sequences for IRE1 were omitted because they were not used in functional assays. The plasmid bearing the sequence for these shRNAs also contained a puromycin resistance cassette, to allow for selection of successfully transduced cells.

THP1 WT cells were transduced with each shRNA-containing lentivirus, we validated the KD of each sensor by analysing their protein levels in potential KD cell lines compared to the untransduced parent THP1 WT cell line and parent cells transduced with a control shRNA vector (CV) that does not target a known gene in any mammal species. First, we tested THP1 WT cell lines transduced with each of the four PERK-targeted shRNAs. By western blot analysis, three out of four cell lines had reduced expression of the PERK protein (**Figure 4.2.2A**). Two of these confirmed KD lines and one that did not reduce PERK protein level were pre-treated with thapsigargin or the C20:2 lipid agonist, a synthetic derivative of αGC that can bind surface CD1d without internalization and processing. The confirmed PERK KD cells failed to activate iNKT cells upon thapsigargin pre-treatment compared to the CV THP1 WT cells – suggesting that the PERK pathway is involved in ER-stressed APC-mediated iNKT cell activation. The CV and KD cell lines pulsed with C20:2 comparably activated iNKT cells, suggesting that CD1d levels and inherent presentation ability were not affected by the KD.

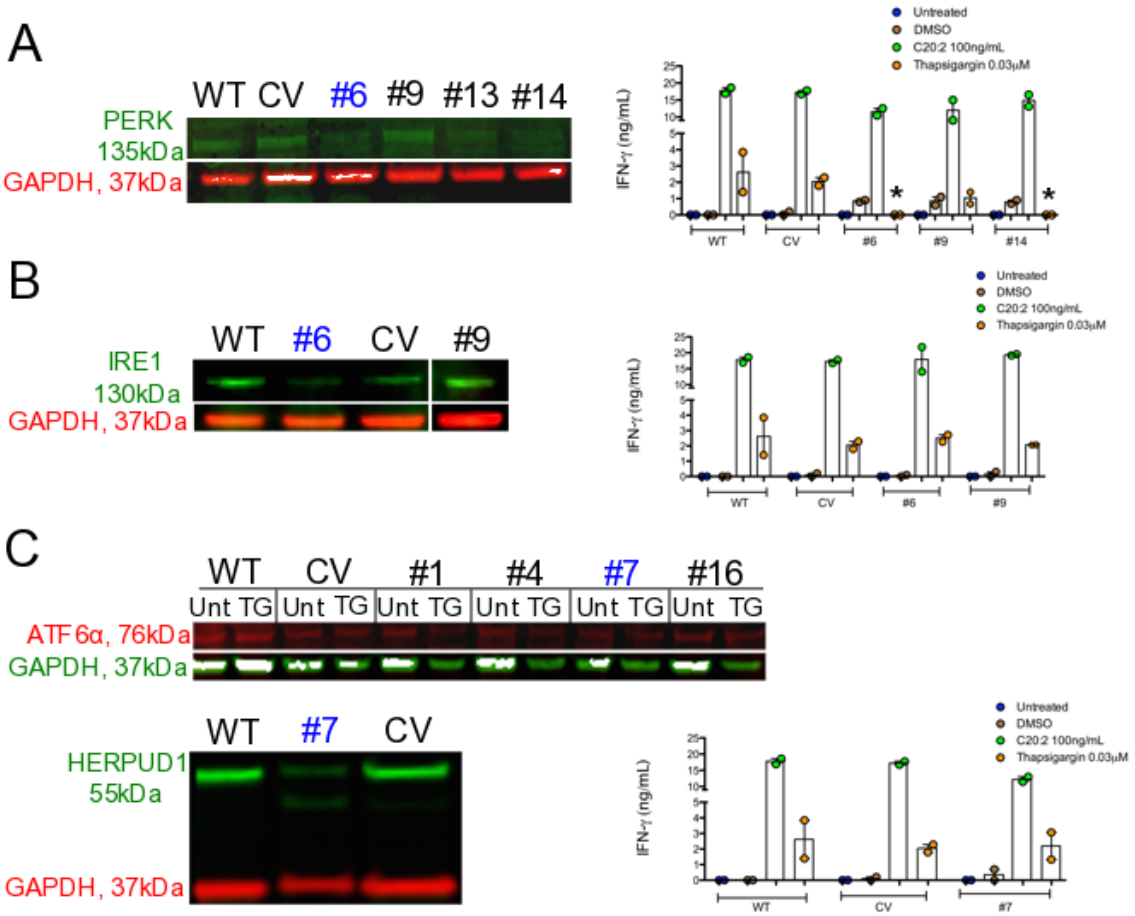

Figure 4.2.2 Confirmation of successful KD of PERK, IRE1, and ATF6α to assess each sensor's role in ER-stressed APC-mediated iNKT cell activation. Lysates from transduced, puromycin-resistant THP1 cells to assess the degree of KD of **(A)** PERK, **(B)** IRE1, and **(C)** ATF6α on the protein level by western blot (**left**). The control vector (CV) cells were transduced with the pKLO.1 plasmid, which contains the identical backbone (including the puromycin resistance cassette) but an shRNA sequence that targets a bacterial protein. THP1 cells transduced with each shRNA were pre-treated as indicated and co-cultured with human iNKT cells (**right**). iNKT cell activation was measured by IFN-γ secretion. * represents $p<0.05$ (compared to the CV thapsigargin condition) by a one-way ANOVA with a Dunnett's Multiple Comparison post-test. IFN-γ secretion is the average of N=3 biological replicates, each performed in technical duplicates.

The same approach was used to test IRE1 KD (**Figure 4.2.2B**) and ATF6α KD (**Figure 4.2.2C**) THP1 WT cells. For the ATF6α KDs, the putative KD based on western blot analysis of ATF6 was confirmed by western blot of HERPUD1, an ER-resident protein whose expression is regulated in part by ATF6. We found that thapsigargin pre-treated IRE1 and ATF6α KD lines were able to activate iNKT

cells comparable to the CV THP1 WT cells, suggesting that these UPR sensors are dispensable in ER-stressed APC-mediated iNKT cell activation.

When comparing the KD cell lines of each of the three sensors side-by-side, we illustrated that ER-stressed APC-mediated iNKT cell activation is only reduced in PERK KD THP1 line (**Figure 4.2.3A**). Since iNKT cell activation to C20:2 does slightly decrease with the PERK KD THP1 line, we wanted to confirm that CD1d surface expression was not altered. PERK KD THP1 WT (**left**) and THP1-CD1d cells (**right**) exhibited surface CD1d levels comparable to the controls (**Figure 4.2.3B**). Together, these results indicate that the PERK pathway is involved in sterile, ER-stressed APC-mediated iNKT cell activation without directly altering CD1d surface expression.

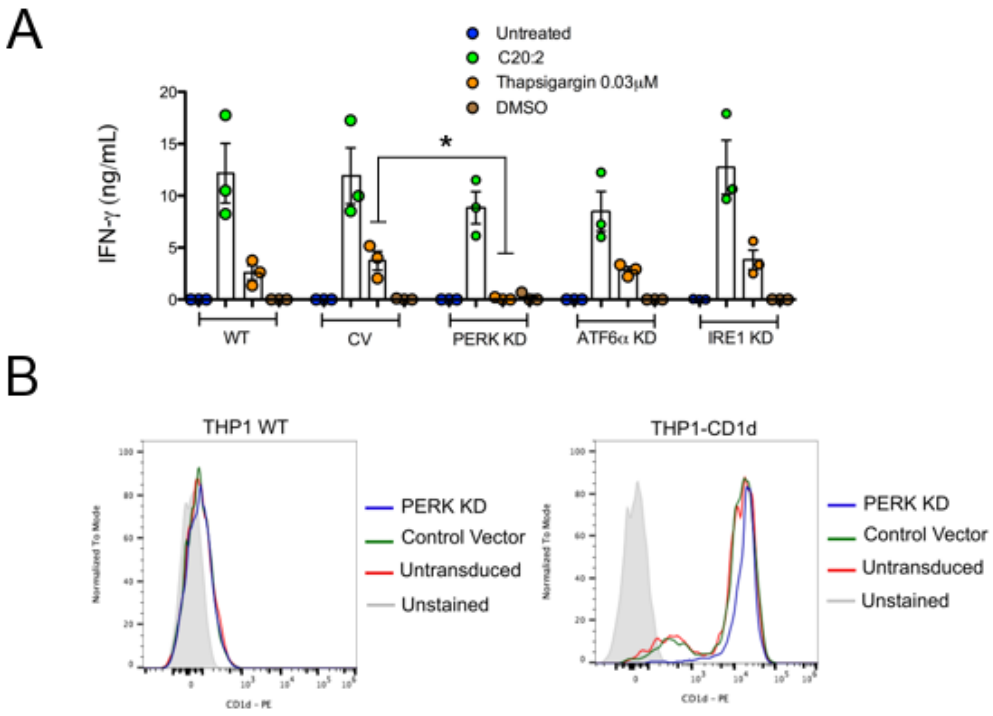

Figure 4.2.3 Comparison of the PERK, IRE1, and ATF6α KD THP1 cells in activating iNKT cells. (A) WT, control vector (CV) and IRE1, ATF6α, or PERK KD vector transduced THP1 wild

type cells were co-cultured with human iNKT cells and activation was assessed by IFN-γ secretion. * represents $p<0.05$ by a one-way ANOVA with a Dunnett's Multiple Comparison post-test. IFN-γ secretion is the average of N=3 biological replicates, each performed in technical duplicates. **(B)** CD1d surface expression, as measured by flow cytometry, in either untransduced, control vector transduced or PERK KD wild type (left) or CD1d-overexpressing (right) THP1 cells. The histograms are representative of N=3 biological replicates, each performed in technical duplicates.

4.3 Small-molecule inhibitors confirm that the PERK pathway regulates ER-stressed APC-mediated iNKT cell activation

We treated THP1 cells with small-molecular inhibitors that target the PERK pathways at different points in the cascade, in the hopes of both confirming the results of the shRNA KD experiments, and narrowing down which specific components of the PERK pathway regulate ER-stressed APC-mediated iNKT cell activation. We tested two different small-molecule inhibitors that would influence PERK-mediated signalling: 1) GSK2606414, which blocks autophosphorylation by targeting the inactive conformation of the PERK ATP-binding region (Axten et al., 2012) and 2) Integrated Stress Response Inhibitor (ISRIB), which blocks the downstream activity of p-eIF2α by promoting eIF2B activity (Sidrauski et al., 2013) (**Figure 4.3.1A**). We confirmed the activity of these inhibitors by western blot, where upon thapsigargin treatments, ISRIB blocked ATF4 upregulation downstream eIF2α phosphorylation, while GSK2606414 blocked both eIF2α phosphorylation and ATF4 upregulation (**Figure 4.3.1B**). THP1 WT cells, untreated, pre-treated with thapsigargin, or pulsed with C20:2, were co-treated with either of the two inhibitors, washed, and co-cultured with iNKT cells.

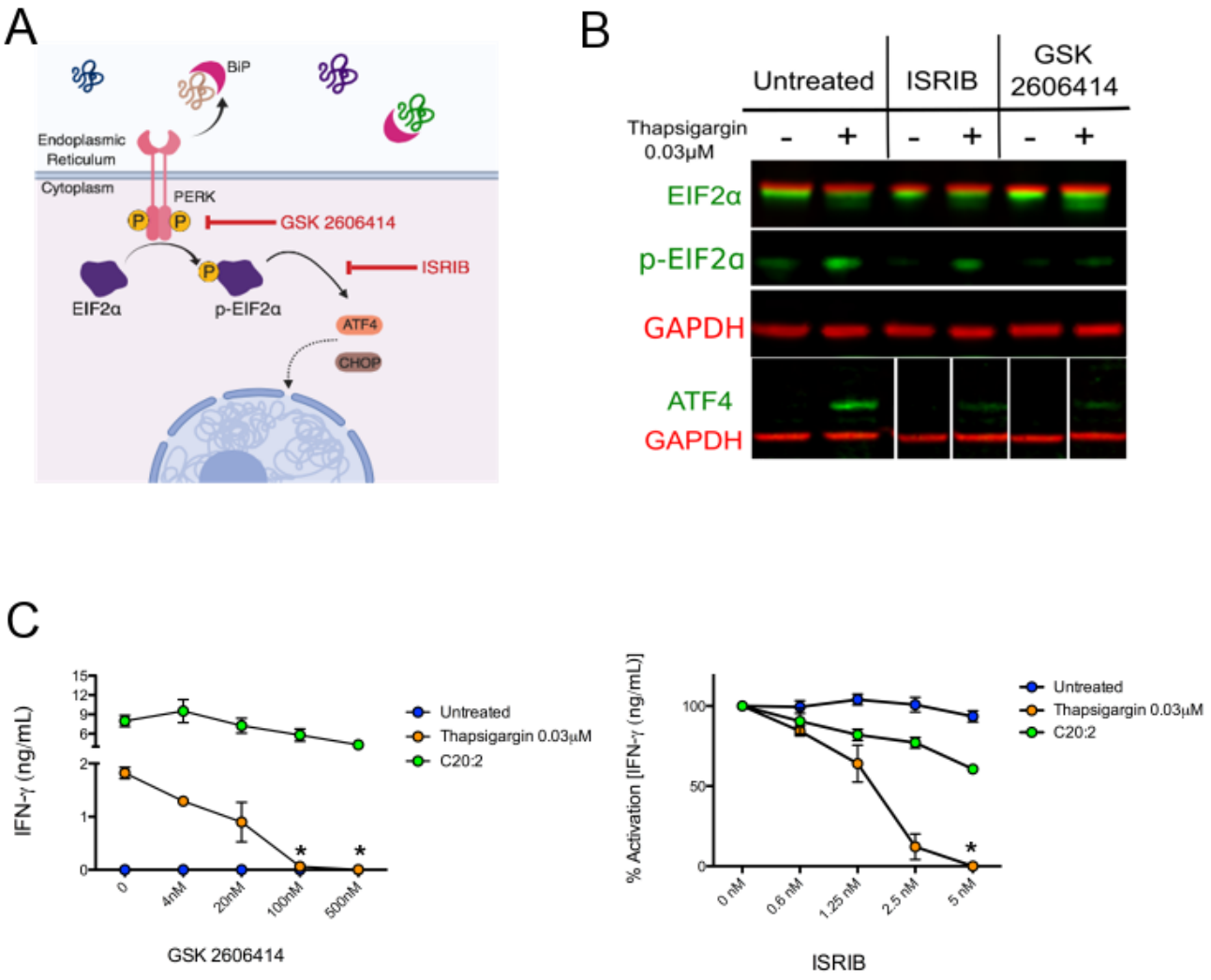

Figure 4.3.1 Small-molecule inhibitors of the PERK pathway block ER-stressed APC-mediated iNKT cell activation. (A) An illustration of the mechanism of action of two inhibitors of the PERK pathway: the PERK kinase inhibitor GSK 2606414 and the phospho-eIF2α inhibitor Integrated Stress Response Inhibitor (ISRIB). **(B)** Validation of ISRIB and GSK2606414 in blocking PERK signalling via western blot of THP1 cells after 6 hours of treatment. ISRIB blocks PERK signalling events beyond eIF2α phosphorylation i.e. ATF4 upregulation. GSK2606414 blocks eIF2α phosphorylation and ATF4 upregulation. **(C)** Effect of GSK2606144 (left) and ISRIB (right) on human iNKT cell activation by thapsigargin-treated THP1 WT cells. THP1 WT cells pulsed with C20:2, an analogue of αGC that binds surface CD1d molecules were used a control for non-specific inhibitor toxicity and functional CD1d presentation. * represents $p<0.01$ compared to thapsigargin treatment without inhibitor by a one-way ANOVA with a Dunnett's Multiple Comparison post-test. The starred data points are compared to the thapsigargin condition without inhibitor added. The data points represent the average of N=3 biological replicates, each performed in technical duplicates.

With both inhibitors, there was a dose-dependent decrease in IFN-γ secretion with increased doses of the inhibitor (**Figure 4.3.1C**). iNKT cell activation to C20:2-

pulsed cells did not change significantly with increased concentrations of the inhibitors, suggesting that surface levels and functionality of CD1d, and THP1 WT cell death was not affected by the inhibitor treatments. Those doses of the inhibitors were based on the reported IC50 of each inhibitor, and confirmed that eIF2α phosphorylation by PERK contributes to the phenotype.

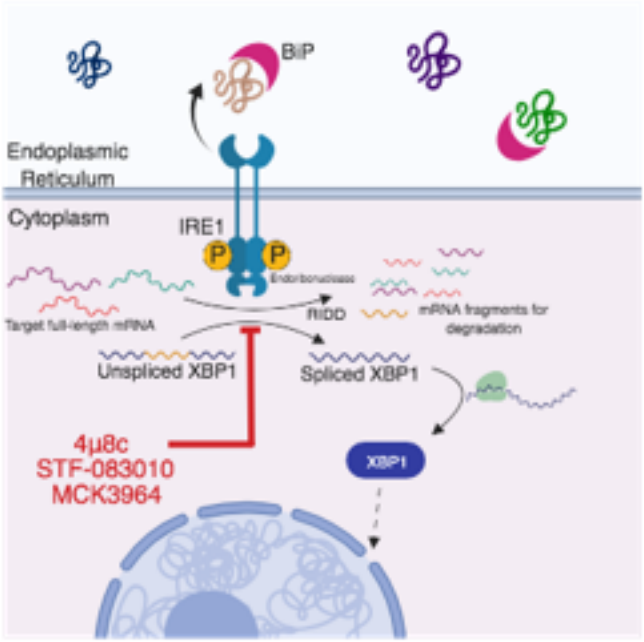

Figure 4.3.2 Mechanism of action of IRE1-targeted small-molecule inhibitors. An illustration of the mechanism of action of the inhibitors of the IRE1 pathway: 4μ8C, STF083010, and MCK-3964, which block the endoribonuclease activity of the dimerized IRE1 kinase.

To confirm the lack of involvement of IRE1 and ATF6α in the observed phenotype, we tested small-molecule inhibitors of these two pathways. To assess the IRE1 pathway, we used small-molecule inhibitors that target the IRE1 endoribonuclease responsible for splicing XBP1: 4μ8C (Cross et al., 2012), STF-083010 (Papandreou et al., 2011), and MCK3964 (Volkmann et al., 2011) (**Figure 4.3.2**). We found that while 4μ8C preventd XBP1 splicing when co-treated with thapsigargin (**Figure 4.3.3A**), it reduced activation of iNKT cells to both

thapsigargin pre-treated and C20:2-pulsed THP1 WT cells (**Figure 4.3.3B**), which we attribute to reduced CD1d surface expression (**Figure 4.3.3C**).

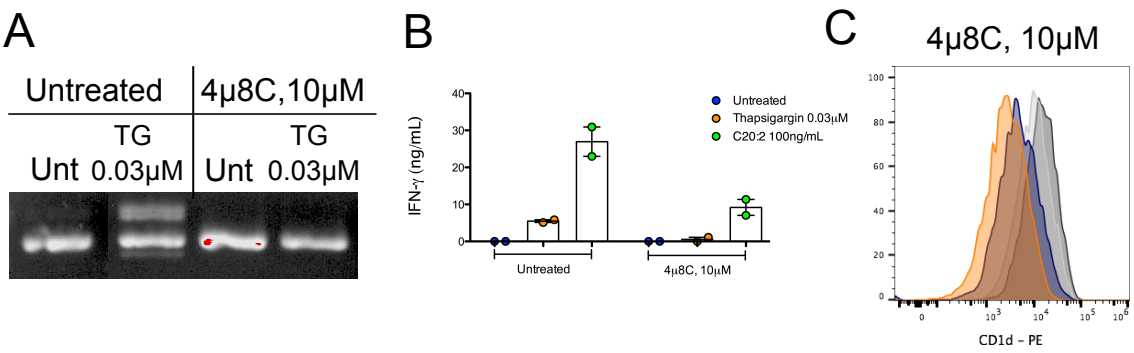

Figure 4.3.3 4μ8C blocks ER-stressed APC-mediated iNKT cell activation. (A) Co-treatment of THP1 WT cells with thapsigargin and 4μ8C blocks XBP1 splicing that cells treated with thapsigargin alone exhibit, confirm the activity of 4μ8C. **(B)** Activation of iNKT cells, as measured by IFN- γ secretion, upon co-culture with THP1 WT cells treated as indicated. **(C)** CD1d surface expression on THP1-CD1d cells either untreated or thapsigargin-treated (dark gray and light gray) or with the addition of the inhibitor (blue and orange). IFN-γ secretion is the average of N=2 biological replicates, each performed in technical duplicates.

Due to the adverse effects of this particular inhibitor, we tested two other commercially available inhibitors: STF-083010 and MCK3964. Both these inhibitors similarly blocked XBP1 splicing, as analysed by PCR analysis (**Figure 4.3.4A**). Both inhibitors reduced CD1d surface expression, though not to the same extent as the 4μ8C inhibitor (**Figure 4.3.4B**). However, when tested in a functional assay, these two inhibitors did not significantly reduce iNKT cell activation to C20:2 or to thapsigargin pre-treated THP1 WT cells (**Figure 4.3.4C**). This result not only confirmed that the reduction in CD1d surface expression with these inhibitors does not strongly impact the functionally readout, but that IRE1 is not the main contributor to ER-stressed APC-mediated iNKT cell activation.

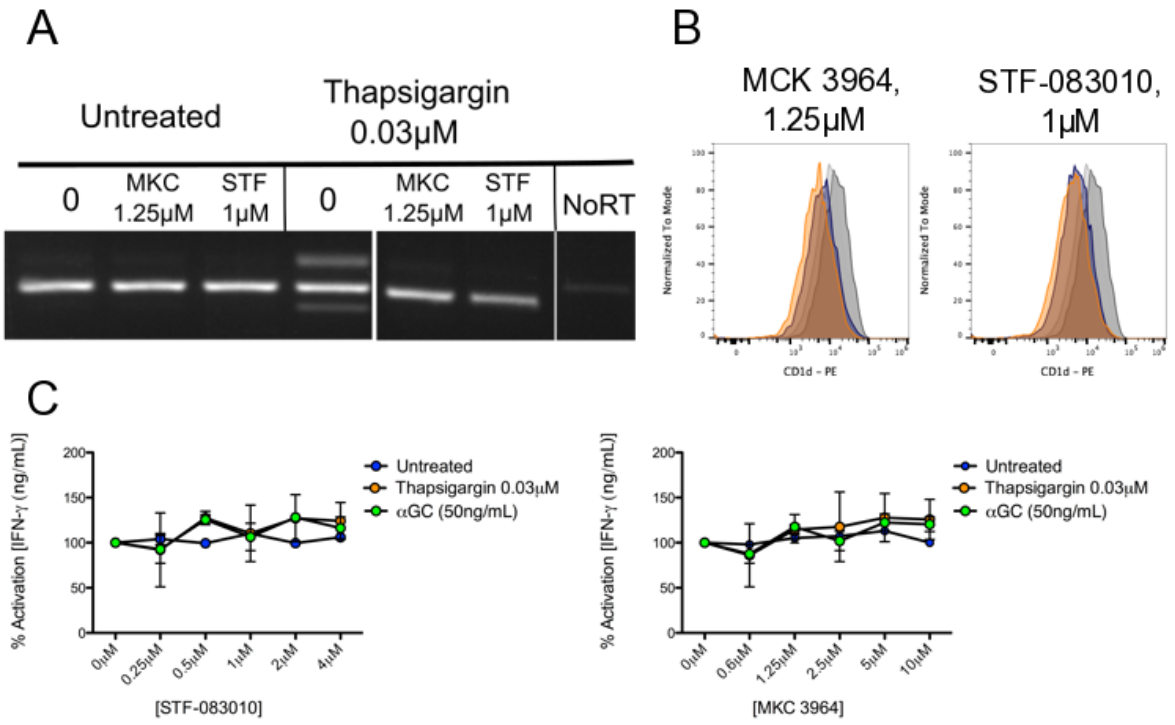

Figure 4.3.4 Small-molecule inhibitors of the IRE1 pathway do not reduce to ER-stressed APC-mediated iNKT cell activation. (A) The IRE1 inhibitors MKC 3964 and STF-083010 inhibit thapsigargin-induced XBP1 splicing **(B)** CD1d surface expression on THP1 cells treated as indicated. **(C)** The IRE1 inhibitors MKC 3964 (left) and STF-083010 (right) do not inhibit human iNKT cell activation by thapsigargin-treated THP1 cells. CD1d surface expression on THP1-CD1d cells that were either untreated or thapsigargin-treated (dark grey and light grey respectively) with or without the inhibitor (blue and orange, respectively). IFN-γ secretion is the average of N=2 biological replicates, each performed in technical duplicates.

We confirmed ATF6α is not involved in this mode of iNKT cell activation using the ATF6α-specific inhibitor ceapin-A7 (Gallagher et al., 2016). This inhibitor blocks transport of the ATF6α protein to the Golgi for site-specific cleavage into a transcription factor, thereby blocking the ATF6α transcriptional response during ER-stress (Gallagher and Walter, 2016) (**Figure 4.3.5A**). The HERPUD1 protein level, which is transcriptionally regulated by ATF6α, was reduced in 0.1μM ceapin-A7-treated THP1 WT cells co-treated with thapsigargin, compared to thapsigargin-treated cells alone (**Figure 4.3.5B**). At this concentration, we also saw no decrease in CD1d surface expression (**Figure 4.3.5C**). Finally when we titrated the

inhibitor in a functional assay, we saw no change in activation to C20:2 pulsed or thapsigargin pre-treated THP1 WT cells (**Figure 4.3.3D**). These findings confirm the lentiviral KD results – that neither IRE1 nor ATF6α are involved in ER-stress APC-mediated iNKT cell activation, but PERK and p-eIF2α signalling contribute to this mode of sterile activation.

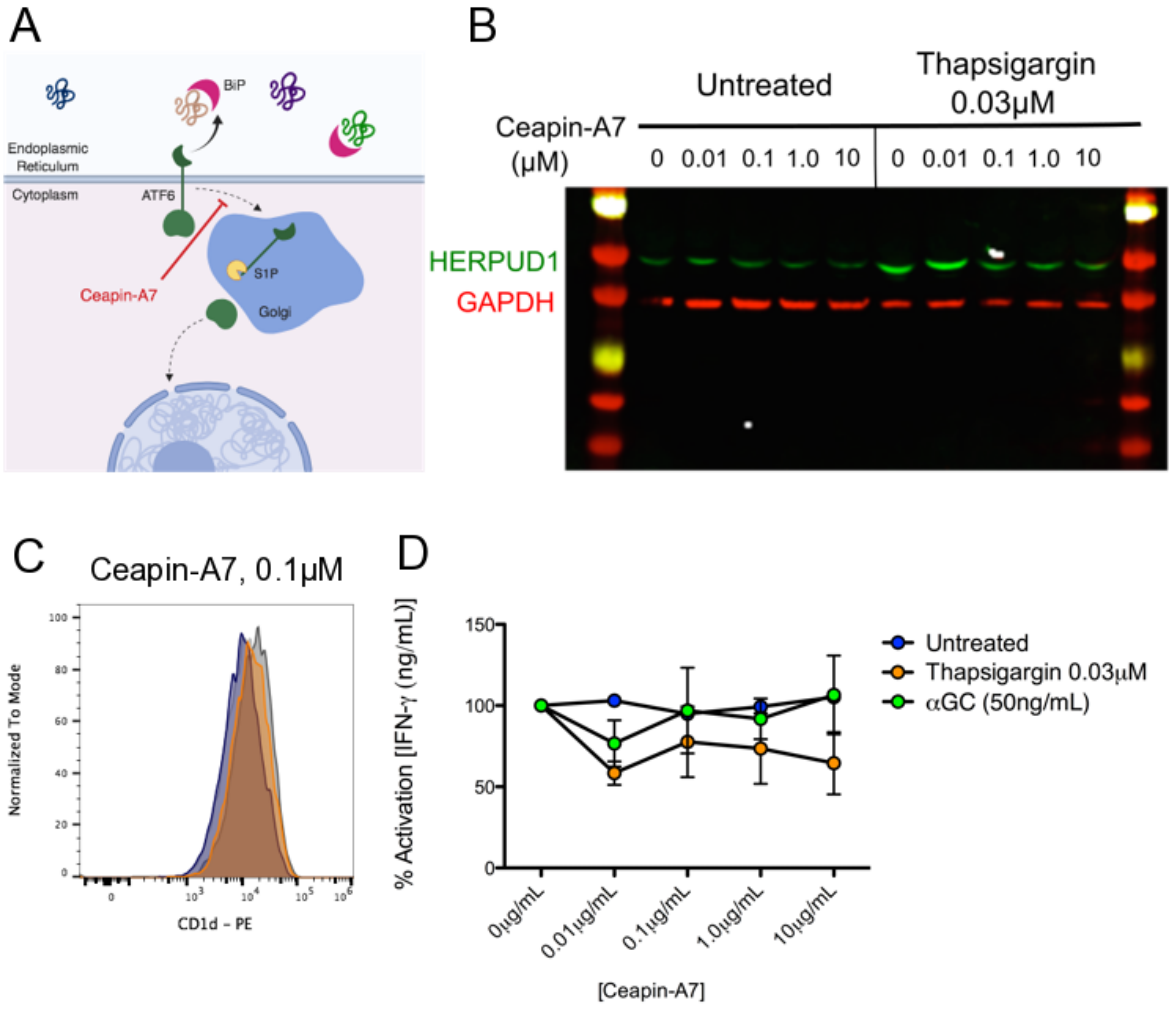

Figure 4.3.5 Small-molecule inhibition of the ATF6α pathway does not reduce ER-stressed APC-mediated iNKT cell activation. (A) The mechanism of action of the small molecule inhibitor of the ATF6α pathway, Ceapin-A7, which blocks translocation of ATF6α to the Golgi where it is cleaved into an active transcription factor **(B)** The ATF6α inhibitor Ceapin-A7 reduces expression of the downstream ATF6α target HERPUD1 **(C)** CD1d surface expression on THP1-CD1d cells either untreated or thapsigargin-treated (dark grey and light grey) or with the addition of the inhibitor (blue and orange). **(D)** Co-treatment of THP1 cells with Ceapin-A7 and thapsigargin co-

cultured with human iNKT cells. IFN-γ secretion is the average of N=3 biological replicates, each performed in technical duplicates.

4.4 ER-stressed APC-mediated iNKT cell activation is ATF4-independent

One of the hallmark transcription factors translated upon phosphorylation of eIF2α is ATF4, which, as previously described, acts a master regulator of a range of genes aimed at coping with a variety of stresses. Since ATF4 generation and translocation into the nucleus is an important event downstream of eIF2α phosphorylation, we generated a lentiviral transduced ATF4 KD THP1 cell line to assess this transcription factor's role in PERK-mediated iNKT cell activation. We assessed the degree of KD in THP1 WT cells that were treated with thapsigargin over a time course, as ATF4 protein expression is temporally regulated and only detected in the cytosolic protein fraction for a relatively brief time before translocating into the nucleus. In THP1 WT cells, ATF4 expression and detection in the cytosol peaked at roughly four to six hours (**Figure 4.4A, top**), whereas expression was drastically reduced or non-existent at the equivalent time point in ATF4 KD THP1 cells (**Figure 4.4A, bottom**). We tested whether thapsigargin pre-treated ATF4 KD THP1 WT cells altered iNKT cell activation compared to untransduced ATF4 KD cells. We found that KD of ATF4 in THP1 cells did not reduce, but in fact marginally increased iNKT cell activation (**Figure 4.4B**), suggesting that ATF4-mediated transcription does not effect or perhaps counteracts ER-stressed APC-mediated iNKT cell activation.

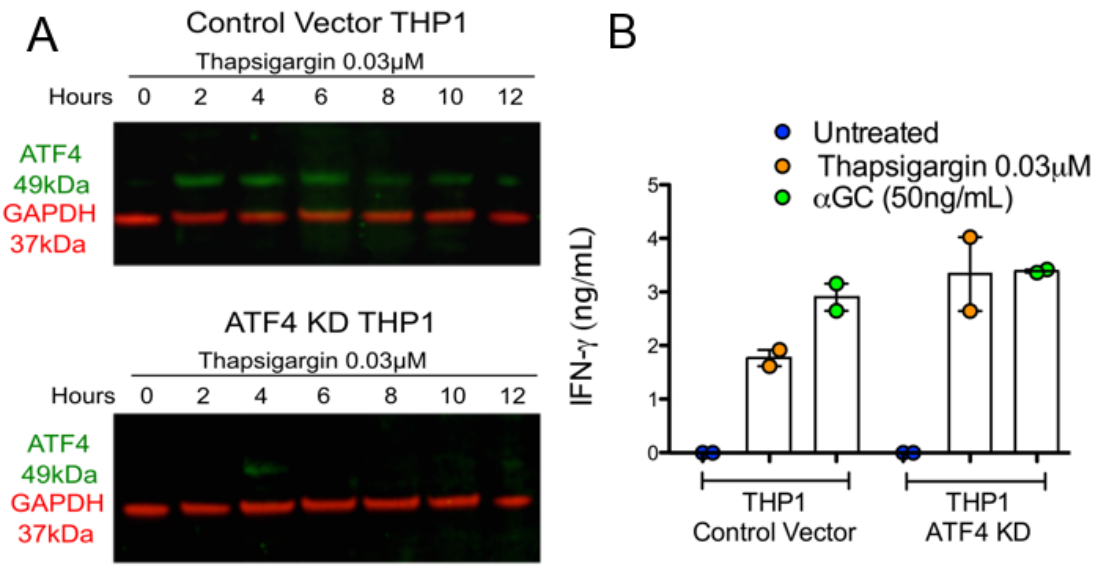

Figure 4.4 ER-stressed APC-mediated iNKT cell activation is ATF4-independent. (A) ATF4 induction upon thapsigargin treatment in control THP1 cells (top), but not in ATF4 KD cells (bottom). **(B)** Human iNKT cell activation by thapsigargin-treated APC is independent of ATF4 activity. IFN-γ secretion is the average of N=2 biological replicates, each performed in technical duplicates.

4.5 Discussion

This chapter focuses on defining the steps downstream the UPR that drives CD1d-dependent iNKT cell activation during ER-stress. To do so, we employed molecular biological and biochemical techniques to manipulate the pathways of the UPR, including shRNA KDs and small-molecule inhibitors. The results suggest that the signalling through eIF2α downstream the PERK pathway drives this mode of iNKT cell activation.

To confirm the role of the UPR in the phenotype, we needed to use an ER-stress inducing reagent without the off-target effects of thapsigargin. This led us to test the SubAB5 toxin, originally described by James Paton. Derived from Shiga-toxogenic *E.coli*, it resemble a typical subtilase cytotoxin; the A subunit is a serine protease that bears the conserved catalytic triad Asp-His-Ser, akin to that of

Bacillus anthracis; the pentameric B unit mediates cellular entry (Paton et al., 2006). In this paper, to determine the toxin's substrate, Vero cells were treated with either the WT SubAB5 or the $SubA_{A272}B5$ mutant, which is inactive due to mutagenesis of the crucial serine residue to an alanine residue in the enzyme cleft (Paton et al., 2006). Protein from the two treated samples was analysed by two-dimensional gel analysis, revealing 4 spots specific to the WT SubAB5-treated cells. Further mass spectrometry analysis identified that the only spot with significant size discrepancy corresponded to the master ER chaperone BiP. *In vitro* and *in vivo* assays confirmed the specificity for BiP, as 28kDa cleavage appeared in western blots from toxin-treated murine liver tissue and cell lines. The Paton group also confirmed that cleavage of BiP results in dissociation of the chaperone from the sensors of the UPR – IRE1, PERK, and ATF6. This dissociation is sufficient to trigger the UPR in the absence of a misfolded protein burden while minimizing off-target effects. However, the levels of IFN-γ secretion were not as high as that of iNKT cells co-cultured with thapsigargin pre-treated APCs, suggesting that off-target effects of thapsigargin contribute to the ER-stressed APC-mediated iNKT cell activation in addition to direct UPR signalling. Furthermore, the inactive mutant $SubA_{A272}B5$ toxin was an important negative control, as it assured us that the UPR, and not any contaminating bacterial product in the preparation, drove the iNKT cell activation. Assuming there is trace endotoxin in the preps of both the active an inactive mutant, this would support the idea that TLR signalling events altering the self-lipid repertoire on APCs are not predominantly contributing to this specific mode of activation, despite the

confusing results using the MyD88$^{-/-}$ BMDCs. However, we did not formally assess whether treatment with the toxin (both active and inactive) induces APC maturation.

Since the UPR contributes to ER-stressed APC-mediated iNKT cell activation, we sought to determine which branch(es) of the UPR are involved. To do so, we purchased lentiviral vectors bearing shRNAs targeted at the sensors of the UPR. When selecting shRNAs, we selected five shRNAs per sensor distributed across the length of the transcript, as certain regions might be more accessible to the shRNA or result in a more efficient knock down. When possible, we selected shRNAs that had been validated in A549 cells, although we understood that validation in one human cell line might not ensure equally good KD in a different cell line, especially since the A549 are lung epithelial cells while the THP1 cells are of myeloid lineage.

Two paralogs of IRE1 exist – IRE1α and IRE1β – that can form homodimers and signal. We chose to target IRE1α for several reasons. First and foremost, IRE1α is ubiquitously expressed across cell types, whereas IRE1β is specifically expressed in the intestinal and bronchial epithelium. IRE1β is not as efficient at splicing XBP1 through its endoribonuclease domain as its paralog, but it targets RNAs involved in ribosomal function to limit protein translation (Tsuru et al., 2013, Martino et al., 2013, Nakamura et al., 2011). As we provide evidence suggesting that PERK signalling contributes in part to ER-stressed APC-mediated iNKT cell activation, perhaps in the tissue sites where IRE1β is expressed (intestine and bronchus), IRE1β signalling might also have a greater contribution

to this mode of iNKT cell activation than in myeloid cells. Of course, it is not clear whether the same proteins are targeted by the translational blockade by both PERK and IRE1β. Had IRE1 been implicated in ER-stressed APC-mediated iNKT cell activation, we would have proceeded to knock down XBP1 to distinguish if activation was driven by the XBP1-directed transcriptional events or whether the RIDD activity of IRE1 was involved.

We also had the option of targeting shRNAs to either protein isoform, ATF6α or ATF6β. While ATF6α exerts UPR activating functions, driving the transcription of chaperones including BiP and generating the full length XBP1 transcript, ATF6β serves as repressor of ATF6α-mediated transcriptional activation, establishing a key regulatory mechanism in place to control ATF6 UPR responses (Thuerauf et al., 2007). Since we are largely concerned with the downstream effects of UPR activation, we used shRNA constructs targeting ATF6α.

To assess whether lentiviral transduction of shRNAs in THP1 cells had resulted in successful KD of each of the three sensors, we checked the total protein levels of each sensor in its respective KD cell line. We opted not to test the KD on the RNA level by qPCR since reduction at the protein level was mandatory. Both IRE1 and PERK are high molecular weight proteins (above 100kDa) the conditions for western blot were slightly different (a high molecular weight ladder was used and the transfer time was increased by three minutes). Detection of ATF6α is notoriously difficult, as it is expressed a relatively low level and there is a lack of good commercial antibodies. We used an antibody targeting the N-terminus

and detected a decrease at the corresponding with the weight of intact full ATF6α. The reduced protein expression at this molecular weight might represent cleavage and translocation of the C-terminal ATF6α fragment into the nucleus. However, we were cautious about this conclusion, as we saw no difference in expression in the WT cells treated with thapsigargin. Despite a few attempts, using stronger detergents and a shorter centrifugation step during the protein harvesting protocol, we were unable to detect the ATF6α cleavage product with by western blot. Due to these technical issues, we opted to use HERPUD1, and downstream transcriptional target (Kroeger et al., 2018), as a readout for ATF6α pathway signalling.

All three pathways regulate downstream molecules aimed at restoring ER homeostasis. IRE1 and ATF6 pathway mediate common or functionally similar chaperones aimed at reduced the misfolded protein burden, while persistent UPR signalling can initiate apoptosis via the PERK pathway. Therefore, we would expect that in functionally removing even one of the three pathways, there should be enhanced, compensatory signalling through the remaining intact pathways. This model is used routinely in the form of 'transgenic' ER-stress, such as $XBP1^{-/-}$ mouse models used by the Blumberg group (Hosomi et al., 2017, Kaser et al., 2008, Niederreiter et al., 2013, Zeissig et al., 2012). Given this information, we expected enhanced iNKT cell activation across the various treatments in the IRE1 and ATF6α KD cells lines. However, the activation levels were very similar across the treatments to the control vector cells, suggesting that this was not the case. It is possible that the additional KD of those two branches alone was not sufficient to

induce a detectable difference in the UPR and therefore iNKT cell activation. Generation of individual IRE1 and ATF6α knock outs using siRNAs or generation of an IRE1/ATF6α double KD might have allows us to test this theory further.

In this set of experiments we utilized an analogue of αGC, C20:2, which can surface bind CD1d rather than being loaded upon endocytosis. This allows us to test whether CD1d levels are comparable at the surface of KD cell lines and whether this surface CD1d is functional. While αGC can surface bind CD1d at high concentrations, there is the possibility that the KD cell lines would have defects in endocytosis and processing exogenous material and lipids. Exogenous GSLs are reported to be taken up through caveolar endocytosis (Singh et al., 2003) but under oxidative stress, which can trigger the UPR, caveolin 1 can be preferentially degraded (Mougeolle et al., 2015). In contrast, in early stages of ER-stress, caveolin-1 is reported to block ER-mitochondrial communication, in turn promoting apoptosis (Bravo-Sagua et al., 2019). When testing the small molecule inhibitors, we were unfortunately forced to switch to αGC due to a lack of C20:2.

We wanted to confirm the results with the lentiviral KDs of the sensors with small-molecule inhibitors for the three pathways. Small-molecule inhibitors have their drawbacks – they can be toxic at certain levels, have off target effects, and in co-culture system, treated cells must be washed before co-culturing. This matter is further complicated by the fact that they might be reversible or irreversible. Therefore, use of these small-molecule inhibitors required a wide dose curve and ample time to be taken up on cells (~6 hours).

Small-molecule inhibitors confirmed our findings with the shRNA KDs, but can also induce off-target effects. The PERK kinase inhibitor GSK2606414 was recently reported to also inhibit RIPK1, an important factor in TNF receptor-family mediated apoptosis (Rojas-Rivera et al., 2017). Interestingly, RIPK1 activity is reported to improve ConA, iNKT-cell dependent hepatic disease *in vivo*. Given the involvement of lipid dysfunction and presentation in ConA hepatitis, this finding suggests that the PERK inhibitor, through alternative RIPK1 signalling, might contribute to the ER-stress-driven mode of iNKT cell activation (Jouan-Lanhouet et al., 2012).

As the results indicate that eIF2α is required for ER-stressed APC-mediated iNKT cell activation, this opens up several new avenues of potential study. Since eIF2α is the central node of the Integrated Stress Response (ISRE), a variety of inputs can lead to phosphorylation and activation, including the GCN2, PKR, and HRI pathways. These pathways can be triggered by a variety of perturbations, there expanding the breadth of conditions by which this mechanism could apply.

Another new avenue to consider was what events downstream eIF2α is controlling the CD1d-dependent iNKT cell activation. Our results using ATF4 KD THP1 cells indicate that ER-stressed APC-mediated iNKT cell activation is not dependent on ATF4. This finding suggests that the activation phenotype might be driven by the decreased translation of a protein that either regulates the generation of an immunogenic self-lipid species or the loading of immunogenic self-lipid(s) onto CD1d. Had we continued to probe this pathway, we would

consider using cyclohexamide to block translation in an effort to mimic p-eIF2α. However, unlike eIF2α, it inhibits global translation.

Harding et al. found multiple transcriptional targets whose expression is upregulated in a PERK-dependent, ATF4-independent manner (Harding et al., 2003). RNAs that are selectively translated upon eIF2α phosphorylation contain a specific pattern of 5' proximal uORF that allows for certain proteins to be translated by the 'delayed initiation' mechanism that occurs when eIF2α is phosphorylated. Using RNA-sequencing and ribosomal profiling, we could seek out mRNA transcripts that both contain this uORF sequence and correspond to lipid synthesis or CD1d loading genes. We could compare mRNA transcripts involved in similar lipid modulations that do not contain the uORF sequence, and therefore whose translation would be blocked. A similar approach has been used to identify biological targets under the translational control exerted by eIF1, which directs selective translation through an alternative 'leaky scanning' mechanism (Fijalkowska et al., 2017). However, it would be helpful to first, or in parallel, determine the identity of the self-lipid agonist(s), as that will guide us on which classes of enzymes to focus, based on whether they promote *de novo* synthesis, lipid catabolism, or biochemical alteration of an existing lipid to produce the agonist, as will be discussed in the coming chapter.

Chapter 5: Signalling through the PERK pathway modulates the repertoire of self-lipid antigen(s) presented on CD1d

Multiple foreign lipid antigens have been characterized through a series of biochemical and structural strategies. The structures of some of these high-affinity foreign lipid antigens have been manipulated to generate synthetic agonists with improved iNKT cell activation and therapeutic potential. However, the characterization of self-lipid antigens in this manner is lacking by comparison, mainly due to technical difficulties. At this point, we have determined that iNKT cells can undergo sterile activation by ER-stressed APCs in a CD1d-dependent manner via PERK pathway signalling. However, since CD1d levels are minimally altered in ER-stressed cells, it begs the questions of how the PERK pathway is modulating CD1d-presentation to activate iNKT cells. In this chapter, we explore the possibility that the PERK pathway alters the self-lipid repertoire presented by CD1d molecules on ER-stressed cells to activate iNKT cells.

5.1 PERK signalling alters the presentation of self-lipids on CD1d recognized by iNKT cells

The fluorescently-labelled CD1d-αGC tetramer identifies iNKT cells by FACS by binding the iNKT-TCR with reasonable avidity to visualize a distinct iNKT cell population. Applying this principle in reverse, an APC presenting a very high affinity lipid antigen on CD1d will potentially bind the iNKT-TCR tetramer. We therefore used fluorescently-labelled iNKT-TCR tetramer to probe CD1d molecules

on the surface of ER-stressed APCs for presentation of high-affinity self-lipid antigens (Salio et al., 2007).

We found that iNKT-TCR staining was increased in thapsigargin pre-treated THP1-CD1d cells, and increased, though to a lesser extent, in SubAB5 pre-treated cells (**Figure 5.1A**). This increase was present but less evident in the control vector THP1-CD1d cells (**Figure 5.1B**), and completely abrogated in THP1-CD1d PERK KD cells (**Figure 5.1C**). Interestingly, the baseline tetramer staining profile of the THP1-CD1d PERK KD cells differed from the control cell lines, suggesting that PERK KD might have an inherent effect on CD1d or on a broad array of self-lipid antigens. We tested CD1d levels in parallel with the iNKT-TCR staining, and found no difference in CD1d surface expression between the three lines (**Figure 5.1D**). Together these results suggest that ER-stress alters CD1d-binding cellular lipids to enhance iNKT-TCR staining. We hypothesized that the enhanced iNKT-TCR tetramer staining in ER-stressed cells reflects the presentation of a more immunogenic self-lipid antigen(s) that activate iNKT cells.

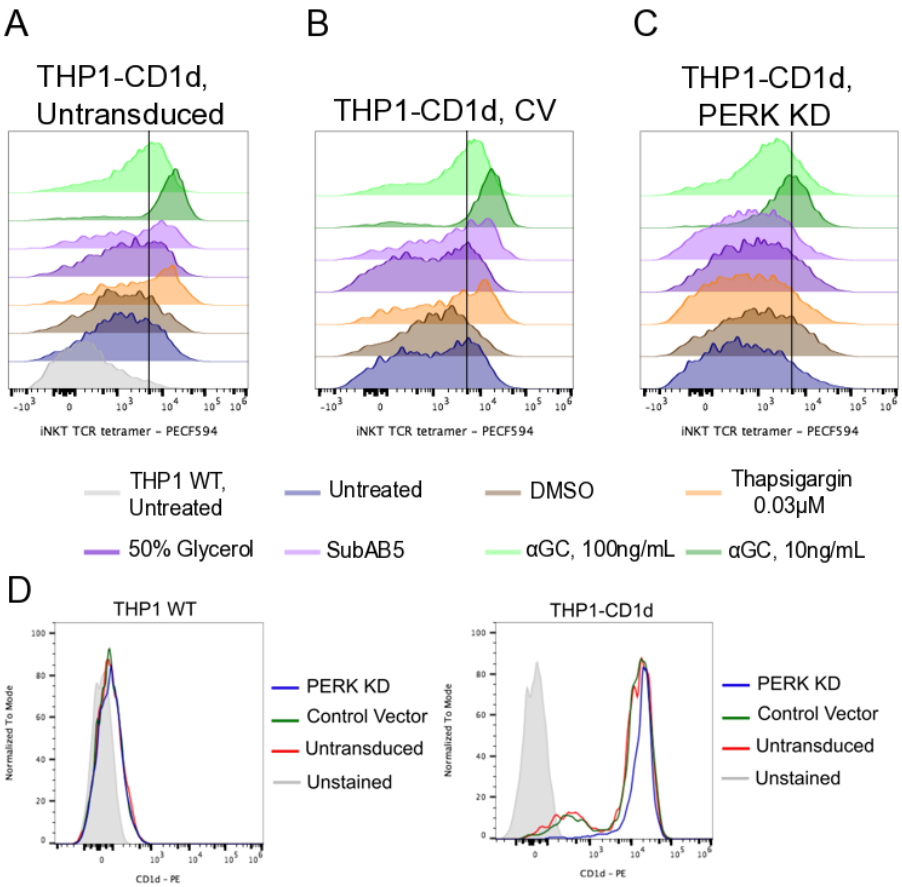

Figure 5.1 Soluble iNKT-TCR staining suggests a marginal shift towards a more immunogenic CD1d binding self-lipid repertoire in ER-stressed APCs. Untransduced THP1 WT cells (grey) or untransduced **(A)**, control vector (CV) transduced **(B)**, or PERK KD **(C)** THP1-CD1d cells were stained using a fluorescently labelled, soluble iNKT-TCR tetramer and analysed by flow cytometry. ER-stress was induced in these cells using thapsigargin or the SubAB5 toxin, and the corresponding solvent controls were included. As a positive control, THP1-CD1d cells were treated with two concentrations of αGC. **(D)** CD1d surface level on the untransduced, CV transduced, and PERK KD THP1 WT (left) and THP1-CD1d cells (right) performed in parallel with the iNKT-TCR staining. These results are representative of N=3 biological replicates, each performed in technical duplicates.

5.2 Fractions from whole lipid extracts of THP1 WT and PERK KD ER-stressed cells differentially activate iNKT cells

We wanted to determine whether ER-stressed APCs, through PERK signalling, alter their lipid composition such that an immunogenic self-lipid species is presented on CD1d to activate iNKT cells. To this end, we extracted whole lipids

from THP1 WT or PERK KD cell lines that were either left untreated or pre-treated with thapsigargin. The lipids were then separated into fractions based on hydrophobicity, with the more hydrophobic lipids theoretically eluting in the early fractions and more hydrophilic lipids eluting in the later fractions. These lipid fractions were pulsed onto recombinant CD1d molecules in a CD1d-plate bound assay. The results of this experiment indicated that lipids in Fractions I and II from ER-stressed THP1 WT cells are capable of activating iNKT cells in a dose-dependent manner, whereas lipids from the same fractions in ER-stressed PERK KD THP1 WT cells fail to activate iNKT cells (**Figure 5.2A**). Given the possibility that these lipids might bind outside the CD1d cleft and activate iNKT cells in an unexpected manner, we added a CD1d blocking antibody to the plate bound assay. Addition of the blocking antibody did reduce stimulation to activating ER-stress lipid fraction (**Figure 5.2B**). This finding suggested that PERK regulates self-lipids that can bind CD1d and activate iNKT cells.

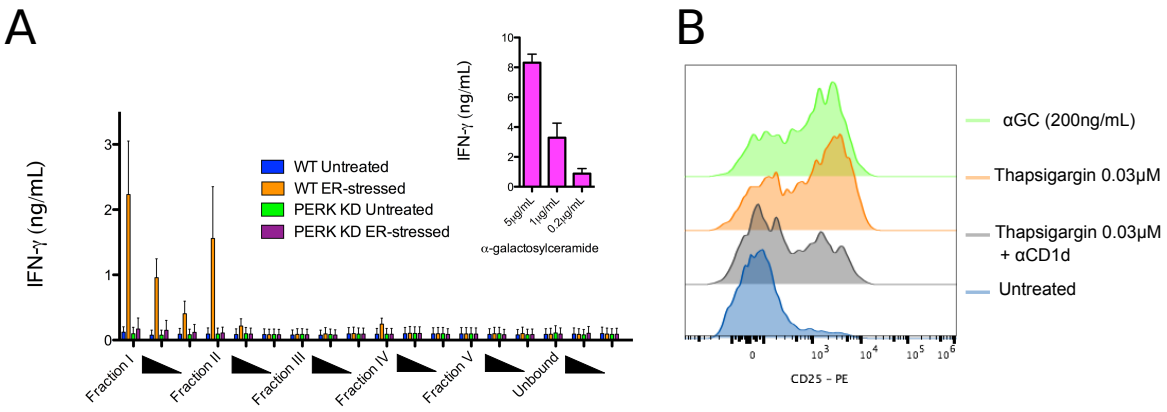

Figure 5.2 Hydrophobic lipid fractions isolated from ER-stressed THP1 WT cells, but not PERK KD cells, activated iNKT cells. (A) Lipids extracted from untreated or thapsigargin-treated WT or PERK KD THP1 cells as described in the methods were pulsed in three decreasing concentrations (solid triangles) onto recombinant, plate-bound CD1d molecules and co-cultured with human iNKT cells. Activation is measured by IFN-γ secretion. As a control αGC was added to the CD1d-coated plates (inset). * represents $p<0.05$ by one-way ANOVA with a Bonferroni post-test comparing ER-stressed WT group with the untreated WT group IFN-γ secretion is the average

of N=5 biological replicates, each performed in technical duplicates. **(B)** Activation of human iNKT cells cultured with lipids from Fraction I with and without a CD1d-blocking antibody (20 μg/mL) on the CD1d plate bound assay as measured by CD25 expression by flow cytometry. The histograms are representative of N=2 biological replicates.

5.3 Mass spectrometry confirms lipid classes, species, and relative abundance in each lipid fraction

At this point, we wanted to narrow down what types of lipids are present in the activating fraction. We analysed the lipid classes in each fraction by mass spectrometry (MS) to confirm that the fractionation had worked as expected. Indeed, more hydrophobic lipid classes eluted in the early fractions, predominately cholesterol and headless ceramides, and more hydrophilic lipids eluted in the later fractions, predominantly phospholipids (**Figure 5.3.1**).

When examining Fraction I, which is predominately the activating fraction, we found that most of the lipids were headless ceramides. However, when examining lipid species that contain classical iNKT cell agonists in the activating fraction, i.e. the hexosylceramides, we detected a species that contains 34 carbons, 1 double bond, and 2 hydroxyl groups (**Figure 5.3.2**) This species, like many other lipids in this fraction, seems to have a pattern of abundance that mirrors the pattern of activation i.e. a higher amount of lipid in the ER-stressed WT THP1 cells than the ER-stressed PERK KD THP1 cells. This hexosylceramide species constitutes only a small fraction of the total lipid content, especially compared to the headless ceramides class, but potentially very little lipid agonist is required to bind CD1d and activate iNKT cells. Furthermore, the length of this hexosylceramide species would fit in the CD1d cleft.

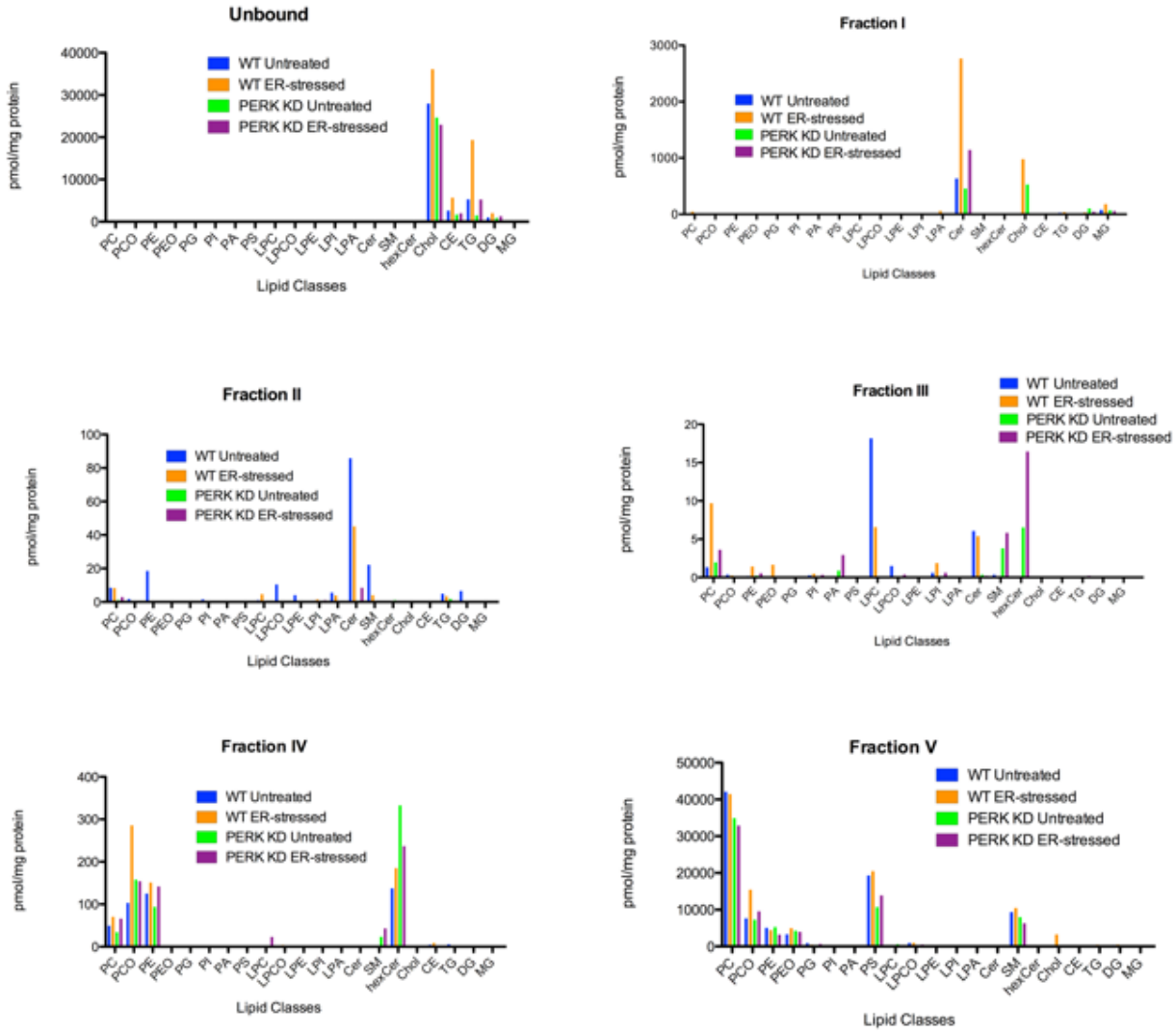

Figure 5.3.1 Mass spectrometry analysis of the lipid fractions confirms the presence of the predicted lipids in each fraction. The lipid classes in the six fractions from WT and PERK KD unstressed and ER-stressed cells were identified and quantified by shotgun mass spectrometry. Lipid quantity (in picomoles) was normalized to protein concentration for each sample. Lipid quantity represents the average of N=2 biological replicates, each performed in technical triplicate.

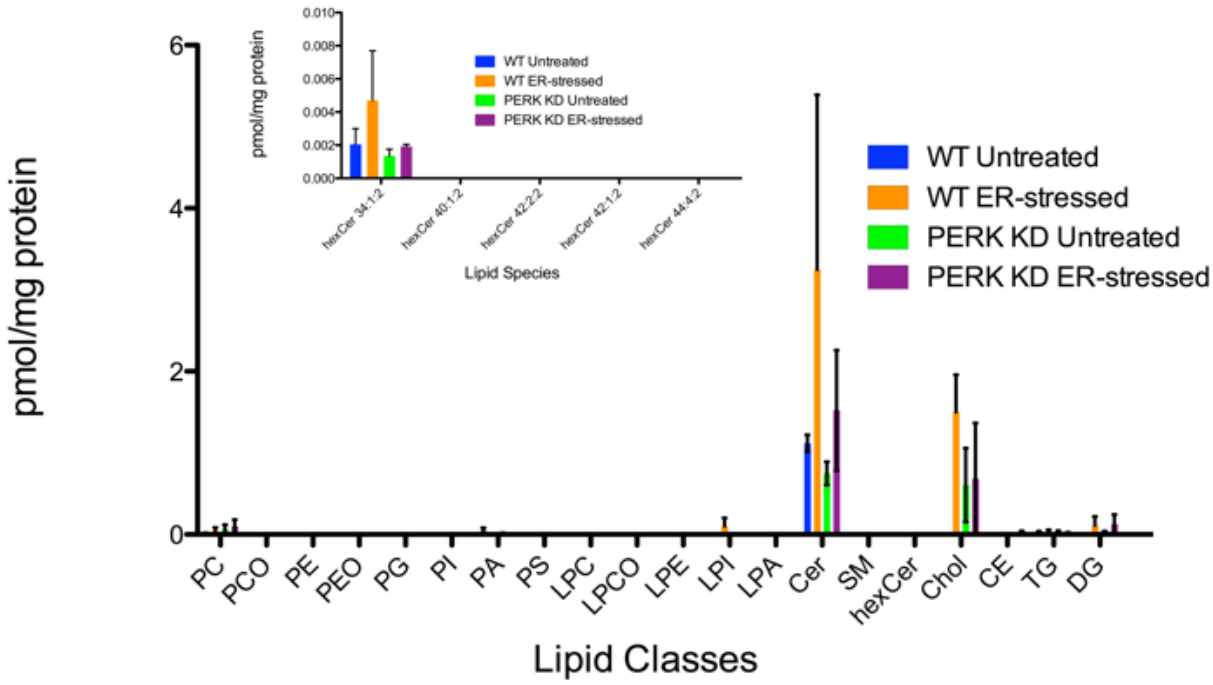

Figure 5.3.2 Lipid species that potentially correspond to iNKT cell agonists are present in the activating fraction. The lipid classes and species in Fraction I were identified and quantified by shotgun mass spectrometry. Hexosylceramide species were annotated by carbon length:double bond; hydroxyl groups (see inset). Lipid quantity (in picomoles) was normalized to protein concentration for each sample. Lipid quantity represents the average of N=2 biological replicates, each performed in technical triplicate.

5.4 Enzymatic digestion of the activating fractions suggests a role for β-glucosylceramide

In an effort to further narrow down the class in which the immunogenic lipid(s) belongs, we attempted to digest the activating fraction with a panel of enzymes that target specific lipids classes, with the hopes of reducing the activation when the particular lipid class is digested. We tested two enzymes: (1) the alkaline ceramidase ACER1, expressed highly in the skin, which hydrolyses long chain ceramides into sphingosine (Mao and Obeid, 2008) and (2) Cerezyme, commercial drug containing imiglucerase, an analogue of β-glucocerebrosidase that cleaves β-glucosylceramide (βGluCer) by hydrolyzing the β-glucosidic linkage

to release ceramide and glucose (Weinreb, 2008). These digested lipids were resuspended in DMSO and pulsed on the CD1d-plate bound assay as previously described. Whether the activation was contained in Fraction I or Fraction II of ER-stressed WT THP1 cells, separate treatment with ACER1 and Cerezyme reduced the activation to almost baseline levels, by both flow cytometry analysis of the iNKT cells in the CD1d plate bound assay and IFN-γ secretion (**Figure 5.4.1**).

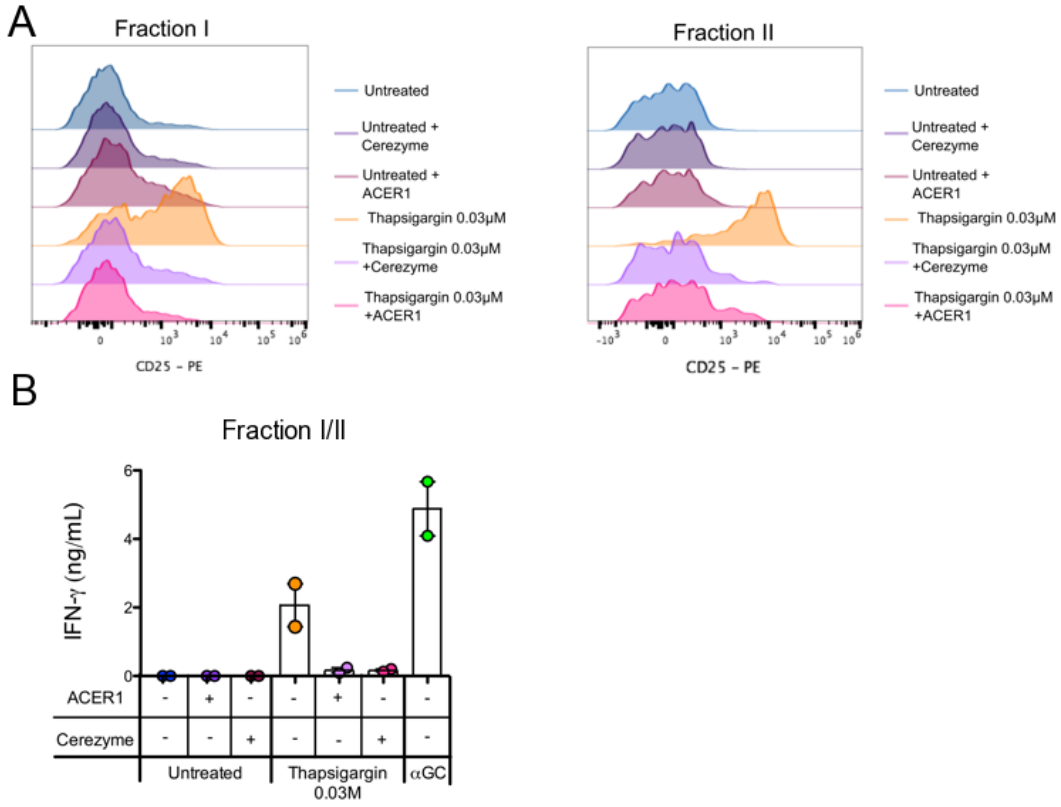

Figure 5.4.1 Digestion of the activating lipid fraction with the enzymes ACER1 and Cerezyme abrogates iNKT cell activation. Activation of human iNKT cells against plate bound CD1d pulsed with lipid fractions I and II from unstressed and ER-stressed WT THP1 cells. These fractions were either undigested or digested with Cerezyme or ACER1. Activation was measured by increased expression of CD25 on the iNKT cells **(A)** and IFN-γ secretion **(B)**. These results represent the average of N=2 biological replicates, each performed in technical duplicate.

This observation gave rise to four different possible explanations: (1) both enzymes are targeting the same immunogenic lipid species (2) there are multiple

immunogenic lipid species, and the enzymes target different species (3) the enzymes are cleaving multiple lipids in a non-specific manner and (4) the enzymes or their buffers are inhibiting activation in an off-target manner. To help determine which options are at play, the activating fraction, both undigested and digested with ACER1 and Cerezyme was analysed by MS to confirm the effect they are having on the lipids in the fraction (**Figure 5.4.2**). MS analysis suggested that ACER1 did cleave the ceramides, as evidenced by lower abundance of that class in both untreated and ER-stress samples, but other lipid classes were altered by the ACER1 treatment, that should not be affected, namely the decrease in phospholipids and increase in triacylglycerols in the ER-stressed fraction. The effect of Cerezyme treatment was unclear; there was no clear decrease in the hexosylceramide class (although Cerezyme only targets one species of hexosylceramide, βGluCer, and the class likely represents other species), and the treatment seemed to affect other lipid classes. When looking at the 34:1:2 hexosylceramide species in the undigested and digested fractions, the amount increases upon ER-stress, which is reduced upon ACER1 and Cerezyme treatment in both unstressed and ER-stressed samples. However, this is a very speculative hypothesis given this data, and many more experiments are required to prove or disprove it.

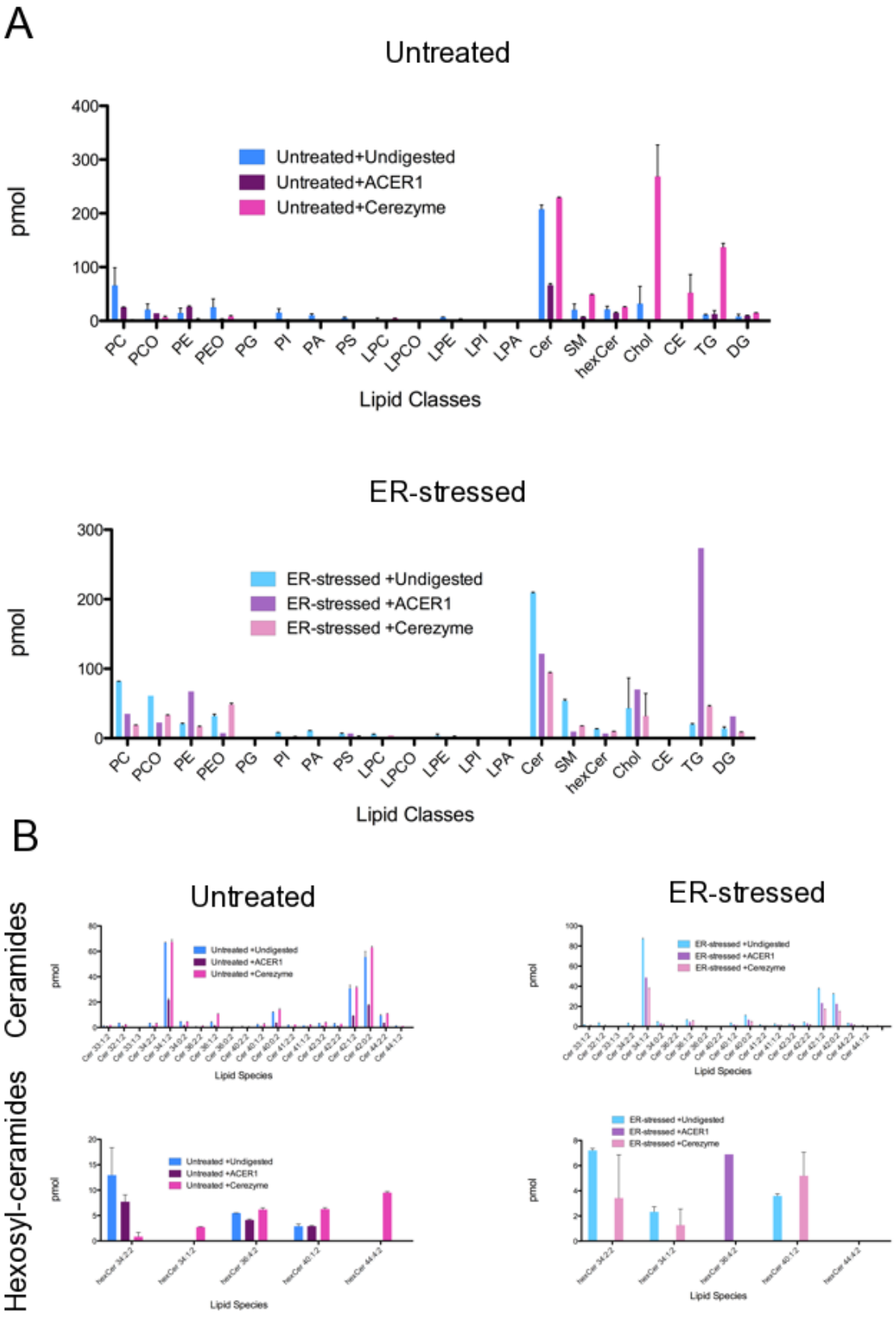
A
Untreated
pmol
400
300
200
100
0
Untreated+Undigested
Untreated+ACER1
Untreated+Cerezyme
PC
PCO
PE
PEO
PG
PI
PA
PS
LPC
LPCO
LPE
LPI
LPA
Cer
SM
hexCer
Chol
CE
TG
DG
Lipid Classes
ER-stressed
pmol
300
200
100
0
ER-stressed +Undigested
ER-stressed +ACER1
ER-stressed +Cerezyme
PC
PCO
PE
PEO
PG
PI
PA
PS
LPC
LPCO
LPE
LPI
LPA
Cer
SM
hexCer
Chol
CE
TG
DG
Lipid Classes
B
Ceramides
Hexosyl-ceramides
Untreated
ER-stressed
pmol
Untreated +Undigested
Untreated +ACER1
Untreated +Cerezyme
ER-stressed +Undigested
ER-stressed +ACER1
ER-stressed +Cerezyme
Lipid Species

Figure 5.4.2 Mass spectrometry of the digested fractions to assess the efficiency and specific of the enzymes. (A) The lipid classes in the activating fraction from unstressed and ER-stressed THP1 WT cells were identified and quantified by shotgun mass spectrometry (blue). The abundance of lipid classes the same fraction digested with ACER1 (pink) and Cerezyme (purple) are also plotted. **(B)** The abundance of lipid species of particular classes in the activating fraction from unstressed and ER-stressed THP1 WT cells. Lipid quantities (picomoles) represent an N=1 biological replicate, performed in technical triplicate.
.

Our approach to narrowing down the identity of the self-lipid brought about obstacles to confirm the validity of the functional data. The functional data points towards a species of βGluCer, but without sufficient controls and further experimentation we cannot support this hypothesis.

5.5 Loading of immunogenic self-lipids during ER-stress conditions requires CD1d to traffic through the endosomal/lysosomal recycling pathway

Since it became too laborious a process within the time frame to directly identify the immunogenic self lipid(s), we refocused our efforts in determining other attributes about the immunogenic self-lipid(s) involved in ER-stressed APC-mediated iNKT cell activation. Loaded CD1d molecules traffic via the trans-Golgi network to the cell surface, but can be recycled through the AP2/3-mediated endosomal pathway and enter the lysosome through AP2/3-interactions with the cytoplasmic tail of CD1d (Jayawardena-Wolf and Bendelac, 2001), where it can exchange lipids through saposin activity and traffic back to the cell surface to present to the new lipids (Yuan et al., 2007, Salio et al., 2013). Given that lipids could be loaded in different compartments, we wondered in what subcellular location the immunogenic self-lipid(s) in ER-stressed APCs might be loaded. To

this end, we pre-treated three THP1 cell lines each over-expressing different types of CD1d molecules. The first line is THP1-CD1d, used previously, which over-expresses full length CD1d. It traffics normally throughout the cell to present and exchange lipids from the ER, endosomes, and lysosome. The second line is THP1-CD1d tail$^{-/-}$, which overexpresses CD1d lacking the last C-terminal eleven amino acids on the cytoplasmic tail, thereby preventing interaction with AP2/3 and consequently preventing recycling of CD1d molecules into the lysosome (Jayawardena-Wolf et al., 2001). These CD1d molecules can pick up and present lipids from the ER and early endosome, but cannot present lipids that require processing and loading in the acidic lysosome. The third line is THP1-CD1d GPI, in which a glycosylphosphatidylinositol (GPI) is added onto the C-terminal tail of CD1d as a post-translational modification in the ER. GPI glycolipids are composed of a phosphatidylinositol group linked through a carbohydrate-containing linker (glucosamine and mannose bound by a glycosidic linkage to the inositol residue) and via an ethanolamine phosphate bridge to the C-terminal amino acid (Paulick and Bertozzi, 2008). Two fatty acid chains from the hydrophobic phosphatidylinositol group anchors CD1d into the cytoplasmic membrane, thereby preventing it from entering the recycling pathway. These CD1d molecules can present lipids from the ER, but not from the endosome or lysosome.

Since CD1d trafficking is altered in these cell lines, we wanted to confirm that CD1d surface levels and lipid-presentation abilities were comparable across the three cell lines. To assess this, the three cell lines were both stained for CD1d surface expression and pulsed with C20:2. We found that CD1d surface level were

comparable across all three cell lines (**Figure 5.5.1**). To confirm that the CD1d molecules expressed in THP1-CD1d tail$^{-/-}$ and THP1-CD1d GPI cells exhibited impaired trafficking to the recycling pathways, we pulsed all three cell lines with Gal(α1–2)galactosylceramide (GGC), a lipid agonist with two galactose moieties on the head group and requires processing by α -galactosidase A in the acidic lysosome to remove the extra sugar head to activate iNKT cells (Prigozy et al., 2001). In addition to these control conditions, the three cell lines were pre-treated with thapsigargin as previously described.

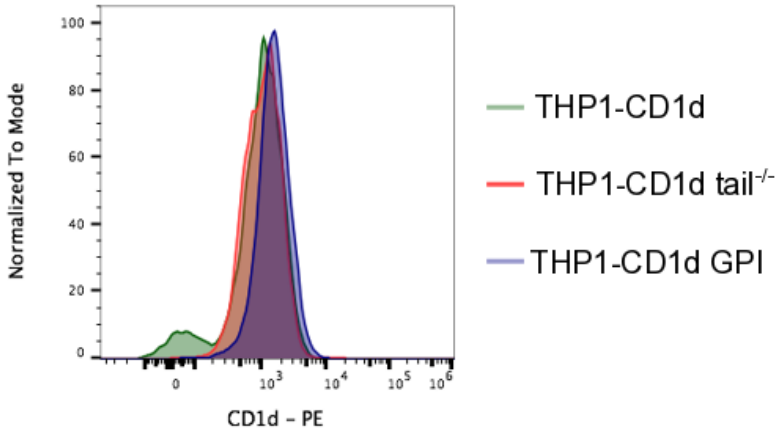

Figure 5.5.1 Cell lines over-expressing modified CD1d molecules express comparable CD1d surface levels. CD1d levels were measured on the surface of THP1 cells overexpressing full length CD1d (THP1-CD1d), CD1d with a deletion of 11 amino acids in the cytoplasmic tail domain (THP-CD1d tail$^{-/-}$) and GPI-linked CD1d (THP1-CD1d GPI).

In a functional assay, the C20:2 presentation was not appreciably reduced (although slightly reduced in the THP1-CD1d GPI cells), the iNKT cell activation to GGC-pulsed and thapsigargin pre-treated cells was reduced in the lines with impaired trafficking (**Figure 5.5.2A and B**). This result points to the possibility that ER-stress related immunogenic self-lipid(s) are loaded onto CD1d molecules in the recycling compartment of the cell, that is, the endosome or lysosome. It is difficult to assess whether these immunogenic self-lipid(s) exist within the

endosome/lysosome, and are modified or upregulated during ER-stress, or whether they exist in other cellular compartments but under ER-stress are trafficked into the endosome/lysosome where they can be loaded on CD1d molecules. Following the latter possibility, we hypothesized that autophagic pathways permit the immunogenic self-lipid loading onto recycling CD1d molecules.

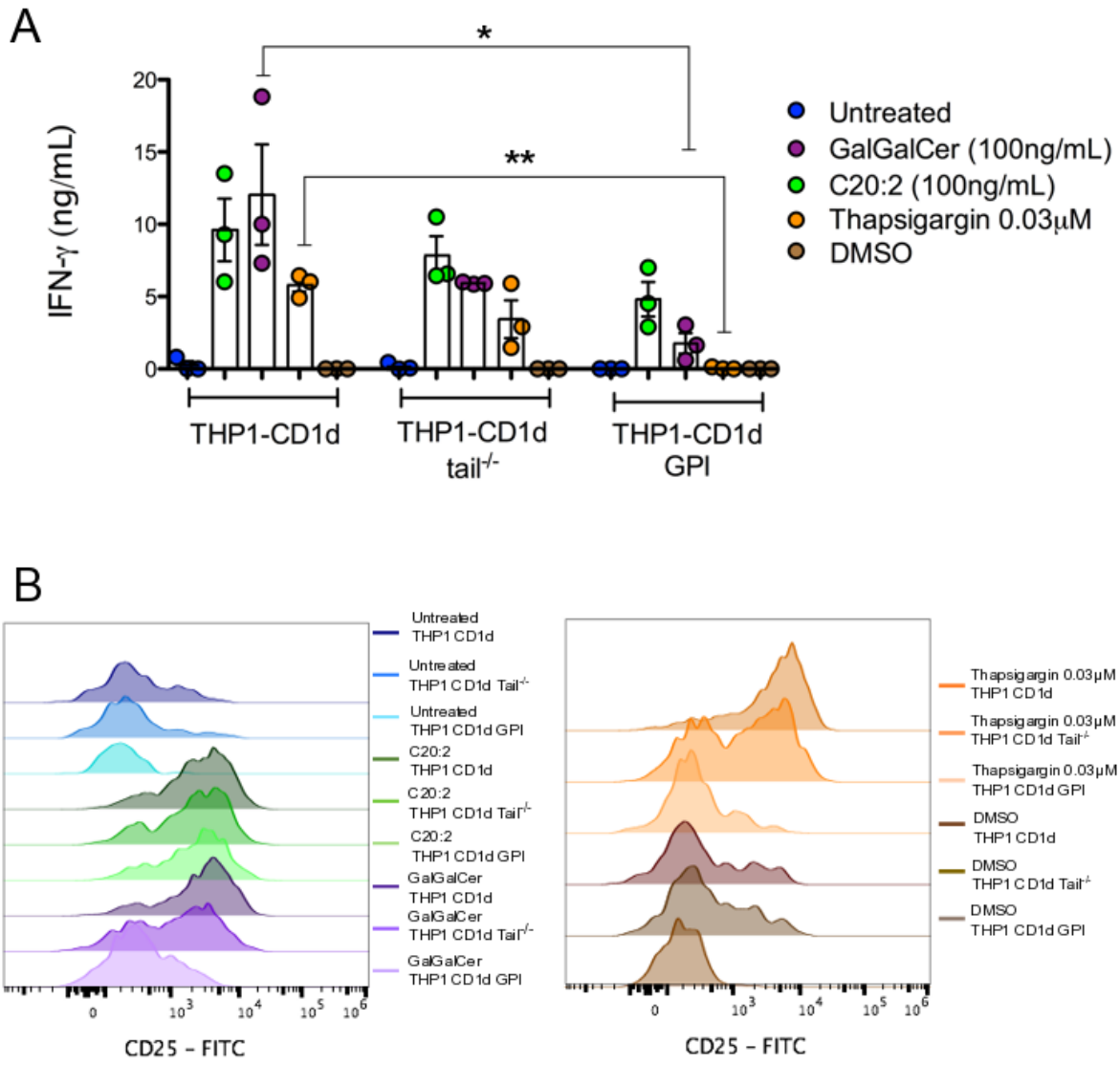

Figure 5.5.2 Immunogenic self-lipid antigen(s) are loaded onto CD1d molecules in the endosomal/lysosomal recycling pathway in ER-stressed APCs. Thapsigargin-treated THP1-CD1d, THP-CD1d tail$^{-/-}$ and THP1-CD1d GPI were co-cultured with human iNKT cells. As a control,

the THP1 cell lines were treated with C20:2. iNKT cell activation was measured by **(A)** IFN-γ secretion and **(B)** CD25 surface expression. Experiments are representative of N=3, each performed in technical duplicates. * and ** represents $p<0.05$ and $p<0.005$, respectively, by a one-way ANOVA with a Dunnett's Multiple Comparison post-test.

5.6 ER-stressed APC-mediated iNKT cell activation does not require autophagy

One of the downstream consequences of ER-stress and PERK signalling in particular, is the induction of autophagy. The PERK/eIF2α/ATF4 axis has been implicated in tipping the balance between autophagy – pushing for cell survival in the face of ER-stress – and apoptosis – committing to cell death in the face of overwhelming ER-stress (Liu et al., 2015). A hallmark of autophagy is the formation of autophagolysosomes, in which double-membraned autophagosomes containing intracellular material, including organelles, fuse with the acidic lysosome so that the cargo is degraded as a source of amino acids, energy etc. (Dikic and Elazar, 2018). Given that the immunogenic self-lipid(s) in ER-stressed APCs are loaded onto CD1d molecules in the endosome/lysosome, we wondered if autophagy provides an opportunity for lipids from other cellular compartments, such as the ER, peroxisome, mitochondria etc. to be processed and loaded onto recycling CD1d molecules.

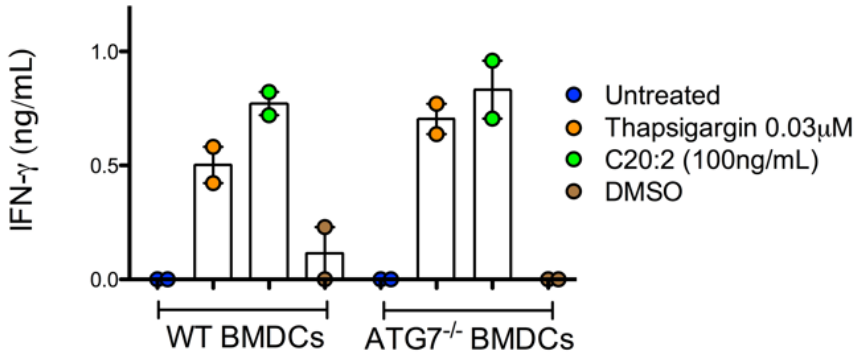

Figure 5.6 ER-stressed APC-mediated iNKT cell activation is autophagy-independent.
Human iNKT cell activation by thapsigargin-treated BMDCs is independent of ATG7 expression. IFN-γ secretion is the average of N=2 biological replicates, each performed in technical duplicates.

To test this hypothesis, we used BMDCs from WT and ATG7$^{-/-}$ mice, as ATG7 is a crucial regulator of autophagosome development in the early stages of autophagy (Mortensen et al., 2011). We found that thapsigargin pre-treated ATG7$^{-/-}$ BMDCs activated iNKT cells at a comparable, if not higher level, than WT BMDCs, as measured by IFN-γ secretion (**Figure 5.6**). This result suggests that ER-stressed APC-mediated iNKT cell activation is autophagy-independent.

5.7 Discussion

Up until this point, efforts to tease out the mechanism of iNKT cell activation focused on defining the components of the UPR that contribute to the ER-stressed APC-mediated iNKT cell activation. However, in this chapter, we studied the mechanism from 'the other end', by characterizing the activating self-lipid antigen(s) presented by CD1d molecules on ER-stressed APCs. Extensive future experimentation is required to build on our current knowledge of the ER-stress-dependent self-lipid(s), and rule out the possibility of activating contaminants.

Apart from work by the Gumperz group, who reported that signalling via ATP has been proposed to boost sterile activation of iNKT cells upon recognition of basal auto-antigens on CD1d (Xu et al., 2016b), most previous work in this field has identified lipids that bind CD1d and activate iNKT cells but, as mentioned in Chapter 1, fell short of placing their presentation in a relevant physiological setting. Our research sets itself apart by both describing both functional characteristics of an activating self-lipid species and providing a sterile, physiologically context in which they would be presented by CD1d molecules. However, we did not elucidate the specific identity and structure of the self-lipid(s) in question. The task of identifying self-lipid antigens has previously been wrought with obstacles, largely stemming from contamination of α-linked GSLs that can strongly activate iNKT cells (Brennan et al., 2014). For this reason, the experimental pipeline to accurately determine the ER-stressed APC-mediated self-lipid(s) would be rigorous.

To determine if there was a link between PERK signalling and the generation of immunogenic self-lipid antigen(s), we performed a CD1d plate bound assay using lipid fractions derived from unstressed and ER-stressed WT and PERK KD THP1 cells. A major benefit of this assay is that it removes confounding factors such as APC cell death, both from drug treatments and activated iNKT cells, and bidirectional cytokine secretion, to assess iNKT cell activation by direct CD1d:lipid and iNKT-TCR interaction. However, performing this assay is not without pitfalls. The first is that we cannot know the exact amount of lipid loaded onto the plate-bound CD1d molecules. Although the lipid samples were

normalized to the protein content of each sample to better compare across biological replicates, this amount varied slightly between experiments (in some cases, due to lower levels of protein). Also, micelles might have formed in certain fractions at high lipid concentrations, which would sequester certain lipids from binding into the CD1d groove. This phenomenon is a particular concern for certain ambipathic lipid species, such as phospholipids with a hydrophilic head group but long, hydrophobic fatty acid tails. Lysophospholipids have been previously identified as ER-stress-induced self-antigens (Zeissig et al., 2012), so we wonder whether micelle formation prevented us from detecting them as potential antigens in our experiments. While we titrated our lipid samples by three-fold dilutions in the assay in an attempt to see a dose-dependent effect and reduce the chance of micelle formation, we cannot rule it out.

A second limitation of the CD1d plate-bound assay is that we cannot be certain that the lipids are activating iNKT cells by binding directly in the CD1d groove. Activating contaminants from the elution buffers can be ruled out, as unbound and washing fractions from each lipid fractionation was prepared and pulsed alongside the actual lipid fractions in initial experiments, and showed no reactivity. Although we washed unbound lipids from the plate bound assay before adding iNKT cells, it is possible that lipids were bound to the well or the outside of the CD1d groove. Addition of the CD1d-blocking antibody to the assay partially blocked the activating self-lipid(s) suggesting that there is a contribution from a non-CD1d binding component of the lipid fractions. The fact that activation is not

reduced to the level of untreated lipid fraction might also be due to an insufficiently high concentration of blocking antibody.

Based on the findings of the CD1d plate bound assay, we subjected the fractions to MS analysis. Each lipid fraction was split into two: one was sent for MS analysis and the other was used in a CD1d plate bound assay. We also compared the identity of lipid species in the fractions to that in the THP1 cellular lipidome by analysing the whole lipid content extracted from lysed THP1 cell (from the step preceding the fractionation). A blank sample tube washed with buffer served as a control for background signal. With these controls in place, we ensured that we only considered lipid species coming from the THP1 cell lysate, and not potential exogenous lipid contaminants introduced during the fractionation and drying down procedure. While it was tempting to pick out candidate activating lipids based on the abundance of different classes and species, lipid molecules in very low abundance could still be sufficient to bind CD1d and activate iNKT cells, especially if it interacts with CD1d and the TCR with a sufficiently high affinity. We also scanned the fractions for lipids that could constitute classical iNKT cell agonists. This includes lipids with a polar head group, such as hexosylceramides to interact with the TCR, and hydrophobic lipid tails to anchor the antigen in the deep A' and C' pockets of CD1d, with the acyl tail and conserved sphingosine chain, respectively. Diacylglycerols, which we detected in the activating fraction, have also been implicated in binding CD1d and activating iNKT cells when derived from *Streptococcus* species (Kinjo et al., 2011). Trace phospholipids in the activating fraction constitute another possible activating lipid species (Zeissig et al., 2012).

As we adopted a reductionist approach to identifying the lipid agonist(s), we wanted to enzymatically digest the fractions to determine which lipid class or classes contribute to this mode of iNKT cell activation. The enzymes were selected based on availability and the spectrum of lipids theoretically affected by the digestion. Since the ceramides were the dominant lipid class in the activating fraction, we opted for the enzyme alkaline ceramidase 1, or ACER1, and Cerezyme. To assess the relevance of the trace phospholipids, we included a basic KOH treatment, to strip the phosphate head groups from the phospholipids. To confirm that the treatments had worked, we tested the digests on the activating fraction as well as positive control fractions that, according to previous MS analysis, were most abundance in hexosylceramides (Fraction IV) and phospholipids (Fraction V). However, due to limited time and resources, we only received the analysis for digests of the activating fraction. The results for the KOH treatment were omitted, as the samples ionized poorly, perhaps due to the interference of salts from the treatment. The level of ceramides in the activating fraction decreased upon ACER1 digestion, while other lipid classes were largely unchanged (with the clear exception of triacylglycerol class from ER-stressed sample). The digestion with Cerezyme was inconclusive. While βGluCer is a relatively abundant mammalian glycosphingolipid, when considering all hexosylceramides in mammalian cells, any decrease due to digestion is not likely to be observable. Furthermore, it seemed to have differential effects on other lipid classes that should theoretically be unaffected by Cerezyme digestion, and there was further variation between unstressed and ER-stressed samples. Nonetheless,

we decided to take the lipids digested with the two enzymes forward to the CD1d plate bound assay. Here we found that both enzymes abolished the iNKT stimulatory activity of the activating fraction. The reported high specificity of Cerezyme for βGluCer, coupled with the fact that ceramidases are reported to cleave hexosylceramide as well as headless ceramides (Ferraz et al., 2016), provides evidence that βGluCer might be our candidate lipid agonist.

In future we could confirm that both enzymes cleave βGluCer by digesting the synthetic form of the lipid with the enzymes and running the product on high performance thin layer chromatography, where the lack of a sugar moiety would cause the lipid to migrate faster on the gel. We also need to perform several additional controls to ensure that activation in this fraction is abolished due the cleavage of βGluCer, and not due to an off-target effect. These controls include testing the specificity of the enzymes by digesting fractions from cells pulsed with synthetic αGC, αGluCer, or βGalCer, or digesting the activating lipid fraction with β-galactosidase, after which the fraction should remain activating. MS analysis would accompany these treatments. Other groups have reported being able to differentiate between α- and β-linked GSLs via MS – their approaches could be useful in our analyses (von Gerichten et al., 2017).

An understanding of the structure and size limits of the CD1d binding groove might help guide our identification of the activating lipid species, be it βGluCer or another type of lipid. For example, αGC, with an acyl tail 26 carbons in length, and a sphingosine tail of the 18 carbons in length fits well into the groove and generated a predominantly Th1 response for iNKT cells. In contrast, OCH,

and short chain αGC analogue, exhibits a weaker TCR affinity and skews iNKT cell response towards a Th2 profiles (Zajonc and Girardi, 2015). Given this, we can focus our attention on species whose predicted fatty acid tail lengths adhere to size of the A' and C' pockets. For βGluCer, the sphingosine tail is derived from palmitate condensation and therefore is always 16 carbons in length. Focusing on the acyl tail, most of the species of hexosylceramides detected in our MS analysis would likely contain βGluCer species with 16-26 carbon acyl tails. Given that C20:2, the surface binding αGC analogue, has a 20-carbon acyl tail with 2 double bonds, the potential βGluCer self-lipid might be a similar size.

If future experiments point more cleanly to a specific lipid class or species, for example, βGluCer, we would continue to confirm its role in iNKT cell activation by testing multiple species of synthetic βGluCer on the CD1d plate bound assay and use the candidate species to refold and form CD1d:βGluCer tetramers to confirm the presence of βGluCer-reactive iNKT cells. An alternative approach, moving away from the plate bound assay, is to harvest soluble CD1d molecules from a CD1d-secreting unstressed and ER-stressed cell line and perform the TCR trap method (Brennan et al., 2017). Briefly, using soluble CD1d and soluble iNKT-TCR molecules, lipid antigens are 'trapped' when bound to CD1d and engaging the soluble TCR. This tri-molecular complex can be identified and purified by size-exclusion gel chromatography; the bound lipid eluted using chloroform/methanol, and is subject to MS analysis to identify the lipid. This method would more efficiently narrow down the identity of the CD1d-bound lipid, which can interact with the TCR, on ER-stressed APCs. Our earlier experiment using the iNKT-TCR

tetramer showed only slightly elevated staining, which might foreshadow difficulties in terms of abundance of tri-molecular complexes bearing the activating self-lipid(s). Ultimately, we would have to obtain a crystal structure of the self-lipid(s) bound to CD1d and interacting with the iNKT-TCR to confirm the structure and functional relevance of the putative activating self-lipid antigen(s).

In our efforts to determine the self-lipid antigen(s) implicated in ER-stressed APC-mediated iNKT cell activation, we have focused on lipids with a polar moiety, such as glucose that would interact with the iNKT-TCR. However, recent findings indicate that T cell autoreactivity against the group 1 CD1 molecule, CD1c, is mediated not by the direct recognition of a specific lipid presented by CD1c, but rather by direct recognition of the altered conformation of CD1c when binding self-lipids (Wun et al., 2018), a finding reminiscent of CD1a. It is currently unclear if this paradigm-shifting finding can apply to any other members of the CD1 family, including CD1d. However, the possibility exists that a species of the most abundant lipid class in the activating fraction, headless ceramides, might in fact mediate iNKT cell autoreactivity in ER-stress conditions, despite lacking the polar head group necessary for CDR3 interaction.

It remains unclear whether the lipid(s) involved in ER-stressed APC-mediated iNKT cell activation are generated *de novo* or are modified pre-existing self-lipids that are preferentially loaded onto CD1d. βGluCer is abundant in the lysosome, in which the ER-stress mediated self-lipid(s) are loaded, at steady-state conditions. The Brenner group has postulated that βGluCer is a human self-lipid antigen (Brennan et al., 2011), though contamination with αGluCer called this

finding into question (Brennan et al., 2014). However, in the context of ER-stress βGluCer might be modified to more readily bind or stabilize CD1d, or be more immunogenic. Enzymes involved in lipid synthesis, through catabolism of longer lipids, or in modification of structural features of the lipid, might also be altered by a changing transcriptional and translational profile of ER-stressed cells. XBP1-mediated transcription has been shown to drive expression of lipogenic enzymes in hepatocytes, linking ER-stress to modulated lipogenesis (Lee et al., 2008). Furthermore, changes in the location of doubled bonds in the fatty acyl chains are known to alter immunogenicity of CD1d-bound glycolipid antigens (Girardi et al., 2011), and unsaturated double bonds in the acyl tail of αGC is important in its interaction with the A' pocket of CD1d (Koch et al., 2005).

While we have focused on ER-stress as a means of upregulating activating self-lipids, an alternative hypothesis is that ER-stressed APCs down regulate presentation of inhibitory self-lipids, such as GM3 (Park et al., 2008, Tiper et al., 2016). These hypotheses are not mutual exclusive, as a skewed balance between the presentation of activating and inhibitory self-lipids might account for the ER-stressed APC-mediated phenotype.

We also cannot rule out the possibility that changes in the CD1d-loading machinery under ER-stress conditions might contribute to the preferential loading of immunogenic self-lipid antigens. Microsomal triglyceride transfer protein (MTTP) is involved in CD1d loading of lipids in the ER (Dougan et al., 2005). Its function can be modified when it forms heterodimers with PDI, a chaperone upregulated upon ER-stress (Wang et al., 2012). Independent of PDI, MTTP was also shown to

regulate lysosomal CD1d trafficking (Sagiv et al., 2007). These observations point to a potential role for MTTP/PDI in loading lipid antigens onto CD1d molecules in ER-stressed APC-mediated iNKT cell activation. Given this necessity for CD1d to recycling the endosome/lysosome, it is also possible the saposins are involved self-lipid loading onto CD1d under ER-stress conditions. Altered localization of the lipid from its native compartment into the endosomal/lysosomal recycling pathway might also allow for the self-lipid(s) from other compartments to be better presented on CD1d.

To this end, we also considered autophagy as an additional stress-related pathway that might influence ER-stressed APC-mediated iNKT cell activation, particularly given the overlap between PERK signalling and autophagic pathways. It would provide a means of lysosomal loading of lipids from other cellular compartments onto CD1d through the formation of autophagolysosomes, as might occur during ER-phagy or mitophagy. It is reported that ether linked self-lipids derived from the peroxisome can activate iNKT cells (Facciotti et al., 2012), but where it is loaded is not clear – inclusion into the autophagolysosome is a potential explanation. However, we showed using ATG7$^{-/-}$ BMDCs that autophagy is dispensable in thapsigargin-mediated iNKT cell activation. This finding is consistent with the report by Ganley et al, which, contrary to other literature, illustrates that thapsigargin blocks autophagy by inhibiting formation of autophagosomes (Ganley et al., 2011).

The necessity for the ER-stress driven self-lipid antigen to be loaded in the recycling pathways has several potential implications for our understanding of this

mechanism of activation. Firstly, it opens up the possibility that the activating self-lipid might be acquired exogenously from dead or dying cells, such as those experiencing overwhelming ER-stress, and loaded onto CD1d in endosomal or lysosomal compartments in a manner akin cross-presentation (Wu et al., 2003). Secondly, the fact that the self-lipid(s) must be loaded in the endosomal and lysosomal compartment suggests that altered localization of the lipid from its native compartment into the endosomal/lysosomal recycling pathway might be required for CD1d presentation. While autophagy might not be implicated in this process, the lipid(s) might require processing by enzymes, perhaps active in a low pH, that reside in the recycling compartments, like GGC. In order to eliminate irrelevant lipids when narrowing down the identity of the self-lipid antigen, we could pool lysosomes isolated from unstressed or ER-stressed cells (typically through differential centrifugal and bead isolation) and perform MS on those lipids, as the self-lipid antigen(s) of interest would likely be enriched in these preparations.

While our findings are focused on the upregulation of lipids bound to CD1d molecules during ER stress that activate iNKT cells, it is tempting to speculate that the enhanced lipogenesis observed during ER-stress (Lee et al., 2008) might have a broader effect on the activation of group I CD1-restricted T cells. Consistent with this possibility, it is known that endogenous lipid hydrocarbon chains can be incorporated as spacer molecules into the groove of CD1 molecules, enhancing functionality of CD1 binding (Ly and Moody, 2014), which potentially lends itself to the ER-stress-driven mechanism of lipid loading described.

The identity of the self-lipid(s) that mediates positive selection of human iNKT cells remains uncertain. While lacking identification, our findings provide a context for the immunogenic self-lipid upregulation on human $CD1d^+$ cells that might have important implications for our understanding of thymic iNKT cell development. Given that ER-stress contributes to the maturation of thymocytes (Amantini et al., 2017), it is possible that ER-stress driven self-lipid antigen(s) are involved in iNKT cell thymic selection and development.

Chapter 6: Pathological settings in which physiologically ER-stressed APCs might activate iNKT cells

To this point, we have primarily investigated the mechanisms underlying ER-stressed APC-mediated iNKT cell activation using a variety of drugs and a toxin to induce the UPR. However, there are physiological and pathological conditions that perturb ER homeostasis and activate the UPR. We aimed to determine whether sterile pathological sources of ER-stress, such as cancer, trigger the UPR in $CD1d^+$ cells, which in turn could activate iNKT cells in human disease.

6.1 An ER-stressed murine tumour line can activate iNKT cells

We wondered if a murine solid tumour line, typically used in tumour models with iNKT cells, were able to activate iNKT cells upon ER-stress induction. We found that the murine Lewis Lung carcinoma cell line (3LL), either untransduced or transduced with human CD1d (**Figure 6.1A**), could activate the murine iNKT cell hybridoma DN32 when pre-treated with thapsigargin (**Figure 6.1B**). The fact that

αGC is presented by untransduced 3LL cells suggests that they express endogenous CD1d. Under physiological ER-stress typical of tumourgenesis, these cells might naturally activate iNKT cells.

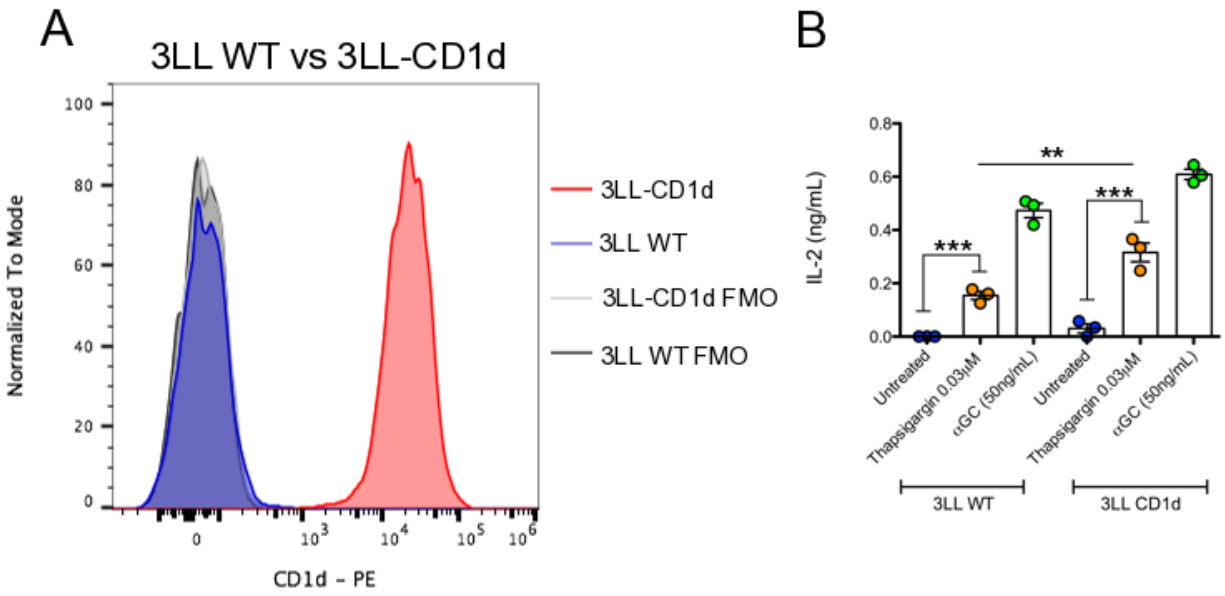

Figure 6.1 Murine lung tumour cells pre-treated with thapsigargin activate a murine iNKT cell hybridoma. (A) CD1d surface expression on Lewis Lung Carcinoma cells (3LL WT), either wild type or lentivirally transduced to overexpress CD1d (3LL-CD1d). **(B)** Murine iNKT (hybridoma DN32.2) cell activation by Lewis Lung Carcinoma cells (3LL), either wild type or overexpressing CD1d molecules, thapsigargin-treated or pulsed with αGC. ** and *** represents $p<0.005$ and $p<0.001$, respectively, by one-way ANOVA with a Bonferroni post-test. Average of N=3 biological replicates, each performed in technical duplicates.

6.2 Human solid tumours exhibit ER-stress in proximal and infiltrating immune cells

Established solid tumours are complex, consisting of many different cell types, including malignant cells, fibroblasts, and immune cells, in multiple layers and occasionally enervated with tumour-specific vasculature. The high concentration of various cells, with different metabolic demands, often leads to a suboptimal tumour microenvironment – the extracellular milieu in and surrounding

the tumour. Tumour cells are highly metabolically active due to their relatively rapid replication, and have acquired adaptions by mutation to survive in suboptimal environments lacking oxygen, amino acids, and glucose. A lack of such nutrients triggers UPR: amino acid deprivation triggers the GCN2 pathway, which feeds into the ISRE, hypoxia triggers the HIFα pathway, which can intersect with XBP1 and PERK signalling (Pereira et al., 2014), and factors involved in glucose sensing and transport are transcriptionally regulated by transcription factors downstream the UPR pathways, particularly PERK, as demonstrated by its requirement in glucose regulation in β-islet cells of the pancreas (Harding et al., 2001). However, non-malignant cells in the tumour microenvironment, including tumour-infiltrating and proximal immune cells, are typically not as well adapted to deal with the cell-extrinsic challenges. They are therefore more susceptible to ER-stress and likely undergo the UPR. Given the role of iNKT cells in tumour immunosurveillance (Crowe et al., 2002), and the mechanism of sterile iNKT cell activation described herein, $CD1d^+$ tumour-infiltrating immune cells undergoing the UPR could present immunogenic self-lipids that activate iNKT cells. To confirm the existence of ER-stressed immune cells in the tumour microenvironment, we stained sequential sections of human solid tumours, the cells via immunohistochemistry for (1) BiP, as a marker of ER-stress and (2) CD11c, as a marker an infiltrating immune cells and in particular, APCs that would express CD1d.

We first tested control tissues with reported expression of the markers at different concentrations based around the recommendations from the suppliers.

For the BiP antibody, we used a breast carcinoma section (as recommended by the antibody supplier), and for CD11c antibody we used a healthy spleen section (as recommended by the antibody supplier). We detected specific staining for BiP in the breast carcinoma and colorectal cancer cells (**Figure 6.2.1**) and CD11c on immune cells in the healthy spleen cells (**Figure 6.2.2**). After this validation, we stained a variety of solid tumour sections for these markers. BiP staining for UPR activation was present in almost all the tumours evaluated; however, staining the sections with immune cell infiltrate was rare. BiP^+ immune cells in and around the tumour were detected in three cases – one melanoma, one lung cancer and one colorectal cancer. We further tested sections from these cases for CD11c staining, to confirm that the infiltrating immune cells that were BiP^+ might be antigen-presenting cells. Despite some background staining, we detected $CD11c^+$ infiltrating immune cells in the areas where, in sequential sections, we detected BiP^+ infiltrating immune cells (**Figure 6.2.3).** These results illustrate that ER-stress in the context of cancer is perhaps a relevant condition in which the mechanism of ER-stressed APC-mediated iNKT cell activation might hold true, where these cells, with $CD1d^+$ presentation potential, could activate iNKT cells within the tumour or in the draining lymph node.

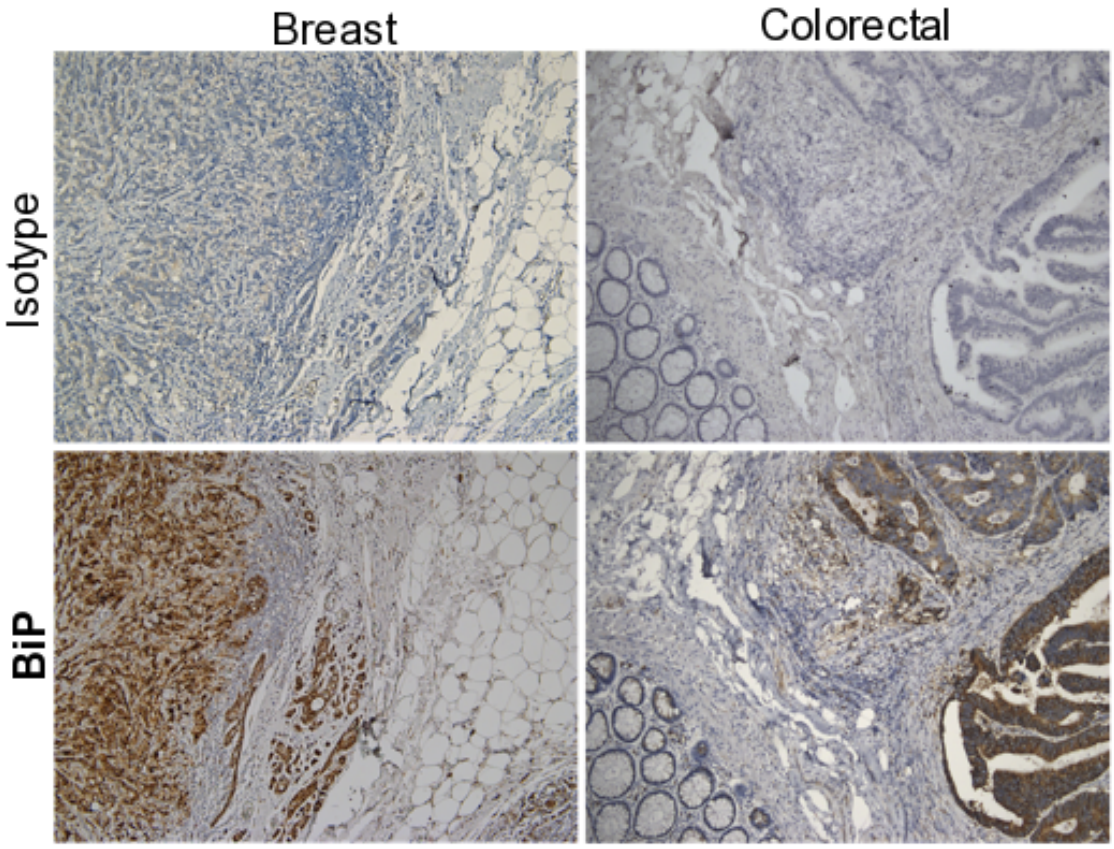

Figure 6.2.1 Positive control staining of BiP^{+} staining in breast and colorectal cancer. Sections from a breast and colorectal cancer sections stained for BiP (brown) with an additional staining for the corresponding isotype control.

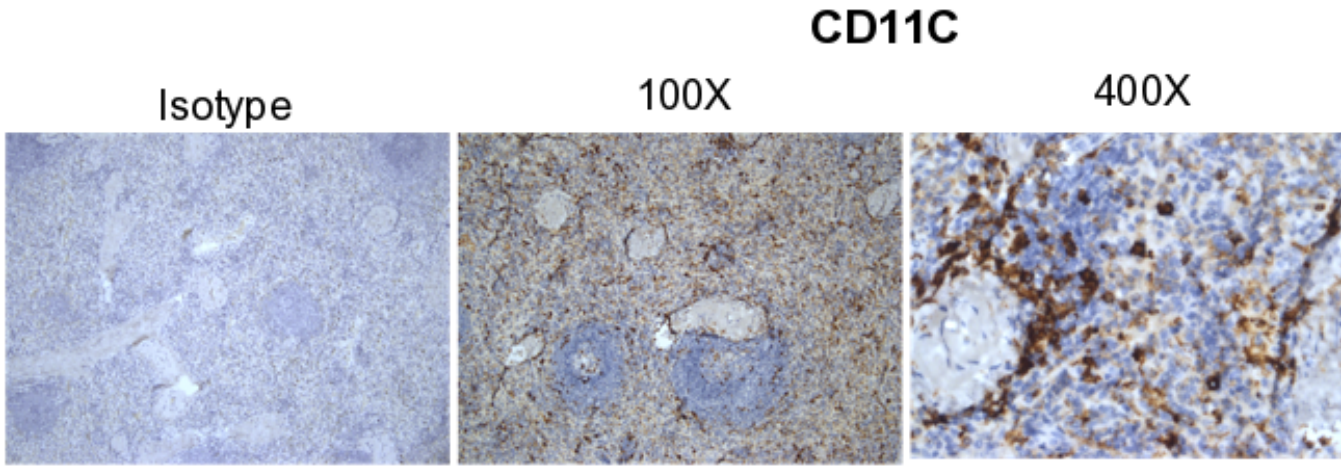

Figure 6.2.2 Positive control staining of CD11c^{+} staining in healthy spleen cells. Sections from a healthy spleen and prostate cancer stained for CD11c (brown) with an additional staining for the corresponding isotype control.

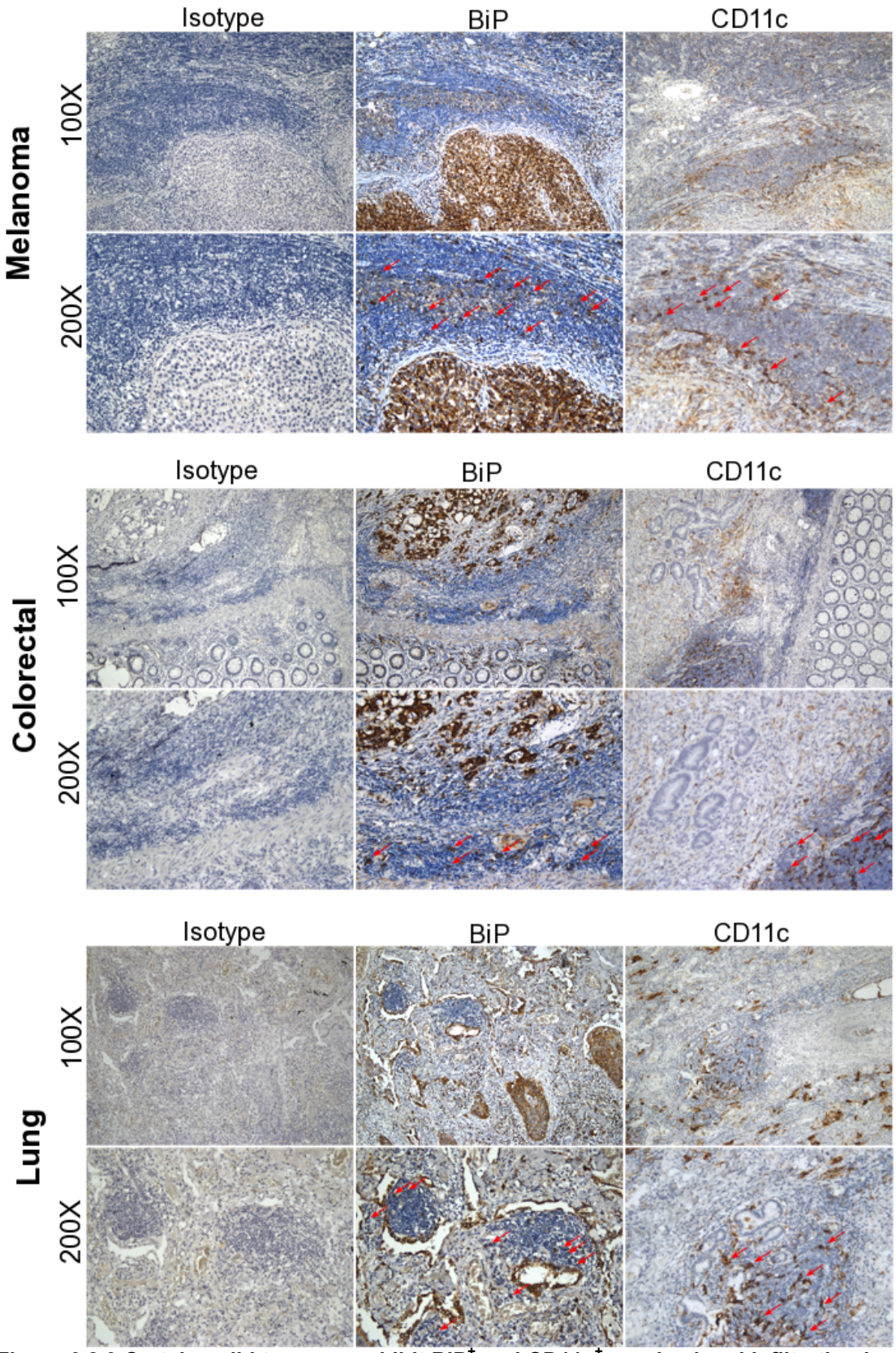

Figure 6.2.3 Certain solid tumours exhibit BiP^{+} and CD11c^{+} proximal and infiltrating immune cells. Sequential sections of paraffin-embedded human tumour tissue from patients with

melanoma (top), colorectal (middle) and lung (bottom) cancer were stained for BiP and CD11c (brown), with an additional staining for the corresponding isotype controls. Arrows indicate immune cells with positive staining for the given marker.

6.3 Multiple myeloma cell lines, some with higher levels of basal UPR, activate iNKT cells when expressing CD1d

While solid tumours are predominantly $CD1d^-$, so-called 'liquid' tumours, which predominantly comprise of malignancies of hematopoietic and lymphoid tissues, tend to express CD1d at one stage or another, including the plasma cell malignancy, multiple myeloma (Bedard et al., 2017, Dhodapkar et al., 2003, Spanoudakis et al., 2009).

Multiple myeloma is an attractive model to test if physiological induction of the UPR in $CD1d^+$ cells can lead to sterile activation of iNKT cells. To this end, we obtained three cell line models of multiple myeloma: U266, JJN3, and JIM3. To initially test if these cell lines expressed functional CD1d, we pulsed them, along with THP1 WT cells, with C20:2. We found that while pulsed THP1 WT cells were able to activate iNKT cells, the pulsed myeloma cells were unable to do so. This indicated that the multiple myeloma cell lines did not express functional CD1d. This finding is consistent with reported downregulation of surface CD1d during multiple myeloma disease progression (Dhodapkar et al., 2003, Spanoudakis et al., 2009). Indeed, these three cell lines were established from patients with late stage multiple myeloma, which would explain their inability to activate iNKT cells with C20:2. This hypothesis was confirmed by surface staining of WT multiple myeloma cell lines for CD1d (**Figure 6.3.1**). To remedy this, we transduced the cell lines to overexpress CD1d (**Figure 6.3.1**).

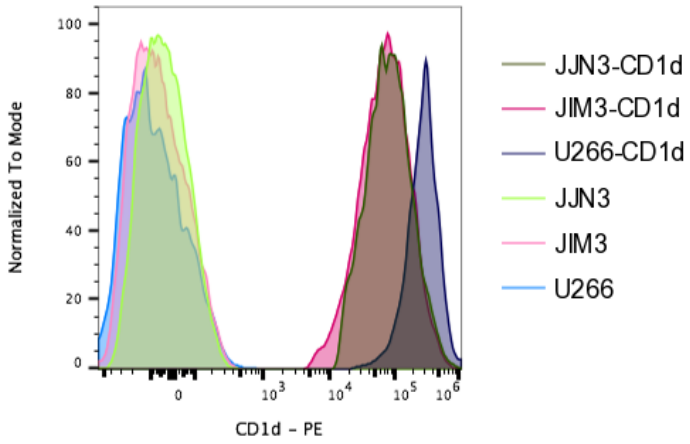

Figure 6.3.1 CD1d expression on WT and CD1d-overexpressing multiple myeloma cell lines. CD1d surface levels are measured by flow cytometry on wild type and CD1d overexpressing U266, JIM3 and JJN3 cell lines. The histograms represent an N=1 biological replicate.

We compared the ability of the untransduced or transduced multiple myeloma cell lines, either unpulsed, pre-treated with thapsigargin, or pulsed with C20:2, to activate iNKT cells (**Figure 6.3.2A**).

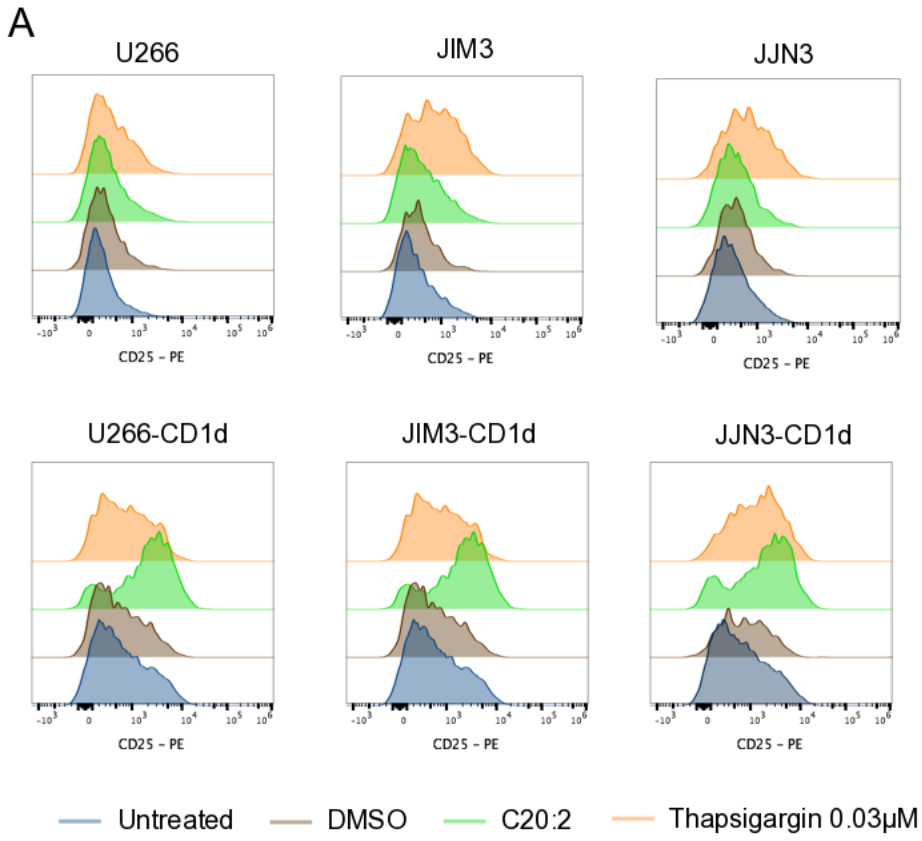

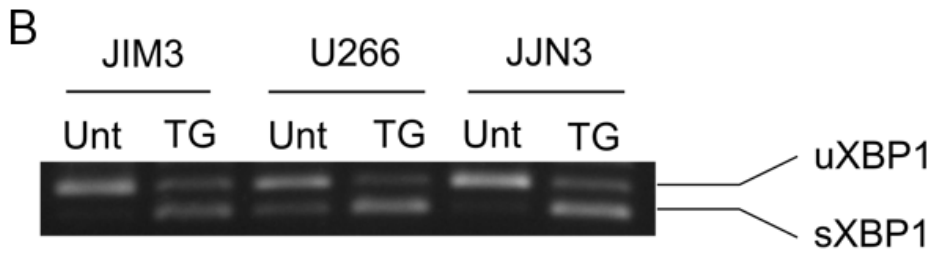

Figure 6.3.2 ER-stressed CD1d-expressing, not wild type, human multiple myeloma cell lines activate iNKT cells. **(A)** Human iNKT cell activation, as measure by increased expression of CD25, against untransduced (top) or CD1d-overexpressing (bottom) U266, JIM3 and JJN3 cell lines. **(B)** XBP1 splicing, as a measure of UPR activation, in U266, JIM3 and JJN3 cell lines, untreated or pre-treated with thapsigargin 0.03μM. Histograms are representative of N=3 biological replicates, performed in technical duplicate.

We confirmed that transduced lines overexpressing CD1d could activate iNKT cells with C20:2, whereas untransduced cells could not do so. We also noticed that the WT lines pre-treated with thapsigargin induced some iNKT cell activation, which was augmented in CD1d-transduced cell lines. Most intriguing observation was that basal activation (from untreated lines) of iNKT cells was shifted upon CD1d transduction, which might reflect the generation of an UPR-driven immunogenic self-lipid(s) in multiple myeloma cells that can be presented on CD1d. To this end, we performed an XBP1 splicing assay from untreated and thapsigargin-treated multiple myeloma cells to assess their UPR activation. There was no evidence of spliced XBP1 in the untreated JJN3 and JIM3 cell lines, but there was evidence of spliced XBP1 in the untreated U266 cells **(Figure 6.3.2B**). Given that all three untreated myeloma lines were able to activate iNKT cells upon CD1d-transduction, yet only one line exhibits basal ER-stress, the increase in CD1d-mediated iNKT cell activation might not be due to an immunogenic self-lipid species upregulated by ER-stress, but perhaps simply due to the increased surface expression of endogenous-lipid-presenting CD1d.

While the role of iNKT cells in tumour immunity largely involves modulating the activity of other immune cell subsets, including cytotoxic ones, there are reports of direct iNKT cell cytotoxic activity against tumours cells (Nieda et al., 2001). Therefore, in parallel with the previous experiments, we tested if iNKT cells activated by the ER-stress-driven self-lipid(s) could kill the $CD1d^+$ myeloma cells. To the end, we performed the *in vitro*/*in vivo* technique for assessing lysis (VITAL) assay, to determine whether specific ER-stressed and/or $CD1d^+$ populations could be targeted and killed by iNKT cells. We first optimized this assay using THP1 WT cells either unpulsed or pulsed with αGC. We observed a dose-dependent killing of the THP1 cells that correlated with the iNKT cell titration; however, the killing was not restricted to the αGC-pulsed THP1 cells, but the unpulsed cells were also target (**Figure 6.3.3**). We hypothesized that the indiscriminate killing of $CD1d^+$ cells by activated iNKT cells might explain iNKT cell killing of both populations. Assuming this hypothesis was true, we tested the VITAL assay on the transduced $CD1d^+$ and untransduced $CD1d^-$ multiple myeloma cell lines.

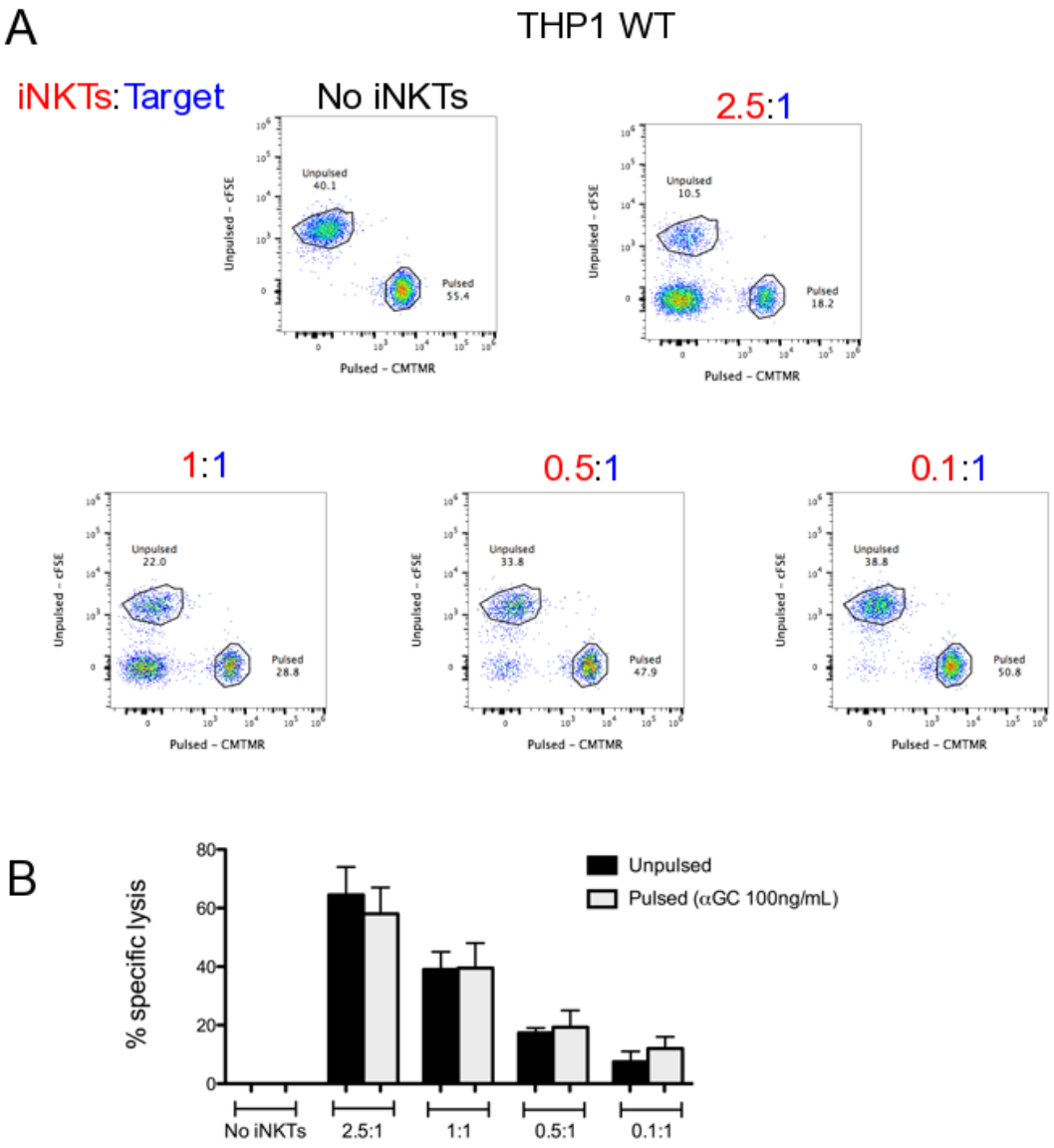

Figure 6.3.3 VITAL assay confirms that activated iNKT cells kill unpulsed and αGC-pulsed THP1 cells. **(A)** Dot plots show the decreasing percentage of target unpulsed and αGC-pulsed THP1 WT cells, each labelled with different fluorescent dyes, with an increasing proportion of effector human iNKT cells. Dot plots are representative of N=3 biological replicates, performed in technical duplicates **(B)** Specific lysis of unpulsed and αGC-pulsed THP1 cells by iNKT cells is quantified. These results are the average of a single experiment representative of N=3 biological replicates, performed in technical duplicates.

We compared the untransduced and transduced cells for each multiple myeloma cell lines that were untreated, pre-treated with thapsigargin, or αGC-

pulsed with a titration of iNKT cells. The untreated U266-CD1d cell line did not exhibit any specific lysis compared to the untreated U266 cells, but the thapsigargin pre-treatment did induce some specific lysis of U266-CD1d cells (**Figure 6.3.4**). However, while the αGC-pulsed U266-CD1d cells did induce some specific lysis compared to their untransduced counterparts with a higher proportion of iNKT cells, the result of this positive control was not convincing, making the experimental condition with thapsigargin difficult to interpret.

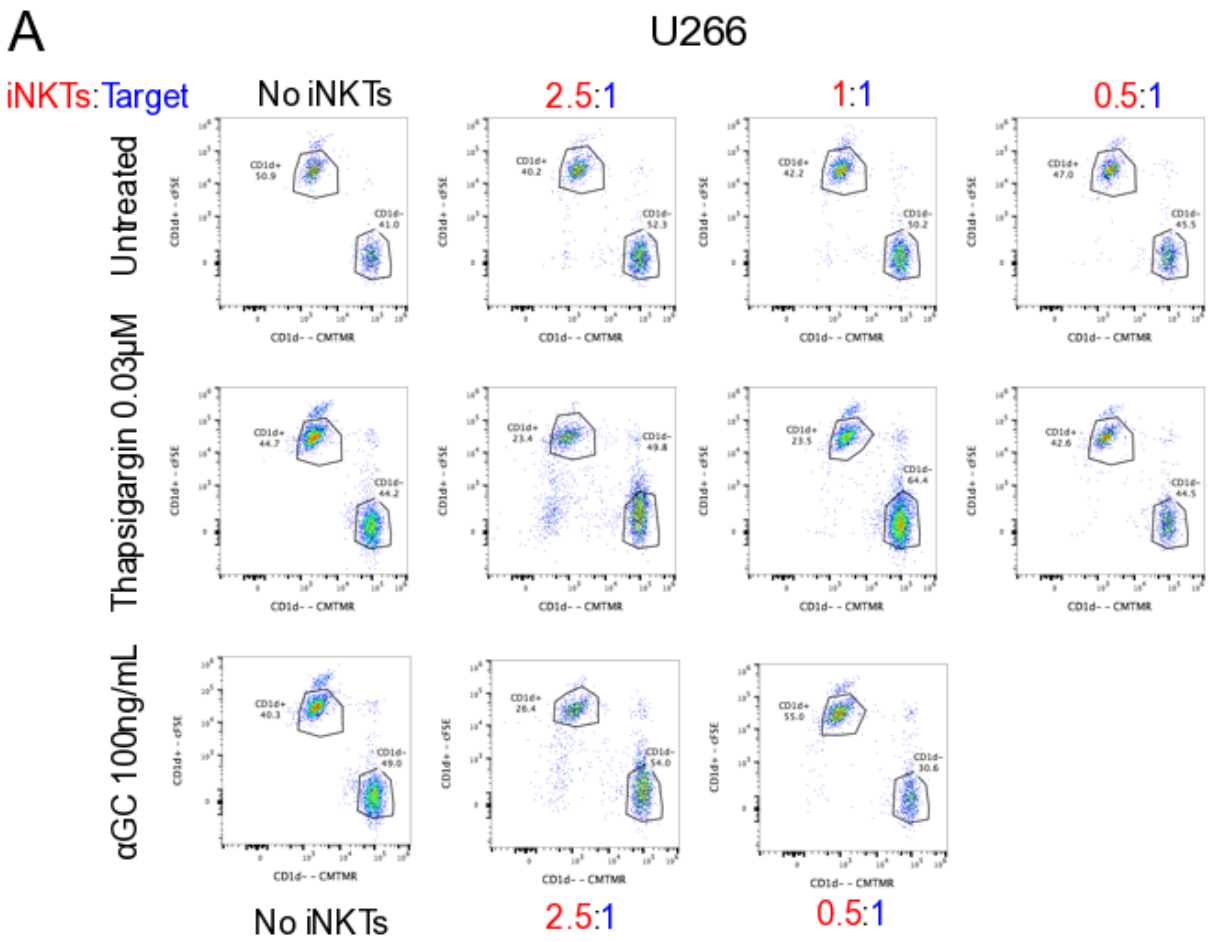

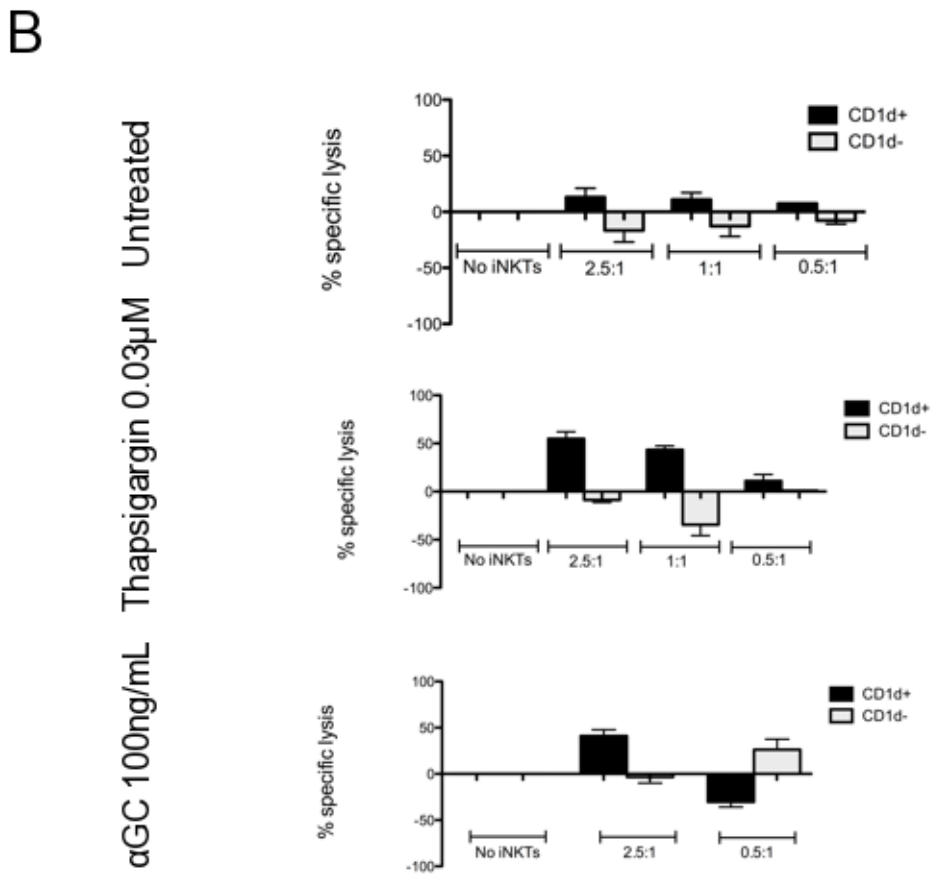

Figure 6.3.4 VITAL assay assesses whether iNKT cells target and kill ER-stressed CD1d^{+} U266 cells. (A) Dot plots show the percentage of WT or CD1d-overexpressing U226 cell lines, each labelled with different fluorescent dyes that are untreated, thapsigargin pre-treated, or αGC pulsed, with an increasing proportion of effector human iNKT cells. Dot plots are representative of N=2 biological replicates, performed in technical duplicates **(B)** Specific lysis of the U266 WT and CD1d-overexpressing cells, under the different conditions is quantified. These results are the average of an experiment representative of N=2 biological replicates, performed in technical duplicates.

When we examined the JIM3 cells, we did not see any specific lysis in the untreated or thapsigargin pre-treated cells, although the αGC control at the higher proportion of iNKT cells did induced a high degree of specific lysis (**Figure 6.3.5**).

A

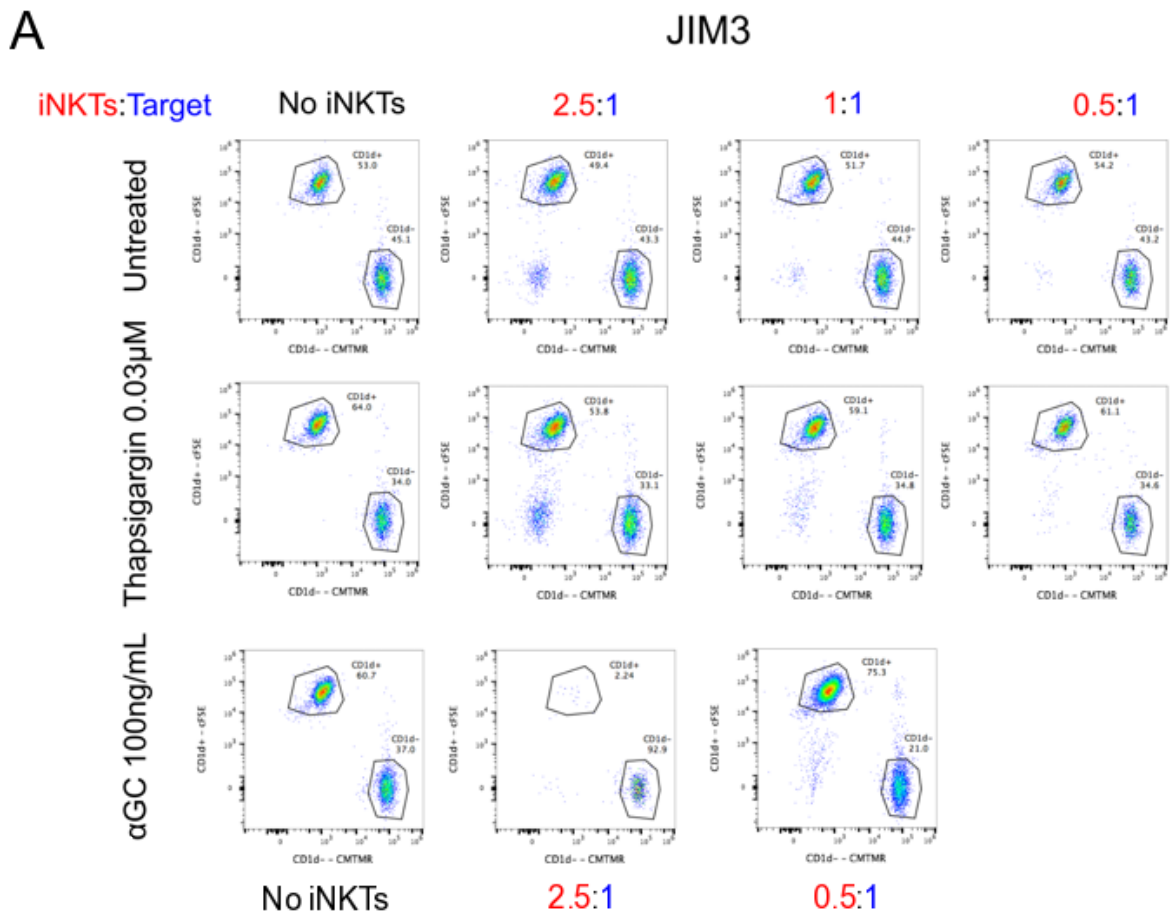
JIM3
iNKTs:Target
No iNKTs
2.5:1
1:1
0.5:1
Untreated
Thapsigargin 0.03µM
αGC 100ng/mL
CD1d+ - CFSE
CD1d- - CMTMR
No iNKTs
2.5:1
0.5:1

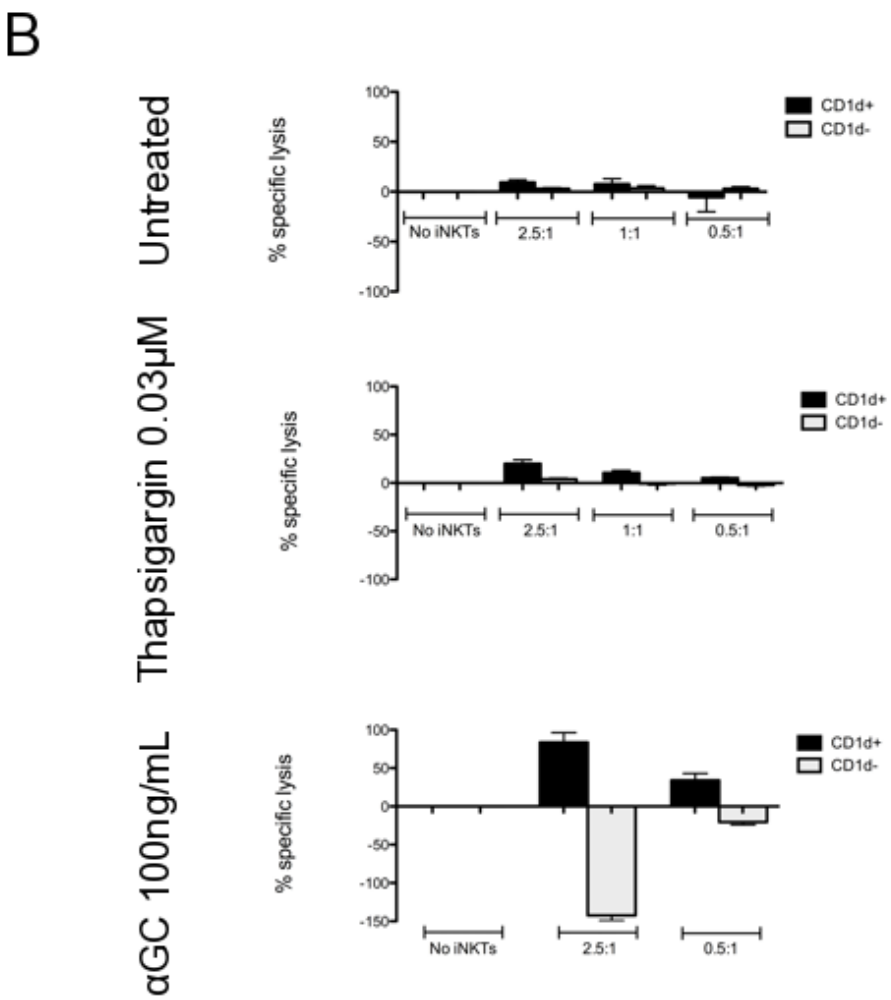

Figure 6.3.5 VITAL assay assesses whether iNKT cells target and kill ER-stressed CD1d^{+}JIM3 cells. (A) Dot plots show the percentage of WT or CD1d-overexpressing JIM3 cell lines, each labelled with different fluorescent dyes that are untreated, thapsigargin pre-treated, or αGC pulsed, with an increasing proportion of effector human iNKT cells. Dot plots are representative of N=2 biological replicates, performed in technical duplicates **(B)** Specific lysis of the JIM3 WT and CD1d-overexpressing cells, under the different conditions is quantified. These results are the average of an experiment representative of N=2 biological replicates, performed in technical duplicates.

When we examined the JJN3 cells, there was no specific lysis in the untreated or thapsigargin pre-treated conditions, but there was also no specific lysis in the αGC-pulsed condition, calling into question the interpretation of the results in the other treatments (**Figure 6.3.6**).

In this set of experiments, restricted to three multiple myeloma cell lines, our results indicate that CD1d^{+} multiple myeloma cells might induce greater iNKT cell activation. However, this observation is not likely due to the generation of immunogenic self-lipids, as the UPR is not consistently upregulated at baseline across the myeloma cell lines. Treatment of the multiple myeloma cell lines with thapsigargin did induce iNKT cell activation in a CD1d-dependent manner, but induced iNKT cell specific killing only in treated U266-CD1d cells, and not the other CD1d-transduced multiple myeloma lines.

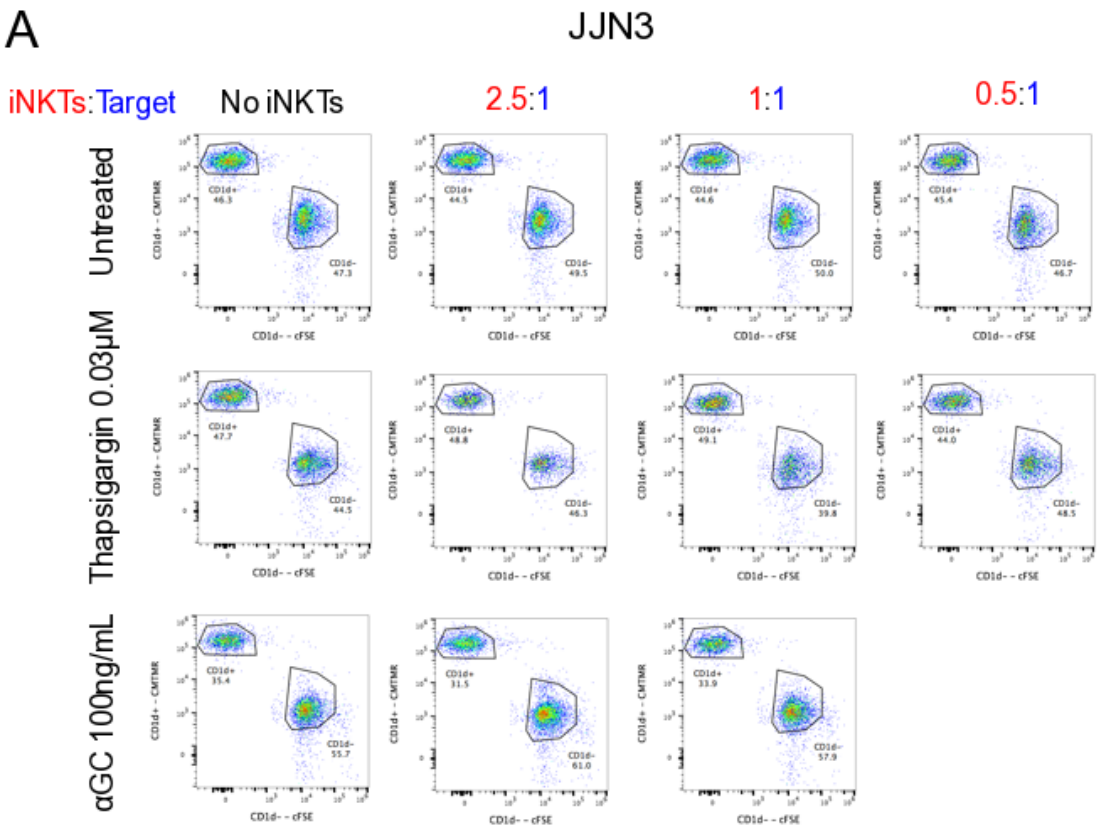

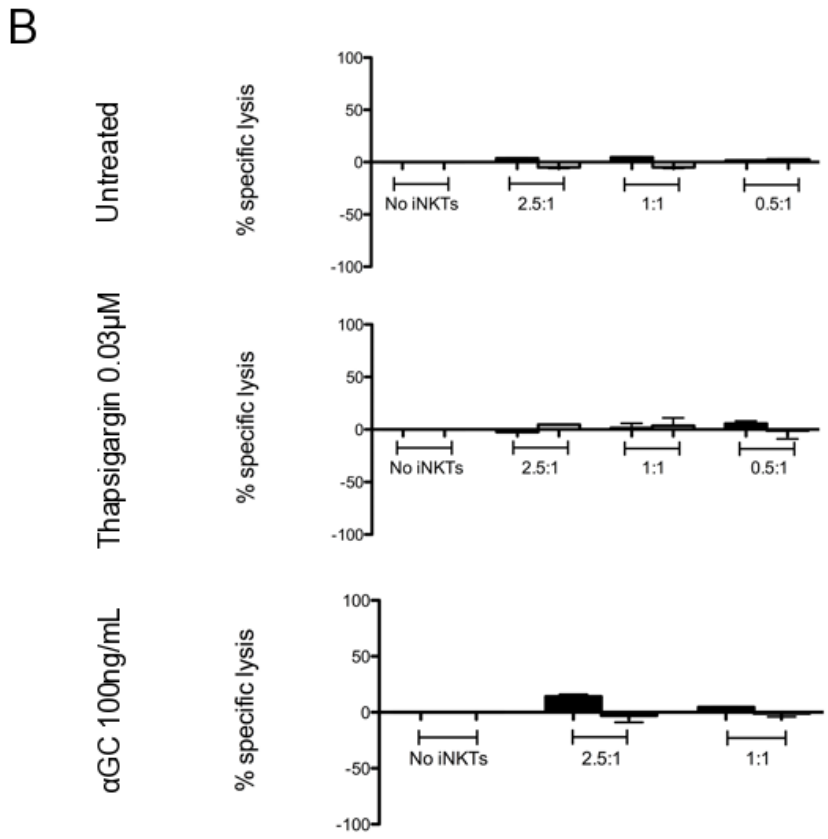

Figure 6.3.6 VITAL assay assesses whether iNKT cells target and kill ER-stressed CD1d^{+} JJN3 cells. (A) Dot plots show the percentage of WT or CD1d-overexpressing JJN3 cell lines, each labelled with different fluorescent dyes that are untreated, thapsigargin pre-treated, or αGC pulsed, with an increasing proportion of effector human iNKT cells. Dot plots are representative of N=2 biological replicates, performed in technical duplicates **(B)** Specific lysis of the JJN3 WT and CD1d-overexpressing cells, under the different conditions is quantified. These results are the average of an experiment representative of N=2 biological replicates, performed in technical duplicates.

6.4 Discussion

In this chapter we attempt to bring the mechanism of ER-stressed APC-mediated iNKT cell activation into a biologically relevant light. There are a variety of physiological stimuli that could drive ER-stress and the UPR, particularly in pathologies such as cancer. One top of that, since the role of iNKT cells in tumour immunosurveillance is well-defined but their mode of activation is unclear, we

wondered whether there might be a role for the ER-stress mediated mechanism of iNKT cell activation in a tumour setting. By testing models of both solid and liquid tumours, we investigated whether (1) ER-stress is prevalent in tumours and (2) whether there was opportunity for iNKT cells to be activated in a CD1d-dependent manner in these settings. While our investigation was limited by a lack of suitable reagents and samples, we generated mixed results regarding the relevance of our mechanism in a cancer setting.

While in the first chapter we illustrate that murine iNKT cells can be activated by ER-stressed DCs *in vivo*, we failed to further characterize the downstream consequences of this activation, including in tumour setting. We found the thapsigargin-treated Lewis Lung Carcinoma (3LL) cells activated iNKT cells. Unfortunately, we did not perform any formal experiments to confirm that 3LL cells pre-treated with thapsigargin induced the UPR.

3LL cells have been used previously to study iNKT cell responses to solid tumours, along with B16 melanoma. Intravenous injection of 3LL cell results in the formation of metastases in the liver, an anatomical region rich in iNKT cells (Smyth et al., 2002). Given that WT 3LL cells appear to be functionally $CD1d^{+}$, we wonder if ER-stressed 3LL metastases are more readily controlled through iNKT cell activation than unstressed 3LL cells. To perform this experiment, we would inject either untreated or thapsigargin pre-treated 3LL cells into wild type or $TRAJ18^{-/-}$ mice. αGC- or IMM60-pulsed cells would serve a positive control. In this model we hypothesize that the tumour burden would be reduced in wild type mice receiving the ER-stressed 3LL cells compared to those receiving the unstressed 3LL cells.

Ideally the difference in tumour growth between TRAJ18$^{-/-}$ mice receiving unstressed and ER-stressed 3LL cells would be minimized to illustrate that control of the ER-stressed 3LL tumour burden is iNKT cell dependent, and that the inherent reduced fitness associated with ER-stressing the cells is not the main determinant of tumour growth.

Another biological source of ER-stress we did not explore is the response to amino acid starvation. Upon activation, GCN2 phosphorylates serine 51 of eIF2α, a step that converges on the central node of the ISRE – similar to PERK. This common convergence point is integral to ER-stressed APC-mediated iNKT cell activation – therefore the GCN2 pathway might serve as an alternative means of iNKT cell activation. Given that amino acid deprivation is hallmark in the tumour microenvironment, and that multiple tumours types upregulate enzymes involved in amino acid transport and synthesis, it might serve a biologically relevant stimulus for sterile iNKT cell activation in a tumour setting (Battu et al., 2017, Timosenko et al., 2016). Furthermore, CD1d^{+} infiltrating immune cells might be more sensitive to amino acid deprivation in the tumour microenvironment and exhibit GCN2 signalling.

To understand whether our *in vitro* mechanistic findings were relevant in a tumour setting, we opted to determine if human solid tumours exhibit ER-stressed immune cells with CD1d-presenting potential that could activate iNKT cells within the tumour or draining lymph node. To address this, we performed immunohistochemistry on sequential sections of a variety of human solid tumours. An advantage of immunohistochemistry is that cells can be characterized in

natural setting within the tumour tissue, without dissociation from the tumour microenvironment as would occur for flow cytometry analysis of samples. This fact is particularly important when determining how tumour proximity influences immune cells, i.e. location in the tumour microenvironment is sufficient to induce the UPR in immune cells. However, unless immunohistochemical staining is multiplexed, it is difficult to properly characterize specific cells accurately and quantifiably. The observations and findings related to the immunohistochemical analysis presented here are largely qualitative and assume consistency in sequential sections. Lack of sufficient reagents for immunohistochemistry, particularly when using paraffin sections, was also very limiting in this set of experiments.

To assess whether cells in these sections were undergoing the UPR, we stained using an antibody against BiP. This marker was used in other studies of ER-stress in solid tumours, and appeared sufficient to distinguish between healthy tissue and tumour tissues. All cells express certain levels of BiP and total protein levels do not change upon initial induction of ER-stress. However, ATF6-mediated transcription drives synthesis of BiP as a chaperone, so upregulation of BiP is a marker of the UPR. Selection of a different marker downstream the PERK pathway, such as ATF4, might have been better suited for these experiments. ATF4 is only translated upon ER-stress, thereby exhibiting a higher dynamic range and sensitivity than BiP, which is constitutively translated even in unstressed cells.

To assess whether cells in these sections were myeloid cells with CD1d-presenting potential, we stained for DCs using an antibody against CD11c, as DC

subsets that are likely most efficient in presenting lipids on CD1d; however, we are excluding tumour-associated macrophages.

We assessed whether tumour cells or proximal and infiltrating immune cells in these sections were $CD1d^+$. The majority of solid tumours were, as expected, $CD1d^-$ (Bedard et al., 2017). However we were surprised to not detect staining on any infiltrating immune cells, and no specific staining in the spleen. There are two possible explanations for this result: (1) wild type levels of CD1d on APCs are low, and difficult to detect by flow cytometry, so it is possible that the apparent negative staining reflects this fact and/or (2) the antibody is of poor quality.

It is difficult to properly compare the staining across the different sections as the staining for BiP was performed many months before the staining for CD11c. This also meant the sections were no longer sequential, so in some cases it was difficult to identified identical regions to compare between the BiP^+ and $CD11c^+$ tissue. The bluing coloration of the hematoxylin was reduced in later samples, despite identical treatment times with the same ammoniated water, which likely reflects that the hematoxylin was nearing the end of its shelf life.

When we initially conducted performed these IHC stainings, we tested with the 6B11 antibody, which stains human iNKT cells by recognizing the invariant CDR3 region of TCR Vα24Jα18 expressed on human iNKT cells (Exley et al., 2008). However, we failed to detect iNKT cells in the healthy human liver tissue, likely because we only had access to paraffin-embedded tissue, and not frozen tissue for which the antibody is reported to stain. To primarily identify iNKT cells, we considered using a two-color staining approach using Vα24 and Vβ11 as

markers, but we could not take this idea forward due to the lack of good quality antibodies raised in different animals combined with a limited number of sections for optimization.

However, several hematological or 'liquid' tumours are $CD1d^+$, including early stages of multiple myeloma. Multiple myeloma was an attractive model due to its characteristic high levels of ER-stress, and reports indicate that surface CD1d is downregulated as the disease progresses (Spanoudakis et al., 2009, Dhodapkar et al., 2003). It is tempting to speculate that this is an immune-evasion mechanism. Our *in vitro* findings were conflicting, although proper controls would have improved interpretation. While overexpression of CD1d in myeloma cells drove iNKT cell activation, which we attributed to ER-stress, it is possible that the activation is simply a result of high levels of CD1d presenting endogenous lipids. By including a control with THP1 WT and THP1-CD1d cells in the functional assay, we could determine if the increase in iNKT cell activation with the myeloma lines ± CD1d exceeds that of the THP1 cells ± CD1d. However, variation in the types of lipids presented by myeloid cells and B cells might remain a confounding factor.

Despite reports of higher levels of ER-stress in myeloma cells compared to non-transformed cells, most myeloma lines did not exhibit XBP1 splicing at a basal level. However, more appropriate controls, like non-malignant plasma cell line, might clarify the interpretation, particularly with the U266 cell line. The difference in ER-stress might be more evident when examining primary myeloma versus plasma cells.

ER-stress is traditionally considered as a cell-intrinsic effect, but certain findings suggest that it can be transferred in between cells in what is termed transmissible ER-stress, or TERS. Work pioneered by Zanetti and Mahadevan found that immune cells become ER-stressed when sharing an environment with ER-stressed tumour cells, observing that macrophages cultured in conditioned medium from ER-stress tumours become stressed themselves (Rodvold et al., 2017). Downstream effects of TERS, when acting on innate immune cells, ranges from modulated pro-inflammatory cytokine secretion and impaired T cell priming due to reduced expression of costimulatory molecules on APCs (Mahadevan et al., 2010, Mahadevan et al., 2011). While these papers suggest that ER-stressed tumour cells are the source of unidentified soluble factors that mediate TERS, it is also possible that a lack of oxygen, glucose, and other nutrients in the shared tumour microenvironment might inadvertently induce ER-stress in infiltrating immune cells (Rodvold et al., 2016).

There are reports supporting and refuting the role of glycolysis in boosting Th1 T cell responses. Metabolic reprogramming appears to direct and imprint myeloid cell plasticity and development. There are reports supporting and refuting the role of glycolysis in boosting Th1 T cell responses. The direction in which glycolytic or oxidative profiles shift responses remains controversial (Assmann and Finlay, 2016). These examples together just scratch the surface on the ways in which the extracellular environment can passively modulate immune responses through nutrient deprivation and other stressful conditions rather than active secretion of immunomodulatory factors.

There is the possibility that lipids from dead and dying cells are cross-presented on CD1d, as discussed in the previous chapter. This could extend to dead and dying tumour cells, as it is known that iNKT cells can recognize cross-present GD3 from melanoma cells (Wu et al., 2003). Furthermore, αGC-pulsed glioma cells, which are $CD1d^{-}$, can activate iNKT cells as part of a tumour vaccine strategy in mice. This effect was boosted if the tumour cells were first irradiated, hinting that the presentation of exogenous, self-lipid agonists could improve adjuvanting iNKT cell responses in tumour immunotherapy (Hunn et al., 2012).

Defining the role of ER-stress in cancer has been an area of intensive research. Indeed, ER-stress in tumour cells is a double-edged sword – some findings implicate ER-stress in tumour cells with chemoresistance, improved survival, increased metastatic potential etc. while others cite that ER-stress is beneficial for patient survival (Urra et al., 2016). Work from multiple groups, including the Glimcher and Cubillos-Ruiz groups, aimed to dissect the role of ER-stress in anti-tumour immune responses. These two groups in particular led investigations in the role of XBP1, the main transcription factor downstream the IRE1 pathway, in tumour infiltrating DCs and T cells. Their studies using CD11c-Cre $XBP1^{fl/fl}$ mice and CD4-Cre $XBP1^{fl/fl}$ mice suggest that XBP1 signalling promotes ovarian tumourigenesis by compromising the anti-tumour responses of DCs and T cells (Cubillos-Ruiz et al., 2015, Song et al., 2018a). However, given that XBP1-dependent transcription largely mediates recovery from the misfolded protein burden, in the absence of this branch, there could in fact be enhanced ER-stress and signalling through the other two branches, PERK and ATF6α, an idea

which we considered *in vitro* in an earlier chapter. The enhanced PERK signalling in the XBP1$^{-/-}$ DCs might contribute to the improved anti-tumour responses compared to control DCs, perhaps through sterile activation of iNKT cells.

Another mouse model of disease that might be worth investigating in future is that of hepatic disease. ER-stress is a hallmark of non-alcoholic fatty liver disease (NAFLD), non-alcoholic steatohepatitis, and hepatic steatosis, and contributes greatly to dysregulated lipid metabolism, particularly triglycerides (Jo et al., 2013, Oyadomari et al., 2008). Notably, iNKT cells contribute to the sterile inflammatory component of these pathologies (Adler et al., 2011, Tajiri et al., 2009). Perhaps using murine model of these diseases in PERK$^{-/-}$ or PERK$^{-/-}$ TRAJ18$^{-/-}$ mice, we could monitor ER-stress, iNKT cell activation and examine disease progression, as measured by ALT release and histological scoring.

Chapter 7: Summary and Conclusions

The discovery of iNKT cells paved the way for a new class of unconventional T lymphocytes – ones that exhibit limited TCR diversity, recognize non-peptide antigens, and generate innate-like immune responses. There has been great progress in characterizing iNKT cell activation and responses in the face of disease, ranging from foreign infection to sterile inflammation and cancer. The identification of foreign lipid antigens has guided the generation of synthetic compounds to induce iNKT activation as cellular adjuvants for immunotherapy. However, there are fundamental aspects of iNKT cell biology that remain unclear, amongst them, how iNKT cells are activated in sterile inflammation. This project aimed to elucidate a molecular mechanism leading to sterile activation of iNKT cells that would apply to physiological and pathological conditions that feature, in part, iNKT cell-driven inflammation. To this end, we hypothesized that the UPR, commonly triggered in cancer, could alter the repertoire of self-lipid antigen(s) presented by CD1d to enhance sterile iNKT cell activation.

We showed *in vitro* that human and murine DCs experiencing ER-stress upon thapsigargin treatment, or more specifically triggering the UPR upon SubAB5-treatment, activate iNKT cells in CD1d-dependent manner. We extended these findings to an *in vivo* setting, where WT ER-stressed BMDCs activated splenic iNKT cells, while their $CD1d^{-/-}$ ER-stressed counterparts failed to do so.

We demonstrated that ER-stressed APC-mediated iNKT cell activation drives the secretion of IFN-γ, important in anti-tumour immunity, amongst other cytokines. Importantly, we ruled out the possibility that increased CD1d levels

mediated this mode of activation. Instead we illustrate that APCs undergoing the UPR present a self-lipid(s) on CD1d that activate iNKT cells. We also showed that the mode of activation promotes maturation of DCs, a key aspect of the adjuvant role ascribed to iNKT cells in anti-tumour immune responses.

Using a combination of immunological and molecular biological techniques, we defined a mechanism driving the presentation of the immunogenic self-lipid(s) in ER-stressed APCs, whereby signalling through the PERK-eIF2α axis promotes the loading of the self-lipid antigen(s) onto CD1d in the endosomal/lysosomal compartment of APCs. Surprisingly, ATF4 was dispensable in this mode of activation, suggesting that either a less-well characterized transcription factor is involved or that suppressed protein translation underpins the mechanism.

Finally, we attempted to illustrate the physiological and pathological relevance of this mechanism by assessing the presence of ER-stressed APCs in tumour microenvironment. Using immunohistochemistry, we observed BiP^+ and $CD11c^+$ immune cells (that is DCs with CD1d-presenting potential) in sections of human solid tumours to illustrate a situation in a human cancer setting where iNKT cells, present either in the tumour or draining lymph node, could come in contact with ER-stressed APCs. Future studies along this line of experimentation would benefit from the use of other clean markers of APCs or TAMs, like CD68. If repeated on frozen sections, the 6B11 antibody, which can detect human iNKT cells, could assess the presence and activation of iNKT cells in these tumours in relation to levels of ER-stress.

In conclusion, we have provided key insights into a novel mechanism of sterile iNKT cell activation with relevance to anti-tumour immune responses. Identification of the self-lipid antigen(s) and the enzymes involved in their production is a priority in future experiments to fully characterize this mechanism of sterile iNKT cell activation. While it tempting to speculate that this mechanism is at play during thymic selection of iNKT cells, or plays a role in activation of other lipid-restricted T cells, it is rare to have an *in vivo* setting where solely $CD1d^+$ cells are undergoing the UPR. Gaining a better understanding of (1) the ER-stress conditions within the circulation and tissues in cancer, as well as (2) the ER-stress thresholds of different immune cell subsets in that environment, is essential in understanding and manipulating the holistic effects of ER-stress on this and a variety of immune cell responses.

Chapter 8: References

Acosta-Alvear, D., Zhou, Y., Blais, A., Tsikitis, M., Lents, N. H., Arias, C., Lennon, C. J., Kluger, Y. & Dynlacht, B. D. 2007. XBP1 controls diverse cell type- and condition-specific transcriptional regulatory networks. *Mol Cell,* 27**,** 53-66.

Adams, E. J. 2013. Diverse antigen presentation by the Group 1 CD1 molecule, CD1c. *Mol Immunol,* 55**,** 182-5.

Adler, M., Taylor, S., Okebugwu, K., Yee, H., Fielding, C., Fielding, G. & Poles, M. 2011. Intrahepatic natural killer T cell populations are increased in human hepatic steatosis. *World J Gastroenterol,* 17**,** 1725-31.

Alvarez, J. G. & Touchstone, J. C. 1992. Separation of acidic and neutral lipids by aminopropyl-bonded silica gel column chromatography. *J Chromatogr,* 577**,** 142-5.

Amantini, C., Farfariello, V., Cardinali, C., Morelli, M. B., Marinelli, O., Nabissi, M., Santoni, M., Bonfili, L., Cecarini, V., Eleuteri, A. M. & Santoni, G. 2017. The TRPV1 ion channel regulates thymocyte differentiation by modulating autophagy and proteasome activity. *Oncotarget,* 8**,** 90766-90780.

Ambrosino, E., Terabe, M., Halder, R. C., Peng, J., Takaku, S., Miyake, S., Yamamura, T., Kumar, V. & Berzofsky, J. A. 2007. Cross-regulation between type I and type II NKT cells in regulating tumor immunity: a new immunoregulatory axis. *J Immunol,* 179**,** 5126-36.

Amin-Wetzel, N., Saunders, R. A., Kamphuis, M. J., Rato, C., Preissler, S., Harding, H. P. & Ron, D. 2017. A J-Protein Co-chaperone Recruits BiP to Monomerize IRE1 and Repress the Unfolded Protein Response. *Cell,* 171**,** 1625-1637 e13.

Angenieux, C., Salamero, J., Fricker, D., Cazenave, J. P., Goud, B., Hanau, D. & De La Salle, H. 2000. Characterization of CD1e, a third type of CD1 molecule expressed in dendritic cells. *J Biol Chem,* 275**,** 37757-64.

Aragon, I. V., Barrington, R. A., Jackowski, S., Mori, K. & Brewer, J. W. 2012. The specialized unfolded protein response of B lymphocytes: ATF6alpha-

independent development of antibody-secreting B cells. *Mol Immunol,* 51**,** 347-55.

Aspeslagh, S., Li, Y., Yu, E. D., Pauwels, N., Trappeniers, M., Girardi, E., Decruy, T., Van Beneden, K., Venken, K., Drennan, M., Leybaert, L., Wang, J., Franck, R. W., Van Calenbergh, S., Zajonc, D. M. & Elewaut, D. 2011. Galactose-modified iNKT cell agonists stabilized by an induced fit of CD1d prevent tumour metastasis. *EMBO J,* 30**,** 2294-305.

Assmann, N. & Finlay, D. K. 2016. Metabolic regulation of immune responses: therapeutic opportunities. *J Clin Invest,* 126**,** 2031-9.

Axten, J. M., Medina, J. R., Feng, Y., Shu, A., Romeril, S. P., Grant, S. W., Li, W. H., Heerding, D. A., Minthorn, E., Mencken, T., Atkins, C., Liu, Q., Rabindran, S., Kumar, R., Hong, X., Goetz, A., Stanley, T., Taylor, J. D., Sigethy, S. D., Tomberlin, G. H., Hassell, A. M., Kahler, K. M., Shewchuk, L. M. & Gampe, R. T. 2012. Discovery of 7-methyl-5-(1-{[3-(trifluoromethyl)phenyl]acetyl}-2,3-dihydro-1H-indol-5-yl)-7H-p yrrolo[2,3-d]pyrimidin-4-amine (GSK2606414), a potent and selective first-in-class inhibitor of protein kinase R (PKR)-like endoplasmic reticulum kinase (PERK). *J Med Chem,* 55**,** 7193-207.

Babcock, D. F., First, N. L. & Lardy, H. A. 1976. Action of ionophore A23187 at the cellular level. Separation of effects at the plasma and mitochondrial membranes. *J Biol Chem,* 251**,** 3881-6.

Bagchi, S., He, Y., Zhang, H., Cao, L., Van Rhijn, I., Moody, D. B., Gudjonsson, J. E. & Wang, C. R. 2017. CD1b-autoreactive T cells contribute to hyperlipidemia-induced skin inflammation in mice. *J Clin Invest,* 127**,** 2339-2352.

Bagley, K. C., Abdelwahab, S. F., Tuskan, R. G. & Lewis, G. K. 2004. Calcium signaling through phospholipase C activates dendritic cells to mature and is necessary for the activation and maturation of dendritic cells induced by diverse agonists. *Clin Diagn Lab Immunol,* 11**,** 77-82.

Bagriacik, E. U., Kirkpatrick, A. & Miller, K. S. 1996. Glycosylation of native MHC class Ia molecules is required for recognition by allogeneic cytotoxic T lymphocytes. *Glycobiology,* 6**,** 413-21.

Bai, L., Picard, D., Anderson, B., Chaudhary, V., Luoma, A., Jabri, B., Adams, E. J., Savage, P. B. & Bendelac, A. 2012. The majority of CD1d-sulfatide-specific T cells in human blood use a semiinvariant Vdelta1 TCR. *Eur J Immunol,* 42**,** 2505-10.

Barral, D. C., Cavallari, M., Mccormick, P. J., Garg, S., Magee, A. I., Bonifacino, J. S., De Libero, G. & Brenner, M. B. 2008a. CD1a and MHC class I follow a similar endocytic recycling pathway. *Traffic,* 9**,** 1446-57.

Barral, P., Eckl-Dorna, J., Harwood, N. E., De Santo, C., Salio, M., Illarionov, P., Besra, G. S., Cerundolo, V. & Batista, F. D. 2008b. B cell receptor-mediated uptake of CD1d-restricted antigen augments antibody responses by recruiting invariant NKT cell help in vivo. *Proc Natl Acad Sci U S A,* 105**,** 8345-50.

Barral, P., Polzella, P., Bruckbauer, A., Van Rooijen, N., Besra, G. S., Cerundolo, V. & Batista, F. D. 2010. CD169(+) macrophages present lipid antigens to mediate early activation of iNKT cells in lymph nodes. *Nat Immunol,* 11**,** 303-12.

Bassiri, H., Das, R., Guan, P., Barrett, D. M., Brennan, P. J., Banerjee, P. P., Wiener, S. J., Orange, J. S., Brenner, M. B., Grupp, S. A. & Nichols, K. E. 2014. iNKT cell cytotoxic responses control T-lymphoma growth in vitro and in vivo. *Cancer Immunol Res,* 2**,** 59-69.

Battu, S., Minhas, G., Mishra, A. & Khan, N. 2017. Amino Acid Sensing via General Control Nonderepressible-2 Kinase and Immunological Programming. *Front Immunol,* 8**,** 1719.

Bedard, M., Salio, M. & Cerundolo, V. 2017. Harnessing the Power of Invariant Natural Killer T Cells in Cancer Immunotherapy. *Front Immunol,* 8**,** 1829.

Bellone, M., Ceccon, M., Grioni, M., Jachetti, E., Calcinotto, A., Napolitano, A., Freschi, M., Casorati, G. & Dellabona, P. 2010. iNKT cells control mouse spontaneous carcinoma independently of tumor-specific cytotoxic T cells. *PLoS One,* 5**,** e8646.

Bendelac, A. 1995. Positive selection of mouse NK1+ T cells by CD1-expressing cortical thymocytes. *J Exp Med,* 182**,** 2091-6.

Bendelac, A., Lantz, O., Quimby, M. E., Yewdell, J. W., Bennink, J. R. & Brutkiewicz, R. R. 1995. CD1 recognition by mouse NK1+ T lymphocytes. *Science,* 268**,** 863-5.

Berzins, S. P., Smyth, M. J. & Baxter, A. G. 2011. Presumed guilty: natural killer T cell defects and human disease. *Nat Rev Immunol,* 11**,** 131-42.

Bettigole, S. E. & Glimcher, L. H. 2015. Endoplasmic reticulum stress in immunity. *Annu Rev Immunol,* 33**,** 107-38.

Beyaz, S., Kim, J. H., Pinello, L., Xifaras, M. E., Hu, Y., Huang, J., Kerenyi, M. A., Das, P. P., Barnitz, R. A., Herault, A., Dogum, R., Haining, W. N., Yilmaz, O. H., Passegue, E., Yuan, G. C., Orkin, S. H. & Winau, F. 2017. The histone demethylase UTX regulates the lineage-specific epigenetic program of invariant natural killer T cells. *Nat Immunol,* 18**,** 184-195.

Bhattacharyya, S. 2014. Can't RIDD off viruses. *Front Microbiol,* 5**,** 292.

Bobrovnikova-Marjon, E., Hatzivassiliou, G., Grigoriadou, C., Romero, M., Cavener, D. R., Thompson, C. B. & Diehl, J. A. 2008. PERK-dependent regulation of lipogenesis during mouse mammary gland development and adipocyte differentiation. *Proc Natl Acad Sci U S A,* 105**,** 16314-9.

Borg, N. A., Wun, K. S., Kjer-Nielsen, L., Wilce, M. C., Pellicci, D. G., Koh, R., Besra, G. S., Bharadwaj, M., Godfrey, D. I., Mccluskey, J. & Rossjohn, J. 2007. CD1d-lipid-antigen recognition by the semi-invariant NKT T-cell receptor. *Nature,* 448**,** 44-9.

Bourgeois, E., Van, L. P., Samson, M., Diem, S., Barra, A., Roga, S., Gombert, J. M., Schneider, E., Dy, M., Gourdy, P., Girard, J. P. & Herbelin, A. 2009. The pro-Th2 cytokine IL-33 directly interacts with invariant NKT and NK cells to induce IFN-gamma production. *Eur J Immunol,* 39**,** 1046-55.

Boyce, M., Bryant, K. F., Jousse, C., Long, K., Harding, H. P., Scheuner, D., Kaufman, R. J., Ma, D., Coen, D. M., Ron, D. & Yuan, J. 2005. A selective inhibitor of eIF2alpha dephosphorylation protects cells from ER stress. *Science,* 307**,** 935-9.

Bradbury, A., Belt, K. T., Neri, T. M., Milstein, C. & Calabi, F. 1988. Mouse CD1 is distinct from and co-exists with TL in the same thymus. *EMBO J,* 7**,** 3081-6.

Bravo-Sagua, R., Parra, V., Ortiz-Sandoval, C., Navarro-Marquez, M., Rodriguez, A. E., Diaz-Valdivia, N., Sanhueza, C., Lopez-Crisosto, C., Tahbaz, N., Rothermel, B. A., Hill, J. A., Cifuentes, M., Simmen, T., Quest, A. F. G. & Lavandero, S. 2019. Caveolin-1 impairs PKA-DRP1-mediated remodelling of ER-mitochondria communication during the early phase of ER stress. *Cell Death Differ,* 26**,** 1195-1212.

Brennan, P. J., Cheng, T. Y., Pellicci, D. G., Watts, G. F. M., Veerapen, N., Young, D. C., Rossjohn, J., Besra, G. S., Godfrey, D. I., Brenner, M. B. & Moody, D. B. 2017. Structural determination of lipid antigens captured at the CD1d-T-cell receptor interface. *Proc Natl Acad Sci U S A,* 114**,** 8348-8353.

Brennan, P. J., Tatituri, R. V., Brigl, M., Kim, E. Y., Tuli, A., Sanderson, J. P., Gadola, S. D., Hsu, F. F., Besra, G. S. & Brenner, M. B. 2011. Invariant natural killer T cells recognize lipid self antigen induced by microbial danger signals. *Nat Immunol,* 12**,** 1202-11.

Brennan, P. J., Tatituri, R. V., Heiss, C., Watts, G. F., Hsu, F. F., Veerapen, N., Cox, L. R., Azadi, P., Besra, G. S. & Brenner, M. B. 2014. Activation of iNKT cells by a distinct constituent of the endogenous glucosylceramide fraction. *Proc Natl Acad Sci U S A,* 111**,** 13433-8.

Brigl, M. & Brenner, M. B. 2004. CD1: antigen presentation and T cell function. *Annu Rev Immunol,* 22**,** 817-90.

Brigl, M., Tatituri, R. V., Watts, G. F., Bhowruth, V., Leadbetter, E. A., Barton, N., Cohen, N. R., Hsu, F. F., Besra, G. S. & Brenner, M. B. 2011. Innate and cytokine-driven signals, rather than microbial antigens, dominate in natural killer T cell activation during microbial infection. *J Exp Med,* 208**,** 1163-77.

Bronner, D. N., Abuaita, B. H., Chen, X., Fitzgerald, K. A., Nunez, G., He, Y., Yin, X. M. & O'riordan, M. X. 2015. Endoplasmic Reticulum Stress Activates the Inflammasome via NLRP3- and Caspase-2-Driven Mitochondrial Damage. *Immunity,* 43**,** 451-62.

Brutkiewicz, R. R. 2016. Cell Signaling Pathways That Regulate Antigen Presentation. *J Immunol,* 197**,** 2971-2979.

Bu, Y. & Diehl, J. A. 2016. Stressing out melanoma with an anti-GRP78 compound. *Pigment Cell Melanoma Res,* 29**,** 490-1.

Cameron, G., Pellicci, D. G., Uldrich, A. P., Besra, G. S., Illarionov, P., Williams, S. J., La Gruta, N. L., Rossjohn, J. & Godfrey, D. I. 2015. Antigen Specificity of Type I NKT Cells Is Governed by TCR beta-Chain Diversity. *J Immunol,* 195**,** 4604-14.

Cao, Y., Trillo-Tinoco, J., Sierra, R. A., Anadon, C., Dai, W., Mohamed, E., Cen, L., Costich, T. L., Magliocco, A., Marchion, D., Klar, R., Michel, S., Jaschinski, F., Reich, R. R., Mehrotra, S., Cubillos-Ruiz, J. R., Munn, D. H., Conejo-Garcia, J. R. & Rodriguez, P. C. 2019. ER stress-induced mediator C/EBP homologous protein thwarts effector T cell activity in tumors through T-bet repression. *Nat Commun,* 10**,** 1280.

Carnaud, C., Lee, D., Donnars, O., Park, S. H., Beavis, A., Koezuka, Y. & Bendelac, A. 1999. Cutting edge: Cross-talk between cells of the innate immune system: NKT cells rapidly activate NK cells. *J Immunol,* 163**,** 4647-50.

Carra, G., Gerosa, F. & Trinchieri, G. 2000. Biosynthesis and posttranslational regulation of human IL-12. *J Immunol,* 164**,** 4752-61.

Catala, A. 2014. Lipid peroxidation modifies the assembly of biological membranes "The Lipid Whisker Model". *Front Physiol,* 5**,** 520.

Cavanagh, C. R., Chao, S., Wang, S., Huang, B. E., Stephen, S., Kiani, S., Forrest, K., Saintenac, C., Brown-Guedira, G. L., Akhunova, A., See, D., Bai, G., Pumphrey, M., Tomar, L., Wong, D., Kong, S., Reynolds, M., Da Silva, M. L., Bockelman, H., Talbert, L., Anderson, J. A., Dreisigacker, S., Baenziger, S., Carter, A., Korzun, V., Morrell, P. L., Dubcovsky, J., Morell, M. K., Sorrells, M. E., Hayden, M. J. & Akhunov, E. 2013. Genome-wide comparative diversity uncovers multiple targets of selection for improvement in hexaploid wheat landraces and cultivars. *Proc Natl Acad Sci U S A,* 110**,** 8057-62.

Chancellor, A., Tocheva, A. S., Cave-Ayland, C., Tezera, L., White, A., Al Dulayymi, J. R., Bridgeman, J. S., Tews, I., Wilson, S., Lissin, N. M., Tebruegge, M., Marshall, B., Sharpe, S., Elliott, T., Skylaris, C. K., Essex, J. W., Baird, M. S., Gadola, S., Elkington, P. & Mansour, S. 2017. CD1b-restricted GEM T cell responses are modulated by Mycobacterium tuberculosis mycolic acid meromycolate chains. *Proc Natl Acad Sci U S A,* 114**,** E10956-E10964.

Chang, J. S., Ocvirk, S., Berger, E., Kisling, S., Binder, U., Skerra, A., Lee, A. S. & Haller, D. 2012. Endoplasmic reticulum stress response promotes cytotoxic phenotype of CD8alphabeta+ intraepithelial lymphocytes in a mouse model for Crohn's disease-like ileitis. *J Immunol,* 189**,** 1510-20.

Chang, P. P., Barral, P., Fitch, J., Pratama, A., Ma, C. S., Kallies, A., Hogan, J. J., Cerundolo, V., Tangye, S. G., Bittman, R., Nutt, S. L., Brink, R., Godfrey, D. I., Batista, F. D. & Vinuesa, C. G. 2011. Identification of Bcl-6-dependent follicular helper NKT cells that provide cognate help for B cell responses. *Nat Immunol,* 13**,** 35-43.

Chang, Y. J., Huang, J. R., Tsai, Y. C., Hung, J. T., Wu, D., Fujio, M., Wong, C. H. & Yu, A. L. 2007. Potent immune-modulating and anticancer effects of NKT cell stimulatory glycolipids. *Proc Natl Acad Sci U S A,* 104**,** 10299-304.

Chen, Y. H., Wang, B., Chun, T., Zhao, L., Cardell, S., Behar, S. M., Brenner, M. B. & Wang, C. R. 1999. Expression of CD1d2 on thymocytes is not sufficient for the development of NK T cells in CD1d1-deficient mice. *J Immunol,* 162**,** 4560-6.

Cheung, K. L., Jarrett, R., Subramaniam, S., Salimi, M., Gutowska-Owsiak, D., Chen, Y. L., Hardman, C., Xue, L., Cerundolo, V. & Ogg, G. 2016. Psoriatic T cells recognize neolipid antigens generated by mast cell phospholipase delivered by exosomes and presented by CD1a. *J Exp Med,* 213**,** 2399-2412.

Clapham, D. E. 2007. Calcium signaling. *Cell,* 131**,** 1047-58.

Colla, E., Coune, P., Liu, Y., Pletnikova, O., Troncoso, J. C., Iwatsubo, T., Schneider, B. L. & Lee, M. K. 2012. Endoplasmic reticulum stress is important for the manifestations of alpha-synucleinopathy in vivo. *J Neurosci,* 32**,** 3306-20.

Cooke, R. E., Gherardin, N. A., Harrison, S. J., Quach, H., Godfrey, D. I., Prince, M., Koldej, R. & Ritchie, D. S. 2016. Spontaneous onset and transplant models of the Vk*MYC mouse show immunological sequelae comparable to human multiple myeloma. *J Transl Med,* 14**,** 259.

Coppieters, K., Dewint, P., Van Beneden, K., Jacques, P., Seeuws, S., Verbruggen, G., Deforce, D. & Elewaut, D. 2007. NKT cells: manipulable managers of joint inflammation. *Rheumatology (Oxford),* 46**,** 565-71.

Coquet, J. M., Chakravarti, S., Kyparissoudis, K., Mcnab, F. W., Pitt, L. A., Mckenzie, B. S., Berzins, S. P., Smyth, M. J. & Godfrey, D. I. 2008. Diverse cytokine production by NKT cell subsets and identification of an IL-17-producing CD4-NK1.1- NKT cell population. *Proc Natl Acad Sci U S A,* 105**,** 11287-92.

Corbett, A. J., Eckle, S. B., Birkinshaw, R. W., Liu, L., Patel, O., Mahony, J., Chen, Z., Reantragoon, R., Meehan, B., Cao, H., Williamson, N. A., Strugnell, R. A., Van Sinderen, D., Mak, J. Y., Fairlie, D. P., Kjer-Nielsen, L., Rossjohn, J. & Mccluskey, J. 2014. T-cell activation by transitory neo-antigens derived from distinct microbial pathways. *Nature,* 509**,** 361-5.

Cox, D., Fox, L., Tian, R., Bardet, W., Skaley, M., Mojsilovic, D., Gumperz, J. & Hildebrand, W. 2009. Determination of cellular lipids bound to human CD1d molecules. *PLoS One,* 4**,** e5325.

Credle, J. J., Finer-Moore, J. S., Papa, F. R., Stroud, R. M. & Walter, P. 2005. On the mechanism of sensing unfolded protein in the endoplasmic reticulum. *Proc Natl Acad Sci U S A,* 102**,** 18773-84.

Crosby, C. M. & Kronenberg, M. 2018. Tissue-specific functions of invariant natural killer T cells. *Nat Rev Immunol,* 18**,** 559-574.

Cross, B. C., Bond, P. J., Sadowski, P. G., Jha, B. K., Zak, J., Goodman, J. M., Silverman, R. H., Neubert, T. A., Baxendale, I. R., Ron, D. & Harding, H. P. 2012. The molecular basis for selective inhibition of unconventional mRNA splicing by an IRE1-binding small molecule. *Proc Natl Acad Sci U S A,* 109**,** E869-78.

Crowe, N. Y., Smyth, M. J. & Godfrey, D. I. 2002. A critical role for natural killer T cells in immunosurveillance of methylcholanthrene-induced sarcomas. *J Exp Med,* 196**,** 119-27.

Cubillos-Ruiz, J. R., Bettigole, S. E. & Glimcher, L. H. 2017. Tumorigenic and Immunosuppressive Effects of Endoplasmic Reticulum Stress in Cancer. *Cell,* 168**,** 692-706.

Cubillos-Ruiz, J. R., Silberman, P. C., Rutkowski, M. R., Chopra, S., Perales-Puchalt, A., Song, M., Zhang, S., Bettigole, S. E., Gupta, D., Holcomb, K., Ellenson, L. H., Caputo, T., Lee, A. H., Conejo-Garcia, J. R. & Glimcher, L.

H. 2015. ER Stress Sensor XBP1 Controls Anti-tumor Immunity by Disrupting Dendritic Cell Homeostasis. *Cell,* 161**,** 1527-38.

Cutting, G. R. 2015. Cystic fibrosis genetics: from molecular understanding to clinical application. *Nat Rev Genet,* 16**,** 45-56.

Dang, E. V., Barbi, J., Yang, H. Y., Jinasena, D., Yu, H., Zheng, Y., Bordman, Z., Fu, J., Kim, Y., Yen, H. R., Luo, W., Zeller, K., Shimoda, L., Topalian, S. L., Semenza, G. L., Dang, C. V., Pardoll, D. M. & Pan, F. 2011. Control of T(H)17/T(reg) balance by hypoxia-inducible factor 1. *Cell,* 146**,** 772-84.

Das, H., Groh, V., Kuijl, C., Sugita, M., Morita, C. T., Spies, T. & Bukowski, J. F. 2001. MICA engagement by human Vgamma2Vdelta2 T cells enhances their antigen-dependent effector function. *Immunity,* 15**,** 83-93.

Dashtsoodol, N., Shigeura, T., Ozawa, R., Harada, M., Kojo, S., Watanabe, T., Koseki, H., Nakayama, M., Ohara, O. & Taniguchi, M. 2016. Generation of Novel Traj18-Deficient Mice Lacking Valpha14 Natural Killer T Cells with an Undisturbed T Cell Receptor alpha-Chain Repertoire. *PLoS One,* 11**,** e0153347.

De Calisto, J., Wang, N., Wang, G., Yigit, B., Engel, P. & Terhorst, C. 2014. SAP-Dependent and -Independent Regulation of Innate T Cell Development Involving SLAMF Receptors. *Front Immunol,* 5**,** 186.

De Jong, A., Cheng, T. Y., Huang, S., Gras, S., Birkinshaw, R. W., Kasmar, A. G., Van Rhijn, I., Pena-Cruz, V., Ruan, D. T., Altman, J. D., Rossjohn, J. & Moody, D. B. 2014. CD1a-autoreactive T cells recognize natural skin oils that function as headless antigens. *Nat Immunol,* 15**,** 177-85.

De La Salle, H., Mariotti, S., Angenieux, C., Gilleron, M., Garcia-Alles, L. F., Malm, D., Berg, T., Paoletti, S., Maitre, B., Mourey, L., Salamero, J., Cazenave, J. P., Hanau, D., Mori, L., Puzo, G. & De Libero, G. 2005. Assistance of microbial glycolipid antigen processing by CD1e. *Science,* 310**,** 1321-4.

De Santo, C., Arscott, R., Booth, S., Karydis, I., Jones, M., Asher, R., Salio, M., Middleton, M. & Cerundolo, V. 2010. Invariant NKT cells modulate the suppressive activity of IL-10-secreting neutrophils differentiated with serum amyloid A. *Nat Immunol,* 11**,** 1039-46.

De Santo, C., Salio, M., Masri, S. H., Lee, L. Y., Dong, T., Speak, A. O., Porubsky, S., Booth, S., Veerapen, N., Besra, G. S., Grone, H. J., Platt, F. M., Zambon, M. & Cerundolo, V. 2008. Invariant NKT cells reduce the immunosuppressive activity of influenza A virus-induced myeloid-derived suppressor cells in mice and humans. *J Clin Invest,* 118**,** 4036-48.

Deeks, E. D. 2016. Lumacaftor/Ivacaftor: A Review in Cystic Fibrosis. *Drugs,* 76**,** 1191-201.

Del Rio, M. L., Bernhardt, G., Rodriguez-Barbosa, J. I. & Forster, R. 2010. Development and functional specialization of CD103+ dendritic cells. *Immunol Rev,* 234**,** 268-81.

Delia, D., Cattoretti, G., Polli, N., Fontanella, E., Aiello, A., Giardini, R., Rilke, F. & Della Porta, G. 1988. CD1c but neither CD1a nor CD1b molecules are expressed on normal, activated, and malignant human B cells: identification of a new B-cell subset. *Blood,* 72**,** 241-7.

Dellabona, P., Padovan, E., Casorati, G., Brockhaus, M. & Lanzavecchia, A. 1994. An invariant V alpha 24-J alpha Q/V beta 11 T cell receptor is expressed in all individuals by clonally expanded CD4-8- T cells. *J Exp Med,* 180**,** 1171-6.

Deng, Z. B., Zhuang, X., Ju, S., Xiang, X., Mu, J., Liu, Y., Jiang, H., Zhang, L., Mobley, J., Mcclain, C., Feng, W., Grizzle, W., Yan, J., Miller, D., Kronenberg, M. & Zhang, H. G. 2013. Exosome-like nanoparticles from intestinal mucosal cells carry prostaglandin E2 and suppress activation of liver NKT cells. *J Immunol,* 190**,** 3579-89.

Denzel, M. S., Storm, N. J., Gutschmidt, A., Baddi, R., Hinze, Y., Jarosch, E., Sommer, T., Hoppe, T. & Antebi, A. 2014. Hexosamine pathway metabolites enhance protein quality control and prolong life. *Cell,* 156**,** 1167-1178.

Dhodapkar, K. M., Cirignano, B., Chamian, F., Zagzag, D., Miller, D. C., Finlay, J. L. & Steinman, R. M. 2004. Invariant natural killer T cells are preserved in patients with glioma and exhibit antitumor lytic activity following dendritic cell-mediated expansion. *Int J Cancer,* 109**,** 893-9.

Dhodapkar, M. V., Geller, M. D., Chang, D. H., Shimizu, K., Fujii, S., Dhodapkar, K. M. & Krasovsky, J. 2003. A reversible defect in natural killer T cell

function characterizes the progression of premalignant to malignant multiple myeloma. *J Exp Med,* 197**,** 1667-76.

Di Pietro, C., De Giorgi, L., Cosorich, I., Sorini, C., Fedeli, M. & Falcone, M. 2016. MicroRNA-133b Regulation of Th-POK Expression and Dendritic Cell Signals Affect NKT17 Cell Differentiation in the Thymus. *J Immunol,* 197**,** 3271-3280.

Dias, J., Leeansyah, E. & Sandberg, J. K. 2017. Multiple layers of heterogeneity and subset diversity in human MAIT cell responses to distinct microorganisms and to innate cytokines. *Proc Natl Acad Sci U S A,* 114**,** E5434-E5443.

Dikic, I. & Elazar, Z. 2018. Mechanism and medical implications of mammalian autophagy. *Nat Rev Mol Cell Biol,* 19**,** 349-364.

Dobenecker, M. W., Kim, J. K., Marcello, J., Fang, T. C., Prinjha, R., Bosselut, R. & Tarakhovsky, A. 2015. Coupling of T cell receptor specificity to natural killer T cell development by bivalent histone H3 methylation. *J Exp Med,* 212**,** 297-306.

Dolen, Y., Kreutz, M., Gileadi, U., Tel, J., Vasaturo, A., Van Dinther, E. A., Van Hout-Kuijer, M. A., Cerundolo, V. & Figdor, C. G. 2016. Co-delivery of PLGA encapsulated invariant NKT cell agonist with antigenic protein induce strong T cell-mediated antitumor immune responses. *Oncoimmunology,* 5**,** e1068493.

Dong, H., Adams, N. M., Xu, Y., Cao, J., Allan, D. S. J., Carlyle, J. R., Chen, X., Sun, J. C. & Glimcher, L. H. 2019. The IRE1 endoplasmic reticulum stress sensor activates natural killer cell immunity in part by regulating c-Myc. *Nat Immunol,* 20**,** 865-878.

Dougan, S. K., Salas, A., Rava, P., Agyemang, A., Kaser, A., Morrison, J., Khurana, A., Kronenberg, M., Johnson, C., Exley, M., Hussain, M. M. & Blumberg, R. S. 2005. Microsomal triglyceride transfer protein lipidation and control of CD1d on antigen-presenting cells. *J Exp Med,* 202**,** 529-39.

Durai, V. & Murphy, K. M. 2016. Functions of Murine Dendritic Cells. *Immunity,* 45**,** 719-736.

Durgan, K., Ali, M., Warner, P. & Latchman, Y. E. 2011. Targeting NKT cells and PD-L1 pathway results in augmented anti-tumor responses in a melanoma model. *Cancer Immunol Immunother,* 60**,** 547-58.

Dutta, M., Kraus, Z. J., Gomez-Rodriguez, J., Hwang, S. H., Cannons, J. L., Cheng, J., Lee, S. Y., Wiest, D. L., Wakeland, E. K. & Schwartzberg, P. L. 2013. A role for Ly108 in the induction of promyelocytic zinc finger transcription factor in developing thymocytes. *J Immunol,* 190**,** 2121-8.

Ellgaard, L., Sevier, C. S. & Bulleid, N. J. 2018. How Are Proteins Reduced in the Endoplasmic Reticulum? *Trends Biochem Sci,* 43**,** 32-43.

Exley, M., Garcia, J., Balk, S. P. & Porcelli, S. 1997. Requirements for CD1d recognition by human invariant Valpha24+ CD4-CD8- T cells. *J Exp Med,* 186**,** 109-20.

Exley, M. A., Bigley, N. J., Cheng, O., Tahir, S. M., Smiley, S. T., Carter, Q. L., Stills, H. F., Grusby, M. J., Koezuka, Y., Taniguchi, M. & Balk, S. P. 2001. CD1d-reactive T-cell activation leads to amelioration of disease caused by diabetogenic encephalomyocarditis virus. *J Leukoc Biol,* 69**,** 713-8.

Exley, M. A., Hou, R., Shaulov, A., Tonti, E., Dellabona, P., Casorati, G., Akbari, O., Akman, H. O., Greenfield, E. A., Gumperz, J. E., Boyson, J. E., Balk, S. P. & Wilson, S. B. 2008. Selective activation, expansion, and monitoring of human iNKT cells with a monoclonal antibody specific for the TCR alpha-chain CDR3 loop. *Eur J Immunol,* 38**,** 1756-66.

Exley, M. A., Friedlander, P., Alatrakchi, N., Vriend, L., Yue, S., Sasada, T., Zeng, W., Mizukami, Y., Clark, J., Nemer, D., Leclair, K., Canning, C., Daley, H., Dranoff, G., Giobbie-Hurder, A., Hodi, F. S., Ritz, J. & Balk, S. P. 2017. Adoptive Transfer of Invariant NKT Cells as Immunotherapy for Advanced Melanoma: A Phase I Clinical Trial. Clin Cancer Res, 23, 3510-3519.

Facciotti, F., Cavallari, M., Angenieux, C., Garcia-Alles, L. F., Signorino-Gelo, F., Angman, L., Gilleron, M., Prandi, J., Puzo, G., Panza, L., Xia, C., Wang, P. G., Dellabona, P., Casorati, G., Porcelli, S. A., De La Salle, H., Mori, L. & De Libero, G. 2011. Fine tuning by human CD1e of lipid-specific immune responses. *Proc Natl Acad Sci U S A,* 108**,** 14228-33.

Facciotti, F., Ramanjaneyulu, G. S., Lepore, M., Sansano, S., Cavallari, M., Kistowska, M., Forss-Petter, S., Ni, G., Colone, A., Singhal, A., Berger, J.,

Xia, C., Mori, L. & De Libero, G. 2012. Peroxisome-derived lipids are self antigens that stimulate invariant natural killer T cells in the thymus. *Nat Immunol,* 13**,** 474-80.

Fallarini, S., Paoletti, T., Orsi Battaglini, N. & Lombardi, G. 2012. Invariant NKT cells increase drug-induced osteosarcoma cell death. *Br J Pharmacol,* 167**,** 1533-49.

Farin, H. F., Karthaus, W. R., Kujala, P., Rakhshandehroo, M., Schwank, G., Vries, R. G., Kalkhoven, E., Nieuwenhuis, E. E. & Clevers, H. 2014. Paneth cell extrusion and release of antimicrobial products is directly controlled by immune cell-derived IFN-gamma. *J Exp Med,* 211**,** 1393-405.

Fedeli, M., Napolitano, A., Wong, M. P., Marcais, A., De Lalla, C., Colucci, F., Merkenschlager, M., Dellabona, P. & Casorati, G. 2009. Dicer-dependent microRNA pathway controls invariant NKT cell development. *J Immunol,* 183**,** 2506-12.

Ferraz, M. J., Marques, A. R., Appelman, M. D., Verhoek, M., Strijland, A., Mirzaian, M., Scheij, S., Ouairy, C. M., Lahav, D., Wisse, P., Overkleeft, H. S., Boot, R. G. & Aerts, J. M. 2016. Lysosomal glycosphingolipid catabolism by acid ceramidase: formation of glycosphingoid bases during deficiency of glycosidases. *FEBS Lett,* 590**,** 716-25.

Fesnak, A. D., June, C. H. & Levine, B. L. 2016. Engineered T cells: the promise and challenges of cancer immunotherapy. *Nat Rev Cancer,* 16**,** 566-81.

Fichtner-Feigl, S., Strober, W., Kawakami, K., Puri, R. K. & Kitani, A. 2006. IL-13 signaling through the IL-13alpha2 receptor is involved in induction of TGF-beta1 production and fibrosis. *Nat Med,* 12**,** 99-106.

Fijalkowska, D., Verbruggen, S., Ndah, E., Jonckheere, V., Menschaert, G. & Van Damme, P. 2017. eIF1 modulates the recognition of suboptimal translation initiation sites and steers gene expression via uORFs. *Nucleic Acids Res,* 45**,** 7997-8013.

Fowlkes, B. J., Kruisbeek, A. M., Ton-That, H., Weston, M. A., Coligan, J. E., Schwartz, R. H. & Pardoll, D. M. 1987. A novel population of T-cell receptor alpha beta-bearing thymocytes which predominantly expresses a single V beta gene family. *Nature,* 329**,** 251-4.

Fox, L. M., Cox, D. G., Lockridge, J. L., Wang, X., Chen, X., Scharf, L., Trott, D. L., Ndonye, R. M., Veerapen, N., Besra, G. S., Howell, A. R., Cook, M. E., Adams, E. J., Hildebrand, W. H. & Gumperz, J. E. 2009. Recognition of lyso-phospholipids by human natural killer T lymphocytes. *PLoS Biol,* 7**,** e1000228.

Freigang, S., Zadorozhny, V., Mckinney, M. K., Krebs, P., Herro, R., Pawlak, J., Kain, L., Schrantz, N., Masuda, K., Liu, Y., Savage, P. B., Bendelac, A., Cravatt, B. F. & Teyton, L. 2010. Fatty acid amide hydrolase shapes NKT cell responses by influencing the serum transport of lipid antigen in mice. *J Clin Invest,* 120**,** 1873-84.

Fujii, S., Liu, K., Smith, C., Bonito, A. J. & Steinman, R. M. 2004. The linkage of innate to adaptive immunity via maturing dendritic cells in vivo requires CD40 ligation in addition to antigen presentation and CD80/86 costimulation. *J Exp Med,* 199**,** 1607-18.

Fujii, S., Shimizu, K., Hemmi, H. & Steinman, R. M. 2007. Innate Valpha14(+) natural killer T cells mature dendritic cells, leading to strong adaptive immunity. *Immunol Rev,* 220**,** 183-98.

Fujii, S., Shimizu, K., Kronenberg, M. & Steinman, R. M. 2002. Prolonged IFN-gamma-producing NKT response induced with alpha-galactosylceramide-loaded DCs. *Nat Immunol,* 3**,** 867-74.

Fujii, S., Shimizu, K., Smith, C., Bonifaz, L. & Steinman, R. M. 2003. Activation of natural killer T cells by alpha-galactosylceramide rapidly induces the full maturation of dendritic cells in vivo and thereby acts as an adjuvant for combined CD4 and CD8 T cell immunity to a coadministered protein. *J Exp Med,* 198**,** 267-79.

Fusakio, M. E., Willy, J. A., Wang, Y., Mirek, E. T., Al Baghdadi, R. J., Adams, C. M., Anthony, T. G. & Wek, R. C. 2016. Transcription factor ATF4 directs basal and stress-induced gene expression in the unfolded protein response and cholesterol metabolism in the liver. *Mol Biol Cell,* 27**,** 1536-51.

Gadola, S. D., Koch, M., Marles-Wright, J., Lissin, N. M., Shepherd, D., Matulis, G., Harlos, K., Villiger, P. M., Stuart, D. I., Jakobsen, B. K., Cerundolo, V. & Jones, E. Y. 2006. Structure and binding kinetics of three different human CD1d-alpha-galactosylceramide-specific T cell receptors. *J Exp Med,* 203**,** 699-710.

Gadola, S. D., Zaccai, N. R., Harlos, K., Shepherd, D., Castro-Palomino, J. C., Ritter, G., Schmidt, R. R., Jones, E. Y. & Cerundolo, V. 2002. Structure of human CD1b with bound ligands at 2.3 A, a maze for alkyl chains. *Nat Immunol,* 3**,** 721-6.

Gallagher, C. M., Garri, C., Cain, E. L., Ang, K. K., Wilson, C. G., Chen, S., Hearn, B. R., Jaishankar, P., Aranda-Diaz, A., Arkin, M. R., Renslo, A. R. & Walter, P. 2016. Ceapins are a new class of unfolded protein response inhibitors, selectively targeting the ATF6alpha branch. *Elife,* 5.

Gallagher, C. M. & Walter, P. 2016. Ceapins inhibit ATF6alpha signaling by selectively preventing transport of ATF6alpha to the Golgi apparatus during ER stress. *Elife,* 5.

Galli, G., Nuti, S., Tavarini, S., Galli-Stampino, L., De Lalla, C., Casorati, G., Dellabona, P. & Abrignani, S. 2003. CD1d-restricted help to B cells by human invariant natural killer T lymphocytes. *J Exp Med,* 197**,** 1051-7.

Ganley, I. G., Wong, P. M., Gammoh, N. & Jiang, X. 2011. Distinct autophagosomal-lysosomal fusion mechanism revealed by thapsigargin-induced autophagy arrest. *Mol Cell,* 42**,** 731-43.

Gapin, L. 2008. The making of NKT cells. *Nat Immunol,* 9**,** 1009-11.

Gapin, L. 2016. Development of invariant natural killer T cells. *Curr Opin Immunol,* 39**,** 68-74.

Gardner, B. M. & Walter, P. 2011. Unfolded proteins are Ire1-activating ligands that directly induce the unfolded protein response. *Science,* 333**,** 1891-4.

Gehrmann, U., Hiltbrunner, S., Georgoudaki, A. M., Karlsson, M. C., Naslund, T. I. & Gabrielsson, S. 2013. Synergistic induction of adaptive antitumor immunity by codelivery of antigen with alpha-galactosylceramide on exosomes. *Cancer Res,* 73**,** 3865-76.

Gherardin, N. A., Souter, M. N., Koay, H. F., Mangas, K. M., Seemann, T., Stinear, T. P., Eckle, S. B., Berzins, S. P., D'udekem, Y., Konstantinov, I. E., Fairlie, D. P., Ritchie, D. S., Neeson, P. J., Pellicci, D. G., Uldrich, A. P., Mccluskey, J. & Godfrey, D. I. 2018. Human blood MAIT cell subsets defined using MR1 tetramers. *Immunol Cell Biol,* 96**,** 507-525.

Girardi, E., Yu, E. D., Li, Y., Tarumoto, N., Pei, B., Wang, J., Illarionov, P., Kinjo, Y., Kronenberg, M. & Zajonc, D. M. 2011. Unique interplay between sugar and lipid in determining the antigenic potency of bacterial antigens for NKT cells. *PLoS Biol,* 9**,** e1001189.

Godfrey, D. I., Uldrich, A. P., Mccluskey, J., Rossjohn, J. & Moody, D. B. 2015. The burgeoning family of unconventional T cells. *Nat Immunol,* 16**,** 1114-23.

Goodall, J. C., Wu, C., Zhang, Y., Mcneill, L., Ellis, L., Saudek, V. & Gaston, J. S. 2010. Endoplasmic reticulum stress-induced transcription factor, CHOP, is crucial for dendritic cell IL-23 expression. *Proc Natl Acad Sci U S A,* 107**,** 17698-703.

Gorini, F., Azzimonti, L., Delfanti, G., Scarfo, L., Scielzo, C., Bertilaccio, M. T., Ranghetti, P., Gulino, A., Doglioni, C., Di Napoli, A., Capri, M., Franceschi, C., Caligaris-Cappio, F., Ghia, P., Bellone, M., Dellabona, P., Casorati, G. & De Lalla, C. 2017. Invariant NKT cells contribute to chronic lymphocytic leukemia surveillance and prognosis. *Blood*.

Govindarajan, S., Gaublomme, D., Van Der Cruyssen, R., Verheugen, E., Van Gassen, S., Saeys, Y., Tavernier, S., Iwawaki, T., Bloch, Y., Savvides, S. N., Lambrecht, B. N., Janssens, S., Elewaut, D. & Drennan, M. B. 2018. Stabilization of cytokine mRNAs in iNKT cells requires the serine-threonine kinase IRE1alpha. *Nat Commun,* 9**,** 5340.

Greene, C. M. & Mcelvaney, N. G. 2010. Z alpha-1 antitrypsin deficiency and the endoplasmic reticulum stress response. *World J Gastrointest Pharmacol Ther,* 1**,** 94-101.

Griewank, K., Borowski, C., Rietdijk, S., Wang, N., Julien, A., Wei, D. G., Mamchak, A. A., Terhorst, C. & Bendelac, A. 2007. Homotypic interactions mediated by Slamf1 and Slamf6 receptors control NKT cell lineage development. *Immunity,* 27**,** 751-62.

Grootjans, J., Kaser, A., Kaufman, R. J. & Blumberg, R. S. 2016. The unfolded protein response in immunity and inflammation. *Nat Rev Immunol,* 16**,** 469-84.

Gu, X., Li, K., Laybutt, D. R., He, M. L., Zhao, H. L., Chan, J. C. & Xu, G. 2010. Bip overexpression, but not CHOP inhibition, attenuates fatty-acid-induced

endoplasmic reticulum stress and apoptosis in HepG2 liver cells. *Life Sci,* 87**,** 724-32.

Hagglof, T., Sedimbi, S. K., Yates, J. L., Parsa, R., Salas, B. H., Harris, R. A., Leadbetter, E. A. & Karlsson, M. C. 2016. Neutrophils license iNKT cells to regulate self-reactive mouse B cell responses. *Nat Immunol,* 17**,** 1407-1414.

Halder, R. C., Aguilera, C., Maricic, I. & Kumar, V. 2007. Type II NKT cell-mediated anergy induction in type I NKT cells prevents inflammatory liver disease. *J Clin Invest,* 117**,** 2302-12.

Han, M., Hannick, L. I., Dibrino, M. & Robinson, M. A. 1999. Polymorphism of human CD1 genes. *Tissue Antigens,* 54**,** 122-7.

Harding, H. P., Zeng, H., Zhang, Y., Jungries, R., Chung, P., Plesken, H., Sabatini, D. D. & Ron, D. 2001. Diabetes mellitus and exocrine pancreatic dysfunction in perk-/- mice reveals a role for translational control in secretory cell survival. *Mol Cell,* 7**,** 1153-63.

Harding, H. P., Zhang, Y. & Ron, D. 1999. Protein translation and folding are coupled by an endoplasmic-reticulum-resident kinase. *Nature,* 397**,** 271-4.

Harding, H. P., Zhang, Y., Zeng, H., Novoa, I., Lu, P. D., Calfon, M., Sadri, N., Yun, C., Popko, B., Paules, R., Stojdl, D. F., Bell, J. C., Hettmann, T., Leiden, J. M. & Ron, D. 2003. An integrated stress response regulates amino acid metabolism and resistance to oxidative stress. *Mol Cell,* 11**,** 619-33.

Hardman, C. S., Chen, Y. L., Salimi, M., Jarrett, R., Johnson, D., Jarvinen, V. J., Owens, R. J., Repapi, E., Cousins, D. J., Barlow, J. L., Mckenzie, A. N. J. & Ogg, G. 2017. CD1a presentation of endogenous antigens by group 2 innate lymphoid cells. *Sci Immunol,* 2.

Heczey, A., Liu, D., Tian, G., Courtney, A. N., Wei, J., Marinova, E., Gao, X., Guo, L., Yvon, E., Hicks, J., Liu, H., Dotti, G. & Metelitsa, L. S. 2014. Invariant NKT cells with chimeric antigen receptor provide a novel platform for safe and effective cancer immunotherapy. *Blood,* 124**,** 2824-33.

Henriksson, J., Chen, X., Gomes, T., Ullah, U., Meyer, K. B., Miragaia, R., Duddy, G., Pramanik, J., Yusa, K., Lahesmaa, R. & Teichmann, S. A. 2019. Genome-wide CRISPR Screens in T Helper Cells Reveal Pervasive Crosstalk between Activation and Differentiation. *Cell,* 176**,** 882-896 e18.

Hermans, I. F., Silk, J. D., Gileadi, U., Salio, M., Mathew, B., Ritter, G., Schmidt, R., Harris, A. L., Old, L. & Cerundolo, V. 2003. NKT cells enhance CD4+ and CD8+ T cell responses to soluble antigen in vivo through direct interaction with dendritic cells. *J Immunol,* 171**,** 5140-7.

Hermans, I. F., Silk, J. D., Yang, J., Palmowski, M. J., Gileadi, U., Mccarthy, C., Salio, M., Ronchese, F. & Cerundolo, V. 2004. The VITAL assay: a versatile fluorometric technique for assessing CTL- and NKT-mediated cytotoxicity against multiple targets in vitro and in vivo. *J Immunol Methods,* 285**,** 25-40.

Herzog, R., Schwudke, D., Schuhmann, K., Sampaio, J. L., Bornstein, S. R., Schroeder, M. & Shevchenko, A. 2011. A novel informatics concept for high-throughput shotgun lipidomics based on the molecular fragmentation query language. *Genome Biol,* 12**,** R8.

Hix, L. M., Shi, Y. H., Brutkiewicz, R. R., Stein, P. L., Wang, C. R. & Zhang, M. 2011. CD1d-expressing breast cancer cells modulate NKT cell-mediated antitumor immunity in a murine model of breast cancer metastasis. *PLoS One,* 6**,** e20702.

Hoglinger, G. U., Melhem, N. M., Dickson, D. W., Sleiman, P. M., Wang, L. S., Klei, L., Rademakers, R., De Silva, R., Litvan, I., Riley, D. E., Van Swieten, J. C., Heutink, P., Wszolek, Z. K., Uitti, R. J., Vandrovcova, J., Hurtig, H. I., Gross, R. G., Maetzler, W., Goldwurm, S., Tolosa, E., Borroni, B., Pastor, P., Group, P. S. P. G. S., Cantwell, L. B., Han, M. R., Dillman, A., Van Der Brug, M. P., Gibbs, J. R., Cookson, M. R., Hernandez, D. G., Singleton, A. B., Farrer, M. J., Yu, C. E., Golbe, L. I., Revesz, T., Hardy, J., Lees, A. J., Devlin, B., Hakonarson, H., Muller, U. & Schellenberg, G. D. 2011. Identification of common variants influencing risk of the tauopathy progressive supranuclear palsy. *Nat Genet,* 43**,** 699-705.

Hokin, L. E. 1966. Effects of calcium omission on acetylcholine-stimulated amylase secretion and phospholipid synthesis in pigeon pancreas slices. *Biochim Biophys Acta,* 115**,** 219-21.

Hollien, J., Lin, J. H., Li, H., Stevens, N., Walter, P. & Weissman, J. S. 2009. Regulated Ire1-dependent decay of messenger RNAs in mammalian cells. *J Cell Biol,* 186**,** 323-31.

Holmstrom, K. M. & Finkel, T. 2014. Cellular mechanisms and physiological consequences of redox-dependent signalling. *Nat Rev Mol Cell Biol,* 15**,** 411-21.

Hong, S., Wilson, M. T., Serizawa, I., Wu, L., Singh, N., Naidenko, O. V., Miura, T., Haba, T., Scherer, D. C., Wei, J., Kronenberg, M., Koezuka, Y. & Van Kaer, L. 2001. The natural killer T-cell ligand alpha-galactosylceramide prevents autoimmune diabetes in non-obese diabetic mice. *Nat Med,* 7**,** 1052-6.

Hoshino, A., Costa-Silva, B., Shen, T. L., Rodrigues, G., Hashimoto, A., Tesic Mark, M., Molina, H., Kohsaka, S., Di Giannatale, A., Ceder, S., Singh, S., Williams, C., Soplop, N., Uryu, K., Pharmer, L., King, T., Bojmar, L., Davies, A. E., Ararso, Y., Zhang, T., Zhang, H., Hernandez, J., Weiss, J. M., Dumont-Cole, V. D., Kramer, K., Wexler, L. H., Narendran, A., Schwartz, G. K., Healey, J. H., Sandstrom, P., Labori, K. J., Kure, E. H., Grandgenett, P. M., Hollingsworth, M. A., De Sousa, M., Kaur, S., Jain, M., Mallya, K., Batra, S. K., Jarnagin, W. R., Brady, M. S., Fodstad, O., Muller, V., Pantel, K., Minn, A. J., Bissell, M. J., Garcia, B. A., Kang, Y., Rajasekhar, V. K., Ghajar, C. M., Matei, I., Peinado, H., Bromberg, J. & Lyden, D. 2015. Tumour exosome integrins determine organotropic metastasis. *Nature,* 527**,** 329-35.

Hosomi, S., Grootjans, J., Tschurtschenthaler, M., Krupka, N., Matute, J. D., Flak, M. B., Martinez-Naves, E., Gomez Del Moral, M., Glickman, J. N., Ohira, M., Lanier, L. L., Kaser, A. & Blumberg, R. 2017. Intestinal epithelial cell endoplasmic reticulum stress promotes MULT1 up-regulation and NKG2D-mediated inflammation. *J Exp Med,* 214**,** 2985-2997.

Hou, N. S., Gutschmidt, A., Choi, D. Y., Pather, K., Shi, X., Watts, J. L., Hoppe, T. & Taubert, S. 2014. Activation of the endoplasmic reticulum unfolded protein response by lipid disequilibrium without disturbed proteostasis in vivo. *Proc Natl Acad Sci U S A,* 111**,** E2271-80.

Huang, J. R., Tsai, Y. C., Chang, Y. J., Wu, J. C., Hung, J. T., Lin, K. H., Wong, C. H. & Yu, A. L. 2014. alpha-Galactosylceramide but not phenyl-glycolipids induced NKT cell anergy and IL-33-mediated myeloid-derived suppressor cell accumulation via upregulation of egr2/3. *J Immunol,* 192**,** 1972-81.

Huang, S., Cheng, T. Y., Young, D. C., Layre, E., Madigan, C. A., Shires, J., Cerundolo, V., Altman, J. D. & Moody, D. B. 2011. Discovery of deoxyceramides and diacylglycerols as CD1b scaffold lipids among diverse groove-blocking lipids of the human CD1 system. *Proc Natl Acad Sci U S A,* 108**,** 19335-40.

Hung, J. T., Huang, J. R. & Yu, A. L. 2017. Tailored design of NKT-stimulatory glycolipids for polarization of immune responses. *J Biomed Sci,* 24**,** 22.

Hunn, M. K., Farrand, K. J., Broadley, K. W., Weinkove, R., Ferguson, P., Miller, R. J., Field, C. S., Petersen, T., Mcconnell, M. J. & Hermans, I. F. 2012. Vaccination with irradiated tumor cells pulsed with an adjuvant that stimulates NKT cells is an effective treatment for glioma. *Clin Cancer Res,* 18**,** 6446-59.

Imai, K., Kanno, M., Kimoto, H., Shigemoto, K., Yamamoto, S. & Taniguchi, M. 1986. Sequence and expression of transcripts of the T-cell antigen receptor alpha-chain gene in a functional, antigen-specific suppressor-T-cell hybridoma. *Proc Natl Acad Sci U S A,* 83**,** 8708-12.

Iwakoshi, N. N., Pypaert, M. & Glimcher, L. H. 2007. The transcription factor XBP-1 is essential for the development and survival of dendritic cells. *J Exp Med,* 204**,** 2267-75.

Iyer, S. S., Gensollen, T., Gandhi, A., Oh, S. F., Neves, J. F., Collin, F., Lavin, R., Serra, C., Glickman, J., De Silva, P. S. A., Sartor, R. B., Besra, G., Hauser, R., Maxwell, A., Llebaria, A. & Blumberg, R. S. 2018. Dietary and Microbial Oxazoles Induce Intestinal Inflammation by Modulating Aryl Hydrocarbon Receptor Responses. *Cell,* 173**,** 1123-1134 e11.

Jackman, R. M., Stenger, S., Lee, A., Moody, D. B., Rogers, R. A., Niazi, K. R., Sugita, M., Modlin, R. L., Peters, P. J. & Porcelli, S. A. 1998. The tyrosine-containing cytoplasmic tail of CD1b is essential for its efficient presentation of bacterial lipid antigens. *Immunity,* 8**,** 341-51.

Jarrett, R., Salio, M., Lloyd-Lavery, A., Subramaniam, S., Bourgeois, E., Archer, C., Cheung, K. L., Hardman, C., Chandler, D., Salimi, M., Gutowska-Owsiak, D., De La Serna, J. B., Fallon, P. G., Jolin, H., Mckenzie, A., Dziembowski, A., Podobas, E. I., Bal, W., Johnson, D., Moody, D. B., Cerundolo, V. & Ogg, G. 2016. Filaggrin inhibits generation of CD1a

neolipid antigens by house dust mite-derived phospholipase. *Sci Transl Med,* 8**,** 325ra18.

Jayawardena-Wolf, J. & Bendelac, A. 2001. CD1 and lipid antigens: intracellular pathways for antigen presentation. *Curr Opin Immunol,* 13**,** 109-13.

Jayawardena-Wolf, J., Benlagha, K., Chiu, Y. H., Mehr, R. & Bendelac, A. 2001. CD1d endosomal trafficking is independently regulated by an intrinsic CD1d-encoded tyrosine motif and by the invariant chain. *Immunity,* 15**,** 897-908.

Jenkins, M. R., Tsun, A., Stinchcombe, J. C. & Griffiths, G. M. 2009. The strength of T cell receptor signal controls the polarization of cytotoxic machinery to the immunological synapse. *Immunity,* 31**,** 621-31.

Jo, H., Choe, S. S., Shin, K. C., Jang, H., Lee, J. H., Seong, J. K., Back, S. H. & Kim, J. B. 2013. Endoplasmic reticulum stress induces hepatic steatosis via increased expression of the hepatic very low-density lipoprotein receptor. *Hepatology,* 57**,** 1366-77.

Johnson, T. R., Hong, S., Van Kaer, L., Koezuka, Y. & Graham, B. S. 2002. NK T cells contribute to expansion of CD8(+) T cells and amplification of antiviral immune responses to respiratory syncytial virus. *J Virol,* 76**,** 4294-303.

Jones, E. Y., Salio, M. & Cerundolo, V. 2007. T cell receptors get back to basics. *Nat Immunol,* 8**,** 1033-5.

Jouan-Lanhouet, S., Arshad, M. I., Piquet-Pellorce, C., Martin-Chouly, C., Le Moigne-Muller, G., Van Herreweghe, F., Takahashi, N., Sergent, O., Lagadic-Gossmann, D., Vandenabeele, P., Samson, M. & Dimanche-Boitrel, M. T. 2012. TRAIL induces necroptosis involving RIPK1/RIPK3-dependent PARP-1 activation. *Cell Death Differ,* 19**,** 2003-14.

Jukes, J. P., Gileadi, U., Ghadbane, H., Yu, T. F., Shepherd, D., Cox, L. R., Besra, G. S. & Cerundolo, V. 2016. Non-glycosidic compounds can stimulate both human and mouse iNKT cells. *Eur J Immunol,* 46**,** 1224-34.

Julier, C. & Nicolino, M. 2010. Wolcott-Rallison syndrome. *Orphanet J Rare Dis,* 5**,** 29.

Kain, L., Webb, B., Anderson, B. L., Deng, S., Holt, M., Costanzo, A., Zhao, M., Self, K., Teyton, A., Everett, C., Kronenberg, M., Zajonc, D. M., Bendelac, A., Savage, P. B. & Teyton, L. 2014. The identification of the endogenous ligands of natural killer T cells reveals the presence of mammalian alpha-linked glycosylceramides. *Immunity,* 41**,** 543-54.

Kammertoens, T., Qin, Z., Briesemeister, D., Bendelac, A. & Blankenstein, T. 2012. B-cells and IL-4 promote methylcholanthrene-induced carcinogenesis but there is no evidence for a role of T/NKT-cells and their effector molecules (Fas-ligand, TNF-alpha, perforin). *Int J Cancer,* 131**,** 1499-508.

Kaser, A., Lee, A. H., Franke, A., Glickman, J. N., Zeissig, S., Tilg, H., Nieuwenhuis, E. E., Higgins, D. E., Schreiber, S., Glimcher, L. H. & Blumberg, R. S. 2008. XBP1 links ER stress to intestinal inflammation and confers genetic risk for human inflammatory bowel disease. *Cell,* 134**,** 743-56.

Kasinrerk, W., Baumruker, T., Majdic, O., Knapp, W. & Stockinger, H. 1993. CD1 molecule expression on human monocytes induced by granulocyte-macrophage colony-stimulating factor. *J Immunol,* 150**,** 579-84.

Kawakami, K., Yamamoto, N., Kinjo, Y., Miyagi, K., Nakasone, C., Uezu, K., Kinjo, T., Nakayama, T., Taniguchi, M. & Saito, A. 2003. Critical role of Valpha14+ natural killer T cells in the innate phase of host protection against Streptococcus pneumoniae infection. *Eur J Immunol,* 33**,** 3322-30.

Kee, S. J., Kwon, Y. S., Park, Y. W., Cho, Y. N., Lee, S. J., Kim, T. J., Lee, S. S., Jang, H. C., Shin, M. G., Shin, J. H., Suh, S. P. & Ryang, D. W. 2012. Dysfunction of natural killer T cells in patients with active Mycobacterium tuberculosis infection. *Infect Immun,* 80**,** 2100-8.

Kemp, K. & Poe, C. 2019. Stressed: The Unfolded Protein Response in T Cell Development, Activation, and Function. *Int J Mol Sci,* 20.

Kim, J. H., Hu, Y., Yongqing, T., Kim, J., Hughes, V. A., Le Nours, J., Marquez, E. A., Purcell, A. W., Wan, Q., Sugita, M., Rossjohn, J. & Winau, F. 2016. CD1a on Langerhans cells controls inflammatory skin disease. *Nat Immunol,* 17**,** 1159-66.

Kim, S., Joe, Y., Jeong, S. O., Zheng, M., Back, S. H., Park, S. W., Ryter, S. W. & Chung, H. T. 2014. Endoplasmic reticulum stress is sufficient for the

induction of IL-1beta production via activation of the NF-kappaB and inflammasome pathways. *Innate Immun,* 20**,** 799-815.

King, I. L., Fortier, A., Tighe, M., Dibble, J., Watts, G. F., Veerapen, N., Haberman, A. M., Besra, G. S., Mohrs, M., Brenner, M. B. & Leadbetter, E. A. 2011. Invariant natural killer T cells direct B cell responses to cognate lipid antigen in an IL-21-dependent manner. *Nat Immunol,* 13**,** 44-50.

Kinjo, Y., Illarionov, P., Vela, J. L., Pei, B., Girardi, E., Li, X., Li, Y., Imamura, M., Kaneko, Y., Okawara, A., Miyazaki, Y., Gomez-Velasco, A., Rogers, P., Dahesh, S., Uchiyama, S., Khurana, A., Kawahara, K., Yesilkaya, H., Andrew, P. W., Wong, C. H., Kawakami, K., Nizet, V., Besra, G. S., Tsuji, M., Zajonc, D. M. & Kronenberg, M. 2011. Invariant natural killer T cells recognize glycolipids from pathogenic Gram-positive bacteria. *Nat Immunol,* 12**,** 966-74.

Kjer-Nielsen, L., Patel, O., Corbett, A. J., Le Nours, J., Meehan, B., Liu, L., Bhati, M., Chen, Z., Kostenko, L., Reantragoon, R., Williamson, N. A., Purcell, A. W., Dudek, N. L., Mcconville, M. J., O'hair, R. A., Khairallah, G. N., Godfrey, D. I., Fairlie, D. P., Rossjohn, J. & Mccluskey, J. 2012. MR1 presents microbial vitamin B metabolites to MAIT cells. *Nature,* 491**,** 717-23.

Koay, H. F., Gherardin, N. A., Enders, A., Loh, L., Mackay, L. K., Almeida, C. F., Russ, B. E., Nold-Petry, C. A., Nold, M. F., Bedoui, S., Chen, Z., Corbett, A. J., Eckle, S. B., Meehan, B., D'udekem, Y., Konstantinov, I. E., Lappas, M., Liu, L., Goodnow, C. C., Fairlie, D. P., Rossjohn, J., Chong, M. M., Kedzierska, K., Berzins, S. P., Belz, G. T., Mccluskey, J., Uldrich, A. P., Godfrey, D. I. & Pellicci, D. G. 2016. A three-stage intrathymic development pathway for the mucosal-associated invariant T cell lineage. *Nat Immunol,* 17**,** 1300-1311.

Koch, M., Stronge, V. S., Shepherd, D., Gadola, S. D., Mathew, B., Ritter, G., Fersht, A. R., Besra, G. S., Schmidt, R. R., Jones, E. Y. & Cerundolo, V. 2005. The crystal structure of human CD1d with and without alpha-galactosylceramide. *Nat Immunol,* 6**,** 819-26.

Koh, J. H., Wang, L., Beaudoin-Chabot, C. & Thibault, G. 2018. Lipid bilayer stress-activated IRE-1 modulates autophagy during endoplasmic reticulum stress. *J Cell Sci,* 131.

Kokame, K., Kato, H. & Miyata, T. 2001. Identification of ERSE-II, a new cis-acting element responsible for the ATF6-dependent mammalian unfolded protein response. *J Biol Chem,* 276**,** 9199-205.

Koldewey, P., Stull, F., Horowitz, S., Martin, R. & Bardwell, J. C. A. 2016. Forces Driving Chaperone Action. *Cell,* 166**,** 369-379.

Korennykh, A. V., Korostelev, A. A., Egea, P. F., Finer-Moore, J., Stroud, R. M., Zhang, C., Shokat, K. M. & Walter, P. 2011. Structural and functional basis for RNA cleavage by Ire1. *BMC Biol,* 9**,** 47.

Kovalovsky, D., Uche, O. U., Eladad, S., Hobbs, R. M., Yi, W., Alonzo, E., Chua, K., Eidson, M., Kim, H. J., Im, J. S., Pandolfi, P. P. & Sant'angelo, D. B. 2008. The BTB-zinc finger transcriptional regulator PLZF controls the development of invariant natural killer T cell effector functions. *Nat Immunol,* 9**,** 1055-64.

Kranz, P., Neumann, F., Wolf, A., Classen, F., Pompsch, M., Ocklenburg, T., Baumann, J., Janke, K., Baumann, M., Goepelt, K., Riffkin, H., Metzen, E. & Brockmeier, U. 2017. PDI is an essential redox-sensitive activator of PERK during the unfolded protein response (UPR). *Cell Death Dis,* 8**,** e2986.

Kroeger, H., Grimsey, N., Paxman, R., Chiang, W. C., Plate, L., Jones, Y., Shaw, P. X., Trejo, J., Tsang, S. H., Powers, E., Kelly, J. W., Wiseman, R. L. & Lin, J. H. 2018. The unfolded protein response regulator ATF6 promotes mesodermal differentiation. *Sci Signal,* 11.

Kumari, S., Curado, S., Mayya, V. & Dustin, M. L. 2014. T cell antigen receptor activation and actin cytoskeleton remodeling. *Biochim Biophys Acta,* 1838**,** 546-56.

Kurioka, A., Walker, L. J., Klenerman, P. & Willberg, C. B. 2016. MAIT cells: new guardians of the liver. *Clin Transl Immunology,* 5**,** e98.

Kuylenstierna, C., Bjorkstrom, N. K., Andersson, S. K., Sahlstrom, P., Bosnjak, L., Paquin-Proulx, D., Malmberg, K. J., Ljunggren, H. G., Moll, M. & Sandberg, J. K. 2011. NKG2D performs two functions in invariant NKT cells: direct TCR-independent activation of NK-like cytolysis and co-stimulation of activation by CD1d. *Eur J Immunol,* 41**,** 1913-23.

Lairson, L. L., Henrissat, B., Davies, G. J. & Withers, S. G. 2008. Glycosyltransferases: structures, functions, and mechanisms. *Annu Rev Biochem,* 77**,** 521-55.

Lang, G. A., Exley, M. A. & Lang, M. L. 2006. The CD1d-binding glycolipid alpha-galactosylceramide enhances humoral immunity to T-dependent and T-independent antigen in a CD1d-dependent manner. *Immunology,* 119**,** 116-25.

Le Nours, J., Shahine, A. & Gras, S. 2018. Molecular features of lipid-based antigen presentation by group 1 CD1 molecules. *Semin Cell Dev Biol,* 84**,** 48-57.

Lee, A. H., Iwakoshi, N. N., Anderson, K. C. & Glimcher, L. H. 2003. Proteasome inhibitors disrupt the unfolded protein response in myeloma cells. *Proc Natl Acad Sci U S A,* 100**,** 9946-51.

Lee, A. H., Scapa, E. F., Cohen, D. E. & Glimcher, L. H. 2008. Regulation of hepatic lipogenesis by the transcription factor XBP1. *Science,* 320**,** 1492-6.

Lee, K., Tirasophon, W., Shen, X., Michalak, M., Prywes, R., Okada, T., Yoshida, H., Mori, K. & Kaufman, R. J. 2002. IRE1-mediated unconventional mRNA splicing and S2P-mediated ATF6 cleavage merge to regulate XBP1 in signaling the unfolded protein response. *Genes Dev,* 16**,** 452-66.

Lemaire, P. A., Anderson, E., Lary, J. & Cole, J. L. 2008. Mechanism of PKR Activation by dsRNA. *J Mol Biol,* 381**,** 351-60.

Lepore, M., Kalinichenko, A., Colone, A., Paleja, B., Singhal, A., Tschumi, A., Lee, B., Poidinger, M., Zolezzi, F., Quagliata, L., Sander, P., Newell, E., Bertoletti, A., Terracciano, L., De Libero, G. & Mori, L. 2014. Parallel T-cell cloning and deep sequencing of human MAIT cells reveal stable oligoclonal TCRbeta repertoire. *Nat Commun,* 5**,** 3866.

Levy, O., Orange, J. S., Hibberd, P., Steinberg, S., Larussa, P., Weinberg, A., Wilson, S. B., Shaulov, A., Fleisher, G., Geha, R. S., Bonilla, F. A. & Exley, M. 2003. Disseminated varicella infection due to the vaccine strain of varicella-zoster virus, in a patient with a novel deficiency in natural killer T cells. *J Infect Dis,* 188**,** 948-53.

Li, Y., Girardi, E., Wang, J., Yu, E. D., Painter, G. F., Kronenberg, M. & Zajonc, D. M. 2010. The Valpha14 invariant natural killer T cell TCR forces microbial glycolipids and CD1d into a conserved binding mode. *J Exp Med,* 207**,** 2383-93.

Liepe, J., Marino, F., Sidney, J., Jeko, A., Bunting, D. E., Sette, A., Kloetzel, P. M., Stumpf, M. P., Heck, A. J. & Mishto, M. 2016. A large fraction of HLA class I ligands are proteasome-generated spliced peptides. *Science,* 354**,** 354-358.

Liew, P. X., Lee, W. Y. & Kubes, P. 2017. iNKT Cells Orchestrate a Switch from Inflammation to Resolution of Sterile Liver Injury. *Immunity,* 47**,** 752-765 e5.

Lind, S. M., Kuylenstierna, C., Moll, M., E, D. J., Winqvist, O., Lundeberg, L., Karlsson, M. A., M, T. L., Johansson, C., Scheynius, A., Sandberg, J. K. & Karlsson, M. C. 2009. IL-18 skews the invariant NKT-cell population via autoreactive activation in atopic eczema. *Eur J Immunol,* 39**,** 2293-301.

Liu, D., Song, L., Wei, J., Courtney, A. N., Gao, X., Marinova, E., Guo, L., Heczey, A., Asgharzadeh, S., Kim, E., Dotti, G. & Metelitsa, L. S. 2012. IL-15 protects NKT cells from inhibition by tumor-associated macrophages and enhances antimetastatic activity. *J Clin Invest,* 122**,** 2221-33.

Liu, Z., Lv, Y., Zhao, N., Guan, G. & Wang, J. 2015. Protein kinase R-like ER kinase and its role in endoplasmic reticulum stress-decided cell fate. *Cell Death Dis,* 6**,** e1822.

Lopez-Sagaseta, J., Sibener, L. V., Kung, J. E., Gumperz, J. & Adams, E. J. 2012. Lysophospholipid presentation by CD1d and recognition by a human Natural Killer T-cell receptor. *EMBO J,* 31**,** 2047-59.

Lu, P., Struijs, M. C., Mei, J., Witte-Bouma, J., Korteland-Van Male, A. M., De Bruijn, A. C., Van Goudoever, J. B. & Renes, I. B. 2013. Endoplasmic reticulum stress, unfolded protein response and altered T cell differentiation in necrotizing enterocolitis. *PLoS One,* 8**,** e78491.

Ly, D. & Moody, D. B. 2014. The CD1 size problem: lipid antigens, ligands, and scaffolds. *Cell Mol Life Sci,* 71**,** 3069-79.

Lynch, L., Hogan, A. E., Duquette, D., Lester, C., Banks, A., Leclair, K., Cohen, D. E., Ghosh, A., Lu, B., Corrigan, M., Stevanovic, D., Maratos-Flier, E.,

Drucker, D. J., O'shea, D. & Brenner, M. 2016. iNKT Cells Induce FGF21 for Thermogenesis and Are Required for Maximal Weight Loss in GLP1 Therapy. *Cell Metab,* 24**,** 510-519.

Lynch, L., Michelet, X., Zhang, S., Brennan, P. J., Moseman, A., Lester, C., Besra, G., Vomhof-Dekrey, E. E., Tighe, M., Koay, H. F., Godfrey, D. I., Leadbetter, E. A., Sant'angelo, D. B., Von Andrian, U. & Brenner, M. B. 2015. Regulatory iNKT cells lack expression of the transcription factor PLZF and control the homeostasis of T(reg) cells and macrophages in adipose tissue. *Nat Immunol,* 16**,** 85-95.

Lynch, L., Nowak, M., Varghese, B., Clark, J., Hogan, A. E., Toxavidis, V., Balk, S. P., O'shea, D., O'farrelly, C. & Exley, M. A. 2012. Adipose tissue invariant NKT cells protect against diet-induced obesity and metabolic disorder through regulatory cytokine production. *Immunity,* 37**,** 574-87.

Ma, Y., Shimizu, Y., Mann, M. J., Jin, Y. & Hendershot, L. M. 2010. Plasma cell differentiation initiates a limited ER stress response by specifically suppressing the PERK-dependent branch of the unfolded protein response. *Cell Stress Chaperones,* 15**,** 281-93.

Mahadevan, N. R., Fernandez, A., Rodvold, J. J., Almanza, G. & Zanetti, M. 2010. Prostate cancer cells undergoing ER stress in vitro and in vivo activate transcription of pro-inflammatory cytokines. *J Inflamm Res,* 3**,** 99-103.

Mahadevan, N. R., Rodvold, J., Sepulveda, H., Rossi, S., Drew, A. F. & Zanetti, M. 2011. Transmission of endoplasmic reticulum stress and pro-inflammation from tumor cells to myeloid cells. *Proc Natl Acad Sci U S A,* 108**,** 6561-6.

Mandic, A., Hansson, J., Linder, S. & Shoshan, M. C. 2003. Cisplatin induces endoplasmic reticulum stress and nucleus-independent apoptotic signaling. *J Biol Chem,* 278**,** 9100-6.

Mansour, S., Tocheva, A. S., Sanderson, J. P., Goulston, L. M., Platten, H., Serhal, L., Parsons, C., Edwards, M. H., Woelk, C. H., Elkington, P. T., Elliott, T., Cooper, C., Edwards, C. J. & Gadola, S. D. 2015. Structural and Functional Changes of the Invariant NKT Clonal Repertoire in Early Rheumatoid Arthritis. *J Immunol,* 195**,** 5582-91.

Mao, C. & Obeid, L. M. 2008. Ceramidases: regulators of cellular responses mediated by ceramide, sphingosine, and sphingosine-1-phosphate. *Biochim Biophys Acta,* 1781**,** 424-34.

Martino, M. B., Jones, L., Brighton, B., Ehre, C., Abdulah, L., Davis, C. W., Ron, D., O'neal, W. K. & Ribeiro, C. M. 2013. The ER stress transducer IRE1beta is required for airway epithelial mucin production. *Mucosal Immunol,* 6**,** 639-54.

Martinon, F., Chen, X., Lee, A. H. & Glimcher, L. H. 2010. TLR activation of the transcription factor XBP1 regulates innate immune responses in macrophages. *Nat Immunol,* 11**,** 411-8.

Matsuda, J. L., Gapin, L., Baron, J. L., Sidobre, S., Stetson, D. B., Mohrs, M., Locksley, R. M. & Kronenberg, M. 2003. Mouse V alpha 14i natural killer T cells are resistant to cytokine polarization in vivo. *Proc Natl Acad Sci U S A,* 100**,** 8395-400.

Mattner, J., Debord, K. L., Ismail, N., Goff, R. D., Cantu, C., 3rd, Zhou, D., Saint-Mezard, P., Wang, V., Gao, Y., Yin, N., Hoebe, K., Schneewind, O., Walker, D., Beutler, B., Teyton, L., Savage, P. B. & Bendelac, A. 2005. Exogenous and endogenous glycolipid antigens activate NKT cells during microbial infections. *Nature,* 434**,** 525-9.

Mattoo, R. U. & Goloubinoff, P. 2014. Molecular chaperones are nanomachines that catalytically unfold misfolded and alternatively folded proteins. *Cell Mol Life Sci,* 71**,** 3311-25.

Maurel, M., Chevet, E., Tavernier, J. & Gerlo, S. 2014. Getting RIDD of RNA: IRE1 in cell fate regulation. *Trends Biochem Sci,* 39**,** 245-54.

Mazor, K. M., Dong, L., Mao, Y., Swanda, R. V., Qian, S. B. & Stipanuk, M. H. 2018. Effects of single amino acid deficiency on mRNA translation are markedly different for methionine versus leucine. *Sci Rep,* 8**,** 8076.

Mccarthy, N. E., Jones, H. A., Marks, N. A., Shiner, R. J., Ind, P. W., Al-Hassi, H. O., English, N. R., Murray, C. M., Lambert, J. R., Knight, S. C. & Stagg, A. J. 2007. Inhaled allergen-driven CD1c up-regulation and enhanced antigen uptake by activated human respiratory-tract dendritic cells in atopic asthma. *Clin Exp Allergy,* 37**,** 72-82.

Mcknight, C. G., Morris, S. C., Perkins, C., Zhu, Z., Hildeman, D. A., Bendelac, A. & Finkelman, F. D. 2017. NKT cells contribute to basal IL-4 production but are not required to induce experimental asthma. *PLoS One,* 12**,** e0188221.

Medel, B., Costoya, C., Fernandez, D., Pereda, C., Lladser, A., Sauma, D., Pacheco, R., Iwawaki, T., Salazar-Onfray, F. & Osorio, F. 2018. IRE1alpha Activation in Bone Marrow-Derived Dendritic Cells Modulates Innate Recognition of Melanoma Cells and Favors CD8(+) T Cell Priming. *Front Immunol,* 9**,** 3050.

Melandri, D., Zlatareva, I., Chaleil, R. a. G., Dart, R. J., Chancellor, A., Nussbaumer, O., Polyakova, O., Roberts, N. A., Wesch, D., Kabelitz, D., Irving, P. M., John, S., Mansour, S., Bates, P. A., Vantourout, P. & Hayday, A. C. 2018. The gammadeltaTCR combines innate immunity with adaptive immunity by utilizing spatially distinct regions for agonist selection and antigen responsiveness. *Nat Immunol,* 19**,** 1352-1365.

Menu, P., Mayor, A., Zhou, R., Tardivel, A., Ichijo, H., Mori, K. & Tschopp, J. 2012. ER stress activates the NLRP3 inflammasome via an UPR-independent pathway. *Cell Death Dis,* 3**,** e261.

Michell, R. H., Jafferji, S. S. & Jones, L. M. 1977. The possible involvement of phosphatidylinositol breakdown in the mechanism of stimulus-response coupling at receptors which control cell-surface calcium gates. *Adv Exp Med Biol,* 83**,** 447-64.

Miura, S., Kawana, K., Schust, D. J., Fujii, T., Yokoyama, T., Iwasawa, Y., Nagamatsu, T., Adachi, K., Tomio, A., Tomio, K., Kojima, S., Yasugi, T., Kozuma, S. & Taketani, Y. 2010. CD1d, a sentinel molecule bridging innate and adaptive immunity, is downregulated by the human papillomavirus (HPV) E5 protein: a possible mechanism for immune evasion by HPV. *J Virol,* 84**,** 11614-23.

Miyamoto, K., Miyake, S. & Yamamura, T. 2001. A synthetic glycolipid prevents autoimmune encephalomyelitis by inducing TH2 bias of natural killer T cells. *Nature,* 413**,** 531-4.

Montoya, C. J., Jie, H. B., Al-Harthi, L., Mulder, C., Patino, P. J., Rugeles, M. T., Krieg, A. M., Landay, A. L. & Wilson, S. B. 2006. Activation of plasmacytoid dendritic cells with TLR9 agonists initiates invariant NKT cell-mediated cross-talk with myeloid dendritic cells. *J Immunol,* 177**,** 1028-39.

Montoya, C. J., Pollard, D., Martinson, J., Kumari, K., Wasserfall, C., Mulder, C. B., Rugeles, M. T., Atkinson, M. A., Landay, A. L. & Wilson, S. B. 2007. Characterization of human invariant natural killer T subsets in health and disease using a novel invariant natural killer T cell-clonotypic monoclonal antibody, 6B11. *Immunology,* 122**,** 1-14.

Moody, D. B., Reinhold, B. B., Guy, M. R., Beckman, E. M., Frederique, D. E., Furlong, S. T., Ye, S., Reinhold, V. N., Sieling, P. A., Modlin, R. L., Besra, G. S. & Porcelli, S. A. 1997. Structural requirements for glycolipid antigen recognition by CD1b-restricted T cells. *Science,* 278**,** 283-6.

Moore, K. & Hollien, J. 2015. Ire1-mediated decay in mammalian cells relies on mRNA sequence, structure, and translational status. *Mol Biol Cell,* 26**,** 2873-84.

Moreno, J. A., Halliday, M., Molloy, C., Radford, H., Verity, N., Axten, J. M., Ortori, C. A., Willis, A. E., Fischer, P. M., Barrett, D. A. & Mallucci, G. R. 2013. Oral treatment targeting the unfolded protein response prevents neurodegeneration and clinical disease in prion-infected mice. *Sci Transl Med,* 5**,** 206ra138.

Moreno, J. A., Radford, H., Peretti, D., Steinert, J. R., Verity, N., Martin, M. G., Halliday, M., Morgan, J., Dinsdale, D., Ortori, C. A., Barrett, D. A., Tsaytler, P., Bertolotti, A., Willis, A. E., Bushell, M. & Mallucci, G. R. 2012. Sustained translational repression by eIF2alpha-P mediates prion neurodegeneration. *Nature,* 485**,** 507-11.

Moreno, M., Molling, J. W., Von Mensdorff-Pouilly, S., Verheijen, R. H., Hooijberg, E., Kramer, D., Reurs, A. W., Van Den Eertwegh, A. J., Von Blomberg, B. M., Scheper, R. J. & Bontkes, H. J. 2008. IFN-gamma-producing human invariant NKT cells promote tumor-associated antigen-specific cytotoxic T cell responses. *J Immunol,* 181**,** 2446-54.

Morgan, A. J. & Jacob, R. 1994. Ionomycin enhances Ca2+ influx by stimulating store-regulated cation entry and not by a direct action at the plasma membrane. *Biochem J,* 300 (Pt 3)**,** 665-72.

Mori, K. 2009. Signalling pathways in the unfolded protein response: development from yeast to mammals. *J Biochem,* 146**,** 743-50.

Mortensen, M., Soilleux, E. J., Djordjevic, G., Tripp, R., Lutteropp, M., Sadighi-Akha, E., Stranks, A. J., Glanville, J., Knight, S., Jacobsen, S. E., Kranc, K. R. & Simon, A. K. 2011. The autophagy protein Atg7 is essential for hematopoietic stem cell maintenance. *J Exp Med,* 208**,** 455-67.

Motomura, Y., Kitamura, H., Hijikata, A., Matsunaga, Y., Matsumoto, K., Inoue, H., Atarashi, K., Hori, S., Watarai, H., Zhu, J., Taniguchi, M. & Kubo, M. 2011. The transcription factor E4BP4 regulates the production of IL-10 and IL-13 in CD4+ T cells. *Nat Immunol,* 12**,** 450-9.

Mougeolle, A., Poussard, S., Decossas, M., Lamaze, C., Lambert, O. & Dargelos, E. 2015. Oxidative stress induces caveolin 1 degradation and impairs caveolae functions in skeletal muscle cells. *PLoS One,* 10**,** e0122654.

Murphy, K. & Weaver, C. 2016. *Janeway's immunobiology,* New York, NY, Garland Science/Taylor & Francis Group, LLC.

Nakamura, D., Tsuru, A., Ikegami, K., Imagawa, Y., Fujimoto, N. & Kohno, K. 2011. Mammalian ER stress sensor IRE1beta specifically down-regulates the synthesis of secretory pathway proteins. *FEBS Lett,* 585**,** 133-8.

Nedellec, S., Sabourin, C., Bonneville, M. & Scotet, E. 2010. NKG2D costimulates human V gamma 9V delta 2 T cell antitumor cytotoxicity through protein kinase C theta-dependent modulation of early TCR-induced calcium and transduction signals. *J Immunol,* 185**,** 55-63.

Nguyen, G. T., Green, E. R. & Mecsas, J. 2017. Neutrophils to the ROScue: Mechanisms of NADPH Oxidase Activation and Bacterial Resistance. *Front Cell Infect Microbiol,* 7**,** 373.

Nie, H., Yang, Q., Zhang, G., Wang, A., He, Q., Liu, M., Li, P., Yang, J., Huang, Y., Ding, X., Yu, H. & Hu, S. 2015. Invariant NKT cells act as an adjuvant to enhance Th2 inflammatory response in an OVA-induced mouse model of asthma. *PLoS One,* 10**,** e0119901.

Nieda, M., Nicol, A., Koezuka, Y., Kikuchi, A., Lapteva, N., Tanaka, Y., Tokunaga, K., Suzuki, K., Kayagaki, N., Yagita, H., Hirai, H. & Juji, T. 2001. TRAIL expression by activated human CD4(+)V alpha 24NKT cells induces in vitro and in vivo apoptosis of human acute myeloid leukemia cells. *Blood,* 97**,** 2067-74.

Niederreiter, L., Fritz, T. M., Adolph, T. E., Krismer, A. M., Offner, F. A., Tschurtschenthaler, M., Flak, M. B., Hosomi, S., Tomczak, M. F., Kaneider, N. C., Sarcevic, E., Kempster, S. L., Raine, T., Esser, D., Rosenstiel, P., Kohno, K., Iwawaki, T., Tilg, H., Blumberg, R. S. & Kaser, A. 2013. ER stress transcription factor Xbp1 suppresses intestinal tumorigenesis and directs intestinal stem cells. *J Exp Med,* 210**,** 2041-56.

Nieuwenhuis, E. E., Matsumoto, T., Exley, M., Schleipman, R. A., Glickman, J., Bailey, D. T., Corazza, N., Colgan, S. P., Onderdonk, A. B. & Blumberg, R. S. 2002. CD1d-dependent macrophage-mediated clearance of Pseudomonas aeruginosa from lung. *Nat Med,* 8**,** 588-93.

Nieuwenhuis, E. E., Matsumoto, T., Lindenbergh, D., Willemsen, R., Kaser, A., Simons-Oosterhuis, Y., Brugman, S., Yamaguchi, K., Ishikawa, H., Aiba, Y., Koga, Y., Samsom, J. N., Oshima, K., Kikuchi, M., Escher, J. C., Hattori, M., Onderdonk, A. B. & Blumberg, R. S. 2009. Cd1d-dependent regulation of bacterial colonization in the intestine of mice. *J Clin Invest,* 119**,** 1241-50.

Nijholt, D. A., Nolle, A., Van Haastert, E. S., Edelijn, H., Toonen, R. F., Hoozemans, J. J. & Scheper, W. 2013. Unfolded protein response activates glycogen synthase kinase-3 via selective lysosomal degradation. *Neurobiol Aging,* 34**,** 1759-71.

Ntimbane, T., Comte, B., Mailhot, G., Berthiaume, Y., Poitout, V., Prentki, M., Rabasa-Lhoret, R. & Levy, E. 2009. Cystic fibrosis-related diabetes: from CFTR dysfunction to oxidative stress. *Clin Biochem Rev,* 30**,** 153-77.

Obeng, E. A., Carlson, L. M., Gutman, D. M., Harrington, W. J., Jr., Lee, K. P. & Boise, L. H. 2006. Proteasome inhibitors induce a terminal unfolded protein response in multiple myeloma cells. *Blood,* 107**,** 4907-16.

Oh, S. J., Ahn, S., Jin, Y. H., Ishifune, C., Kim, J. H., Yasutomo, K. & Chung, D. H. 2015. Notch 1 and Notch 2 synergistically regulate the differentiation and function of invariant NKT cells. *J Leukoc Biol,* 98**,** 781-9.

Okada, T., Yoshida, H., Akazawa, R., Negishi, M. & Mori, K. 2002. Distinct roles of activating transcription factor 6 (ATF6) and double-stranded RNA-activated protein kinase-like endoplasmic reticulum kinase (PERK) in transcription during the mammalian unfolded protein response. *Biochem J,* 366**,** 585-94.

Olszak, T., Neves, J. F., Dowds, C. M., Baker, K., Glickman, J., Davidson, N. O., Lin, C. S., Jobin, C., Brand, S., Sotlar, K., Wada, K., Katayama, K., Nakajima, A., Mizuguchi, H., Kawasaki, K., Nagata, K., Muller, W., Snapper, S. B., Schreiber, S., Kaser, A., Zeissig, S. & Blumberg, R. S. 2014. Protective mucosal immunity mediated by epithelial CD1d and IL-10. *Nature,* 509**,** 497-502.

Osorio, F., Tavernier, S. J., Hoffmann, E., Saeys, Y., Martens, L., Vetters, J., Delrue, I., De Rycke, R., Parthoens, E., Pouliot, P., Iwawaki, T., Janssens, S. & Lambrecht, B. N. 2014. The unfolded-protein-response sensor IRE-1alpha regulates the function of CD8alpha+ dendritic cells. *Nat Immunol,* 15**,** 248-57.

Oyadomari, S., Harding, H. P., Zhang, Y., Oyadomari, M. & Ron, D. 2008. Dephosphorylation of translation initiation factor 2alpha enhances glucose tolerance and attenuates hepatosteatosis in mice. *Cell Metab,* 7**,** 520-32.

Paget, C., Mallevaey, T., Speak, A. O., Torres, D., Fontaine, J., Sheehan, K. C., Capron, M., Ryffel, B., Faveeuw, C., Leite De Moraes, M., Platt, F. & Trottein, F. 2007. Activation of invariant NKT cells by toll-like receptor 9-stimulated dendritic cells requires type I interferon and charged glycosphingolipids. *Immunity,* 27**,** 597-609.

Papandreou, I., Denko, N. C., Olson, M., Van Melckebeke, H., Lust, S., Tam, A., Solow-Cordero, D. E., Bouley, D. M., Offner, F., Niwa, M. & Koong, A. C. 2011. Identification of an Ire1alpha endonuclease specific inhibitor with cytotoxic activity against human multiple myeloma. *Blood,* 117**,** 1311-4.

Parekh, V. V., Lalani, S., Kim, S., Halder, R., Azuma, M., Yagita, H., Kumar, V., Wu, L. & Kaer, L. V. 2009. PD-1/PD-L blockade prevents anergy induction and enhances the anti-tumor activities of glycolipid-activated invariant NKT cells. *J Immunol,* 182**,** 2816-26.

Parekh, V. V., Wilson, M. T., Olivares-Villagomez, D., Singh, A. K., Wu, L., Wang, C. R., Joyce, S. & Van Kaer, L. 2005. Glycolipid antigen induces long-term natural killer T cell anergy in mice. *J Clin Invest,* 115**,** 2572-83.

Park, J. E., Wu, D. Y., Prendes, M., Lu, S. X., Ragupathi, G., Schrantz, N. & Chapman, P. B. 2008. Fine specificity of natural killer T cells against GD3 ganglioside and identification of GM3 as an inhibitory natural killer T-cell ligand. *Immunology,* 123**,** 145-55.

Park, S. H., Kyin, T., Bendelac, A. & Carnaud, C. 2003. The contribution of NKT cells, NK cells, and other gamma-chain-dependent non-T non-B cells to IL-12-mediated rejection of tumors. *J Immunol,* 170**,** 1197-201.

Paton, A. W., Beddoe, T., Thorpe, C. M., Whisstock, J. C., Wilce, M. C., Rossjohn, J., Talbot, U. M. & Paton, J. C. 2006. AB5 subtilase cytotoxin inactivates the endoplasmic reticulum chaperone BiP. *Nature,* 443**,** 548-52.

Paulick, M. G. & Bertozzi, C. R. 2008. The glycosylphosphatidylinositol anchor: a complex membrane-anchoring structure for proteins. *Biochemistry,* 47**,** 6991-7000.

Pei, B., Zhao, M., Miller, B. C., Vela, J. L., Bruinsma, M. W., Virgin, H. W. & Kronenberg, M. 2015. Invariant NKT cells require autophagy to coordinate proliferation and survival signals during differentiation. *J Immunol,* 194**,** 5872-84.

Pereira, E. R., Frudd, K., Awad, W. & Hendershot, L. M. 2014. Endoplasmic reticulum (ER) stress and hypoxia response pathways interact to potentiate hypoxia-inducible factor 1 (HIF-1) transcriptional activity on targets like vascular endothelial growth factor (VEGF). *J Biol Chem,* 289**,** 3352-64.

Pobezinsky, L. A., Etzensperger, R., Jeurling, S., Alag, A., Kadakia, T., Mccaughtry, T. M., Kimura, M. Y., Sharrow, S. O., Guinter, T. I., Feigenbaum, L. & Singer, A. 2015. Let-7 microRNAs target the lineage-specific transcription factor PLZF to regulate terminal NKT cell differentiation and effector function. *Nat Immunol,* 16**,** 517-24.

Porcelli, S., Yockey, C. E., Brenner, M. B. & Balk, S. P. 1993. Analysis of T cell antigen receptor (TCR) expression by human peripheral blood CD4-8- alpha/beta T cells demonstrates preferential use of several V beta genes and an invariant TCR alpha chain. *J Exp Med,* 178**,** 1-16.

Porcelli, S. A. 1995. The CD1 family: a third lineage of antigen-presenting molecules. *Adv Immunol,* 59**,** 1-98.

Porubsky, S., Speak, A. O., Luckow, B., Cerundolo, V., Platt, F. M. & Grone, H. J. 2007. Normal development and function of invariant natural killer T cells in mice with isoglobotrihexosylceramide (iGb3) deficiency. *Proc Natl Acad Sci U S A,* 104**,** 5977-82.

Porubsky, S., Speak, A. O., Salio, M., Jennemann, R., Bonrouhi, M., Zafarulla, R., Singh, Y., Dyson, J., Luckow, B., Lehuen, A., Malle, E., Muthing, J., Platt, F. M., Cerundolo, V. & Grone, H. J. 2012. Globosides but not isoglobosides can impact the development of invariant NKT cells and their interaction with dendritic cells. *J Immunol,* 189**,** 3007-17.

Prigozy, T. I., Naidenko, O., Qasba, P., Elewaut, D., Brossay, L., Khurana, A., Natori, T., Koezuka, Y., Kulkarni, A. & Kronenberg, M. 2001. Glycolipid antigen processing for presentation by CD1d molecules. *Science,* 291**,** 664-7.

Radford, H., Moreno, J. A., Verity, N., Halliday, M. & Mallucci, G. R. 2015. PERK inhibition prevents tau-mediated neurodegeneration in a mouse model of frontotemporal dementia. *Acta Neuropathol,* 130**,** 633-42.

Rahimpour, A., Koay, H. F., Enders, A., Clanchy, R., Eckle, S. B., Meehan, B., Chen, Z., Whittle, B., Liu, L., Fairlie, D. P., Goodnow, C. C., Mccluskey, J., Rossjohn, J., Uldrich, A. P., Pellicci, D. G. & Godfrey, D. I. 2015. Identification of phenotypically and functionally heterogeneous mouse mucosal-associated invariant T cells using MR1 tetramers. *J Exp Med,* 212**,** 1095-108.

Ranson, T., Vosshenrich, C. A., Corcuff, E., Richard, O., Laloux, V., Lehuen, A. & Di Santo, J. P. 2003. IL-15 availability conditions homeostasis of peripheral natural killer T cells. *Proc Natl Acad Sci U S A,* 100**,** 2663-8.

Ratner, D. & Mueller, C. 2012. Immune responses in cystic fibrosis: are they intrinsically defective? *Am J Respir Cell Mol Biol,* 46**,** 715-22.

Raulet, D. H. 2003. Roles of the NKG2D immunoreceptor and its ligands. *Nat Rev Immunol,* 3**,** 781-90.

Reantragoon, R., Corbett, A. J., Sakala, I. G., Gherardin, N. A., Furness, J. B., Chen, Z., Eckle, S. B., Uldrich, A. P., Birkinshaw, R. W., Patel, O., Kostenko, L., Meehan, B., Kedzierska, K., Liu, L., Fairlie, D. P., Hansen, T. H., Godfrey, D. I., Rossjohn, J., Mccluskey, J. & Kjer-Nielsen, L. 2013. Antigen-loaded MR1 tetramers define T cell receptor heterogeneity in mucosal-associated invariant T cells. *J Exp Med,* 210**,** 2305-20.

Reichmann, D., Voth, W. & Jakob, U. 2018. Maintaining a Healthy Proteome during Oxidative Stress. *Mol Cell,* 69**,** 203-213.

Reiling, J. H., Clish, C. B., Carette, J. E., Varadarajan, M., Brummelkamp, T. R. & Sabatini, D. M. 2011. A haploid genetic screen identifies the major facilitator domain containing 2A (MFSD2A) transporter as a key mediator in the response to tunicamycin. *Proc Natl Acad Sci U S A,* 108**,** 11756-65.

Richter, J., Neparidze, N., Zhang, L., Nair, S., Monesmith, T., Sundaram, R., Miesowicz, F., Dhodapkar, K. M. & Dhodapkar, M. V. 2013. Clinical regressions and broad immune activation following combination therapy targeting human NKT cells in myeloma. Blood, 121, 423-30.

Rodvold, J. J., Chiu, K. T., Hiramatsu, N., Nussbacher, J. K., Galimberti, V., Mahadevan, N. R., Willert, K., Lin, J. H. & Zanetti, M. 2017. Intercellular transmission of the unfolded protein response promotes survival and drug resistance in cancer cells. *Sci Signal,* 10.

Rodvold, J. J., Mahadevan, N. R. & Zanetti, M. 2016. Immune modulation by ER stress and inflammation in the tumor microenvironment. *Cancer Lett,* 380**,** 227-36.

Rogers, S. L. & Kaufman, J. 2016. Location, location, location: the evolutionary history of CD1 genes and the NKR-P1/ligand systems. *Immunogenetics,* 68**,** 499-513.

Rojas-Rivera, D., Delvaeye, T., Roelandt, R., Nerinckx, W., Augustyns, K., Vandenabeele, P. & Bertrand, M. J. M. 2017. When PERK inhibitors turn out to be new potent RIPK1 inhibitors: critical issues on the specificity and use of GSK2606414 and GSK2656157. *Cell Death Differ,* 24**,** 1100-1110.

Rossjohn, J., Gras, S., Miles, J. J., Turner, S. J., Godfrey, D. I. & Mccluskey, J. 2015. T cell antigen receptor recognition of antigen-presenting molecules. *Annu Rev Immunol,* 33**,** 169-200.

Rubio, C., Pincus, D., Korennykh, A., Schuck, S., El-Samad, H. & Walter, P. 2011. Homeostatic adaptation to endoplasmic reticulum stress depends on Ire1 kinase activity. *J Cell Biol,* 193**,** 171-84.

Sachet, M., Tardieu, M., Durand, P., Ozanne, A., Soubrier, F., Tissieres, P., Chevret, L., Husson, B., Adamsbaum, C., Bellesme, C., Senat, M. V., Ducreux, D., Saliou, G. & Centre De Reference Des Maladies Neurovasculaires Malformatives De, L. E. 2013. [Medical care of brain

malformative vascular diseases discovered during the pre- or neonatal period]. *Arch Pediatr,* 20**,** 74-81.

Saez De Guinoa, J., Jimeno, R., Gaya, M., Kipling, D., Garzon, M. J., Dunn-Walters, D., Ubeda, C. & Barral, P. 2018. CD1d-mediated lipid presentation by CD11c(+) cells regulates intestinal homeostasis. *EMBO J,* 37.

Sagiv, Y., Bai, L., Wei, D. G., Agami, R., Savage, P. B., Teyton, L. & Bendelac, A. 2007. A distal effect of microsomal triglyceride transfer protein deficiency on the lysosomal recycling of CD1d. *J Exp Med,* 204**,** 921-8.

Salio, M., Gasser, O., Gonzalez-Lopez, C., Martens, A., Veerapen, N., Gileadi, U., Verter, J. G., Napolitani, G., Anderson, R., Painter, G., Besra, G. S., Hermans, I. F. & Cerundolo, V. 2017. Activation of Human Mucosal-Associated Invariant T Cells Induces CD40L-Dependent Maturation of Monocyte-Derived and Primary Dendritic Cells. *J Immunol,* 199**,** 2631-2638.

Salio, M., Ghadbane, H., Dushek, O., Shepherd, D., Cypen, J., Gileadi, U., Aichinger, M. C., Napolitani, G., Qi, X., Van Der Merwe, P. A., Wojno, J., Veerapen, N., Cox, L. R., Besra, G. S., Yuan, W., Cresswell, P. & Cerundolo, V. 2013. Saposins modulate human invariant Natural Killer T cells self-reactivity and facilitate lipid exchange with CD1d molecules during antigen presentation. *Proc Natl Acad Sci U S A,* 110**,** E4753-61.

Salio, M., Puleston, D. J., Mathan, T. S., Shepherd, D., Stranks, A. J., Adamopoulou, E., Veerapen, N., Besra, G. S., Hollander, G. A., Simon, A. K. & Cerundolo, V. 2014. Essential role for autophagy during invariant NKT cell development. *Proc Natl Acad Sci U S A,* 111**,** E5678-87.

Salio, M., Speak, A. O., Shepherd, D., Polzella, P., Illarionov, P. A., Veerapen, N., Besra, G. S., Platt, F. M. & Cerundolo, V. 2007. Modulation of human natural killer T cell ligands on TLR-mediated antigen-presenting cell activation. *Proc Natl Acad Sci U S A,* 104**,** 20490-5.

Salou, M., Legoux, F., Gilet, J., Darbois, A., Du Halgouet, A., Alonso, R., Richer, W., Goubet, A. G., Daviaud, C., Menger, L., Procopio, E., Premel, V. & Lantz, O. 2019. A common transcriptomic program acquired in the thymus defines tissue residency of MAIT and NKT subsets. *J Exp Med,* 216**,** 133-151.

Savage, A. K., Constantinides, M. G., Han, J., Picard, D., Martin, E., Li, B., Lantz, O. & Bendelac, A. 2008. The transcription factor PLZF directs the effector program of the NKT cell lineage. *Immunity,* 29**,** 391-403.

Scharf, L., Li, N. S., Hawk, A. J., Garzon, D., Zhang, T., Fox, L. M., Kazen, A. R., Shah, S., Haddadian, E. J., Gumperz, J. E., Saghatelian, A., Faraldo-Gomez, J. D., Meredith, S. C., Piccirilli, J. A. & Adams, E. J. 2010. The 2.5 A structure of CD1c in complex with a mycobacterial lipid reveals an open groove ideally suited for diverse antigen presentation. *Immunity,* 33**,** 853-62.

Scheper, W. & Hoozemans, J. J. 2015. The unfolded protein response in neurodegenerative diseases: a neuropathological perspective. *Acta Neuropathol,* 130**,** 315-31.

Schipper, H. S., Rakhshandehroo, M., Van De Graaf, S. F., Venken, K., Koppen, A., Stienstra, R., Prop, S., Meerding, J., Hamers, N., Besra, G., Boon, L., Nieuwenhuis, E. E., Elewaut, D., Prakken, B., Kersten, S., Boes, M. & Kalkhoven, E. 2012. Natural killer T cells in adipose tissue prevent insulin resistance. *J Clin Invest,* 122**,** 3343-54.

Schuhmann, K., Almeida, R., Baumert, M., Herzog, R., Bornstein, S. R. & Shevchenko, A. 2012. Shotgun lipidomics on a LTQ Orbitrap mass spectrometer by successive switching between acquisition polarity modes. *J Mass Spectrom,* 47**,** 96-104.

Schuhmann, K., Thomas, H., Ackerman, J. M., Nagornov, K. O., Tsybin, Y. O. & Shevchenko, A. 2017. Intensity-Independent Noise Filtering in FT MS and FT MS/MS Spectra for Shotgun Lipidomics. *Anal Chem,* 89**,** 7046-7052.

Schumacher, T. N. & Schreiber, R. D. 2015. Neoantigens in cancer immunotherapy. *Science,* 348**,** 69-74.

Seiler, M. P., Mathew, R., Liszewski, M. K., Spooner, C. J., Barr, K., Meng, F., Singh, H. & Bendelac, A. 2012. Elevated and sustained expression of the transcription factors Egr1 and Egr2 controls NKT lineage differentiation in response to TCR signaling. *Nat Immunol,* 13**,** 264-71.

Shaffer, A. L., Shapiro-Shelef, M., Iwakoshi, N. N., Lee, A. H., Qian, S. B., Zhao, H., Yu, X., Yang, L., Tan, B. K., Rosenwald, A., Hurt, E. M., Petroulakis, E., Sonenberg, N., Yewdell, J. W., Calame, K., Glimcher, L. H. & Staudt, L. M.

2004. XBP1, downstream of Blimp-1, expands the secretory apparatus and other organelles, and increases protein synthesis in plasma cell differentiation. *Immunity,* 21**,** 81-93.

Shah, H. B., Joshi, S. K., Rampuria, P., Devera, T. S., Lang, G. A., Stohl, W. & Lang, M. L. 2013. BAFF- and APRIL-dependent maintenance of antibody titers after immunization with T-dependent antigen and CD1d-binding ligand. *J Immunol,* 191**,** 1154-63.

Sharif, S., Arreaza, G. A., Zucker, P., Mi, Q. S., Sondhi, J., Naidenko, O. V., Kronenberg, M., Koezuka, Y., Delovitch, T. L., Gombert, J. M., Leite-De-Moraes, M., Gouarin, C., Zhu, R., Hameg, A., Nakayama, T., Taniguchi, M., Lepault, F., Lehuen, A., Bach, J. F. & Herbelin, A. 2001. Activation of natural killer T cells by alpha-galactosylceramide treatment prevents the onset and recurrence of autoimmune Type 1 diabetes. *Nat Med,* 7**,** 1057-62.

Shenderov, K., Riteau, N., Yip, R., Mayer-Barber, K. D., Oland, S., Hieny, S., Fitzgerald, P., Oberst, A., Dillon, C. P., Green, D. R., Cerundolo, V. & Sher, A. 2014. Cutting edge: Endoplasmic reticulum stress licenses macrophages to produce mature IL-1beta in response to TLR4 stimulation through a caspase-8- and TRIF-dependent pathway. *J Immunol,* 192**,** 2029-2033.

Shpilka, T. & Haynes, C. M. 2018. The mitochondrial UPR: mechanisms, physiological functions and implications in ageing. *Nat Rev Mol Cell Biol,* 19**,** 109-120.

Sidobre, S., Hammond, K. J., Benazet-Sidobre, L., Maltsev, S. D., Richardson, S. K., Ndonye, R. M., Howell, A. R., Sakai, T., Besra, G. S., Porcelli, S. A. & Kronenberg, M. 2004. The T cell antigen receptor expressed by Valpha14i NKT cells has a unique mode of glycosphingolipid antigen recognition. *Proc Natl Acad Sci U S A,* 101**,** 12254-9.

Sidrauski, C., Acosta-Alvear, D., Khoutorsky, A., Vedantham, P., Hearn, B. R., Li, H., Gamache, K., Gallagher, C. M., Ang, K. K., Wilson, C., Okreglak, V., Ashkenazi, A., Hann, B., Nader, K., Arkin, M. R., Renslo, A. R., Sonenberg, N. & Walter, P. 2013. Pharmacological brake-release of mRNA translation enhances cognitive memory. *Elife,* 2**,** e00498.

Siegmann, N., Worbs, D., Effinger, F., Bormann, T., Gebhardt, M., Ulrich, M., Wermeling, F., Muller-Hermelink, E., Biedermann, T., Tighe, M., Edwards,

M. J., Caldwell, C., Leadbetter, E., Karlsson, M. C., Becker, K. A., Gulbins, E. & Doring, G. 2014. Invariant natural killer T (iNKT) cells prevent autoimmunity, but induce pulmonary inflammation in cystic fibrosis. *Cell Physiol Biochem,* 34**,** 56-70.

Silk, J. D., Hermans, I. F., Gileadi, U., Chong, T. W., Shepherd, D., Salio, M., Mathew, B., Schmidt, R. R., Lunt, S. J., Williams, K. J., Stratford, I. J., Harris, A. L. & Cerundolo, V. 2004. Utilizing the adjuvant properties of CD1d-dependent NK T cells in T cell-mediated immunotherapy. *J Clin Invest,* 114**,** 1800-11.

Silk, J. D., Salio, M., Reddy, B. G., Shepherd, D., Gileadi, U., Brown, J., Masri, S. H., Polzella, P., Ritter, G., Besra, G. S., Jones, E. Y., Schmidt, R. R. & Cerundolo, V. 2008. Cutting edge: nonglycosidic CD1d lipid ligands activate human and murine invariant NKT cells. *J Immunol,* 180**,** 6452-6.

Singh, A. K., Wilson, M. T., Hong, S., Olivares-Villagomez, D., Du, C., Stanic, A. K., Joyce, S., Sriram, S., Koezuka, Y. & Van Kaer, L. 2001. Natural killer T cell activation protects mice against experimental autoimmune encephalomyelitis. *J Exp Med,* 194**,** 1801-11.

Singh, R. D., Puri, V., Valiyaveettil, J. T., Marks, D. L., Bittman, R. & Pagano, R. E. 2003. Selective caveolin-1-dependent endocytosis of glycosphingolipids. *Mol Biol Cell,* 14**,** 3254-65.

Smith, J. A., Turner, M. J., Delay, M. L., Klenk, E. I., Sowders, D. P. & Colbert, R. A. 2008. Endoplasmic reticulum stress and the unfolded protein response are linked to synergistic IFN-beta induction via X-box binding protein 1. *Eur J Immunol,* 38**,** 1194-203.

Smyth, M. J., Cretney, E., Takeda, K., Wiltrout, R. H., Sedger, L. M., Kayagaki, N., Yagita, H. & Okumura, K. 2001. Tumor necrosis factor-related apoptosis-inducing ligand (TRAIL) contributes to interferon gamma-dependent natural killer cell protection from tumor metastasis. *J Exp Med,* 193**,** 661-70.

Smyth, M. J., Crowe, N. Y., Pellicci, D. G., Kyparissoudis, K., Kelly, J. M., Takeda, K., Yagita, H. & Godfrey, D. I. 2002. Sequential production of interferon-gamma by NK1.1(+) T cells and natural killer cells is essential for the antimetastatic effect of alpha-galactosylceramide. *Blood,* 99**,** 1259-66.

Song, L., Asgharzadeh, S., Salo, J., Engell, K., Wu, H. W., Sposto, R., Ara, T., Silverman, A. M., Declerck, Y. A., Seeger, R. C. & Metelitsa, L. S. 2009. Valpha24-invariant NKT cells mediate antitumor activity via killing of tumor-associated macrophages. *J Clin Invest,* 119**,** 1524-36.

Song, M., Sandoval, T. A., Chae, C. S., Chopra, S., Tan, C., Rutkowski, M. R., Raundhal, M., Chaurio, R. A., Payne, K. K., Konrad, C., Bettigole, S. E., Shin, H. R., Crowley, M. J. P., Cerliani, J. P., Kossenkov, A. V., Motorykin, I., Zhang, S., Manfredi, G., Zamarin, D., Holcomb, K., Rodriguez, P. C., Rabinovich, G. A., Conejo-Garcia, J. R., Glimcher, L. H. & Cubillos-Ruiz, J. R. 2018a. IRE1alpha-XBP1 controls T cell function in ovarian cancer by regulating mitochondrial activity. *Nature,* 562**,** 423-428.

Song, S., Tan, J., Miao, Y. & Zhang, Q. 2018b. Crosstalk of ER stress-mediated autophagy and ER-phagy: Involvement of UPR and the core autophagy machinery. *J Cell Physiol,* 233**,** 3867-3874.

Spanoudakis, E., Hu, M., Naresh, K., Terpos, E., Melo, V., Reid, A., Kotsianidis, I., Abdalla, S., Rahemtulla, A. & Karadimitris, A. 2009. Regulation of multiple myeloma survival and progression by CD1d. *Blood,* 113**,** 2498-507.

Speak, A. O., Salio, M., Neville, D. C., Fontaine, J., Priestman, D. A., Platt, N., Heare, T., Butters, T. D., Dwek, R. A., Trottein, F., Exley, M. A., Cerundolo, V. & Platt, F. M. 2007. Implications for invariant natural killer T cell ligands due to the restricted presence of isoglobotrihexosylceramide in mammals. *Proc Natl Acad Sci U S A,* 104**,** 5971-6.

Sriram, V., Willard, C. A., Liu, J. & Brutkiewicz, R. R. 2008. Importance of N-linked glycosylation in the functional expression of murine CD1d1. *Immunology,* 123**,** 272-81.

Stetson, D. B., Mohrs, M., Reinhardt, R. L., Baron, J. L., Wang, Z. E., Gapin, L., Kronenberg, M. & Locksley, R. M. 2003. Constitutive cytokine mRNAs mark natural killer (NK) and NK T cells poised for rapid effector function. *J Exp Med,* 198**,** 1069-76.

Streb, H., Irvine, R. F., Berridge, M. J. & Schulz, I. 1983. Release of Ca2+ from a nonmitochondrial intracellular store in pancreatic acinar cells by inositol-1,4,5-trisphosphate. *Nature,* 306**,** 67-9.

Stutzbach, L. D., Xie, S. X., Naj, A. C., Albin, R., Gilman, S., Group, P. S. P. G. S., Lee, V. M., Trojanowski, J. Q., Devlin, B. & Schellenberg, G. D. 2013. The unfolded protein response is activated in disease-affected brain regions in progressive supranuclear palsy and Alzheimer's disease. *Acta Neuropathol Commun,* 1**,** 31.

Subramaniam, S., Aslam, A., Misbah, S. A., Salio, M., Cerundolo, V., Moody, D. B. & Ogg, G. 2016. Elevated and cross-responsive CD1a-reactive T cells in bee and wasp venom allergic individuals. *Eur J Immunol,* 46**,** 242-52.

Sugita, M., Cernadas, M. & Brenner, M. B. 2004. New insights into pathways for CD1-mediated antigen presentation. *Curr Opin Immunol,* 16**,** 90-5.

Sugita, M., Van Der Wel, N., Rogers, R. A., Peters, P. J. & Brenner, M. B. 2000. CD1c molecules broadly survey the endocytic system. *Proc Natl Acad Sci U S A,* 97**,** 8445-50.

Sugiura, K., Muro, Y., Futamura, K., Matsumoto, K., Hashimoto, N., Nishizawa, Y., Nagasaka, T., Saito, H., Tomita, Y. & Usukura, J. 2009. The unfolded protein response is activated in differentiating epidermal keratinocytes. *J Invest Dermatol,* 129**,** 2126-35.

Sullivan, B. A. & Kronenberg, M. 2005. Activation or anergy: NKT cells are stunned by alpha-galactosylceramide. *J Clin Invest,* 115**,** 2328-9.

Sumida, T., Takei, I. & Taniguchi, M. 1984. Activation of acceptor-suppressor hybridoma with antigen-specific suppressor T cell factor of two-chain type: requirement of the antigen- and the I-J-restricting specificity. *J Immunol,* 133**,** 1131-6.

Sundararaj, S., Zhang, J., Krovi, S. H., Bedel, R., Tuttle, K. D., Veerapen, N., Besra, G. S., Khandokar, Y., Praveena, T., Le Nours, J., Matsuda, J. L., Rossjohn, J. & Gapin, L. 2018. Differing roles of CD1d2 and CD1d1 proteins in type I natural killer T cell development and function. *Proc Natl Acad Sci U S A,* 115**,** E1204-E1213.

Syn, W. K., Oo, Y. H., Pereira, T. A., Karaca, G. F., Jung, Y., Omenetti, A., Witek, R. P., Choi, S. S., Guy, C. D., Fearing, C. M., Teaberry, V., Pereira, F. E., Adams, D. H. & Diehl, A. M. 2010. Accumulation of natural killer T cells in progressive nonalcoholic fatty liver disease. *Hepatology,* 51**,** 1998-2007.

Tajiri, K., Shimizu, Y., Tsuneyama, K. & Sugiyama, T. 2009. Role of liver-infiltrating CD3+CD56+ natural killer T cells in the pathogenesis of nonalcoholic fatty liver disease. *Eur J Gastroenterol Hepatol,* 21**,** 673-80.

Takami, M., Ihara, F. & Motohashi, S. 2018. Clinical Application of iNKT Cell-mediated Anti-tumor Activity Against Lung Cancer and Head and Neck Cancer. Front Immunol, 9, 2021.

Tashiro, T., Sekine-Kondo, E., Shigeura, T., Nakagawa, R., Inoue, S., Omori-Miyake, M., Chiba, T., Hongo, N., Fujii, S., Shimizu, K., Yoshiga, Y., Sumida, T., Mori, K., Watarai, H. & Taniguchi, M. 2010. Induction of Th1-biased cytokine production by alpha-carba-GalCer, a neoglycolipid ligand for NKT cells. *Int Immunol,* 22**,** 319-28.

Taylor, S. G., Mckenzie, I. F. & Sandrin, M. S. 2003. Characterization of the rat alpha(1,3)galactosyltransferase: evidence for two independent genes encoding glycosyltransferases that synthesize Galalpha(1,3)Gal by two separate glycosylation pathways. *Glycobiology,* 13**,** 327-37.

Tefit, J. N., Crabe, S., Orlandini, B., Nell, H., Bendelac, A., Deng, S., Savage, P. B., Teyton, L. & Serra, V. 2014. Efficacy of ABX196, a new NKT agonist, in prophylactic human vaccination. *Vaccine,* 32**,** 6138-45.

Terabe, M. & Berzofsky, J. A. 2018. Tissue-Specific Roles of NKT Cells in Tumor Immunity. *Front Immunol,* 9**,** 1838.

Terabe, M., Matsui, S., Noben-Trauth, N., Chen, H., Watson, C., Donaldson, D. D., Carbone, D. P., Paul, W. E. & Berzofsky, J. A. 2000. NKT cell-mediated repression of tumor immunosurveillance by IL-13 and the IL-4R-STAT6 pathway. *Nat Immunol,* 1**,** 515-20.

Terabe, M., Matsui, S., Park, J. M., Mamura, M., Noben-Trauth, N., Donaldson, D. D., Chen, W., Wahl, S. M., Ledbetter, S., Pratt, B., Letterio, J. J., Paul, W. E. & Berzofsky, J. A. 2003. Transforming growth factor-beta production and myeloid cells are an effector mechanism through which CD1d-restricted T cells block cytotoxic T lymphocyte-mediated tumor immunosurveillance: abrogation prevents tumor recurrence. *J Exp Med,* 198**,** 1741-52.

Thuerauf, D. J., Marcinko, M., Belmont, P. J. & Glembotski, C. C. 2007. Effects of the isoform-specific characteristics of ATF6 alpha and ATF6 beta on

endoplasmic reticulum stress response gene expression and cell viability. *J Biol Chem,* 282**,** 22865-78.

Tian, G., Courtney, A. N., Jena, B., Heczey, A., Liu, D., Marinova, E., Guo, L., Xu, X., Torikai, H., Mo, Q., Dotti, G., Cooper, L. J. & Metelitsa, L. S. 2016. CD62L+ NKT cells have prolonged persistence and antitumor activity in vivo. *J Clin Invest,* 126**,** 2341-55.

Timosenko, E., Ghadbane, H., Silk, J. D., Shepherd, D., Gileadi, U., Howson, L. J., Laynes, R., Zhao, Q., Strausberg, R. L., Olsen, L. R., Taylor, S., Buffa, F. M., Boyd, R. & Cerundolo, V. 2016. Nutritional Stress Induced by Tryptophan-Degrading Enzymes Results in ATF4-Dependent Reprogramming of the Amino Acid Transporter Profile in Tumor Cells. *Cancer Res,* 76**,** 6193-6204.

Timosenko, E., Hadjinicolaou, A. V. & Cerundolo, V. 2017. Modulation of cancer-specific immune responses by amino acid degrading enzymes. *Immunotherapy,* 9**,** 83-97.

Tiper, I. V., Temkin, S. M., Spiegel, S., Goldblum, S. E., Giuntoli, R. L., 2nd, Oelke, M., Schneck, J. P. & Webb, T. J. 2016. VEGF Potentiates GD3-Mediated Immunosuppression by Human Ovarian Cancer Cells. *Clin Cancer Res,* 22**,** 4249-58.

Torreno-Pina, J. A., Manzo, C., Salio, M., Aichinger, M. C., Oddone, A., Lakadamyali, M., Shepherd, D., Besra, G. S., Cerundolo, V. & Garcia-Parajo, M. F. 2016. The actin cytoskeleton modulates the activation of iNKT cells by segregating CD1d nanoclusters on antigen-presenting cells. *Proc Natl Acad Sci U S A,* 113**,** E772-81.

Tsagaratou, A., Gonzalez-Avalos, E., Rautio, S., Scott-Browne, J. P., Togher, S., Pastor, W. A., Rothenberg, E. V., Chavez, L., Lahdesmaki, H. & Rao, A. 2017. TET proteins regulate the lineage specification and TCR-mediated expansion of iNKT cells. *Nat Immunol,* 18**,** 45-53.

Tsuru, A., Fujimoto, N., Takahashi, S., Saito, M., Nakamura, D., Iwano, M., Iwawaki, T., Kadokura, H., Ron, D. & Kohno, K. 2013. Negative feedback by IRE1beta optimizes mucin production in goblet cells. *Proc Natl Acad Sci U S A,* 110**,** 2864-9.

Tupin, E., Kinjo, Y. & Kronenberg, M. 2007. The unique role of natural killer T cells in the response to microorganisms. *Nat Rev Microbiol,* 5**,** 405-17.

Tyznik, A. J., Tupin, E., Nagarajan, N. A., Her, M. J., Benedict, C. A. & Kronenberg, M. 2008. Cutting edge: the mechanism of invariant NKT cell responses to viral danger signals. *J Immunol,* 181**,** 4452-6.

Uddin, M. N., Sultana, D. A., Lorentsen, K. J., Cho, J. J., Kirst, M. E., Brantly, M. L., Califano, D., Sant'angelo, D. B. & Avram, D. 2016. Transcription factor Bcl11b sustains iNKT1 and iNKT2 cell programs, restricts iNKT17 cell program, and governs iNKT cell survival. *Proc Natl Acad Sci U S A,* 113**,** 7608-13.

Uldrich, A. P., Le Nours, J., Pellicci, D. G., Gherardin, N. A., Mcpherson, K. G., Lim, R. T., Patel, O., Beddoe, T., Gras, S., Rossjohn, J. & Godfrey, D. I. 2013. CD1d-lipid antigen recognition by the gammadelta TCR. *Nat Immunol,* 14**,** 1137-45.

Urra, H., Dufey, E., Avril, T., Chevet, E. & Hetz, C. 2016. Endoplasmic Reticulum Stress and the Hallmarks of Cancer. *Trends Cancer,* 2**,** 252-262.

Van 'T Wout, E. F., Van Schadewijk, A., Van Boxtel, R., Dalton, L. E., Clarke, H. J., Tommassen, J., Marciniak, S. J. & Hiemstra, P. S. 2015. Virulence Factors of Pseudomonas aeruginosa Induce Both the Unfolded Protein and Integrated Stress Responses in Airway Epithelial Cells. *PLoS Pathog,* 11**,** e1004946.

Van Den Elzen, P., Garg, S., Leon, L., Brigl, M., Leadbetter, E. A., Gumperz, J. E., Dascher, C. C., Cheng, T. Y., Sacks, F. M., Illarionov, P. A., Besra, G. S., Kent, S. C., Moody, D. B. & Brenner, M. B. 2005. Apolipoprotein-mediated pathways of lipid antigen presentation. *Nature,* 437**,** 906-10.

Van Den Heuvel, M. J., Garg, N., Van Kaer, L. & Haeryfar, S. M. 2011. NKT cell costimulation: experimental progress and therapeutic promise. *Trends Mol Med,* 17**,** 65-77.

Van Der Harg, J. M., Nolle, A., Zwart, R., Boerema, A. S., Van Haastert, E. S., Strijkstra, A. M., Hoozemans, J. J. & Scheper, W. 2014. The unfolded protein response mediates reversible tau phosphorylation induced by metabolic stress. *Cell Death Dis,* 5**,** e1393.

Van Haasteren, J., Hyde, S. C. & Gill, D. R. 2018. Lessons learned from lung and liver in-vivo gene therapy: implications for the future. *Expert Opin Biol Ther,* 18**,** 959-972.

Van Rhijn, I., Godfrey, D. I., Rossjohn, J. & Moody, D. B. 2015. Lipid and small-molecule display by CD1 and MR1. *Nat Rev Immunol,* 15**,** 643-54.

Van Rhijn, I., Kasmar, A., De Jong, A., Gras, S., Bhati, M., Doorenspleet, M. E., De Vries, N., Godfrey, D. I., Altman, J. D., De Jager, W., Rossjohn, J. & Moody, D. B. 2013. A conserved human T cell population targets mycobacterial antigens presented by CD1b. *Nat Immunol,* 14**,** 706-13.

Van Rhijn, I., Koets, A. P., Im, J. S., Piebes, D., Reddington, F., Besra, G. S., Porcelli, S. A., Van Eden, W. & Rutten, V. P. 2006. The bovine CD1 family contains group 1 CD1 proteins, but no functional CD1d. *J Immunol,* 176**,** 4888-93.

Van Wilgenburg, B., Scherwitzl, I., Hutchinson, E. C., Leng, T., Kurioka, A., Kulicke, C., De Lara, C., Cole, S., Vasanawathana, S., Limpitikul, W., Malasit, P., Young, D., Denney, L., Consortium, S.-H., Moore, M. D., Fabris, P., Giordani, M. T., Oo, Y. H., Laidlaw, S. M., Dustin, L. B., Ho, L. P., Thompson, F. M., Ramamurthy, N., Mongkolsapaya, J., Willberg, C. B., Screaton, G. R. & Klenerman, P. 2016. MAIT cells are activated during human viral infections. *Nat Commun,* 7**,** 11653.

Vattem, K. M. & Wek, R. C. 2004. Reinitiation involving upstream ORFs regulates ATF4 mRNA translation in mammalian cells. *Proc Natl Acad Sci U S A,* 101**,** 11269-74.

Vijayanand, P., Seumois, G., Pickard, C., Powell, R. M., Angco, G., Sammut, D., Gadola, S. D., Friedmann, P. S. & Djukanovic, R. 2007. Invariant natural killer T cells in asthma and chronic obstructive pulmonary disease. *N Engl J Med,* 356**,** 1410-22.

Volkmann, K., Lucas, J. L., Vuga, D., Wang, X., Brumm, D., Stiles, C., Kriebel, D., Der-Sarkissian, A., Krishnan, K., Schweitzer, C., Liu, Z., Malyankar, U. M., Chiovitti, D., Canny, M., Durocher, D., Sicheri, F. & Patterson, J. B. 2011. Potent and selective inhibitors of the inositol-requiring enzyme 1 endoribonuclease. *J Biol Chem,* 286**,** 12743-55.

Volmer, R., Van Der Ploeg, K. & Ron, D. 2013. Membrane lipid saturation activates endoplasmic reticulum unfolded protein response transducers through their transmembrane domains. *Proc Natl Acad Sci U S A,* 110**,** 4628-33.

Von Gerichten, J., Schlosser, K., Lamprecht, D., Morace, I., Eckhardt, M., Wachten, D., Jennemann, R., Grone, H. J., Mack, M. & Sandhoff, R. 2017. Diastereomer-specific quantification of bioactive hexosylceramides from bacteria and mammals. *J Lipid Res,* 58**,** 1247-1258.

Wang, H., Feng, D., Park, O., Yin, S. & Gao, B. 2013. Invariant NKT cell activation induces neutrophil accumulation and hepatitis: opposite regulation by IL-4 and IFN-gamma. *Hepatology,* 58**,** 1474-85.

Wang, H., Yang, D., Xu, W., Wang, Y., Ruan, Z., Zhao, T., Han, J. & Wu, Y. 2008. Tumor-derived soluble MICs impair CD3(+)CD56(+) NKT-like cell cytotoxicity in cancer patients. *Immunol Lett,* 120**,** 65-71.

Wang, J. & Sevier, C. S. 2016. Formation and Reversibility of BiP Protein Cysteine Oxidation Facilitate Cell Survival during and post Oxidative Stress. *J Biol Chem,* 291**,** 7541-57.

Wang, Z. V., Deng, Y., Gao, N., Pedrozo, Z., Li, D. L., Morales, C. R., Criollo, A., Luo, X., Tan, W., Jiang, N., Lehrman, M. A., Rothermel, B. A., Lee, A. H., Lavandero, S., Mammen, P. P. A., Ferdous, A., Gillette, T. G., Scherer, P. E. & Hill, J. A. 2014. Spliced X-box binding protein 1 couples the unfolded protein response to hexosamine biosynthetic pathway. *Cell,* 156**,** 1179-1192.

Webster, K. E., Kim, H. O., Kyparissoudis, K., Corpuz, T. M., Pinget, G. V., Uldrich, A. P., Brink, R., Belz, G. T., Cho, J. H., Godfrey, D. I. & Sprent, J. 2014. IL-17-producing NKT cells depend exclusively on IL-7 for homeostasis and survival. *Mucosal Immunol,* 7**,** 1058-67.

Weinreb, N. J. 2008. Imiglucerase and its use for the treatment of Gaucher's disease. *Expert Opin Pharmacother,* 9**,** 1987-2000.

Wesley, J. D., Tessmer, M. S., Chaukos, D. & Brossay, L. 2008. NK cell-like behavior of Valpha14i NK T cells during MCMV infection. *PLoS Pathog,* 4**,** e1000106.

Wild, M. K., Cambiaggi, A., Brown, M. H., Davies, E. A., Ohno, H., Saito, T. & Van Der Merwe, P. A. 1999. Dependence of T cell antigen recognition on the dimensions of an accessory receptor-ligand complex. *J Exp Med,* 190**,** 31-41.

Wingender, G., Rogers, P., Batzer, G., Lee, M. S., Bai, D., Pei, B., Khurana, A., Kronenberg, M. & Horner, A. A. 2011. Invariant NKT cells are required for airway inflammation induced by environmental antigens. *J Exp Med,* 208**,** 1151-62.

Wingender, G., Stepniak, D., Krebs, P., Lin, L., Mcbride, S., Wei, B., Braun, J., Mazmanian, S. K. & Kronenberg, M. 2012. Intestinal microbes affect phenotypes and functions of invariant natural killer T cells in mice. *Gastroenterology,* 143**,** 418-28.

Wong, W. L., Brostrom, M. A., Kuznetsov, G., Gmitter-Yellen, D. & Brostrom, C. O. 1993. Inhibition of protein synthesis and early protein processing by thapsigargin in cultured cells. *Biochem J,* 289 (Pt 1)**,** 71-9.

Worah, K., Mathan, T. S. M., Vu Manh, T. P., Keerthikumar, S., Schreibelt, G., Tel, J., Duiveman-De Boer, T., Skold, A. E., Van Spriel, A. B., De Vries, I. J. M., Huynen, M. A., Wessels, H. J., Gloerich, J., Dalod, M., Lasonder, E., Figdor, C. G. & Buschow, S. I. 2016. Proteomics of Human Dendritic Cell Subsets Reveals Subset-Specific Surface Markers and Differential Inflammasome Function. *Cell Rep,* 16**,** 2953-2966.

Wu, D. Y., Segal, N. H., Sidobre, S., Kronenberg, M. & Chapman, P. B. 2003. Cross-presentation of disialoganglioside GD3 to natural killer T cells. *J Exp Med,* 198**,** 173-81.

Wu, L., Parekh, V. V., Gabriel, C. L., Bracy, D. P., Marks-Shulman, P. A., Tamboli, R. A., Kim, S., Mendez-Fernandez, Y. V., Besra, G. S., Lomenick, J. P., Williams, B., Wasserman, D. H. & Van Kaer, L. 2012. Activation of invariant natural killer T cells by lipid excess promotes tissue inflammation, insulin resistance, and hepatic steatosis in obese mice. *Proc Natl Acad Sci U S A,* 109**,** E1143-52.

Wu, T. N., Lin, K. H., Chang, Y. J., Huang, J. R., Cheng, J. Y., Yu, A. L. & Wong, C. H. 2011. Avidity of CD1d-ligand-receptor ternary complex contributes to T-helper 1 (Th1) polarization and anticancer efficacy. *Proc Natl Acad Sci U S A,* 108**,** 17275-80.

Wun, K. S., Cameron, G., Patel, O., Pang, S. S., Pellicci, D. G., Sullivan, L. C., Keshipeddy, S., Young, M. H., Uldrich, A. P., Thakur, M. S., Richardson, S. K., Howell, A. R., Illarionov, P. A., Brooks, A. G., Besra, G. S., Mccluskey, J., Gapin, L., Porcelli, S. A., Godfrey, D. I. & Rossjohn, J. 2011. A molecular basis for the exquisite CD1d-restricted antigen specificity and functional responses of natural killer T cells. *Immunity,* 34**,** 327-39.

Wun, K. S., Reijneveld, J. F., Cheng, T. Y., Ladell, K., Uldrich, A. P., Le Nours, J., Miners, K. L., Mclaren, J. E., Grant, E. J., Haigh, O. L., Watkins, T. S., Suliman, S., Iwany, S., Jimenez, J., Calderon, R., Tamara, K. L., Leon, S. R., Murray, M. B., Mayfield, J. A., Altman, J. D., Purcell, A. W., Miles, J. J., Godfrey, D. I., Gras, S., Price, D. A., Van Rhijn, I., Moody, D. B. & Rossjohn, J. 2018. T cell autoreactivity directed toward CD1c itself rather than toward carried self lipids. *Nat Immunol,* 19**,** 397-406.

Xu, M., Marsh, H. M. & Sevier, C. S. 2016a. A Conserved Cysteine within the ATPase Domain of the Endoplasmic Reticulum Chaperone BiP is Necessary for a Complete Complement of BiP Activities. *J Mol Biol,* 428**,** 4168-4184.

Xu, X., Pocock, G. M., Sharma, A., Peery, S. L., Fites, J. S., Felley, L., Zarnowski, R., Stewart, D., Berthier, E., Klein, B. S., Sherer, N. M. & Gumperz, J. E. 2016b. Human iNKT Cells Promote Protective Inflammation by Inducing Oscillating Purinergic Signaling in Monocyte-Derived DCs. *Cell Rep,* 16**,** 3273-85.

Yang, X., Xia, R., Yue, C., Zhai, W., Du, W., Yang, Q., Cao, H., Chen, X., Obando, D., Zhu, Y., Chen, X., Chen, J. J., Piganelli, J., Wipf, P., Jiang, Y., Xiao, G., Wu, C., Jiang, J. & Lu, B. 2018. ATF4 Regulates CD4(+) T Cell Immune Responses through Metabolic Reprogramming. *Cell Rep,* 23**,** 1754-1766.

Yoboue, E. D., Sitia, R. & Simmen, T. 2018. Redox crosstalk at endoplasmic reticulum (ER) membrane contact sites (MCS) uses toxic waste to deliver messages. *Cell Death Dis,* 9**,** 331.

Yoshida, H., Haze, K., Yanagi, H., Yura, T. & Mori, K. 1998. Identification of the cis-acting endoplasmic reticulum stress response element responsible for transcriptional induction of mammalian glucose-regulated proteins. Involvement of basic leucine zipper transcription factors. *J Biol Chem,* 273**,** 33741-9.

Yoshida, H., Matsui, T., Yamamoto, A., Okada, T. & Mori, K. 2001. XBP1 mRNA is induced by ATF6 and spliced by IRE1 in response to ER stress to produce a highly active transcription factor. *Cell,* 107**,** 881-91.

Yoshida, H., Okada, T., Haze, K., Yanagi, H., Yura, T., Negishi, M. & Mori, K. 2000. ATF6 activated by proteolysis binds in the presence of NF-Y (CBF) directly to the cis-acting element responsible for the mammalian unfolded protein response. *Mol Cell Biol,* 20**,** 6755-67.

Young, S. K. & Wek, R. C. 2016. Upstream Open Reading Frames Differentially Regulate Gene-specific Translation in the Integrated Stress Response. *J Biol Chem,* 291**,** 16927-35.

Yu, L., Lu, M., Jia, D., Ma, J., Ben-Jacob, E., Levine, H., Kaipparettu, B. A. & Onuchic, J. N. 2017. Modeling the Genetic Regulation of Cancer Metabolism: Interplay between Glycolysis and Oxidative Phosphorylation. *Cancer Res,* 77**,** 1564-1574.

Yu, S. M. & Kim, S. J. 2010. Endoplasmic reticulum stress (ER-stress) by 2-deoxy-D-glucose (2DG) reduces cyclooxygenase-2 (COX-2) expression and N-glycosylation and induces a loss of COX-2 activity via a Src kinase-dependent pathway in rabbit articular chondrocytes. *Exp Mol Med,* 42**,** 777-86.

Yuan, W., Qi, X., Tsang, P., Kang, S. J., Illarionov, P. A., Besra, G. S., Gumperz, J. & Cresswell, P. 2007. Saposin B is the dominant saposin that facilitates lipid binding to human CD1d molecules. *Proc Natl Acad Sci U S A,* 104**,** 5551-6.

Zajonc, D. M., Elsliger, M. A., Teyton, L. & Wilson, I. A. 2003. Crystal structure of CD1a in complex with a sulfatide self antigen at a resolution of 2.15 A. *Nat Immunol,* 4**,** 808-15.

Zajonc, D. M. & Girardi, E. 2015. Recognition of Microbial Glycolipids by Natural Killer T Cells. *Front Immunol,* 6**,** 400.

Zeissig, S. & Blumberg, R. S. 2013. Commensal microbiota and NKT cells in the control of inflammatory diseases at mucosal surfaces. *Curr Opin Immunol,* 25**,** 690-6.

Zeissig, S., Murata, K., Sweet, L., Publicover, J., Hu, Z., Kaser, A., Bosse, E., Iqbal, J., Hussain, M. M., Balschun, K., Rocken, C., Arlt, A., Gunther, R., Hampe, J., Schreiber, S., Baron, J. L., Moody, D. B., Liang, T. J. & Blumberg, R. S. 2012. Hepatitis B virus-induced lipid alterations contribute to natural killer T cell-dependent protective immunity. *Nat Med,* 18**,** 1060-8.

Zeissig, S., Peuker, K., Iyer, S., Gensollen, T., Dougan, S. K., Olszak, T., Kaser, A. & Blumberg, R. S. 2017. CD1d-Restricted pathways in hepatocytes control local natural killer T cell homeostasis and hepatic inflammation. *Proc Natl Acad Sci U S A,* 114**,** 10449-10454.

Zhang, Y., Wu, B. X., Metelli, A., Thaxton, J. E., Hong, F., Rachidi, S., Ansa-Addo, E., Sun, S., Vasu, C., Yang, Y., Liu, B. & Li, Z. 2015. GP96 is a GARP chaperone and controls regulatory T cell functions. *J Clin Invest,* 125**,** 859-69.

Zhao, M., Svensson, M. N. D., Venken, K., Chawla, A., Liang, S., Engel, I., Mydel, P., Day, J., Elewaut, D., Bottini, N. & Kronenberg, M. 2018. Altered thymic differentiation and modulation of arthritis by invariant NKT cells expressing mutant ZAP70. *Nat Commun,* 9**,** 2627.